Stony Brook University

Role of Alternative Splicing in Regulating Cancer Cell Metabolism

A Dissertation Presented

by

Deblina Chatterjee

to

The Graduate School

in Partial Fulfillment of the Requirements

for the Degree of

Doctor of Philosophy

in

Molecular and Cellular Biology

(Cellular and Developmental Biology)

Stony Brook University

AUGUST 2012

Stony Brook University

The Graduate School

Deblina Chatterjee

We, the dissertation committee for the above candidate

for the Doctor of Philosophy degree, hereby recommend

acceptance of this dissertation.

Dr. Adrian R Krainer - Dissertation Advisor
Professor, Cold Spring Harbor Laboratory

Dr. Nicholas Tonks - Chairperson of Defense
Professor, Cold Spring Harbor Laboratory

Dr. David.L. Spector
Professor, Cold Spring Harbor Laboratory

Dr. Raffaella Sordella
Associate Professor, Cold Spring Harbor Laboratory

Dr. Luca Cartegni
Assistant Professor, Memorial Sloan Kettering Cancer Centre

This dissertation is accepted by the Graduate School

Charles Taber
Interim Dean of the Graduate School

Abstract of the Dissertation

Role of Alternative Splicing in Regulating Cancer Cell Metabolism

by

Deblina Chatterjee

Doctor of Philosophy

in

Molecular and Cellular Biology

(Cellular and Developmental Biology)

Stony Brook University

2012

Cancer cells preferentially metabolize glucose by aerobic glycolysis, characterized by increased lactate production. This distinctive metabolism involves expression of the embryonic M2 isozyme of pyruvate kinase, in contrast to the M1 isozyme normally expressed in differentiated cells, and it confers a proliferative advantage to tumor cells. The M1 and M2 pyruvate kinase isozymes are expressed from a single gene through alternative splicing of a pair of mutually exclusive exons. We measured the expression of M1 and M2 mRNA and protein isoforms in mouse and human tissues, tumor cell lines, and during terminal differentiation of muscle cells, and showed that alternative splicing regulation is sufficient to account for the levels of expressed protein isoforms. We further showed that the M1-specific exon is actively repressed in cancer cell lines—although some M1 mRNA is expressed in cell lines derived from brain tumors—and demonstrated that the related splicing repressors hnRNPA1 and A2, as well as the

polypyrimidine-tract-binding protein PTB, contribute to this control. Down-regulation of these splicing repressors in cancer cell lines using shRNAs rescues M1 isoform expression and decreases the extent of lactate production. We further identified the oncogenic SR protein SRSF3 as a regulator that recognizes an exonic splicing enhancer to activate exon 10 and mediate changes in glucose metabolism. To systematically detect additional splicing factors that promote PK-M1 expression, I carried out a directed, high-throughput lentivirus screen using a novel qPCR approach. Using this approach, I identified additional players that may participate in the tissue-specific regulation of alternative splicing of PK-M. These findings extend the links between alternative splicing and cancer, and begin to define some of the factors responsible for the switch to aerobic glycolysis.

To my Family

Their love and prayers keep me going

Table of Contents

List of Figures

Chapter 1: Introduction

Chapter 2 : **The alternative splicing repressors hnRNP A1/A2 and PTB influence pyruvate kinase isoform expression and cell metabolism**

Chapter 3 : **Regulation of Pyruvate Kinase M alternative splicing by an oncogenic SR Protein SRSF3**

List of Tables

Abbreviations

qPCR Quantitative-Real Time PCR

DNA Deoxy-riboNucleic Acid

DAPI 4',6-Diamidino-2-phenylindole

shRNA short hairpin RNA

siRNA short interfering RNA

RNA RiboNucleic Acid

CLIP Cross-linking and immunoprecipitation

cDNA complementary DNA

NMD Nonsense mediated decay

RBP RNA-Binding protein

EMT Epithelial to mesenchymal transition

MET Mesenchymal to epithelial transition

VEGF Vascular endothelial growth factor

ATP Adenosine triphosphate

PKM Pyruvate kinase M

Ct Cycle threshhold

AS Alternative Splicing

Preface

This thesis is divided into four chapters. Chapter 1 is an introduction describing the role of alternative splicing in cancer, and specifically in cancer-cell metabolism. Chapter 2 deals with the identification of splicing repressor proteins hnRNPs as regulators of pyruvate kinase M (PKM) alternative splicing, and is provided in its original form as published in *Proceedings of the National Academy of Sciences USA*. The C2C12 cell line work in the manuscript is performed by Cynthia Clower, Lewis Cantley Laboratory. Chapter 3 is a manuscript published in the *Journal of Molecular and Cellular Biology*, further elucidating the molecular mechanism of the mutually exclusive alternative splicing of PKM. All the minigene and *cis*-acting experiments have been performed by Zhenxun Wang, Krainer Laboratory. I have performed all the trans-acting factor experiments. Chapter 4 describes a directed shRNA screen, carried out to systematically identify further regulators of pyruvate kinase M (PKM) alternative splicing. Chapter 4 is a collaborative effort between our laboratory and Greg Hannon laboratory. Kenneth Chang (Hannon Laboratory) and Chaolin Zhang (Krainer Laboratory) initially designed and built the shRNA library, I conducted all other experiments.

Acknowledgments

I am deeply appreciative of the many people who have helped me reach this milestone. First and foremost, I must thank my advisor, Adrian Krainer. He has been patient, encouraging and a father figure to me through all the trials and tribulations of my PhD life. He has not just trained me to do good science, but also has taught me the importance of being honest, hardworking, meticulous, appreciative, humble and kind. I am greatly indebted to him for supporting and guiding me in all things science and not-science, and teaching me to be a good human being above all.

I am grateful to all members of the Krainer lab, both past and present. I thank Zuo Zhang for teaching me the basics of splicing in my initial years, Lisa Manche for being the great friend and advisor that she has been; Barbara and Betsy for their help with scheduling. A special thanks to Jackie Novatt, for keeping my spirits up whenever they sagged, to Oliver Fregoso for the music in the lab, to Xavier Roca for his calming presence and help in the lab, and to Shuying Sun for helpful advice along the way.

I would like to thank our collaborators Dr Lewis Cantley and Dr Matthew Vander Heiden for helpful feedback on every step of my project. I would also like to thank Felix and Paloma in the Hannon lab for helping me unconditionally with reagents and advice whenever needed for the library screening, Molly Hammell for help with bioinformatics analysis, and Stephanie Muller for all her help with the Biomek; I definitely would have been lost without their help.

A special thanks to my thesis committee: Nicholas Tonks, David Spector, Raffaella Sordella and Luca Cartegni – I always came out of every meeting with renewed hope and fresh ideas.

Life would not have been half as fulfilling had I not had an endless source of love and inspiration throughout my life from my parents. They have always encouraged me to learn and explore, to appreciate the little joys of life and never to give up. I cannot thank them enough for the many opportunities they have given me, and for always being there when I needed them. I thank my brother Chirantan and his wife Anubrata for standing beside me. I thank my second family – my in-laws – for their love, acceptance and patience. I thank my friends – Mansi, Sanju, Anshul, Sourabh, Kurush and Shailja – for helping me keep my sanity and sense of humor intact outside the lab.

Finally, I am grateful to my husband Arindam for always being there during this tough phase of my life – supporting me, listening to me, believing in me more than I do in myself, making me smile, being patient with me, loving me and encouraging me to see the rainbow behind every cloud. Without him, I never would have made it this far.

Publications

- Clower, C.V., **Chatterjee, D**., Wang, Z., Cantley, L.C., Vander Heiden, M.G., and Krainer, A.R. (2010). The alternative splicing repressors hnRNP A1/A2 and PTB influence pyruvate kinase isoform expression and cell metabolism. Proceedings of the National Academy of Sciences of the United States of America *107*, 1894-1899.**(co-first author)**

- Wang Z, **Chatterjee D**, Akerman M, Vander Heiden MG, Cantley LC, and Krainer AR (2011) Exon-centric regulation of pyruvate kinase M alternative splicing via mutually exclusive exons. J Mol Cell Biol. 2012 Apr;4(2):79-87

Chapter 1

Introduction

1.1 Synopsis

Alternative pre-mRNA splicing is a key molecular event that creates transcriptome and proteome diversity in eukaryotes. Through this process, a single gene increases its coding capacity by expressing several related proteins with diverse and even antagonistic functions. For many genes, alternative splicing (AS) directs the expression of functionally divergent protein isoforms in a cell-specific manner, based on differentiated cell types (Fu et al., 2009), developmental stage (Cooper, 2005), gender, or in response to an external signal (Back et al., 2005; Hartmann et al., 2009). The variety of such cell-specific expression patterns is regulated by the spliceosomal complex – a highly dynamic, precise system in which intron excision and exon joining repeatedly occur at the appropriate places in human pre-mRNA molecules (Black, 2003). Given that splicing is such a highly complex yet exceedingly accurate process, it is not surprising that aberrant splicing has been found to be associated with various diseases, including cancer (Faustino and Cooper, 2003). However, until recently, it was unclear whether abnormal AS changes were a natural consequence of oncogenic transformation, or whether at least some of the RNA and protein isoforms that were produced in cancer cells have actual functional consequences for transformation (Kim et al., 2008). Emerging data suggest that at least in some cases, the aberrant mRNAs and their encoded proteins have unique properties that equip the cancer cell with new

growth, differentiation and other cellular characteristics (Christofk et al. 2008). In this introductory chapter, I briefly summarize the current knowledge about the most important modes of abnormal AS in cancer, the factors governing these splicing events, and the biological consequences associated with the alteration of splicing on the various hallmarks of neoplastic development, with an emphasis on cancer-cell metabolism. In the following sections, I attempt to correlate the role of AS to each hallmark of cancer, and discuss some of the AS processes that are disrupted during the development of tumors. I also discuss recent evidence that correlates specific isoform expression patterns to distinct functional changes in tumors. Finally, I provide my rationale for focusing on AS regulation of Pyruvate Kinase M (PKM) as the subject of my dissertation.

1.2 The Basics of Splicing

The major, classical spliceosome acts on genes transcribed by RNA polymerase II (Pol II) and follows the GU-AG rule, according to which RNPs recognize the 5' splice site beginning with a GU dinucleotide and the 3' splice site ending with an AG dinucleotide. The second, less prevalent type of spliceosome acts on a minor class of Pol II transcribed introns and follows the AU-AC rule (Tarn and Steitz, 1996). When the sequence of a splice site deviates from the consensus, the site can still be used, albeit less efficiently, and a second class of *cis*-acting elements – called silencers and enhancers – influence the splicing outcome in such cases by acting in conjunction with the splicing apparatus. Silencers and enhancers are short conserved sequences (6-10 nucleotides) located in isolation or in clusters within introns or exons, and they inhibit or stimulate the use of weak splice sites. RNA-binding proteins called splicing activators and repressors bind to

silencers and enhancers, respectively, to influence the final outcome of the splicing decision (Black, 2003; Krainer et al., 1990a, b; Mayeda and Krainer, 1992). Aberrant expression or regulation of RNA-binding proteins (RBPs) causes the global deregulation of splicing observed in cancer (Grosso et al., 2008). Regulation of RBPs therefore has an arguably important biological impact because of its downstream effects, yet little is known about the underlying mechanisms and the disruption of the splicing-regulatory machinery in cancer.

1.3 Alternative Splicing

When two or more splice sites compete, AS generates mRNA variants that can yield different polypeptides from a single gene (Matlin et al., 2005). There are mainly five basic patterns of alternative AS prevalent in normal cells that have been described in the literature (Fig 1). Recent studies have compared the amount of AS in cancer cells vis-à-vis normal cells using various biochemical and bioinformatics approaches and determined that cancer cells exhibit lower levels of AS than normal cells (Ghigna et al., 2008). They also showed that the distribution of the types of AS events differs in cancer cells compared to normal cells, the former demonstrating less exon skipping but more alternative 5' and 3' splice site selection and intron retention than the latter (Kim et al., 2008, Ghigna et al., 2008). A contextual point is that AS decisions are not made on a static, pre-synthesized template. As the pre-mRNA emerges from elongating RNA Pol II, it immediately becomes packaged with various processing and general RNA-binding factors. The C-terminal domain of the RNA Pol II large subunit helps to recruit RNA processing factors to the emerging transcript (Misteli and Spector, 1999). Moreover, the

rate of polymerase elongation can influence splicing patterns by accelerating or delaying the synthesis of competing splice sites or regulatory elements (de la Mata et al., 2003). It is in this dynamic setting that AS decisions are made, involving precise coordination between the spliceosomal complex and the transcriptional machinery; hence even minor disruptions in this finely calibrated process can lead to AS aberrations associated with cancer cells. I discuss below the known physiological functions of AS in the process of tumor initiation and progression.

1.4 The hallmarks of cancer and the role of splicing

Hanahan and Weinberg described the hallmarks of cancer – the distinctive capabilities that enable tumor growth and metastatic propagation, which are the main foundation for understanding the biology of cancer (Hanahan and Weinberg, 2000, 2011). All aspects of tumor biology appear to be affected in some manner by AS. Systematic functional studies as well as recent genome-wide approaches have revealed large scale alterations in AS during tumorigenesis. Not only does AS modulate the activities of various oncogenes and tumor suppressors, but at least some splicing factors have also been reported to act as oncogenes (Karni et al., 2008) or tumor suppressors (Shin et al., 2008). Though direct functional correlations between tumor progression and splicing are just beginning to emerge, the expression of alternatively spliced isoforms has been frequently used for the classification of various tumors (Brinkman, 2004).

1.4.1 Sustaining proliferative signalling

The most significant trait of cancer cells is their enduring proliferative state. Normal cells control the cell cycle by tightly regulating growth promoting signals, thereby maintaining a steady-state cell number (Novak et al., 2007). However, tumor cells successfully deregulate the control of these signals and become the masters of their own fates. Defects in feedback mechanisms enhance the proliferative signaling capability by deregulating the homeostatic regulation of the flux of signals coursing through the intracellular circuitry, and are the primary reason for the uncontrolled growth in cancer cells. The prototype of this type of regulation involves the mTOR pathway (Guertin and Sabatini, 2005). Recent findings from our lab have highlighted the role of the splicing activator SRSF1 as a potent proto-oncogene that activates mTORC1, shown to be essential for SRSF1-mediated transformation (Karni et al., 2007).

AS also often acts as an on/off switch to control gene expression at the post-transcriptional level, such that one mRNA isoform results in a functional protein, whereas the other(s) is (are) subject to degradation by NMD, or retained in the nucleus, or result(s) in a truncated/inactive or mis-localized protein. Such regulation in the case of cellular oncogenes and tumor suppressors has widespread implications. One important example in this regard is the *p73* tumor-suppressor gene, which expresses six different proteins with closely related sequences – p73α, p73β, p73γ, p73δ, and p73ζ – as a result of extensive AS in the C-terminal domain (Hofstetter et al., 2010). These C-terminal splice variants exhibit different transcriptional and functional properties and show differential expression across normal human tissues and cell lines, though their

exact functions are still not known in detail. Further, the use of an alternative promoter in exon 3 of the full-length *p73* gene results in expression of the ΔN variants of p73, ΔNp73α and ΔNp73β, which lack the N-terminal transactivation domain and act as dominant-negative forms of both *p73* and *p53*, with resulting oncogenic activity (Ozaki and Nakagawara, 2005). Similar regulation through AS, combined with the use of alternative promoters, has also been reported in the case of *p63* and *p53* (Bourdon et al., 2005, Hofstetter et al., 2010).

Splicing misregulation in the tyrosine kinase family has also been studied for its effects on metastasis. An example of this is SYK (Spleen tyrosine kinase), a soluble tyrosine kinase that suppresses metastasis in vitro in MCF10A cells. Recent studies have shown that exposure of cancer cells to epidermal growth factor (EGF) modulates the SYK splicing pattern to promote the pro-survival isoform associated with cancer tissues *in vivo (Prinos et al., 2011).* This group showed that the splicing of selected genes is specifically modified during tumor development to allow the expression of isoforms that promote cancer-cell survival. For example, increased expression of the SYK long isoform in tumors increases not only cell survival but also cellular proliferation and tumor aggressiveness, as seen by the increased expression of the long isoform in highly aggressive Grade 3 tumors and also by its effect on anchorage-independent growth. Notably, they also observed increased JUN expression when the long isoform of SYK was knocked down, but not when the overall expression of SYK was down-regulated by siRNA against constitutive exons. The fact that changing the splicing pattern of SYK, and not its overall expression, affects the MAPK–JNK signaling pathway indicates that

splicing changes directly affect oncogenesis and tumor progression rather than being mere bystanders.

1.4.2 Evading apoptosis

When cellular systems function properly, programmed cell death or apoptosis is a natural phenomenon to dispose of dead cells and debris. However, malignant cells find ways to not succumb to this natural cleansing and escape apoptosis.

Apoptosis is perhaps the most investigated process in cancer, in which AS plays a role by giving rise to protein isoforms with distinct and sometimes antagonistic properties. Fas and Bcl-2 splicing changes are the most commonly studied AS events in the extrinsic and intrinsic pathways, respectively. A soluble isoform of FasL can be generated by AS, and has been well described for murine FasL. This isoform lacks the transmembrane domain, the intracellular domain, and part of the extracellular domain, and resembles proteolytically derived soluble FasL in inhibiting apoptosis via the Fas receptor pathway (Ayroldi et al., 1999). Several soluble variants of Fas generated by AS and lacking the transmembrane domain have been described in activated human peripheral blood mononuclear cells and T cell tumor lines (Cascino et al., 1995; Hughes and Crispe, 1995). Among these is FasExo6Del, which lacks the transmembrane domain due to AS of the exon 6. FasExo6Del can compete with the membrane-bound form of Fas and functions as a soluble decoy. Another splice variant of Fas, termed FasExo8Del, lacks the intracellular domain, due to a frameshift caused by skipping of exon 8. FasExo8Del was identified in a human lymphoma cell line resistant to Fas-mediated apoptosis, and found

to be responsible for the resistance phenotype in a dominant-negative fashion (Cascino et al., 1996).

The most complex group of apoptotic regulators in the intrinsic pathway is composed of proteins related to Bcl-2. Several Bcl-2 family proteins are also regulated by AS, and modulation of isoform production can lead to a switch in their function during cell death from pro- to anti-apoptotic or vice-versa (Akgul et al., 2004). Importantly, the balance between pro- and anti-apoptotic Bcl-2 proteins can significantly contribute to cancer progression. Possibly the most interesting member of the Bcl-2 family, as relates to AS, is the Bcl-x gene product, a close relative of Bcl-2. A long version of Bcl-x (Bcl-x_L) contains all four BH domains and is inhibitory to programmed cell death. AS leads to the production of several isoforms, one of which (Bcl-x_S) lacks the BH1 and BH2 domains. Bcl-x_S antagonizes the inhibitory functions of Bcl-x_L and Bcl-2. Bcl-x_S mRNA is expressed at high levels in cells that undergo a high rate of turnover (e.g., developing lymphocytes), whereas the Bcl-x_L transcript is found in tissues containing long-lived postmitotic cells (e.g., adult brain)(Boise et al., 1993). Interestingly, whereas Bcl-x_L expression is rather widespread, Bcl-x_S occurs in only some tissues, including thymus and lymph nodes (Hsu and Hsueh, 2000). It is likely that the expression ratio of the Bcl-x isoforms contributes to the control of apoptosis in these tissues.

A recent genome-wide RNAi screen using Bcl-x splicing reporters established coordinated AS as an integral component of cell cycle control (Moore et al., 2010). Knockdown of 52 genes induced pro-apoptotic splicing of both reporters in the study. The list of genes included a network of factors linked to the cell cycle regulator Aurora

kinase A, a central regulator of mitosis. Loss of Aurora kinase A promoted posttranslational degradation of SRSF1, a member of the SR protein family of splicing regulators. Cross-Linking Immuno Precipitation (CLIP) analysis showed that SRSF1 directly binds to Bcl-x RNA, and revealed additional endogenous apoptotic splicing events that shift toward pro-apoptotic splicing upon cell-cycle inhibition.

1.4.3 Sustained angiogenesis

The physiology of microvessels limits the growth and development of tumors. Tumors gain nutrients and excrete waste through growth-associated microvessels. Vascular endothelial growth factor A (VEGF-A) splice isoforms play a role in promoting such microvessel growth (Ladomery et al., 2007). VEGF-A exists in multiple isoforms of variable exon content and strikingly contrasting properties and expression patterns (Harper and Bates, 2008). This range of products from the eight-exon VEGF-A gene on Chromosome 6 contributes to VEGF-A's complex biology, and alterations in the expression of these isoforms are involved in malignant changes in general, and in the pro-angiogenic cascade in particular. The first VEGF-A isoform, VEGF-A_{165}, has been extensively investigated for its function, signaling, expression, and roles in cancer (Ferrara, 2004). Other isoforms, including VEGF-A_{121}, VEGF-A_{145}, VEGF-A_{148}, VEGF-A_{183}, VEGF-A_{189}, and VEGF-A_{206}, are generated by AS of exons 6 and 7, which code for motifs that bind to the highly negatively charged glycosaminoglycan carbohydrate heparin and similar molecules, and are mostly pro-angiogenic (Glass et al., 2006; Harper and Bates, 2008). An additional isoform, VEGF-A_{165}b, is generated either by exon 8 distal splice site

(DSS) selection (Bates et al., 2002) or in conjunction with exon 6 and 7 inclusion or skipping. It is therefore apparent that VEGF-A mRNA splicing generates two families of proteins that differ by their C-terminal six amino acids, and are termed VEGF-A_{xxx} (pro-angiogenic) and VEGF-A_{xxx}b (anti-angiogenic), with xxx denoting the amino acid number of the mature protein. Details of the molecular control of C-terminal splice site choice (and the pro-angiogenic–anti-angiogenic balance) have only recently begun to emerge (Nowak et al., 2008). Based on initial evidence, insulin growth factor can change the balance between pro- and anti-angiogenic forms by activating protein kinase C (PKC), resulting in phosphorylation of SR protein kinases (SRPKs) that in turn activate SRSF1. This process may be dependent on the presence of hypoxia-inducible factor (HIF), a transcription factor involved in VEGF-A_{xxx} up-regulation (Kerbel, 2008). Other splicing factors and kinases may also be involved in PSS and DSS selection, and only a handful of recent studies have so far delved into this area.

1.4.4 Tissue invasion and metastasis

Phenotypic conversion of cells between epithelial and mesenchymal states, known as epithelial–mesenchymal (EMT) and mesenchymal–epithelial (MET) transitions, are fundamental to organ morphogenesis and tissue remodeling (Thiery et al., 2009). EMT and associated markers have been observed in tumor samples, particularly at the invasive front of solid tumors, such as non-small cell lung cancer (NSCLC), pancreatic, colorectal, and hepatocellular cancers (Kalluri and Weinberg, 2009). The loss of epithelial features, including loss of cell adhesion and polarity, is associated with disease progression and metastatic potential, and it is becoming evident that cancer cells can

de-differentiate through activation of specific biological pathways associated with EMT, thereby gaining the ability to migrate and invade.

AS plays a decisive role in EMT through the regulation of multiple splicing events and the utilization of several regulatory proteins (Brown et al., 2011; Ghigna et al., 2008; Valacca et al., 2010; Warzecha et al., 2009) (Figure 1.3). SRSF1 up-regulation is known to trigger EMT through AS of the Ron tyrosine kinase receptor proto-oncogene and expression of a constitutively active, pro-invasive isoform, Δ Ron (Ghigna et al., 2008). Induction of EMT via ERK1/2 activation (Thiery and Sleeman, 2006), proceeds in part through phosphorylation of SAM68, which then up-regulates SRSF1. Down-regulation of the RNA-binding proteins Epithelial Splicing Regulatory Proteins 1 and 2 (ESRP1 and ESRP2), which are expressed in a cell-type-specific manner, have also been shown to determine physiological changes during EMT. Splicing-sensitive microarrays identified nearly 100 splicing events that displayed reciprocal changes in epithelial cells depleted of ESRP1/ESRP2 or mesenchymal cells expressing ectopic ESRP1 (Warzecha et al., 2009). The ESRP target genes were enriched in functions that support EMT, such as cell adhesion, cell migration and cell polarity. Importantly, sustained ESRP1/ESRP2 knockdown resulted in global EMT splicing transitions and EMT-like phenotypic changes. Among ESRP targets, the splice isoforms of the CD44 cell adhesion molecule in particular participate in multiple EMT-relevant functions like proliferation, adhesion, and migration (Ponta et al., 2003). The fibroblast growth factor plasma membrane receptor 2 (FGFR2) contains two mutually exclusive alternative exons, IIIb and IIIc, that correspond to distinct ligand binding specificities in epithelial and mesenchymal cells

(Wagner and Garcia-Blanco, 2002), ensuring appropriate signaling for different mesenchymal-epithelial interactions. The studies of FGFR2 in EMT have also identified a critical interplay between the histone code, adapter proteins, and AS regulators to generate cell-type-specific splice isoforms (De Moerlooze et al., 2000; Luco et al., 2010; Wagner and Garcia-Blanco, 2002).

1.4.5 Deregulated metabolism

The proclivity of rapidly growing cells to metabolize a significant fraction of glucose through fermentation was first elucidated in yeast. Otto Warburg extended these observations to mammalian cells in the 1950s, finding that proliferating ascites tumor cells converted the majority of their glucose carbon to lactate, even in oxygen-rich conditions (Warburg, 1956). Warburg hypothesized that this altered metabolism was specific to cancer cells, and that it arose from mitochondrial defects that repressed their ability to effectively oxidize glucose carbon to CO_2. The Warburg Effect has now been accepted as one of the hallmarks of cancer (Hanahan and Weinberg, 2011).

Though it has long been known that proliferating cells exhibit the Warburg effect, the complexity of the underlying mechanisms has only recently started to be appreciated (Anastasiou et al., 2011; Christofk et al., 2008c). How do proliferating cells re-program their metabolism to engage in aerobic glycolysis? The Warburg effect requires the shunting of pyruvate that provides the substrate for oxidative phosphorylation in differentiated cells, from the mitochondria to the cytosol, and the conversion to lactate catalyzed by lactate dehydrogenase (LDH). An important part of this process is the

increased production of LDH-A necessary for the final step in aerobic glycolysis: the production of lactate from pyruvate (Fantin et al. 2006). The oncogenic transcription factor c-Myc is known to promote the up-regulation of LDH-A, as well as that of several other glycolytic enzymes – an activity that appears to underlie, in part, the effect of Myc on aerobic glycolysis (Gao et al., 2009).

AS has also recently been implicated in the Warburg effect, as it is now known that isoforms of metabolic enzymes can provide cancer cells with a mechanism to select for metabolic alterations during tumorigenesis. Proliferating cells almost universally express the M2 isoform of pyruvate kinase M (PK-M2) (Christofk et al., 2008c). Pyruvate kinase is a glycolytic enzyme that converts phosphoenolpyruvate (PEP) to pyruvate, with concomitant generation of ATP. In contrast to the M1 isoform of pyruvate kinase (PK-M1), the predominant isoform in most differentiated adult tissues, the PK-M2 splice variant is the major isoform in embryonic tissues and in all cancer cells examined to date (Mazurek et al., 2005).

Other significant genes for proliferative cell metabolism are also alternatively spliced. The phosphofructokinase/fructose-2,6-bisphosphatase B3 gene (*PFKFB3*) is highly expressed in human tumors and has six splice variants (Sharma et al., 1990; Tang et al., 1998). Two splice variants predominate in high-grade astrocytoma and colon carcinoma and enhance glycolytic flux, whereas other splice variants are limited to low-grade tumors and normal tissues (Bando et al., 2005; Zscharnack et al., 2009). An alternatively spliced isoform of glutaminase may also be important for the mitochondrial glutamine

metabolism of tumor cells (Cassago et al., 2012). HIFs are also known to be alternatively spliced. HIF-3α is unique among the HIF-α isoforms in that its gene is also subject to extensive AS, which in turn inhibits HIF-1 and HIF-2 functions (Pasanen et al., 2010). The most widely characterized of these alternatively spliced metabolic enzymes is pyruvate kinase. However, the mechanism of the mutually exclusive (ME) mode of PK-M AS, which favors the apparent inclusion of Exon 10 over Exon 9 in tumors and of Exon 9 over Exon 10 in normal tissues, remains poorly understood. The preferential expression of PK-M2 in proliferating cells suggested a pro-tumorigenic role for this splice variant, and xenograft models subsequently demonstrated that PK-M2-expressing cells have a growth advantage in vivo, compared with PK-M1-expressing cells (Christofk et al., 2008a). The switching of isoforms in tumor cells and PK-M2's pro-tumorigenic role prompted us to investigate the AS regulation of this gene and to develop a deeper understanding of the mechanism underlying the regulation of these spliced isoforms in a tissue-specific manner. Three splicing repressors – PTB, hnRNP A1, and hnRNP A2 – were recently shown by us and others to promote the formation of the PK-M2 isoform (Clower and Chatterjee et al., 2010b), in part by binding to sequences upstream of and downstream from E9 (David et al., 2010). PK-M2 expression appears to be universal in tumors, and the up-regulation of hnRNP A1/A2 and PTB is widely observed in cancer (see below), potentially suggesting that pathways shared by many tumor types promote the overexpression of these RBPs. Chen et al. also demonstrated that in addition to its role in up-regulating glycolytic enzymes, c-Myc contributes to the Warburg effect by indirectly regulating PK-M splicing (Chen et al. 2010). However, the effect of c-Myc

knockdown on hnRNP protein levels was not observed in all cells tested (David et al. 2010), implying that additional proliferation-associated transcriptional pathways may play a larger role in inducing over-expression of hnRNP A1/A2 and PTB in other contexts. By studying splicing regulators that mediate the mutual exclusive splicing pattern of PK-M, my dissertation attempts to fill in some of the gaps in understanding the role of splicing in tumor metabolism.

1.5 Thesis Objectives

For my thesis, I aimed to understand the role of AS in regulating one of the hallmarks of cancer – cancer-cell metabolism – by specifically studying the AS regulation of the Pyruvate Kinase M gene. I chose to investigate the role of splicing activators and repressors in regulating the ratio of expressed isoforms in a cell-specific context. Two isoforms of PK-M are expressed, PK-M1 and PK-M2, by the mutual exclusive selection of either exon 9 or 10, respectively. My primary goal was to understand how splicing regulators control the ratio of PKM-1 and PK-M2, and investigate the factors that bind and mediate this mutual exclusivity in a tissue-specific manner, to regulate glucose metabolism in cancer cells. My first aim was to understand the regulation of PK-M by splicing repressors hnRNPA1/A2 and PTB. Because hnRNP proteins are known common repressors of splicing, I reasoned that investigating whether hnRNPA1/A2 and hnRNPI (PTB) can repress exon 9 of PK-M could reveal important aspects of the tissue-specific expression pattern of PK-M.

My second aim was a contribution to another study in the lab, to help understand the mutual exclusive splicing regulation of PK-M by the splicing activator SRSF3. My third aim was to begin to identify other splicing factors that mediate alternative splicing of PK-M. Given the importance of PK-M alternative splicing in cancer metabolism, I speculated that systematically studying the factors involved in this mutual-exclusive splicing regulation by using a shRNA library could significantly contribute to understanding the overall regulation of PK-M AS. By carrying out a directed shRNA screen, I sought to address this possibility.

Alterations in splicing patterns often underlie many of the cancer-associated phenotypic changes, and I decided to focus on the splicing pattern of PK-M, as this was one of a few AS changes known to exhibit a direct correlation between isoform expression and physiological changes at the tissue level. The goals of my thesis were thus to explore the factors that regulate the mutual exclusive splicing pattern of PK-M, and how they mediate altered tumor metabolism.

Splicing Factor	Function	Genomic location	Mechanism	Targets	Cancer type	Mouse models
SRSF1	Oncogene	17q23	Activator	S6K,BIN1,Ron,MNK2	Lung, Breast	Complete KO-embryonic lethal
Tra-2B	Oncogene	3q26	Activator	CD44	Breast, Ovary	Complete KO-embryonic lethality
SRSF3	Oncogene	6p21	Activator	PKM2, PLK1,CDC25	Ovary, Breast	Complete KO, embryonic lethal, E3.5
HnRNPA1	Tumor suppressor	12q13	Repressor	PKM2	Lung, breast, Ovary	Not available
HnRNPA2	Tumor suppressor	7p15	Repressor	PKM2,BIN,Ron,Caspase-9	Glioblastoma,Lung Breast, Ovary	Not available
HnRNPH	Oncogene	5q35	Activator	IG20/MADD, c-src	Colon, Glioblastoma	Not available
PTB	Oncogene	19p13	Repressor	PKM2,MINK1,EIF4G2	Glioblastoma, Lung	Not available
YB1	Oncogene	1p34	Repressor	CD44, Fas,	Breast, Ovary	Complete KO-embryonic lethal, E11.5
Sam68	Oncogene	1p32	Activator	BclL1, CD44	Prostrate, Breast,	Haploinsufficiency impedes mammary tumor onset
SRPK1	-	6p21	Activator	VEGF, HIF	Colorectal, Leukemia, Pancreas	Not available
RBM5	-	3p21	Repressor	caspase-2, Fas	Lung, Breast	Not available

Table1: Key splicing factors involved in cancer

The above table shows key splicing factors that have been categorized as oncogenes or tumor suppressors. They are labeled ‘oncogene’ or ‘tumor suppressor’ if they have at least one known feature consistent with these categories, though some of these assignments are only tentative, and more research will be required.

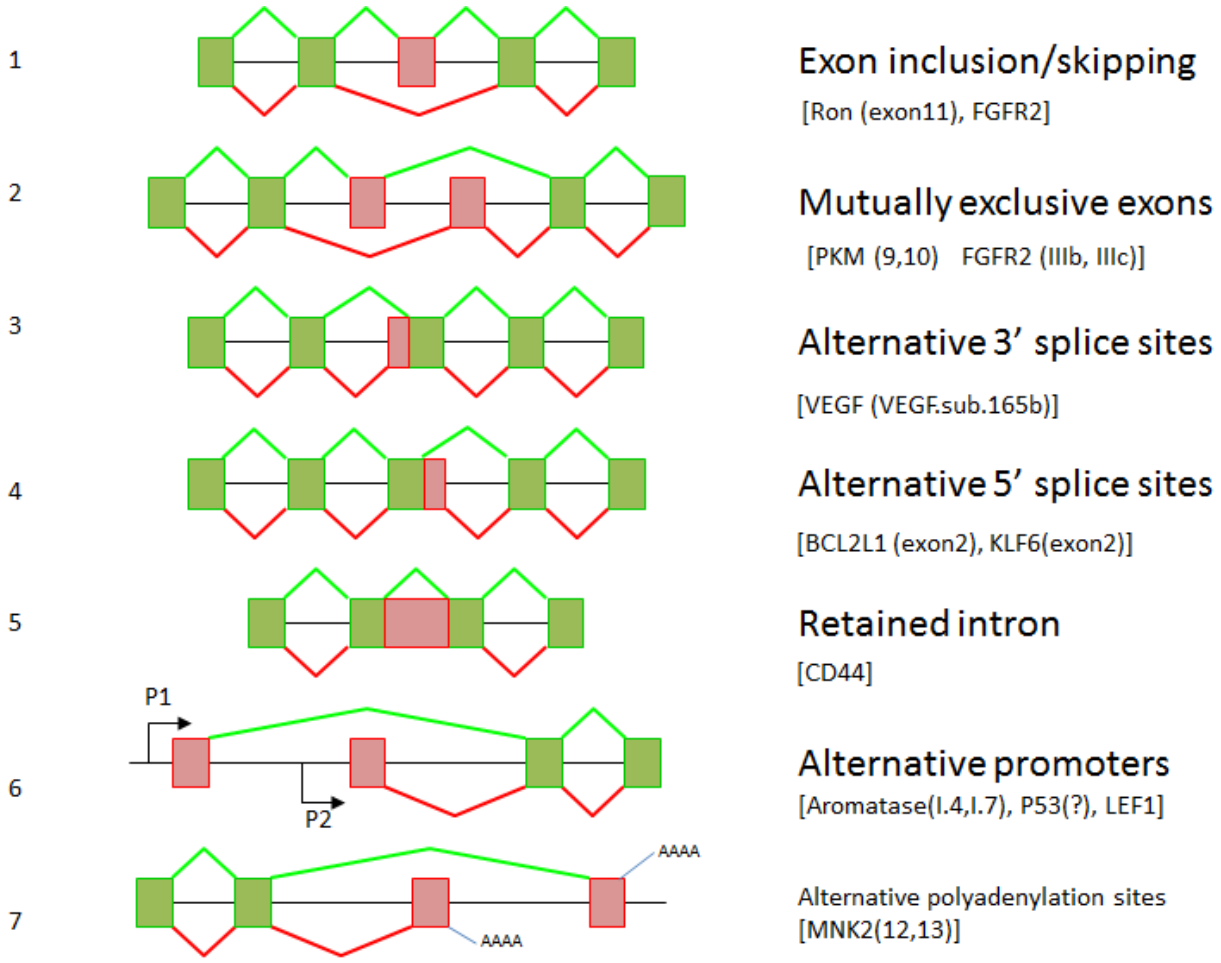

Figure 1.1 Common modes of alternative splicing

The exons are shown in green and red and the mode of splicing is shown with similar colors. In certain complex pre-mRNAs, more than one of these modes of splicing could take place in the same transcript. [Adaptated from Cartegni, Chew and Krainer, Nature Review Genetics, 2002,(Cartegni et al., 2002)]

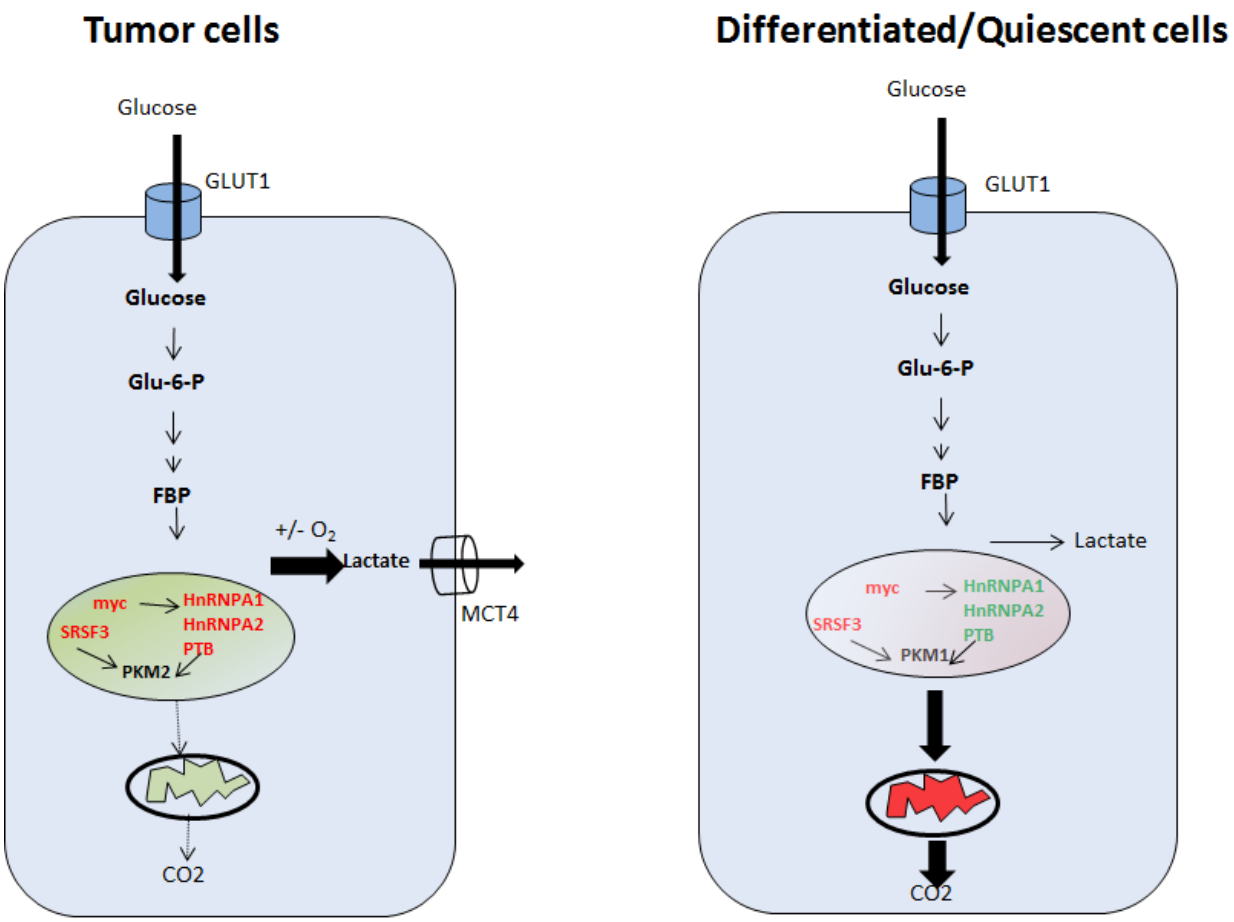

Figure 1.2 Schematic representation of the Warburg effect in tumor and differentiated cells. In differentiated tissues, glucose is metabolized to pyruvate via glycolysis, and then completely oxidizes most of that pyruvate in the mitochondria to CO_2 during the process of oxidative phosphorylation. Tumor cells, regardless of whether oxygen is present or not, can redirect the pyruvate generated by glycolysis away from mitochondrial oxidative phosphorylation by generating lactate (aerobic glycolysis). HnRNPs, SR proteins and likely other factors regulate the balance of expression of the splicing isoforms of PK-M.

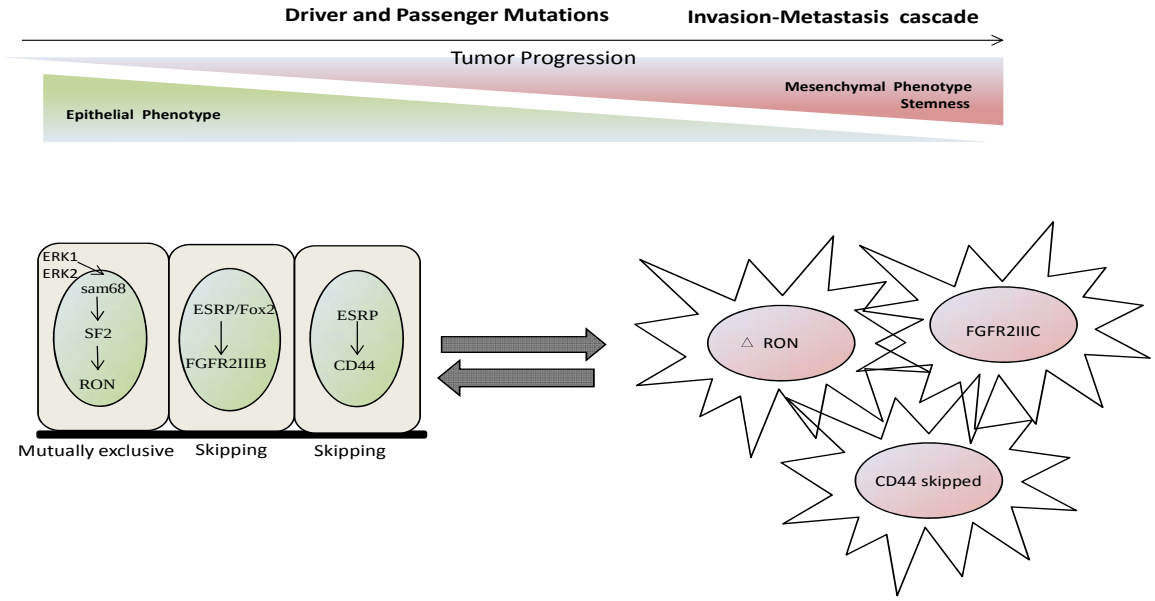

Figure 1.3 Alternative splicing changes during the Epithelial to Mesenchymal Transition. Epithelial (left) and mesenchymal (right) splicing events that directly influence EMT are depicted. SRSF1 promotes exon 11 skipping of the Ron proto-oncogene to produce a constitutively active isoform (ΔRon) that imparts invasive properties. SRSF1 levels are dynamically controlled during EMT through AS-NMD by another splicing factor, Sam68. Epithelial cell-derived soluble factors repress ERK activity, thereby inhibiting Sam68 phosphorylation, which reduces SFRS1 levels through increased AS-NMD. ESRP1 downregulation leads to a switch from CD44(v)ariant to CD44(s)kipped isoforms that is crucial for EMT. Mutually exclusive splicing of fibroblast growth factor receptor 2 (FGFR2) exons IIIb and IIIc is regulated by multiple splicing factors in communication with chromatin modifications. ESRP proteins inhibit exon IIIC, whereas RBFOX2 promotes exon IIIb inclusion in epithelial cells. PTB is expressed similarly in mesenchymal and epithelial cells, but suppresses exon IIIb specifically in mesenchymal cells.

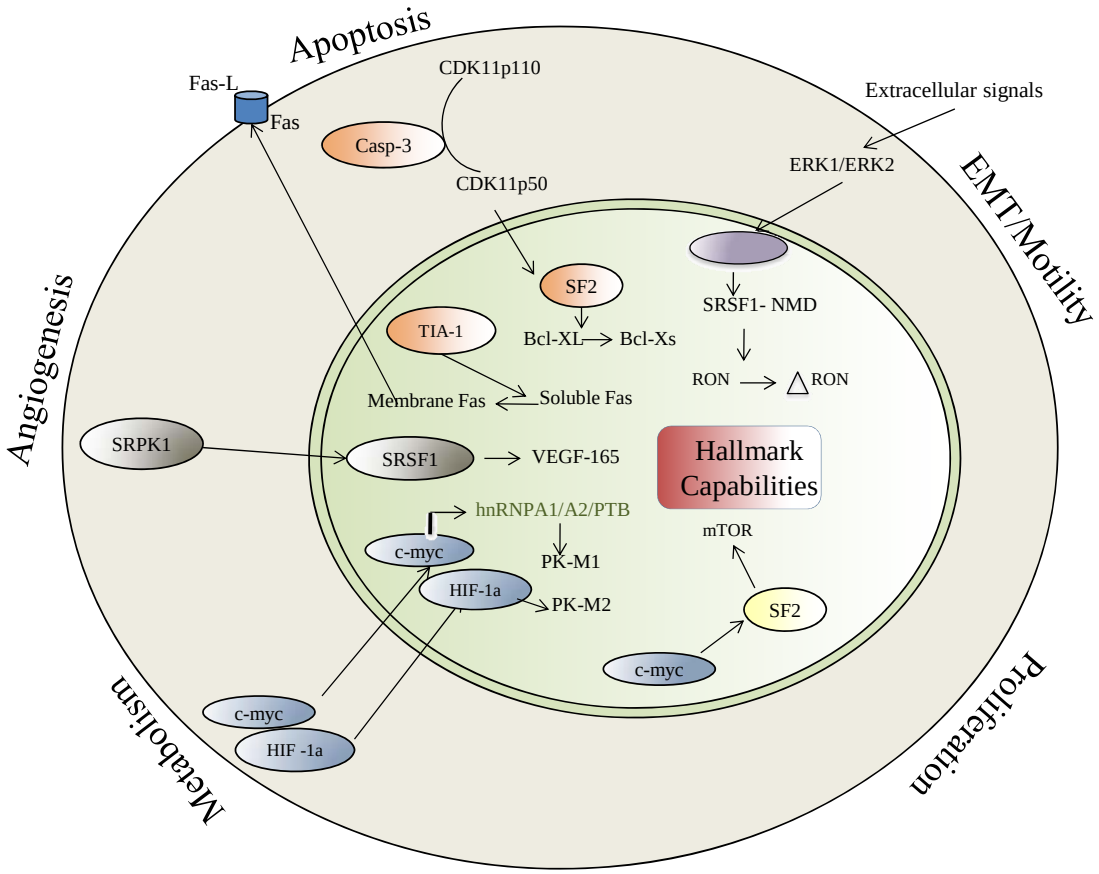

Figure 1.4 Splicing regulations in the context of the hallmarks of cancer

Illustration depicting the hallmarks of tumor progression, in which alternative splicing pathways play an important role. Active research is ongoing in the various aspects of cancer, investigating the role of alternative splicing in giving rise to proteins that act synergistically or antagonistically with each other.

Chapter 2

The alternative splicing repressors hnRNP A1/A2 and PTB influence pyruvate kinase isoform expression and cell metabolism

2.1 Abstract

Cancer cells preferentially metabolize glucose by aerobic glycolysis, characterized by increased lactate production. This distinctive metabolism involves expression of the embryonic M2 isozyme of pyruvate kinase, in contrast to the M1 isozyme normally expressed in differentiated cells, and it confers a proliferative advantage to tumor cells. The M1 and M2 pyruvate kinase isozymes are expressed from a single gene through alternative splicing of a pair of mutually exclusive exons. We measured the expression of M1 and M2 mRNA and protein isoforms in mouse and human tissues, tumor cell lines, and during terminal differentiation of muscle cells, and show that alternative splicing regulation is sufficient to account for the levels of expressed protein isoforms. We further show that the M1-specific exon is actively repressed in cancer cell lines—although some M1 mRNA is expressed in cell lines derived from brain tumors—and demonstrate that the related splicing repressors hnRNP A1 and A2, as well as the polypyrimidine-tract-binding protein PTB, contribute to this control. Downregulation of these splicing repressors in cancer cell lines using shRNAs rescues M1 isoform expression and decreases the extent of lactate production. These findings extend the links between alternative splicing and cancer, and begin to define some of the factors responsible for the switch to aerobic glycolysis.

2.2 Introduction

Cancer cells exhibit a metabolic phenotype characterized by increased glycolysis with lactate generation, regardless of oxygen availability—a phenomenon termed the Warburg effect. Recent work demonstrated that expression of the type II isoform of the pyruvate kinase-M gene (*PKM2*, referred to here as PK-M) is a critical determinant of this metabolic phenotype, and confers a selective proliferative advantage to tumor cells in vivo(Christofk et al., 2008c). This finding adds to the growing body of evidence that alterations in alternative pre-mRNA splicing play important roles in different aspects of cancer progression (Grosso et al., 2008; Karni et al., 2007).

Pyruvate kinase (PK) is the enzyme that catalyzes the final step in glycolysis, generating pyruvate and ATP from phosphoenolpyruvate and ADP (Dombrauckas et al., 2005). The resulting pyruvate can be converted to lactate or it can be incorporated into the TCA cycle to drive oxidative phosphorylation. PK is encoded by two paralogous genes, each of which is alternatively spliced, such that four PK isoforms are expressed in mammals. The L and R isozymes, derived from the *PKLR* gene, show tissue-specific expression in the liver and red-blood cells, respectively. They have different first exons, defined by tissue-specific promoters (Noguchi et al., 1987). The *PKM2* (PK-M) gene consists of 12 exons, of which exons 9 and 10 are alternatively spliced in a mutually exclusive fashion to give rise to the PK-M1 and PK-M2 isoforms, respectively (Noguchi et al., 1986). Exons 9 and 10 each encode a 56 amino acid variable segment that confers distinctive properties to the regulation and activity of PK-M1 and PK-M2 enzymes; as a result, PK-

M1 is constitutively active, whereas the activity of PK-M2 is allosterically regulated by fructose-1,6-bisphosphate levels and interaction with tyrosine-phosphorylated proteins (Christofk et al., 2008d).

The ability of PK-M2 activity to be regulated is thought to provide a mechanism for cells to control the availability of metabolites for anabolic processes, and to confer a proliferative advantage during tumorigenesis (Christofk et al., 2008d). Despite increasing evidence demonstrating the significance of PK-M2 isoform expression in cancer-cell metabolism and tumorigenesis, the mechanisms governing alternative splicing of the PK-M gene are not understood. PK-M2 is expressed in a range of cancer cells, as well as in fetal and undifferentiated adult tissues, whereas PK-M1 is expressed predominantly in terminally differentiated tissues (Christofk et al., 2008c; Christofk et al., 2008d).

Alternative splicing involving pairs of mutually exclusive exons represents only ~2% of all alternative splicing events in human genes (Chacko and Ranganathan, 2009). In terms of gene structure, the regulated exons in such genes are often closely related in sequence—as in the case of PK-M exons 9 and 10—indicating that they originally arose by exon duplication (Letunic et al., 2002a). Well characterized examples of this alternative splicing pattern in mammals include the tropomyosins, fibroblast growth factor receptor 2, and α-actinin. Although some of the trans-acting factors involved in the recognition of individual mutually exclusive exons in these genes have been identified, it remains unclear how these pairs of exons are coordinately regulated in a way that maintains their mutually exclusive properties(Smith, 2005).

We have begun to dissect the molecular mechanisms underlying PK-M2 alternative splicing regulation. Previous work implicated the splicing-repressor paralogs PTB and nPTB in the repression of exon 9 (Spellman et al., 2007). In addition, other splicing repressors, such as hnRNPA1 and hnRNPA2, and activators, such as SF2/ASF, have been implicated in oncogenic transformation (Grosso et al., 2008; Karni et al., 2007), and hence could potentially play a role in PK-M alternative splicing. Here we characterize the expression of PK-M isoforms at the mRNA and protein level in primary tissues and cancer cell lines, as well as during terminal differentiation of muscle cells in culture. We show that hnRNPA1/A2, in addition to PTB, repress the use of exon 9, such that knocking down expression of these splicing repressors allows expression of PK-M1, accompanied by a decrease in lactate production.

2.3 RESULTS

2.3.1 Relative PK-M1 and PK-M2 expression in tissues and cell lines correlates with hnRNPA1/A2 and PTB expression.

Proliferating cells and cancer cells preferentially express PK-M2 over PK-M1 at the protein level (Christofk et al., 2008c; Mazurek et al., 2005). To determine if the expressed protein isozymes are a direct reflection of differences in alternative splicing—as opposed to, e.g., being affected by mRNA stability or translational control—we measured the levels of mRNA and protein isoforms expressed in various tissues and cell lines. Representative organs/tissues isolated from adult mice were perfused with saline, and total protein and RNA were isolated and analyzed. The relative expression of PK-M1

and PK-M2 protein isoforms was organ/tissue-specific: brain and skeletal muscle preferentially expressed PK-M1, whereas spleen and lung expressed mainly PK-M2, as detected by western blotting with isoform-specific antibodies (Fig. 1*A*). As previously reported (Christofk et al., 2008c), several human cell lines expressed PK-M2 protein with no detectable PK-M1 (Fig. 1*B*). Among the cell lines tested, however, two brain-tumor-derived cell lines, namely U-118MG and A-172 glioblastoma cells, expressed detectable levels of PK-M1 protein, in addition to PK-M2, reminiscent of the protein pattern in mouse brain, where both isoforms are also readily detectable (cf. Fig. 1*B*, 1*A*).To accurately measure the relative levels of PK alternatively spliced mRNA isoforms, we simultaneously detected both isoforms by radioactive RT-PCR with a single pair of primers corresponding to the flanking constitutive exons 8 and 11. Because exons 9 and 10 are identical in length (167 nt), the resulting cDNA amplicons were digested with restriction enzymes that cleave either exon 9 or 10 to distinguish the two isoforms (Fig. 1*C*; see also Takenaka et al., 1996). PK-M1 mRNA was the predominant isoform in striated muscle and brain—tissues that are enriched in terminally differentiated, non-proliferating cells. In contrast, PK-M2 mRNA was the major isoform in lung and spleen, presumably reflecting the abundance of proliferating cells in these organs. Similar results were obtained using total RNA harvested from human autopsy tissues (muscle, brain, lung and spleen; data not shown). PK-M2 mRNA was invariably the major isoform in all cancer or transformed cell lines we assayed, consistent with the previous finding that PK-M2 expression at the protein level is strongly correlated with, and facilitates, proliferation and tumorigenesis (Christofk et al., 2008c). However, PK-M1 mRNA was

readily detectable in brain-tumor-derived cancer cell lines, including glioblastoma (U-118MG and A-172) and neuroblastoma (SK-N-BE) cell lines. This finding is consistent with PK-M1 protein being detectable in U-118MG cells and to a lesser extent in A-172 cells (Fig. 1*B*). In general, we observed a strong correlation between PK-M1/M2 isoform ratios measured at the protein and mRNA levels, in both tissues and cell lines.

To facilitate studies of the mechanism underlying the PK-M2 to PK-M1 isoform switch during terminal differentiation, we examined several established systems for cell differentiation in culture. We found that proliferating mouse C2C12 myoblasts induced to terminally differentiate into myotubes (Kislinger et al., 2005)switched protein and mRNA isoform expression from almost exclusively PK-M2 to predominantly PK-M1 (Fig. 2). Consistent with PK-M2 being the predominant isoform in proliferating cells, and PK-M1 being the predominant isoform in muscle (Fig. 1*A*), this switch in PK-M isoform accompanied the morphological differentiation of the C2C12 myoblasts into myotubes (Fig. 2*A*). Normalizing to total PK-M protein expression, it is readily apparent that there was a pronounced increase in PK-M1 upon differentiation, at the expense of the PK-M2 isoform (Fig. 2*B*). Likewise, at the mRNA level, the proportion of the M1 isoform changed from 5% to 55% over a differentiation time course (Fig. 2*C*).

We also measured the protein levels of representative alternative splicing factors, including some known to have oncogenic activities (Grosso et al., 2008). In the C2C12 differentiation model, as well as in mouse or human tissues and cancer cell lines, we observed a correlation between high levels of the alternative splicing factors hnRNP

A1/A2 and PTB, and reduced expression of the PK-M1 isoform (Fig. 2*B*,*D*,*E*). In contrast, there was little or no change in several other splicing factors, such as SF2/ASF and CUG-BP1 (Fig. 2B). U-118MG and A-172 cells, which expressed detectable levels of PK-M1, both at mRNA and protein levels (Fig. 1B, E), had less hnRNP A1/A2 and PTB compared to HeLa, HEK293, and SK-N-BE cells, whereas SF2/ASF was expressed at similar levels in these cell lines (Fig. 2*D*). Both hnRNP A/B and PTB (also known as hnRNP I) protein family members are well characterized splicing repressors, which led us to hypothesize that these factors might be partly responsible for repressing the use of exon 9 during pre-mRNA splicing.

2.3.2 Blocking the 3' splice site of exon 10 causes abnormal skipping of both exons 9 and 10.

To determine if exon 9 is actively repressed in cancer cell lines, or simply fails to compete effectively with exon 10, we blocked the 3' or 5' splice sites of exon 10 using 2'-*O*-methyl, phosphorothioate antisense oligonucleotides complementary to these regions (16)(Fig. 3*A*). The oligonucleotides were transfected into HEK293 cells and the endogenous PK mRNA isoforms were analyzed by radioactive RT-PCR (Fig. 3*B*). As expected, use of exon 10 was partially inhibited by the antisense oligonucleotides. However, in addition to increased use of exon 9 (PK-M1 isoform), we observed an abnormal mRNA arising from skipping of both mutually exclusive exons. These results indicate that even with reduced use of exon 10, there is residual repression of exon 9 use in HEK293 cells (as well as in HeLa and A-172 cells; data not shown).

2.3.3 hnRNP proteins repress exon 9 in a gliobloastoma cell line.

To address whether specific hnRNP proteins are responsible for repression of exon 9, we generated stable cell lines expressing shRNAs directed against hnRNP A1, A2, or PTB (Fig. 4). We chose A-172 glioblastoma cells for this analysis, both because they already express some PK-M1 (Fig. 1*B*,*E*) and because they tolerated simultaneous stable knockdown of hnRNP A1 and A2, in contrast to other cells we examined (data not shown). We achieved ~65% knockdown of hnRNP A1 and ~50% knockdown of hnRNP A2 (Fig. 4*A*). Although individual knockdown of these proteins—which are closely related in structure and function (Mayeda and Krainer, 1992)—had little effect, the combined knockdown elicited a ~6-fold increase in PK-M1 protein (Fig. 4*A*) and ~5-fold increase in PK-M1 mRNA (Fig. 4*B*). PTB or PTB+nPTB siRNA-knockdown in HeLa cells was previously shown by quantitative 2g-gel proteomics to decrease total PK-M expression (Spellman et al., 2007). Although the PK-M1 and PK-M2 spots could not be resolved, RT-PCR revealed a ~4-fold increase in the PK-M1/M2 ratio. We stably expressed PTB shRNA in A-172 cells and performed western blotting and radioactive RT-PCR analyses as above, and detected a ~3-fold increase in PK-M1 protein and mRNA (Fig. 4*C*,*D*). Taken together, these results suggest that hnRNPA1/A2 and PTB directly or indirectly mediate active repression of exon 9 in cancer cells.

2.3.4 Knockdown of splicing repressors inhibits lactate production in a glioblastoma cell line.

To test whether knockdown of hnRNP A1/A2 or PTB, which results in an increase in the PK-M1/PK-M2 protein ratio, is sufficient to affect cancer-cell metabolism, we measured the extent of lactate production in stable-knockdown versus control A-172 cells (Fig. 5). Remarkably, we observed a >2-fold decrease in lactate production upon combined knockdown of hnRNP A1/A2, and a ~1.5-fold reduction upon knockdown of PTB.

2.4 Discussion

We have demonstrated that down-regulation of the splicing repressors hnRNP A1/A2 and PTB relieves repression of PK-M exon 9 inclusion, resulting in higher levels of PK-M1. Both types of hnRNP proteins have been implicated in cancer (Grosso et al., 2008; Karni et al., 2007; Venables, 2006), consistent with their ability to promote expression of the pro-tumorigenic PK-M2 isoform. hnRNP A1 and A2 are closely related proteins encoded by two separate genes (*HNRNPA1* and *HNRNPA2B1*), which express additional minor isoforms (He and Smith, 2009); they are splicing repressors that typically, but not always, recognize exonic splicing silencer elements, and once bound to these elements they can spread along the RNA through cooperative interactions and interfere with the binding of spliceosomal components or activator proteins (Okunola and Krainer, 2009). PTB (hnRNP I) is also an abundant RNA-binding protein that binds to polypyrimidine tracts, such as those present at or upstream of 3' splice sites, and it can regulate alternative splicing by creating a zone of silencing (Wagner and Garcia-Blanco, 2001).

Previous analysis of PK-M splicing using a minigene suggested that inclusion of exon 10 is the default splicing pattern in proliferating cells (Takenaka et al., 1996). This is consistent with our observation that blocking either of the splice sites of exon 10 by means of antisense oligonucleotides leads to simultaneous skipping of both exons 9 and 10, rather than to efficient derepression of exon 9. We have shown that hnRNP A1/A2 and PTB are responsible for, or contribute to the repression of exon 9 in cells that express PK-M2. Although preferred motifs recognized by these repressors are known, we have not determined yet whether hnRNP A1/A2 and PTB regulate PK-M alternative splicing directly, and if so, where the relevant binding sites are located. However, two recent studies reported that PTB can be crosslinked in cells to several regions in intron 8 (Xue et al., 2009) and hnRNP A1 can bind in vitro to an RNA fragment encompassing the 5' splice site of intron 9 (David et al., 2010). Further studies of *cis*-acting elements within and flanking both exon 9 and exon 10 will be necessary to uncover how individual cells achieve predominant or exclusive expression of only one of the two isoforms.

Considering that downregulation of hnRNP A1/A2 or PTB achieved only a 3- to 5-fold increase over the low basal level of exon 9 inclusion, accompanied by a modest increase in PK-M1 protein with the persistence of PK-M2 protein, additional factors likely contribute to the usually tight control of PK-M alternative splicing. As in other instances of regulated alternative splicing [reviewed in (Black, 2003)], combinatorial control by numerous RNA-binding proteins is likely operative for the PK-M gene.

The effects we observed on lactate production following combined knockdown of hnRNP A1/A2 are likely attributable to more than just the switch in PK-M isoform expression. hnRNP A1/A2 knockdown resulted in some PK-M1 protein expression, although cells continued to express appreciable amounts of PK-M2. A nearly complete switch of PK-M2 to PK-M1 using shRNA knockdown and isoform-specific rescue constructs resulted in at most a 30% decrease in lactate production (Christofk et al., 2008c). Thus, the >2-fold reduction in lactate production we observed following combined hnRNP A1+A2 knockdown probably reflects changes in alternative splicing that presumably occur in addition to those involving PK-M1/M2.

Aside from PK-M, additional genes important for cancer-cell metabolism are alternatively spliced. For instance, the bifunctional enzyme phosphofructokinase/ bisphophatase B3 gene (*PFKFB3*) is a key regulator of glycolysis with preferential expression in cancer cells (Atsumi et al., 2002). The kinase activity of this gene product generates fructose 2,6 bisphosphate (F2,6BP), which activates phosphofructokinase-1, a rate-limiting and regulatory control point of glycolysis, and indirectly leads to PK-M2 activation. In addition, HIF-1α and oncoproteins such as Ras activate *PFKFB3*, leading to increased F2-6BP in tumors (Atsumi et al., 2002). Multiple alternatively spliced isoforms of *PFKFB3* exist, though their distinctive properties have not been characterized. There is cross-talk between cell-energy sensing and pyruvate-kinase regulation of this enzyme, suggesting that regulation of splicing to generate specific isoforms may be part of a larger metabolic program to promote proliferative metabolism(Bando et al., 2005). We speculate that hnRNP A1/A2 might modulate the expression of other alternatively

spliced metabolic genes, in addition to PK-M, that collectively account for the large decrease in lactate production following double knockdown of hnRNP A1 and A2.

2.5 MATERIALS AND METHODS

2.5.1 Cells and transfections. HeLa, HEK293, U-118MG, A-172, SK-N-BE, and C2C12 cells were grown in DMEM, supplemented with 10% (v/v) FBS, penicillin and streptomycin. To induce differentiation, near-confluent C2C12 cultures were washed 3X with PBS and maintained for 7 days in medium containing 2% (v/v) horse serum, penicillin, and streptomycin. To select for a more homogenous differentiated culture, myotubes were treated for 4 days with 25 μM cytosine β-D-arabinofuranoside hydrochloride (AraC) (Sigma) beginning on day 7 after inducing differentiation. To generate stable transductant pools, A-172 cells were infected with LMP-puro or LMP-hygro retroviral vectors(Karni et al., 2007). The medium was replaced 24 h after infection, and starting 1 day later, infected cells were selected with puromycin (2 μg ml^{-1}) for 3 days, or hygromycin (200 μg ml^{-1}) for 7 days. In the case of double infections, cells were treated with hygromycin for 7 days after selection with puromycin for 3 days. Short hairpin RNA sequences were as follows: hnRNPA1 - 5' TGCTGTTGACAGTGAGCGAAGGTTACAACAGATTTGTGAATAGTGAAGCCACAGATGTATTCAC AAATCTGTTGTAACCTGTGCCTACTGCCTCGGA-3'; hnRNPA2 – 5' TGCTGTTGACAGTGAGCGCGCCATGGGCTTCACTGTATAATAGTGAAGCCACAGATGTATTATA CAGTGAAGCCCATGGCATGCCTACTGCCTCGGA-3'; PTB – 5'-

CGCGTCCCCGCAGTTGGAGTGACCTTACTTCAAGAGAGTAAGGTCACTTCAGCTGCTTTTTGGA
AAT-3'.

2.5.2 Immunoblotting. Cells were lysed in SDS and total protein concentration was measured). 30 μg of total protein from each lysate was separated by SDS-PAGE and transferred onto a nitrocellulose membrane. This was followed by blocking with 5% milk in TBST, probing with the indicated antibodies, and quantitation using an Odyssey infrared-imaging system (LI-COR Biosciences). Primary antibodies were: β-catenin (Abcam rAb 6302, 1:4000); tubulin (Genscript rAb, 1:5000); SF2/ASF (mAb AK96 culture supernatant, 1:100); hnRNP A1 (Abcam mAb 4B10, 1:1000 or mAb UP1-55 culture supernatant); hnRNP A2 (Abcam mAb DP3, 1:1000); hnRNP A1/A2 (A1/UP1-62 culture supernatant, 1:20); PTB (mAb SH54 culture supernatant, 1:100 (30) or Abcam rAb83897, 1:1000); CUG-BP1 (Abcam mAb 3B1, 1:500); PK-M2 (rabbit, 1:500) and PK-M1 (rabbit, 1:2,000)(1); total PK-M (Abcam gAb6191, 1:1,000). Secondary antibodies were IRdye 800 or 680 anti-rabbit, anti-mouse, or anti-goat (LI-COR Biosciences, 1:10,000).

2.5.3 RT-PCR assays. 2 μg of total RNA was extracted from freshly dissected, saline-perfused mouse tissues, and from cell lines, using Trizol reagent (Invitrogen). Contaminating DNA was removed by treatment with DNase I (Promega). Reverse transcription was carried out using ImPromp-II reverse transcriptase (Promega). Semiquantitative PCR using AmpliTaq polymerase (Applied Biosystems) was performed

by including [α-^{32}P]-dCTP in the reactions. The mouse- and human-specific primer sets anneal to exons 8 and 11, and their sequences are as follows: hPKMF: 5'-AGAAACAGCCAAAGGGGACT-3'; hPKMR: 5'-CATTCATGGCAAAGTTCACC-3' and mPKMF: 5'-ATGCTGGAGAGCATGATCAAGAAGCCACGC-3'; mPKMR: 5'-CAACATCCATGGCCAAGTT-3'. After 22 amplification cycles, the reactions were separated into four aliquots for digestion with NcoI, PstI (New England Biolabs), both, or neither. The products were analyzed on a 5% native polyacrylamide gel, visualized by autoradiography, and quantitated on a FUJIFILM FLA-5100 phosphoimager (Fuji Medical Systems) using Multi Gauge software Version 2.3 (Fujifilm). The %M1 mRNA was calculated using the GC-content-normalized intensities of the top undigested band (M1) and the bottom two digested bands (M2) in the PstI-digest lanes.

2.5.4 Antisense oligonucleotides. 2'-*O*-methyl phosphorothioate oligonucleotides were purchased from TriLink Biotechnologies, and purity was confirmed by gel electrophoresis. 3' splice site antisense oligonucleotide: CGGGCAATCTAGGGGAGCAAC; 5' splice site antisense oligonucleotide: CCGCCTCCTACCTGCCAGAC. HEK293 cells were plated at 50,000 cells per well in 6-well plates in DMEM supplemented with 10% fetal calf serum, 500 units/ml penicillin, and 0.1 mg/ml streptomycin. After allowing cells to adhere, they were transfected with 500 nM oligonucleotide using Lipofectamine 2000 (Invitrogen). After 4 h at 37 °C, the transfecting mixture was replaced with fresh medium with serum. After 48 hr, the cells were washed three times with PBS, trypsinized,

counted, and extracted RNA was analyzed by radioactive RT-PCR as described above.

2.5.5 Lactate assays. Lactate production was measured using a fluorescence-based assay kit (BioVision). Fresh medium was added to a 12-well plate of subconfluent cells and aliquots of media from each well were assessed 30 min later for the amount of lactate present. The cells were counted with a haemocytometer.

2.6 FIGURES AND LEGENDS

Figure 2.1 Protein and transcript expression patterns of pyruvate kinase M1/M2 isoforms in cells and tissues.

(A) Total adult-mouse organ/tissue homogenates were used for Western blotting with the indicated antibodies. rM1 and rM2: Flag-tagged purified recombinant human PK isoforms.

(B) Total cell lysates of five human cancer-cell lines were used for Western blotting with the indicated antibodies.

(C) Primers annealing to exon 8 and exon 11, respectively, were used to amplify mouse or human PK-M transcripts. The alternative exons that encode the distinctive segments of PK-M1 and PK-M2 are indicated in (black) and (gray), respectively. To distinguish between PK-M1 (exon 9 included) and PK-M2 (exon 10 included) isoforms, the PCR products were cleaved with NcoI, PstI, or both. There is an additional NcoI site (*) 11 bp away from the 3' end of mouse exon 11.

(D) Mouse organs were freshly dissected and perfused with saline. Total RNA was analyzed by radioactive RT-PCR followed by digestion with NcoI (N), PstI (P), or both enzymes (NP), plus an uncut control (U). Numbered bands are as follows: 1: Uncut M1 (502 bp); 2: uncut M2 (502 bp); 2*: M2 cleaved with NcoI in exon 11 (491 bp); 3: Pst1-cleaved M2 5' fragment (286 bp); 4: NcoI-cleaved M1 5' fragment (245 bp); 5: NcoI-cleaved M1 3' fragment (240 bp); 6: PstI-cleaved M2 3' fragment (216 bp); 7: PstI + NcoI-

cleaved M2 3’ fragment (205 bp). The %M1 was quantified from band 1 (M1) and bands 3 and 6 (M2) in each P lane.

(E) RT-PCR and restriction digest analysis of total RNA from the indicated human cell lines. The bands are numbered as for the mouse RT-PCR products, but the sizes are different because of the positions of the primers; the sizes are as follows: 1: 398 bp; 2: 398 bp; 3: 185 bp; 4: 144 bp; 5: 248 bp; 6: 213 bp. Note that the PK-M1 bands in the P and U lanes migrate slightly above the PK-M2 bands, which is also the case for the mouse PK-M1 transcripts.

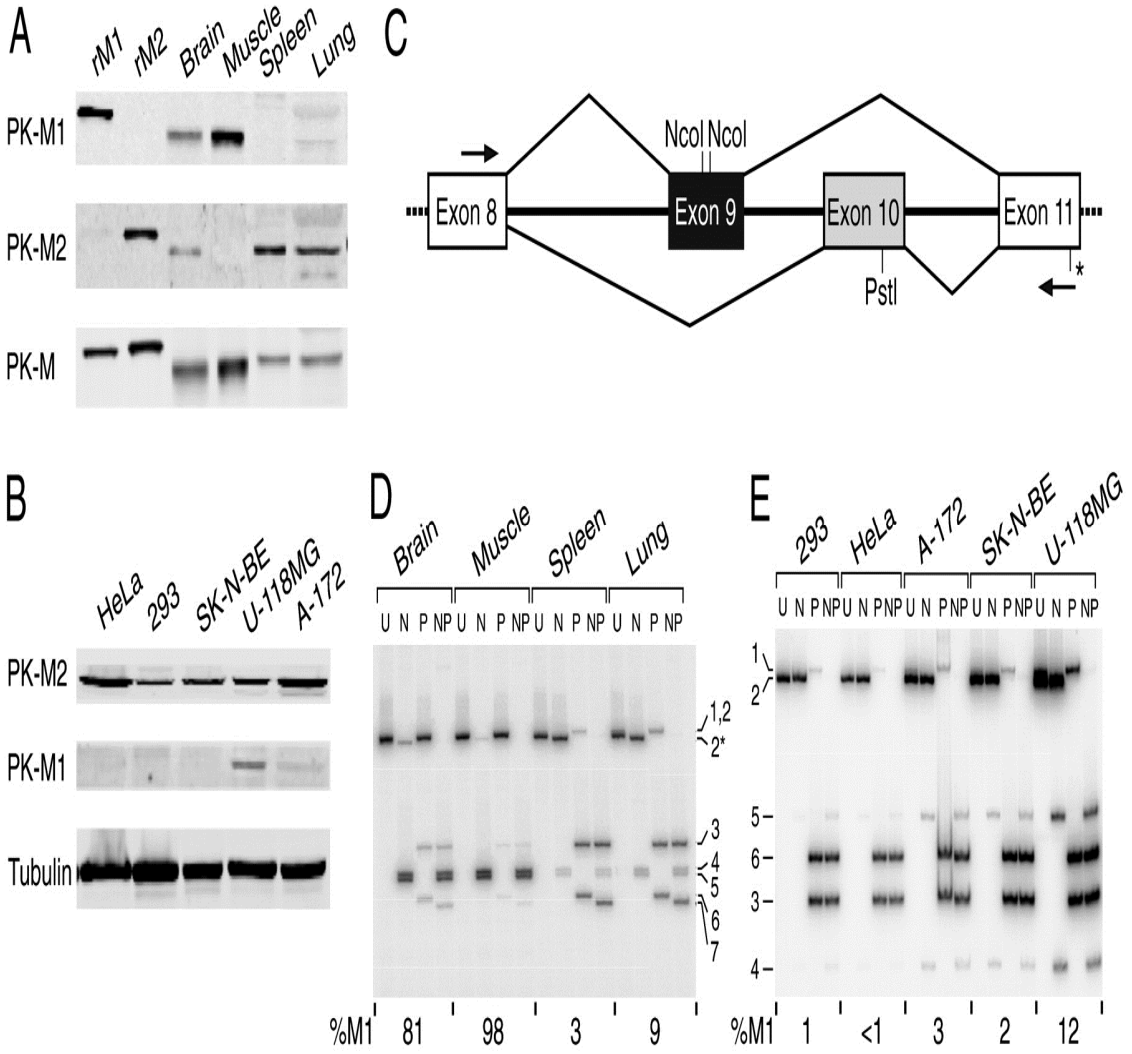
A
rM1
rM2
Brain
Muscle
Spleen
Lung
PK-M1
PK-M2
PK-M
C
NcoI NcoI
Exon 8
Exon 9
Exon 10
Exon 11
PstI
*
B
HeLa
293
SK-N-BE
U-118MG
A-172
PK-M2
PK-M1
Tubulin
D
Brain
Muscle
Spleen
Lung
U N P NP U N P NP U N P NP U N P NP
1,2
2*
3
4
5
6
7
%M1 81 98 3 9
E
293
HeLa
A-172
SK-N-BE
U-118MG
U N P NP U N P NP U N P NP U N P NP U N P NP
1
2
5
6
3
4
%M1 1 <1 3 2 12

Figure 2.2 Expression of pyruvate-kinase isoforms and selected splicing factors in cell lines and tissues.

*(A) Differentiation of mouse C2C12 myoblasts into myotubes. The left field shows proliferating myoblasts, and the right field shows cells after seven days in differentiation medium, when most of the cells have fused into myotubes.

*(B) Western blot of proliferating myoblasts versus AraC-treated myotubes with the indicated antibodies against selected splicing factors, β-catenin, total PK-M, and PK-M1 or PK-M2.

*(C) Radioactive RT-PCR analysis of PK-M1 and PK-M2 expression in C2C12 cells over a differentiation time course. Bands are numbered as in Fig. 1D.

(D) Total cell lysates of five human-tumor or transformed cell lines were used for Western blotting with the indicated specific antibodies. Tubulin was used as an internal control for loading. HeLa (cervical carcinoma); HEK293 (transformed embryonic kidney cells); SK-NB-E (neuroblastoma); U-118MG (glioma); A-172 (glioblastoma).

(E) Mouse tissues were analyzed as in Fig. 1A, with the indicated antibodies.

(* These experiments were done by Cynthia Clower, Cantley Laboratory)

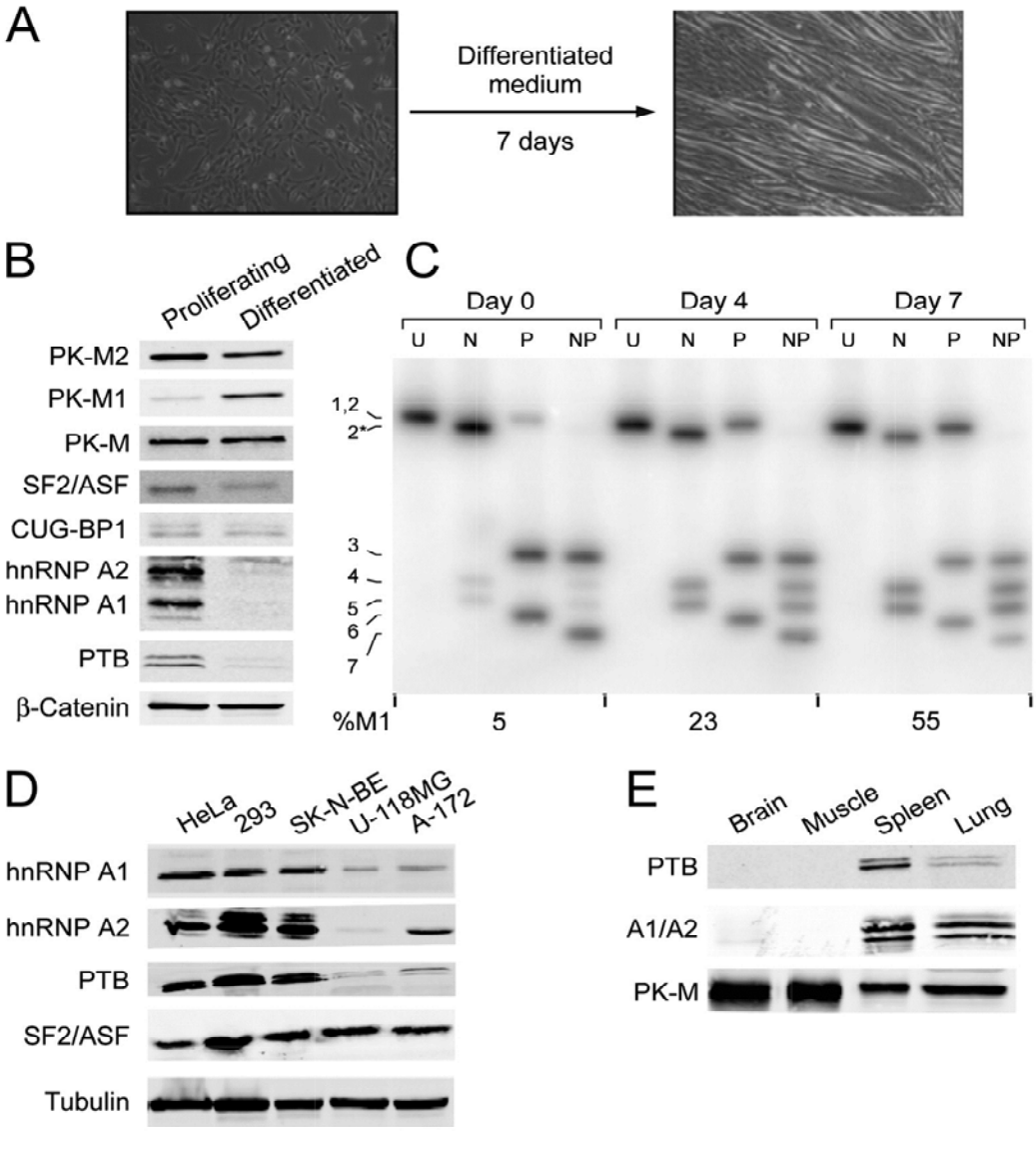
A
Differentiated medium
7 days
B
Proliferating
Differentiated
PK-M2
PK-M1
PK-M
SF2/ASF
CUG-BP1
hnRNP A2
hnRNP A1
PTB
β-Catenin
C
Day 0
Day 4
Day 7
U N P NP U N P NP U N P NP
1,2
2*
3
4
5
6
7
%M1
5
23
55
D
HeLa
293
SK-N-BE
U-118MG
A-172
hnRNP A1
hnRNP A2
PTB
SF2/ASF
Tubulin
E
Brain
Muscle
Spleen
Lung
PTB
A1/A2
PK-M

Figure 2.3 Exon 9 is partially rescued in HEK293 cells when exon 10 is blocked.

(A) Schematic representation of the strategy used to block exon 10 with 2′-O-methyl antisense oligonucleotides. The two arrows above exon 10 denote the oligonucleotides complementary to the 3′ splice site and 5′ splice site regions.

(B) Radioactive RT-PCR assay to measure PK-M1/PK-M2 levels after blocking each of the exon 10 splice sites with antisense oligonucleotides. An abnormal isoform arising from skipping of both exons 9 and 10 is indicated.

(C) Quantitation of multiple experiments. (Error bars show s.d.; n = 3; p-values: = ∗0.007; = ∗∗0.005; = ∗∗∗0.004; = ∗∗∗∗0.001; Student's paired t-test).

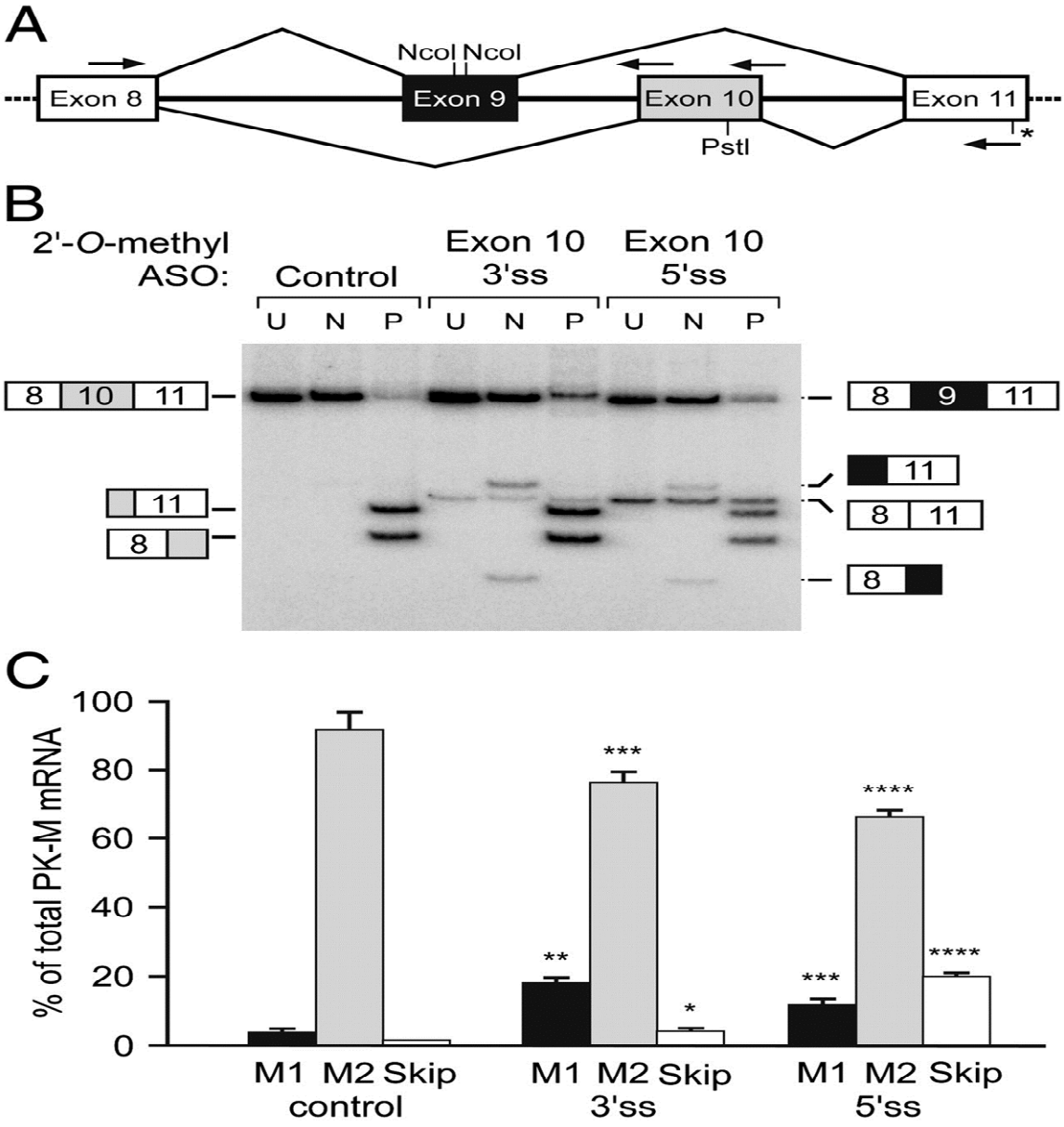
A
NcoI NcoI
Exon 8
Exon 9
Exon 10
Exon 11
PstI
*
B
2'-O-methyl ASO:
Control
Exon 10 3'ss
Exon 10 5'ss
U N P U N P U N P
8 10 11
11
8
8 9 11
11
8 11
8
C
% of total PK-M mRNA
100
80
60
40
20
0
**
***
*
***
****
****
M1 M2 Skip
control
M1 M2 Skip
3'ss
M1 M2 Skip
5'ss

Figure 2.4 Repression of exon 9 by hnRNP proteins.

(A) A-172 glioblastoma cells were transduced with retroviruses expressing hnRNPA1 and hnRNPA2 shRNAs. Total lysates were analyzed by Western blotting with the indicated antibodies. The histogram on the right shows the quantitation of multiple experiments by infrared-imaging (n = 4; error bars show s.d.; p = 0.02 (M1); p = 0.005 (M2); p = 0.05 (A1); p = 0.01 (A2); Student's paired t-test)

(B) Analysis of PK -MRNA transcripts from the cells in (A) using radioactive RT-PCR and NcoI or PstI digestion. Bands are numbered as in Fig. 1E. The histogram on the right shows the quantitation from several experiments (error bars show s.d.; n = 4; p = 10-4 for the A1/A2 double-knockdown; Student's paired t-test)

(C) and (D) As in (A) and (B) but using shRNAs against PTB (hnRNP I). (C) The * on each side indicates the band corresponding to PK-M1. The histogram on the right shows the quantitation (n = 4; error bars show s.d.; p = 0.03 (M1); p = 0.01(M2); p = 0.03 (PTB); Student's paired t-test). (D) The histogram on the right shows the quantitation (error bars show s.d.; n = 3; p = 0.001; Student's paired t-test).

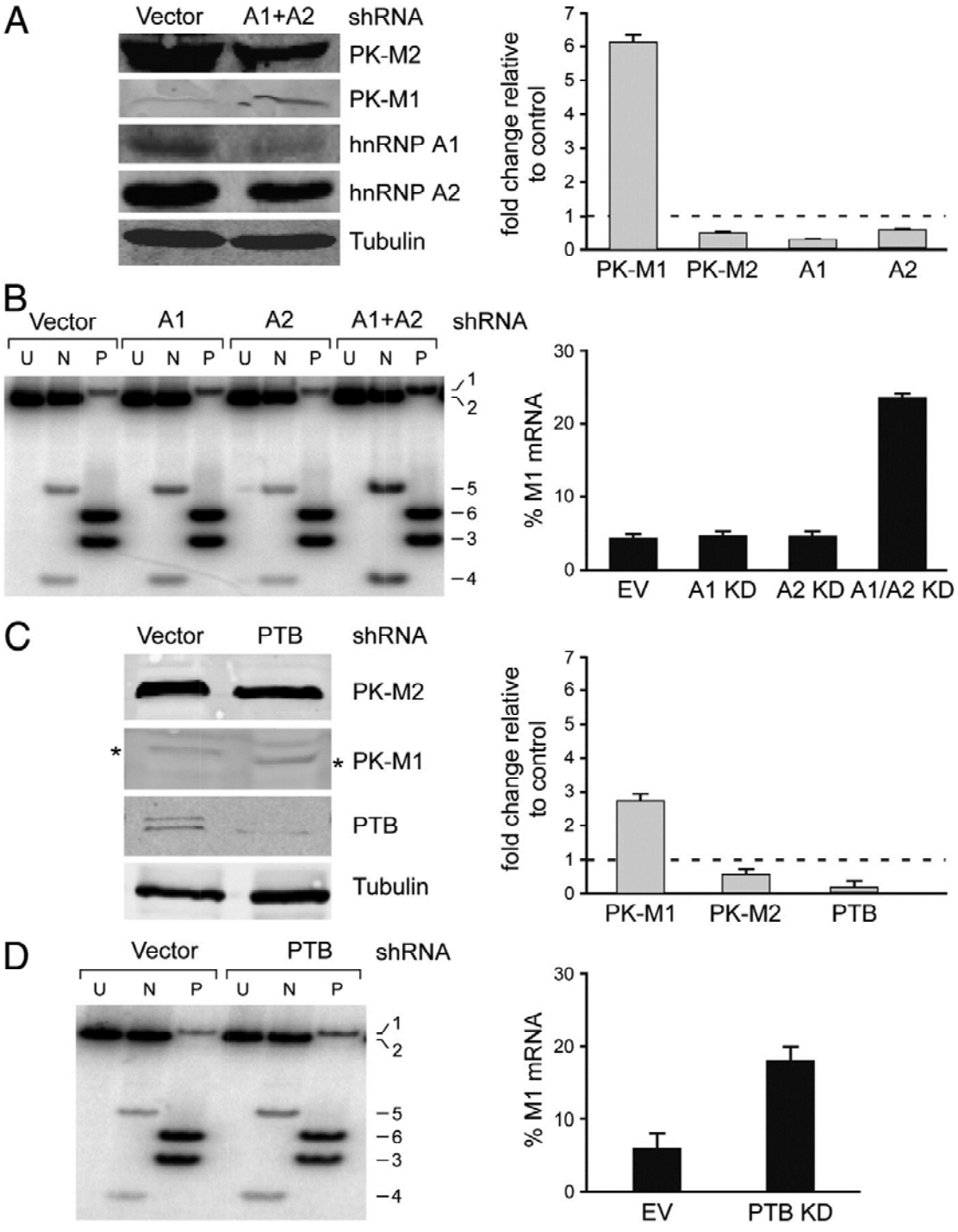
A
Vector
A1+A2
shRNA
PK-M2
PK-M1
hnRNP A1
hnRNP A2
Tubulin
fold change relative to control
PK-M1
PK-M2
A1
A2
B
Vector
A1
A2
A1+A2
shRNA
U N P U N P U N P U N P
1
2
5
6
3
4
% M1 mRNA
EV
A1 KD
A2 KD
A1/A2 KD
C
Vector
PTB
shRNA
PK-M2
PK-M1
PTB
Tubulin
fold change relative to control
PK-M1
PK-M2
PTB
D
Vector
PTB
shRNA
U N P U N P
1
2
5
6
3
4
% M1 mRNA
EV
PTB KD

Figure 2.5 Effect of splicing-repressor knockdown on metabolism of glioblastoma cells. Lactate production was measured in A-172 glioblastoma cells transduced with empty vector or with combined shRNAs against hnRNP A1 and A2, or against PTB. Error bars show s.d.; n = 12 for EV control, and n = 6 for A1/A2 ($p = 0.0034$) and PTB ($p = 0.014$) knockdowns; Student's paired t-test

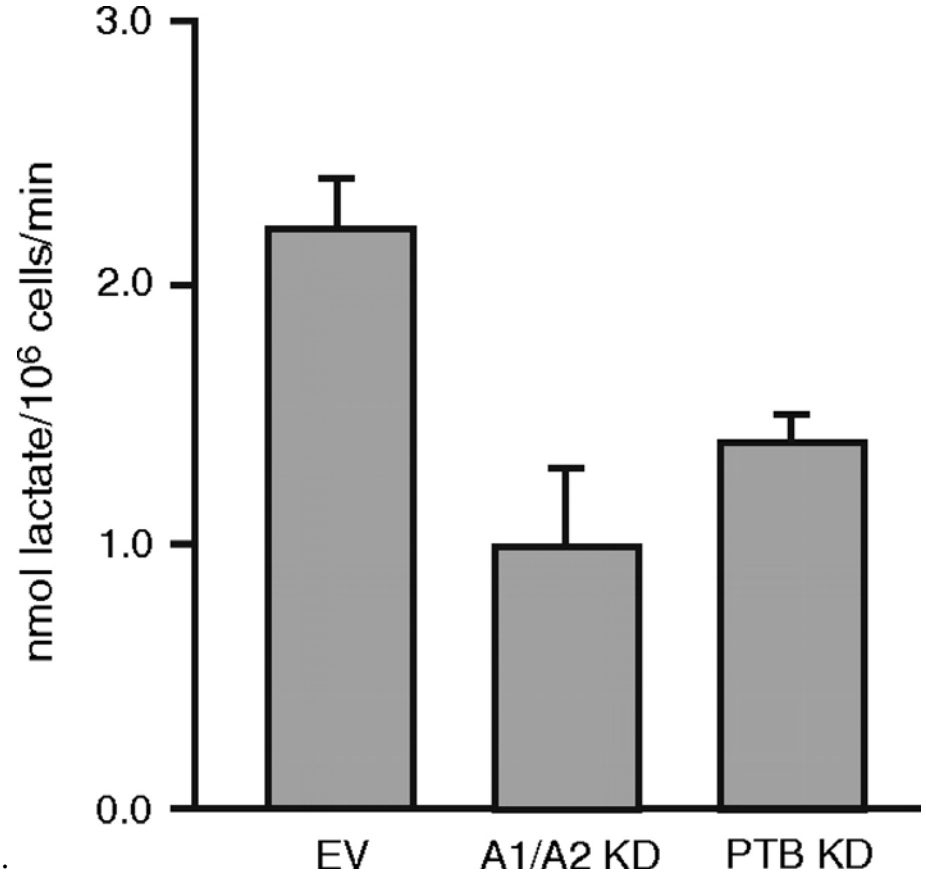
3.0
2.0
1.0
0.0
nmol lactate/10^6 cells/min
EV
A1/A2 KD
PTB KD

Chapter 3

Regulation of Pyruvate Kinase M Alternative Splicing by an Oncogenic SR Protein, SRSF3

SUMMARY

Cancer cells alter their metabolism to efficiently incorporate nutrients, such as glucose, into biomass. Alternative splicing of the pyruvate kinase M gene to generate the M2 isoform promotes aerobic glycolysis and tumor growth, and contributes to anabolic metabolism. Using biochemical, molecular, and bioinformatic approaches, we demonstrate that alternative splicing of *PK-M* is regulated by reciprocal effects on the mutually-exclusive exons 9 and 10, such that exon 9 is repressed and exon 10 is activated in cancer cells. Strikingly, exonic, rather than intronic, *cis*-elements are the key determinants of *PK-M* splicing isoform ratios in cancer cells (the above work is not discussed in details in my thesis). We identify the oncogenic SR protein SRSF3 as a regulator that recognizes an exonic splicing enhancer to activate exon 10 and mediate changes in glucose metabolism. These findings provide insights into the complex regulation of alternative splicing of a key regulator of the Warburg effect.

3.1 INTRODUCTION

Cancer cells exhibit a metabolic phenotype termed aerobic glycolysis, or the Warburg effect, characterized by increased glycolysis with lactate generation, regardless of oxygen availability (Vander Heiden et al., 2009). Expression of the type II isoform of the pyruvate-kinase-M gene (*PKM2*, referred to here as *PK-M*) mediates this metabolic phenotype, and confers a proliferative advantage to tumor cells *in vivo* (Christofk et al., 2008a).

Pyruvate kinase (PK) is the enzyme that catalyzes the final step in glycolysis, generating pyruvate and ATP from phosphoenolpyruvate and ADP (Dombrauckas et al., 2005). The *PK-M* gene consists of 12 exons, of which exons 9 and 10 are alternatively spliced in a mutually exclusive fashion to give rise to M1 and M2 isoforms, respectively (Noguchi et al., 1986). Exons 9 and 10 each encode a 56-amino-acid segment that confers distinctive properties to the regulation and activity of the PK-M isozymes. PK-M1 is constitutively active, whereas PK-M2 is allosterically regulated by fructose-1,6-bisphosphate levels and interaction with tyrosine-phosphorylated signaling proteins (Christofk et al., 2008a; Christofk et al., 2008b).

The growth-signal-mediated inhibition of *PK-M2* activity is thought to contribute to cancer-cell growth by decreasing carbon flux through the catabolic glycolytic pathway, allowing accumulated upstream intermediates to be shunted to anabolic pathways and thereby facilitating cell proliferation (Hitosugi et al., 2009). Consistent with this hypothesis, PK-M2 is expressed in a broad range of cancer cells, as well as in fetal and

undifferentiated adult tissues, whereas PK-M1 is expressed predominantly in terminally differentiated tissues (Christofk et al., 2008a; Clower et al., 2010a). Despite increasing evidence demonstrating the significance of PK-M2 isoform expression in cancer-cell metabolism and tumorigenesis, the mechanisms governing alternative splicing of the PK-M pre-mRNA are not well understood.

Alternative splicing involving pairs of mutually exclusive (ME) exons represents ~2% of all alternative splicing events in human genes (Chacko and Ranganathan, 2009). In terms of gene structure, the regulated exons in such genes are often closely related in sequence—as in the case of *PK-M* exons 9 and 10—indicating that they originally arose by exon duplication (Letunic et al., 2002b). Well characterized examples of this alternative splicing pattern in mammals include the tropomyosins, fibroblast growth factor receptor 2, and α-actinin (reviewed in Smith, 2005). Although some trans-acting factors involved in the recognition of ME exons in these genes have been identified, it remains unclear how these pairs of exons are coordinately selected in a way that maintains their ME properties (Smith, 2005). The mechanism underlying the ME splicing pattern of *PK-M* appears to be novel. For example, in contrast to other cases of ME splicing, doubly-spliced exon 9/exon 10 transcripts are not predicted to be degraded by nonsense mediated decay (Jones et al., 2001; Letunic et al., 2002b), and the length (401bp) and sequence of intron 9 rules out steric interference effects that could prevent double splicing due to the spacing of the branch site and the 5' splice site (5'ss) (Smith and Nadal-Ginard, 1989).

We have begun to dissect the molecular mechanisms underlying *PK-M2* alternative splicing regulation. Recently, we and others demonstrated that the exon-10-included M2 isoform is the default choice in cancer and proliferating cells, and also implicated two pairs of splicing-repressor paralogs—PTB/nPTB and hnRNPA1/A2—in repression of exon 9 as discussed above (Clower et al., 2010a; David et al., 2010). However, it remains unclear whether there are other repressors that also block the use of exon 9, and how exon 9 repression in turn promotes the splicing of exon 10.

To address these questions, Zhenxun Wang (another graduate student) constructed a *PK-M* minigene that recapitulates the splicing-regulatory features of the endogenous gene. Using this minigene and derivatives thereof, he demonstrated that exon 10 is activated in cancer cells independently of exon 9 repression. I performed knockdown of SRSF3 in cancer cells which was found to rescue *PK-M1* expression and a decrease in lactate production. Strikingly I also found that, simultaneous knockdown of the SRSF3 exon-10 activator and the exon-9 repressors hnRNPA1/A2 results in additive rescue of *PK-M1* expression in cancer cell lines. Since I have been focusing on trans-acting elements which regulate ME splicing of PK-M, in this chapter I will describe the results and methods performed by me without going into finer details of exon swapping and pull-down experiments.

3.2 RESULTS

3.2.1 Relative expression of PK-M2 in cancer cell lines correlate with SRSF3 expression.

SRSF3 is known to be overexpressed in ovarian cancers (He et al., 2004) and cervical cancer cell lines, whereas in normal cervical tissue, its expression is restricted to the basal proliferating layers (Jia et al., 2009). Moreover, overexpression of SRSF3 was recently found to be sufficient for transformation of NIH-3T3 immortal mouse fibroblasts (Jia et al., 2010), indicating that similar to its paralog, SRSF1 (Karni et al., 2007), SRSF3 is an oncoprotein. SRSF3 is also a downstream target of the oncogenic β-catenin/TCF-4 pathway in colorectal cancer cells (Gonçalves et al., 2008). Having the knowledge of the above information, to determine if there is a correlation between expression levels of SRSF3 and PKM-2, we measured the levels of mRNA and protein isoforms expressed in the brain (where there is very little PK-M2 expression) and various cancer cell lines. mRNA levels were measured using qPCR and I found that there was a general correlative trend in the expression pattern of PKM-2 and SRSF3. The cell lines that expressed PKM-2 only, noticeably had higher levels of SRSF3 too, whereas the cell lines that expressed lesser amounts of PKM-2, also showed decreased SRSF3 mRNA levels (Figure 3.6.1). I also measured the protein levels in the various cell lines using western blot analysis and found a similar trend. These results implied that there was indeed a direct correlation between exon 10 inclusion (PKM-2) and SRSF3 expression.

3.2.2 SRSF3 Affects Endogenous PK-M Splicing

To test whether SRSF3 could affect endogenous *PK-M* alternative splicing; I used knockdown and overexpression approaches, which, as expected, gave reciprocal effects. Knocking down SRSF3 in HEK-293 cells led to a 3-fold increase in PK-M1 at the mRNA level, which was also reflected at the protein level (Fig 3.6.2). Interestingly, knocking down SRSF3 additionally resulted in some double skipping of both exons 9 and 10—detected by additional cycles of PCR —consistent with the notion that SRSF3 promotes the definition of exon 10. As a reciprocal experiment, I overexpressed SRSF3 in the glioblastoma cell line A172 (Fig. 3.5), which expresses relatively high levels of PK-M1 (Clower et al., 2010a) and has low levels of endogenous SRSF3 protein. Overexpression of SRSF3 promoted an increase in M2 levels, and therefore a decrease in M1 levels (Fig. 3.3 C). Interestingly, knocking down hnRNPA1/A2 or PTB (Fig. 3.3 D and Fig. 3.5 C), which are known repressors of exon 9 (Clower et al. 2010; David et al., 2010), along with SRSF3, led to an additive increase in PK-M1 mRNA and protein levels in HEK-293 cells (Fig.3.3 D), implying that repression of exon 9 and activation of exon 10 both contribute to PK-M isoform selection.

3.2.3 SRSF3 Activates Endogenous PK-M Exon 10

To determine whether the effect of SRSF3 overexpression is due to increased activation of exon 10 and/or repression of exon 9, I first rescued M1 inclusion by knocking down hnRNPA1/A2 and PTB in HEK-293 cells, and then I overexpressed SRSF3 in these cells and assessed its effects on endogenous PK-M transcripts. SRSF3 overexpression

restored PK-M2 transcripts to the original levels, whereas there was little or no change in PK-M1 levels. This observation suggests that SRSF3 only activates PK-M exon 10. Indeed, overexpression of SRSF3 did not elicit a significant change in splicing of the duplicated-exon-9 minigene, further suggesting that SRSF3 does not directly affect exon 9 splicing (data not shown).

3.2.4 SRSF3 Enhances Aerobic Glycolysis

PK-M isoform ratios influence aerobic glycolysis (Christofk et al., 2008), and therefore, we determined the effect of SRSF3 knockdown on this process, as assayed by the extent of cellular lactate production. SRSF3 knockdown in HEK-293 cells resulted in a significant decrease in lactate production (Fig 3.3 A). Because the additive effect of SRSF3 on PK-M1 levels was stronger with hnRNPA1/A2 than PTB knockdown, and simultaneously knocking down all four factors impaired cell viability (data not shown), I assayed for lactate production in HEK-293 cells in which SRSF3, hnRNPA1, and hnRNPA2 were simultaneously knocked down, a situation in which the cells remained viable (Fig. 3.4 B). Strikingly, the extent of lactate production was intermediate between that in the SRSF3 single knockdown and the hnRNPA1/A2 double knockdown. These results are consistent with SRSF3 contributing to the Warburg effect, but further suggest the involvement of metabolic targets other than *PK-M* that presumably respond differently to SRSF3 and hnRNPA1/A2 (see Discussion).

3.2.5 An exonic enhancer element in Exon 10 which binds SRSF3 is necessary and sufficient for activation of the Exon

To analyse whether intronic or exonic *cis*-elements play critical roles in activating exon 10 and/or repressing exon 9 splicing, exon 10 was duplicated in place of exon 9 in a PKM minigene (illustration –Fig 3.7). He observed the appearance of a doubly-included exon 10 RNA species indicating that the upstream exon 10 was still activated, regardless of its position. If exon 9 repression depended on *cis*-elements present in introns 8 or 9, there would have been inefficient use of the upstream copy of exon 10 because it would be under the influence of these repressive elements, and the pattern should be similar to that of the wild-type minigene. This suggested that splicing enhancer elements involved in exon 10 definition are present in the exon itself. Similarly, exon 9 duplication was also carried on in place of exon 10 in the minigene. If exon 10 splicing is normally activated through flanking *cis*-elements in introns 9 or 10, there should be a strong increase in exon-9-included transcripts compared to the wild-type minigene, because the downstream copy of exon 9 would now be under the influence of such elements. However, there was no such increase from the exon-9-duplicated minigene transcripts. This finding suggested that splicing-silencing elements involved in repressing exon 9 are located in the exon itself. When the positions of exons 9 and 10 were swapped, leaving all the introns unchanged, the M1 and M2 isoform ratio was similar to that of the wild-type minigene, although there was a decrease in M1 abundance, and an expected decrease in the use of the cryptic 3'ss upstream of the original exon 10 (i.e., in intron 9), because this 3'ss is now juxtaposed with the repressed exon 9 3'ss. This finding indicates

that exon 10, when moved to exon 9, is spliced as efficiently as in its original location. These results suggested that exonic *cis*-elements involved in *PK-M* splicing are sufficient to activate exon 10 and repress exon 9, in a manner that is independent of their respective positions along the gene and the influence of their flanking introns.

To test the hypothesis that there are critical exonic splicing enhancer elements (ESEs) in exon 10, we systematically searched for such elements. Taking advantage of the high nucleotide-sequence identity between exons 9 and 10, and their identical lengths, he duplicated 15-30 nt stretches of exon 10 into the corresponding location in exon 9, in order to find sub-exonic regions that are sufficient to activate exon 9 inclusion. We found that the last 30 nt, but not the last 15 nt of exon 10 strongly increased exon 9 inclusion, suggesting that a strong ESE is present within, or overlaps with, the penultimate 15 nt of exon 10. We then analyzed the entire 30-nt stretch using SFmap (Akerman et al., 2009; Paz et al., 2010), a method to predict splicing-regulatory motifs based on their inter-species conservation and sequence environment. This analysis yielded a near-consensus, conserved SRSF3 functional-SELEX (systematic evolution of ligands by exponential enrichment) motif (Schaal and Maniatis, 1999) within the penultimate 15-nt segment, adjacent to a 6-nt highly conserved AC-rich stretch. To determine whether this SRSF3 motif alone can account for the observed M1 splicing activation, he duplicated the 7-nt SRSF3 motif from exon 10 into exon 9, by mutating the only two nucleotides that differ between exons 9 and 10 within this heptamer. Duplicating only the SRSF3 motif, but not the flanking 8-nt region, activated exon 9 to a similar extent as that achieved by duplicating the entire 30-nt region. In contrast,

duplicating the AC-rich stretch alone had no effect on exon 9 inclusion, whereas duplicating the AC-rich stretch together with the SRSF3 motif had an intermediate effect. This result suggested that the SRSF3 motif is an actual exon 10 ESE.

3.4 DISCUSSION

We have demonstrated that the SR protein SRSF3 promotes the inclusion of the *PK-M2*-specific alternative exon 10 in transformed cells by binding to an ESE near the 3' end of the exon. Consistent with its expected ability to facilitate cellular proliferation by altering glycolytic metabolism, *SRSF3* is overexpressed in ovarian cancers (He et al., 2004) and cervical cancer cell lines, whereas in normal cervical tissue, its expression is restricted to the basal proliferating layers (Jia et al., 2009). Moreover, overexpression of SRSF3 was recently found to be sufficient for transformation of NIH-3T3 immortal mouse fibroblasts (Jia et al., 2010), indicating that similar to its paralog, SRSF1 (Karni et al., 2007), SRSF3 is an oncoprotein. SRSF3 is also a downstream target of the oncogenic β-catenin/TCF-4 pathway in colorectal cancer cells (Gonçalves et al., 2008).

To address how alternative splicing of the *PK-M* gene switches from the M1 isoform in quiescent cells to the M2 isoform in transformed cells, Wang analyzed a minigene with intact introns flanking the alternative exons. We demonstrated that *PK-M* ME splicing involves a two-component circuit: exon 9 is repressed and exon 10 is activated in proliferating cells, and these two effects are essentially independent of each other (Fig 5.1).

Whereas the 5'ss of exons 9 and 10 do not play a dominant role in exon selection in this system—considering that the levels of M1 and M2 mRNAs do not change upon swapping the 5'ss of the ME exons—mutational analysis indicates that the 3'ss are necessary for definition of their respective exons, and they compete with each other. It appears that exon definition, and ultimately, proper ME exon selection in the *PK-M* gene, are dependent on the outcome of competition between the alternative 3' ss. We therefore expect that a splicing factor that activates one of the exons does so by promoting the recruitment of spliceosomal components to its 3'ss. This would strengthen this 3'ss relative to the other 3'ss, and in effect, enhance the definition of the exon.

By duplicating and swapping ME exons in the *PK-M* minigene, Wang showed that the most important *cis*-elements controlling *PK-M* alternative splicing are located within the ME exons themselves. As a first proof of this principle, he mapped a *bona fide* SRSF3 ESE in exon 10 that proved sufficient to activate exon 9 splicing in cancer cells when placed in this exon. Although double inclusion of exon 10 was not the major product from the exon-10-duplication minigene (Fig. 3), this cannot be due to repression via the flanking intron 8 and 9 regions, because exon 10 was spliced efficiently when it was swapped with exon 9. Instead, we speculate that intronic elements are likely involved in the ME exon selection properties of PK-M.

Remarkably, the SRSF3 ESE motif in exon 10 differs from the corresponding exon 9 sequence by only two nucleotides. Both nucleotides correspond to wobble bases in the

corresponding codons. The first wobble base is unusually conserved, which might reflect the importance of this nucleotide in mediating SRSF3 recruitment and functionality. The corresponding two nucleotides in exon 9 are also conserved, suggesting strong selection against the creation of an exon 9 SRSF3 activation motif, However, because we used exon 9 sequences to replace exon 10 when abrogating the exon 10 SRSF3 ESE, we cannot rule out the existence of a corresponding exonic splicing silencing (ESS) element in exon 9. The co-evolution of splicing signals in both exons exemplifies the requirement for these exons to be coordinately regulated in order to maintain the ME properties of the system. Additionally, the use of two wobble nucleotides to code for a key splicing signal illustrates the impact of sequence changes that are expected to be translationally neutral, but that nevertheless drastically affect the structure of the resulting protein by changing alternative splicing of the entire exon (reviewed in (Cartegni et al., 2002).

Although the SRSF3 motif alone was necessary and sufficient for activation of exon 10 splicing *in vivo*, binding assays using short RNAs *in vitro* indicated that both the SRSF3 motif and the adjacent AC-rich motif are required for SRSF3 binding to exon 10 RNA. Likewise, rescuing SRSF3 binding to a variant exon 9 RNA fragment required both the SRSF3 and adjacent AC-rich motifs from exon 10. This AC-rich-motif-dependent recruitment might occur either through protein-protein interactions or through changes in local RNA secondary structure to make it permissive for SRSF3 binding. An alternative possibility is that SRSF3 directly binds to its cognate ESE without the help of recruitment factors, by mass action, whenever it is abundantly expressed *in vivo*.

We were surprised to find no rescue of exon 9 inclusion when its 5'ss was swapped with that of exon 10—even though it has been reported that hnRNPA1 represses exon 9 inclusion by binding to the exon 9 5'ss (David et al., 2010)—as this swap presumably removed the repressive hnRNPA1 binding site; perhaps this lack of rescue reflects contextual effects. However, our results confirm and extend the data from an earlier study that duplicated the exon 10 5'ss in a heterologous minigene reporter system, and found no change in *PK-M* splicing (Takenaka et al., 1996). Moreover, in the context of intact pre-mRNAs, it is not known how well hnRNPA1 binding to a motif that is part of a 5'ss can compete with binding of spliceosomal components, such as U1 and U6 snRNPs. Given that hnRNPA1 does have strong effects on exon 9 inclusion *in vivo* (Clower et al., 2010a; David et al., 2010), hnRNPA1-induced exon 9 repression could occur either indirectly—through hnRNPA1-mediated regulation of a splicing factor that in turn regulates *PK-M* alternative splicing—or through additional *cis*-elements located elsewhere on the *PK-M* pre-mRNA.

The change in endogenous levels of PK-M1 when SRSF3 was knocked down was roughly comparable to the effects of knocking down the recently identified repressors of exon 9, hnRNPA1/A2 and PTB (Clower et al., 2010a; David et al., 2010). However, even knocking down all three factors did not completely rescue exon 9 inclusion. This could imply the existence of additional activators of exon 10 and/or repressors of exon 9 that presumably work in a combinatorial fashion to maintain exon 10 definition in proliferating cells. It is also possible that there exists another factor(s) with similar specificity as SRSF3, and with partially redundant functions, by analogy to what occurs

with hnRNPA1 and hnRNPA2 (Clower et al., 2010a; David et al., 2010). This would account for the very large reduction in exon 10 inclusion we observed when we mutated the SRSF3 binding site.

Although hnRNPA1/A2 knockdown resulted in a large decrease in lactate production, as we previously reported (Clower et al., 2010a), and SRSF3 knockdown also reduced lactate production, the triple knockdown of SRSF3, hnRNPA1, and hnRNPA2 paradoxically resulted in a smaller overall decrease in lactate production. We speculate that this antagonistic effect between the exon 10 activator and the exon 9 repressors could be due to distinct non-PK-M downstream metabolic targets of SRSF3 and hnRNP A1/A2, each of which may independently influence lactate production.

Important questions that remain unanswered include: What are the additional factors that govern exon 9 and exon 10 usage in tumor cells? Can the PK-M2 isoform be completely switched to the PK-M1 isoform by manipulating the levels of splicing factors in tumor cells? How is exon 9 selected as the default spliced exon in quiescent cells? Are there tissue-specific differences in the mechanisms of exon 9 selection in differentiated cells? Answers to these questions will contribute to a better understanding of the regulation of PK-M isoform expression in the context of tumorigenesis, which could provide the basis to develop splicing-targeted cancer therapeutics.

3.5 MATERIALS AND METHODS

3.5.1 Cells and Transfections

HeLa and HEK-293 cells were grown in DMEM, supplemented with 10% (v/v) FBS, penicillin and streptomycin, at 37 °C and 5% CO_2. 5 μg of minigene plasmid per 10-cm dish was transiently transfected using Lipofectamine 2000 (Invitrogen). Total RNA from transfected cells was harvested 36 hr after minigene transfection.

3.5.2 RNA Interference

siRNA against *SFRS3* was obtained from Dharmacon. siRNAs against hnRNPA1 and hnRNPA2 were used as described (Cartegni et al., 2006).10^6 HEK-293 cells in 6-well plates were transfected with 200 pmol of siRNA duplex using Lipofectamine RNAiMax reagent (Invitrogen) for individual knockdowns and 100 pmol of each duplex for triple knockdowns. Cells were harvested 48 hr after transfection.

3.5.3 Immunoblotting

Cells were lysed in SDS, and total protein concentration was measured by the Bradford assay. 30 μg of total protein from each lysate was separated by SDS-PAGE and transferred onto nitrocellulose. This was followed by blocking with 5% (w/v) milk in Tris-buffered saline with Tween-20, probing with the indicated antibodies, and visualization

by enhanced chemiluminescence (Roche) or infrared imaging. Quantitation was performed using an Odyssey infrared-imaging system (LI-COR Biosciences). Primary antibodies were: β-tubulin (Genscript rAb, 1:5000); hnRNPA1 (mAb UP1-55, culture supernatant (Hua et al., 2008)); SRSF3 (Zymed mAb, 1:1000); PK-M2 (rabbit, 1:2000) and PK-M1 (rabbit, 1:2000 (Christofk et al., 2008a; Christofk et al., 2008b)). Secondary antibodies were: iRdye 800 or 680 anti-rabbit or anti-mouse (LI-COR Biosciences, 1:10,000); anti-mouse (Bio-Rad goat anti-mouse HRP conjugate, 1:20,000).

3.5.4 RT-PCR

2-5 μg of total RNA was extracted from cell lines using Trizol (Invitrogen). Contaminating DNA was removed with DNAase I (Promega). Reverse transcription was carried out using ImPromp-II reverse transcriptase (Promega). Semiquantitative PCR using Amplitaq polymerase (Applied Biosystems) was performed by including [α-^{32}P]-dCTP in the reactions. The human-specific primer sets used to amplify endogenous transcripts anneal to PK-M exons 8 and 11, and their sequences are: hPKMF: 5'-AGAAACAGCCAAAGGGGACT-3'; hPKMR: 5'-CATTCATGGCAAAGTTCACC-3'. To amplify minigene-specific transcripts, the forward primer was replaced with a primer annealing to the pcDNA3.1(+) vector, pcDNAF: 5'-TAATACGACTCACTATAGGG-3'. After 26 amplification cycles for minigene-derived transcripts, and 24 cycles for endogenous transcripts, the reactions were divided into four aliquots for digestion with NcoI, PstI (New England Biolabs), both, or neither. The products were analyzed on a 5% native

polyacrylamide gel, visualized by autoradiography, and quantified on a FLA-5100 phosphoimager (Fuji Medical Systems) using Multi Gauge software Version 2.3. The % M1 mRNA in endogenous transcripts was calculated using the GC-content-normalized intensities of the top undigested band (M1, A) and the bottom two digested bands (M2, B1 B2) in the PstI-digest lanes. The % M1 mRNA from minigene-transcripts was calculated using the GC-content-normalized intensities of the top undigested band (**a,** M1) and other higher-mobility digested bands corresponding to M2 and its variant species (**b – g**, as described above) in the PstI-digest lanes.

3.5.5 RNA Pulldowns

RNA pulldowns were performed as described (Caputi et al., 1999; Hua et al., 2008). RNA oligonucleotides were obtained from Sigma Genosys. After the final wash, the beads were resuspended in 75 μl of 4× Laemmli buffer and boiled for 5 min to elute bound proteins. 5 μl of each protein sample was loaded on a 12 % SDS polyacrylamide gel for immunoblotting.

3.5.6 Lactate Assay

For measurements of lactate secretion, cells were transfected with siRNA in 6-well plates. 24 hr later, the cells were replated (three replicates per condition) at subconfluent density (25,000 cells/well) in 12-well dishes, and after 24 hr, the cells were

switched to serum-free medium without phenol red for 20 min, and lactate secreted into the medium over this time was measured, in triplicate for each sample, using the fluorescence mode of a Lactate Assay Kit (Biovision Inc.). Fluorescent readings were averaged for each sample replicate set, then averaged for each condition replicate set, and finally normalized to the cell number measured from parallel wells.

3.6 FIGURES AND LEGENDS

FIGURE 3.6.1 Comparative analyses of relative levels of SRSF3 and PKM2 in various cancer cell lines.

(A) SRSF3 protein level was measured by Western blotting in brain tissue and in various other cancer cell lines.

(B) qRT-PCR analysis of SRSF3 levels compared to PKM2 levels in various cancer cell lines. The black bars represent SRSF3 mRNA levels, and the grey bar represents PK-M2 levels.

(A)

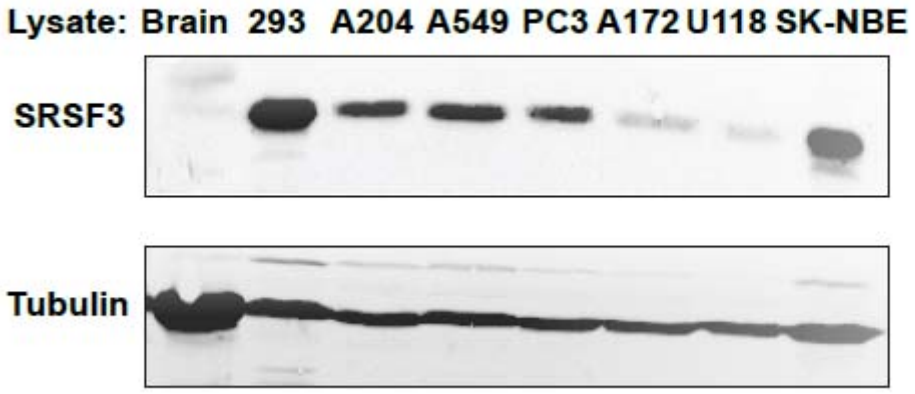
Lysate: Brain 293 A204 A549 PC3 A172 U118 SK-NBE
SRSF3
Tubulin

(B)

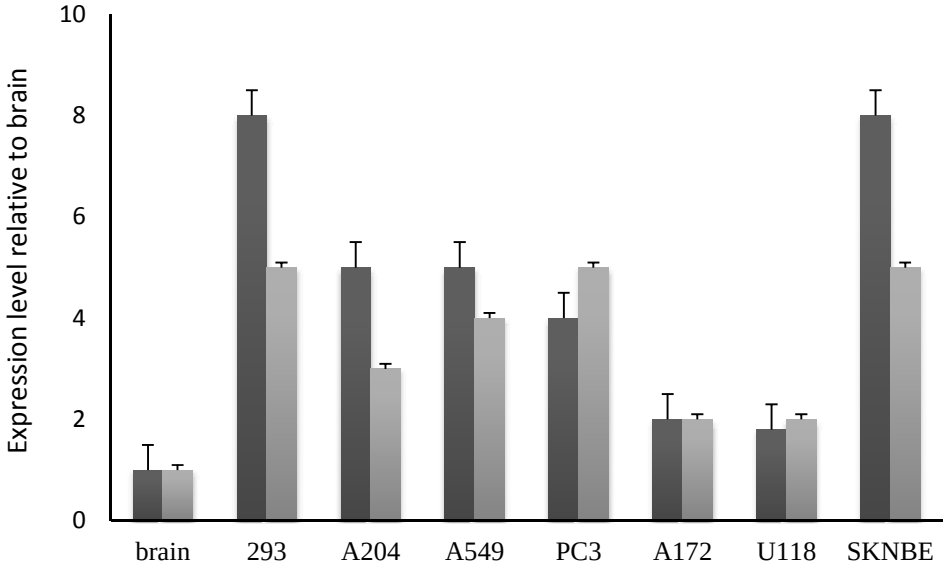
Expression level relative to brain
10
8
6
4
2
0
brain
293
A204
A549
PC3
A172
U118
SKNBE

Figure3.6.2. SRSF3 Affects Endogenous Levels of PK-M1/M2

(A) (B) SRSF3 siRNA alone, or together with hnRNPA1/A2 siRNAs, was transfected into HEK-293 cells. (A) shows transcript-level changes for *PK-M1* and *PK-M2*. % M1 is indicated at the bottom, with the following s.d.: 1% (luc); 2% (SRSF3); 1% (A1/A2); and 1% (SRSF3/A1/A2) (n = 4). (B) shows changes at the protein level; quantitations are shown at the bottom, normalized to the tubulin loading control, with s.d. ≤0.5% in all cases (n=3).

(C) SRSF3 cDNA was transfected in increasing amounts into A172 cells. Cells were harvested after 48 hr. *PK*-M mRNA level was determined by RT-PCR. s.d. ≤1% in all cases (n=5).

(D) hnRNPA1/A2/PTB siRNAs were co-transfected into HEK-293 cells, followed by transfection of SRSF3 cDNA 24 hr later. Cells were harvested 36 hr after the second transfection. Transcript-level changes are indicated at the bottom, with the following s.d.: 1% (A1/A2/PTB siRNA); 3% (A1/A2/PTB siRNA + SRSF3) (n=5). p-value comparing A1/A2/PTB siRNA with A1/A2/PTB+SRSF3 is 0.002.

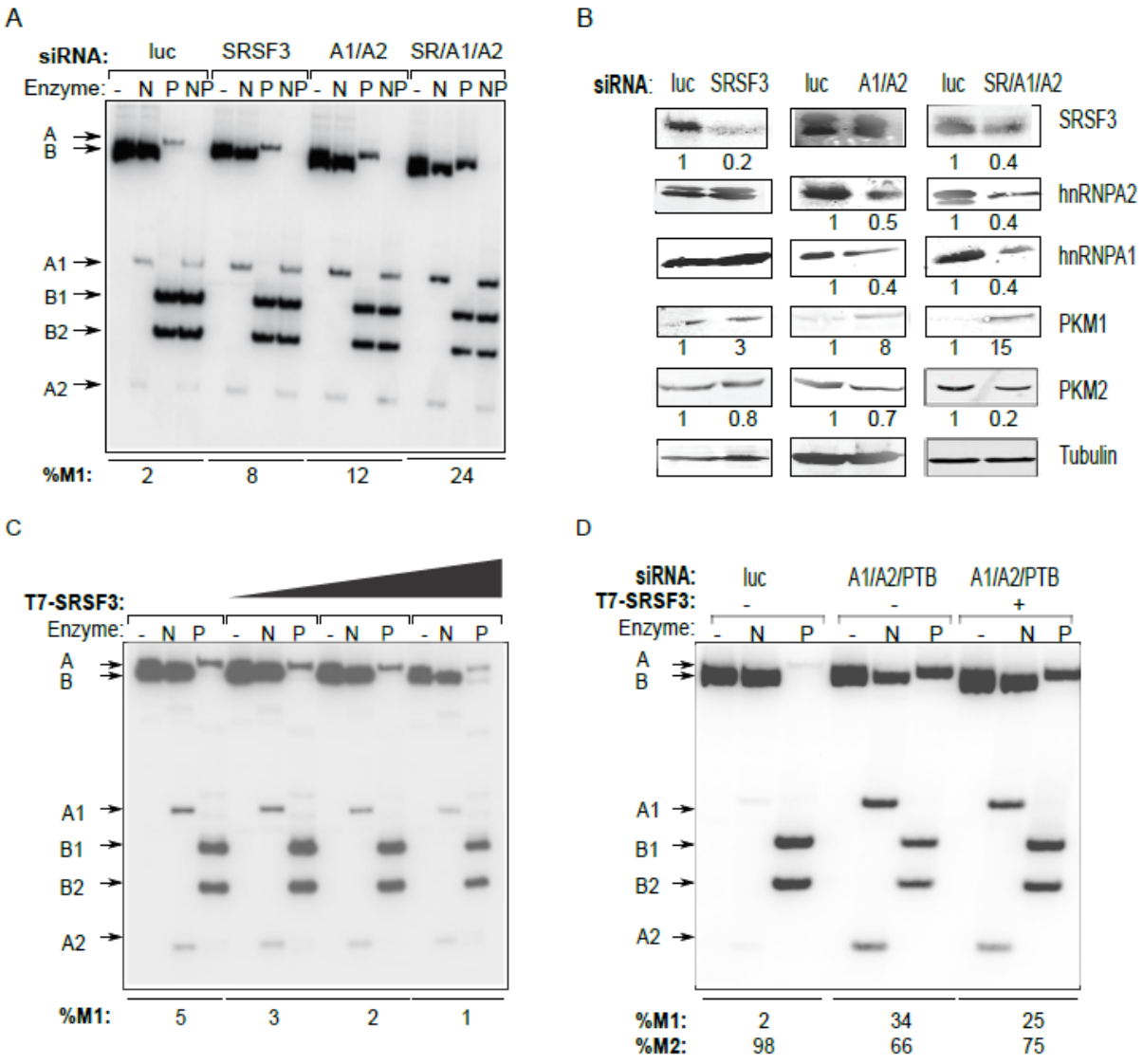
A
siRNA: luc SRSF3 A1/A2 SR/A1/A2
Enzyme: - N P NP - N P NP - N P NP - N P NP
A
B
A1
B1
B2
A2
%M1: 2 8 12 24
B
siRNA: luc SRSF3 luc A1/A2 luc SR/A1/A2
SRSF3
1 0.2 1 0.4
hnRNPA2
1 0.5 1 0.4
hnRNPA1
1 0.4 1 0.4
PKM1
1 3 1 8 1 15
PKM2
1 0.8 1 0.7 1 0.2
Tubulin
C
T7-SRSF3:
Enzyme: - N P - N P - N P - N P
A
B
A1
B1
B2
A2
%M1: 5 3 2 1
D
siRNA: luc A1/A2/PTB A1/A2/PTB
T7-SRSF3: - - +
Enzyme: - N P - N P - N P
A
B
A1
B1
B2
A2
%M1: 2 34 25
%M2: 98 66 75

FIGURE 3.6.3 Lactate levels and viability measurements in SRSF3 knock-down cells

(A) SRSF3 siRNA alone, or together with hnRNPA1/A2 siRNAs, was transfected into HEK-293 cells. Lactate production was measured 48 hr after transfection. Error bars represent s.d.; n = 6. * $p < 0.05$.

(B) Cell viability assay was performed by Trypan-Blue staining and counting the cells with a hemocytometer, after knocking down the indicated factors in HEK-293 cells. Viability is shown as the percentage of living cells.

(A) **(B)**

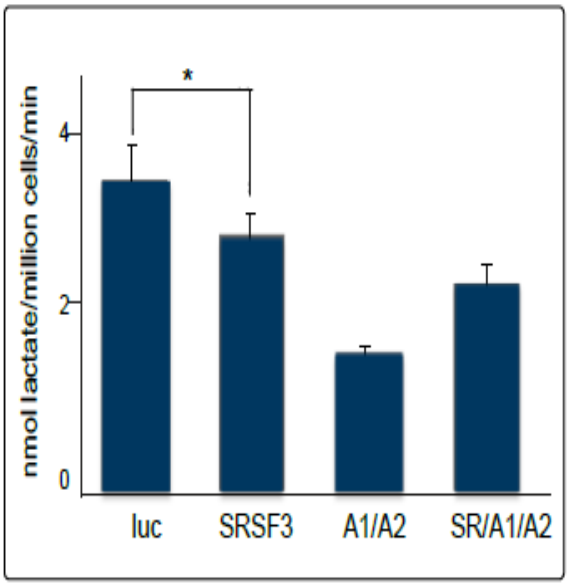
nmol lactate/million cells/min
4
2
0
*
luc
SRSF3
A1/A2
SR/A1/A2

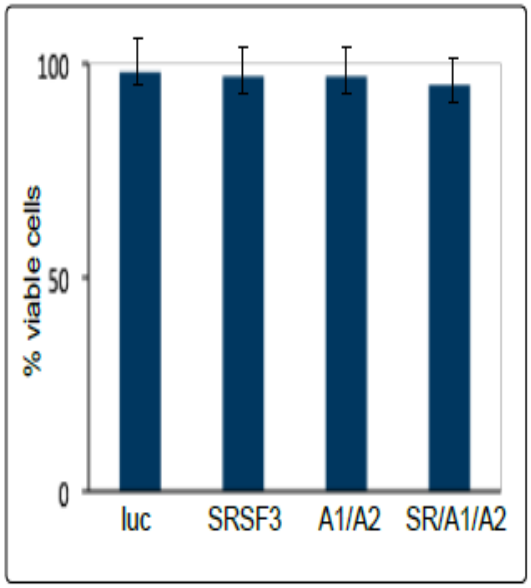
% viable cells
100
50
0
luc
SRSF3
A1/A2
SR/A1/A2

Figure 3.6.4 Western Blots for Overexpression and Knockdown Experiments

(A, B) Overexpression of SRSF3 in HEK-293**(A)** and A172**(B)** cells. Cells were transfected with plasmids encoding T7-tagged SRSF3 cDNA (Cáceres et al., 1998) in increasing amounts. Cell lysates were prepared after 48 hr, and overexpression was verified by immunoblotting with monoclonal antibodies against SRSF3 or the T7 tag, and tubulin as a loading control.

(C) Overexpression of SRSF3 combined with triple-knockdown of hnRNPA1/hnRNPA2/PTB in HEK-293 cells. hnRNPA1/A2 /PTB siRNAs and T7-tagged SRSF3 cDNA were co-transfected into HEK-293 cells. Cell lysates were prepared after 72 hr, and knockdown and overexpression were verified by immunoblotting with monoclonal antibodies against the T7 tag (for SRSF3) and hnRNPA1, A2, and PTB, as well as tubulin as a loading control.

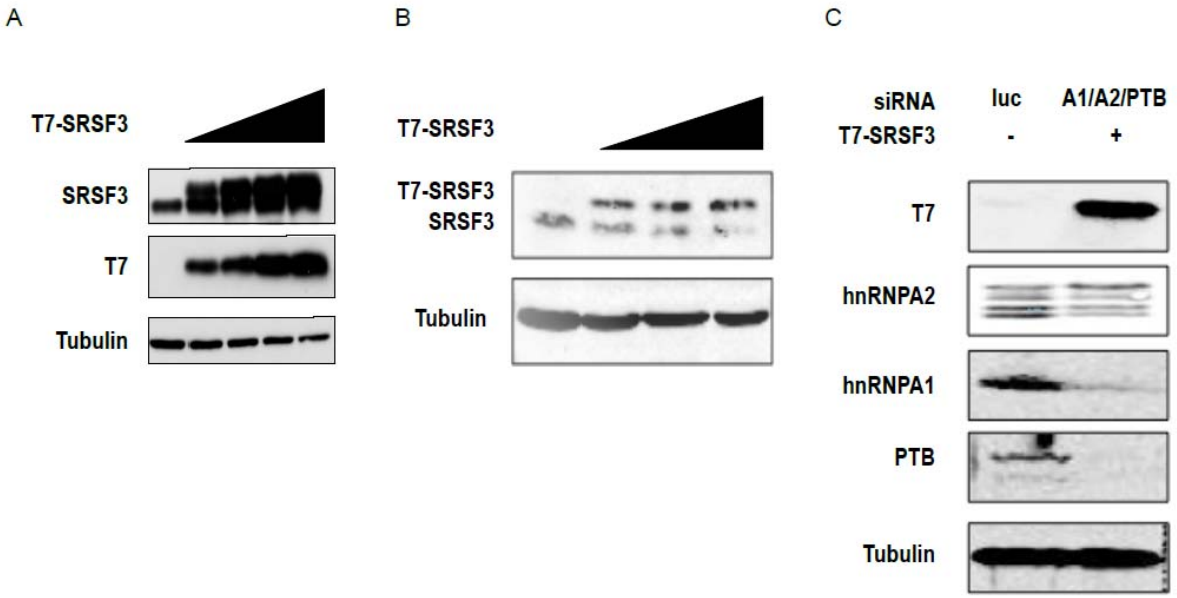
A
T7-SRSF3
SRSF3
T7
Tubulin
B
T7-SRSF3
T7-SRSF3
SRSF3
Tubulin
C
siRNA
luc
A1/A2/PTB
T7-SRSF3
-
+
T7
hnRNPA2
hnRNPA1
PTB
Tubulin

Figure 3.6.5 Additive Effect of SRSF3 and PTB on *PK-M1/M2* Ratio

(A)(B) SRSF3 siRNA alone, or together with PTB siRNAs, or luciferase siRNA control, was transfected into HEK-293 cells. (A) Transcript-level changes for *PK-M1* and *PK-M2*. %M1 transcript is indicated at the bottom, as calculated from the Pst1 digestion lanes (s.d. ≤0.5% in all cases). (B) Changes at the protein level were measured by Western blotting with the indicated antibodies.

(C) *PKM-1/2* transcript-level changes were measured using a control siRNA hnRNPK.

(D) Knock-down levels were measured using western blot analysis.

A

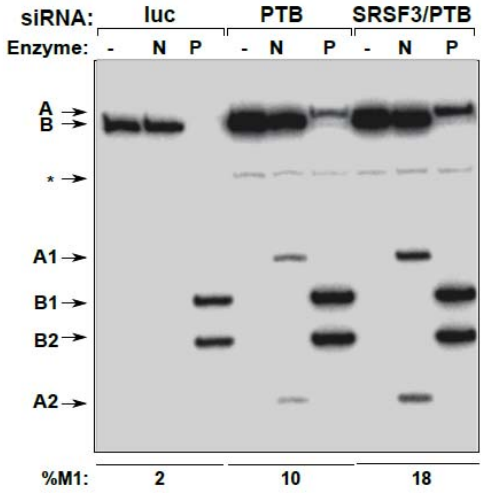
siRNA:
luc
PTB
SRSF3/PTB
Enzyme:
-
N
P
-
N
P
-
N
P
A
B
*
A1
B1
B2
A2
%M1:
2
10
18

B

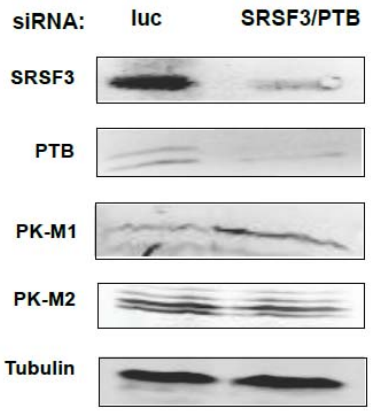
siRNA:
luc
SRSF3/PTB
SRSF3
PTB
PK-M1
PK-M2
Tubulin

C

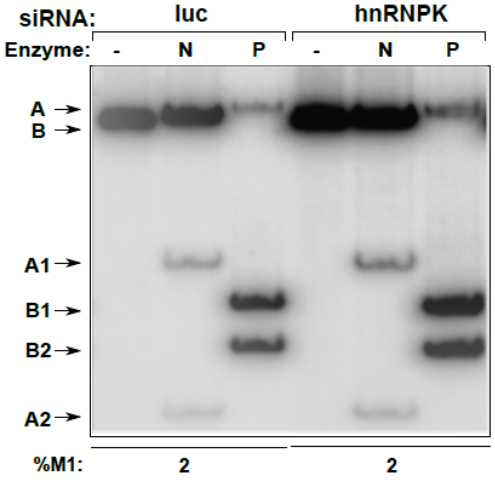
siRNA:
luc
hnRNPK
Enzyme:
-
N
P
-
N
P
A
B
A1
B1
B2
A2
%M1:
2
2

D

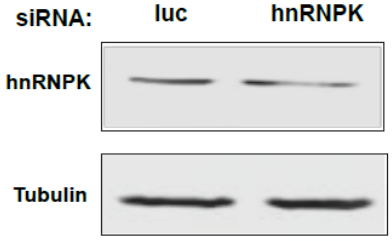
siRNA:
luc
hnRNPK
hnRNPK
Tubulin

3.6.7 Schematic diagram of micro-duplication and swapping experiments from both the 3’ and 5’ end of exon-10 of PK-M.

* the original minigene experiments were done by Zhenxun Wang.

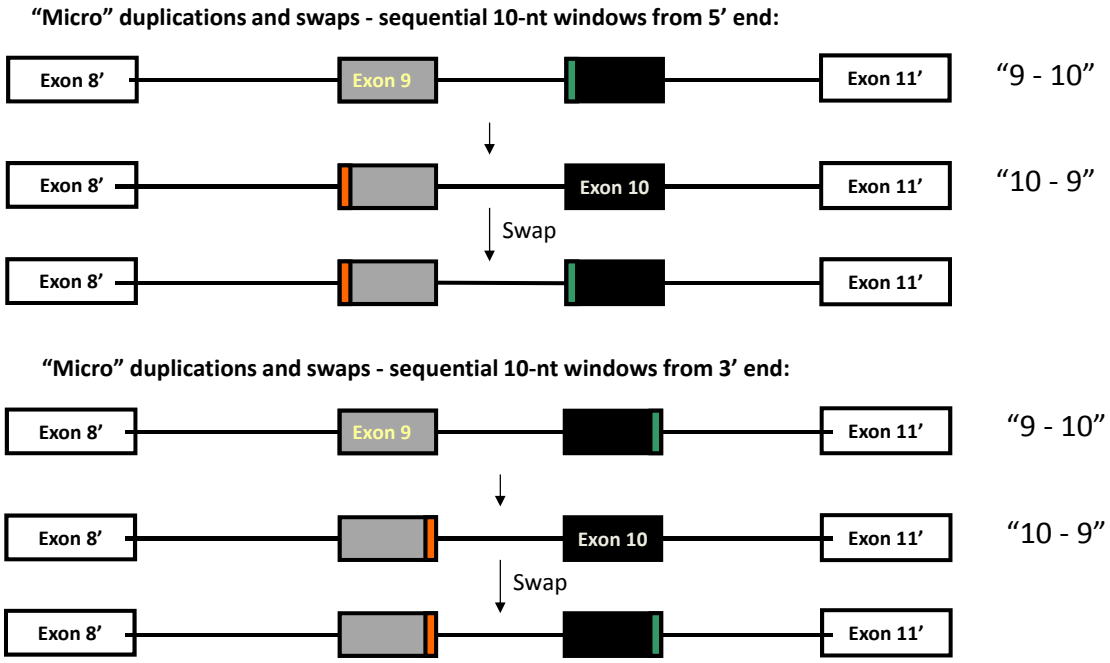

Figure 3.6.8 Regulation of *PK-M* Splicing in Cancer Cells

In quiescent or differentiated cells, exon 9 is the default spliced exon. In transformed cells, overexpression of oncogenic splicing factors leads to the simultaneous repression of exon 9 and activation of exon 10. Binding of SRSF3 to the activation motif near the 3' end of exon 10 enhances exon definition by facilitating spliceosomal recruitment to the 3'ss of this exon. Additional, unknown activators (green ovals) likely contribute to exon 10 recognition. Up regulated splicing repressors (pink ovals) that presumably act through silencing motifs in exon 9 and introns 8 and 9, including hnRNPA1/A2 and PTB (Clower et al., 2010; David et al., 2010), further reinforce exon 10 selection in transformed cells by repressing exon 9 inclusion. When SRSF3 is less abundant (or when we mutated the SRSF3 activation motif), loss of exon 10 definition occurs, and leads to increased exon 10 skipping. The exon 9 3'ss is then able to compete more effectively for spliceosomal components, leading to an increase in exon 9 inclusion. A further additive increase in exon 9 inclusion occurs if the levels of SRSF3 and exon-9 repressors are concomitantly reduced.

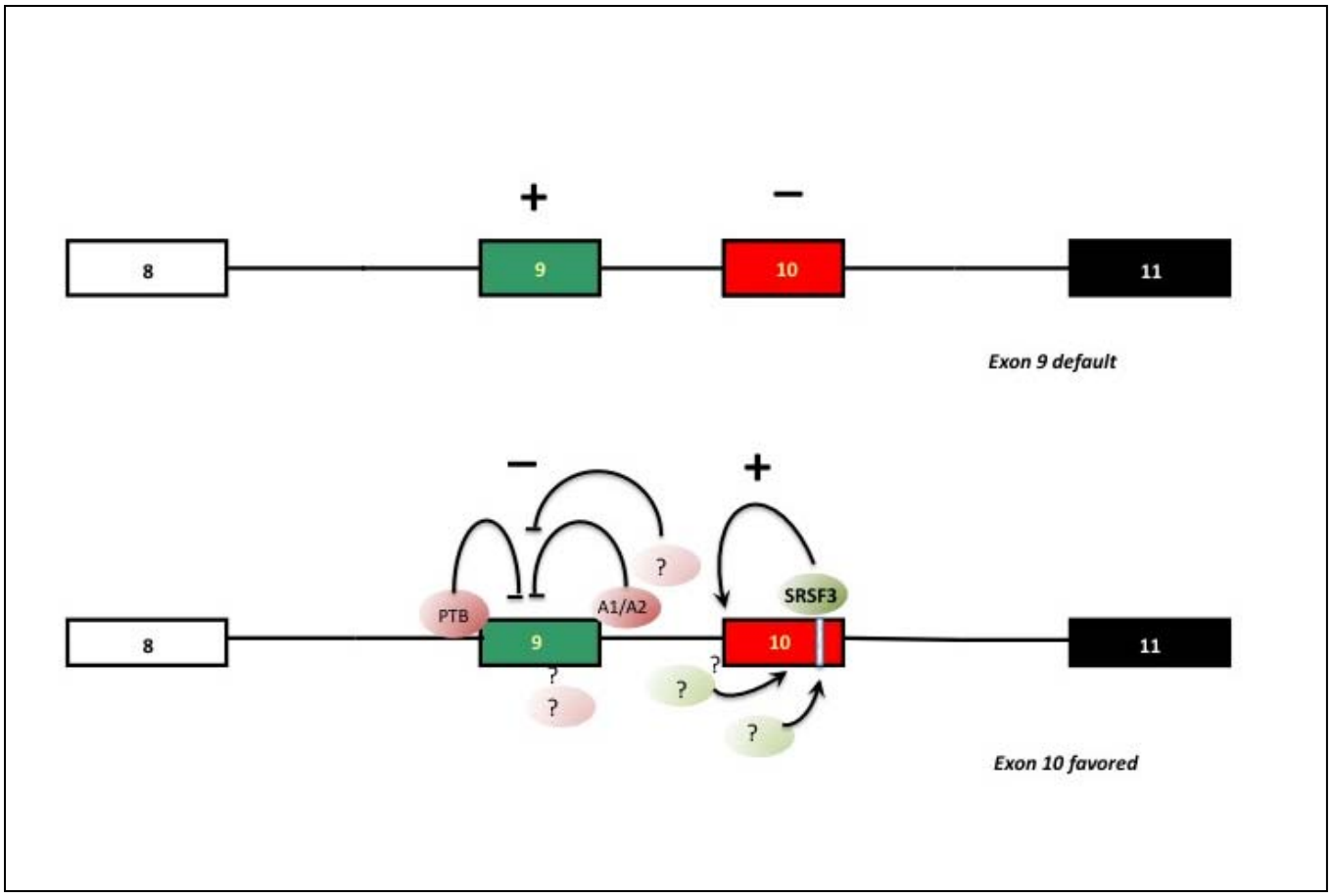
+
−
8
9
10
11
Exon 9 default
−
+
?
PTB
A1/A2
SRSF3
8
9
10
11
?
?
?
?
Exon 10 favored

Chapter 4

Identification of alternative splicing regulators of the Pyruvate Kinase-M gene by RNA interference in glioblastoma cells

4.1 Introduction

Alternative splicing generates multiple mRNAs from a single gene transcript, thereby expanding proteomic diversity in complex organisms (as discussed above). Regulation of splicing is achieved by auxiliary *cis*-elements that bind regulatory proteins that activate or repress splicing of adjacent exons (Black, 2003; Matlin et al., 2005). Most known splicing regulators are RNA-binding proteins (RBPs), such as the SR and hnRNP family of proteins, which are expressed fairly ubiquitously, albeit with quantitative differences in expression between tissues (see chapter 2, also Hanamura et al., 1998). Modulation of the activity and subcellular localization of these proteins by post-translational modifications contributes to cell-type-specific splicing decisions (Allemand et al., 2005; Stamm, 2008). Post-transcriptional regulation of the mRNAs encoding RBPs by microRNAs can also influence cell-type-specific splicing decisions (Boutz et al., 2007; Makeyev et al., 2007). Furthermore, alternatively spliced exons are subject to combinatorial control by numerous splicing regulators with both negative and positive effects on splicing (Black, 2003; Smith, 2005). A handful of mammalian splicing factors have also been identified that are cell-type specific. Nonetheless, the identification of additional splicing regulatory proteins with distinct cell-type-specific differences in expression remains an elusive goal. An alternative splicing event with well-defined cell-

type specificity and functional consequence is the choice between mutually exclusive exons 9 and 10 of the Pyruvate kinase M gene (PK-M). The PK-M2 splice variant is exclusive to proliferating cancer cells, while PKM-1 is found in differentiated, slow-growing cells, and the resulting proteins have distinct properties in ligand binding specificity and allosteric regulation (Christofk et al., 2008c). The compartment-specific expression of these PKM-2 splice variants and their ligands is essential for regulation of cell proliferation and control of the Warburg effect in cancer cells. As discussed in previous chapters, our studies have identified a number of auxiliary *cis*-elements and RBPs that regulate PKM-2 alternative splicing. To systematically identify additional splicing factors that promote PKM-1 expression, I carried out a directed, high-throughput lentivirus screen using a QPCR approach (Arany et al., 2008). Dual fluorescence reporter screening has been previously used as a method to search for splicing regulators of a target, using genomewide libraries (Moore et al., 2010; Nasim and Eperon, 2006; Warzecha et al., 2009). Although the QPCR approach I used is not readily amenable to genome wide screening, it is a novel method of quantitatively examining changes in splicing. The advantage is that one can study endogenous gene targets more efficiently than resorting to using minigene or reporter constructs that are time-consuming to devise.

4.2 RESULTS

4.2.1 Design of a qPCR based PKM splicing screening assay

My main goal was to establish an assay capable of identifying factors that increase the amount of functional PKM-1 isoform level. As stated in previous chapters, alternatively spliced isoforms of pyruvate kinase are important regulators of cancer metabolism and Warburg effect, exon 10 inclusion (PKM-2) being the predominant form expressed in cancer cells and exon 9 inclusion (PKM-1) seen in non-dividing and differentiated tissues. As an approach to systematically identifying splicing factors involved in PK-M alternative splicing, I carried out a directed lentivirus shRNA screen using a focused collection of annotated factors (with the help of the Hannon lab at CSHL). I used the PGIPZ vector (figure 4.1A) with an average of seven hairpins for each of ~400 factors involved in constitutive and/or alternative splicing, including many RNA-binding proteins, spliceosome components, RNA helicases, and modifying enzymes, rather than a large genome-wide library. shRNAs against hnRNPA1, hnRNPA2, PTB, and nPTB served as positive controls; shRNAs specific for hnRNPK and SRSF1 served as negative controls, since I had already determined that these factors do not affect PK-M alternative splicing in cancer cells. To quantitatively measure the relative levels of PK-M1 alternatively spliced mRNA isoform, I designed a single pair of primers corresponding to the flanking constitutive exons 8 and 11 and a VIC-MGB reporter fluorescent probe to the least homologous region of exon 9. Because exons 9 and 10 are identical in length (167 nt) and share a 67% similarity at the amino acid level, it was important to design the exon 9 probe in a manner that would be specific enough to carry out a screen (as shown in

figure 4.3A), without any cross-contaminating signal from exon 10 transcript. The primer and probe pair were tested for specificity using a pcDNAPK-M1 and pcDNAPK-M2 plasmid, in which the primer/probe pair would give an exponentially increasing signal with increasing amounts of the PK-M1 plasmid, but not with the PK-M2 plasmid (results not shown). I also designed a FAM-NFQ reporter fluorescent probe on exon 12, and a forward and reverse primer flanking the probe that served as an endogenous control, to isolate the change in the splicing ratio of PK-M1/PK-M without the influence of transcriptional or other systemic fluctuations. The primers and probes were tested in glioblastoma cell lines and yielded expected results as previously tested with the semi-quantitative PCR assay.

4.2.2 Primary Screening results

An outline of the screen for activators of the PK-M1 spliced isoform is shown in Fig. 1B. In brief, U-118 glioblastoma cells were grown in culture and plated into 96-well plates before shRNA transduction. The cells were then treated with lentivirus and fresh media was added after 24 hrs. Four days after virus infection, the cells were washed and lysed, and the total lysate was reverse transcribed *in situ* to yield cDNA, and this was used as template for quantification of gene expression by qPCR. The measured expression of PKM-1 mRNA was then normalized to the measured expression of total PKM, which served as an internal control. In this way, the response of PKM-1 splicing to any factor in the library to could be determined. U-118 cells were chosen for the screen for a number

of reasons. First, these cells showed the maximum knockdown of all factors initially tested with the lentivirus shRNA (as shown in Figure 3). Second, U-118 cells are grade IV glioblastoma cells that grow very slowly in culture, thus giving flexibility in infection and time after which the cells are lysed without crowding the 96-well plates. And third, my previous research shows that levels of PK-M1 expression in these cells are somewhat higher than in other cultured cells (Chapter 2), with the advantage that changes in PK-M1 levels would be more predisposed to the PK-M2 – to – PK-M1 switch and would make detecting changes in the opposite direction easier. The measurement of endogenous gene expression was also chosen for a number of reasons. First, the common alternative of using luciferase fusion constructs is severely limited when the precise makeup of the promoter in question is not known. Second, gene expression on plasmids is artificial and fails to take into account chromatin modifications. Third, the effects of distant elements such as enhancers and chromatin regulators can only be detected by studying endogenous gene expression.

The feasibility of evaluating PK-M1 gene expression in 96-well plates of U-118 cells was tested by infecting them with varying doses of lentivirus shRNA. As shown in Fig. 1C, infection with virus at a multiplicity of infection (M.O.I) of 10 could reliably infect 100% of the cells in this format, helping bypass the puromycin-selection step. Next, the primer/probe specificity was determined using PK-M1 and PK-M2 plasmids, which yielded an exponentially increasing standard curve (data not shown), and proved the specificity of the primer/probe despite the high homology in exon 9 and exon 10. The assay variability was then determined by measuring PK-M1 expression in 192 wells that

were “mock”-treated with control scrambled shRNA. The standard deviation of the measured C_t value was 0.45. The standard deviation was further reduced to 0.31 when the values were normalized to the internal control, PKM total. This variability is quite small, yielding a *Z* factor of 0.6 for detecting increases in PK-M1 expression of as little as 3-fold. Indeed, in the 192 control samples, not one had a PK-M1 expression that differed >2-fold from the mean.

Thirty two 96-well plates of U-118 cells were then treated with the lentivirus library as described, and the expression of PK-M1 (and total PKM as control) was evaluated in a multiplex QPCR assay. 12 wells in each plate were treated only with control shRNA (luciferase or scrambled), to be used as plate-specific negative controls. The remainder of the wells was treated with lentivirus at MOI 10. Fig. 1B shows representative qPCR amplification curves for PK-M1 for one of these plates; potential activators are identified as wells where PK-M1 cDNA is amplified earlier than the in the other wells, whereas wells where PK-M1 is amplified later reflect either inhibition of PK-M1 or toxicity to the cells. The latter can be distinguished based on whether expression of PKM total is also affected. In my screen, however, I could identify mostly increase in PK-M1, because a strong decrease in PK-M1 levels would push PK-M1 transcript to levels undetectable by qPCR. As shown in Fig. 1B, the qPCR assay identified positive controls that were randomly distributed, and increase confidence in the results. Figure 4.4 shows scatter plots of raw Ct values distributed against the well number and plate number, demonstrating that the screen of all 32 plates did not show any unexpected deviations in Ct values, further adding to confidence in the primary screening results. Forty-five

distinct factors that induce PK-M1 expression 4-fold or greater were identified from the library (Table1) using a regression method per Pradervand et al., 2009. When a compound was identified as a "hit", it was represented by at least two or more independent shRNAs to the same factor in the library, strongly supporting the reproducibility of the screen.

4.3 DISCUSSION

I have outlined here a high-throughput method using qPCR for shRNA library screening for factors that control PK-M1 gene expression. By using this method, my first pass screen identified mRNA processing factors, protein kinases, transcription cofactors, DNA topoisomerases and helicases and chromatin regulators as potent inducers of PK-M1 expression. High-throughput evaluation of isoform expression is generally performed using plasmid-based luciferase assays. These approaches suffer from significant shortcomings, including the artificial nature of unchromatinized plasmids and the assumptions that must be made when constructing reporter plasmids. Methods to assay endogenous gene expression, including array-based and bead-based approaches, often have limited sensitivity/specificity profiles, significant time and cost demands that prohibit true high throughput, and/or the need for highly specialized equipment (Inglese et al., 2007). The screen described here is simple and relatively inexpensive, potentially allowing for scaling up to larger genomewide libraries. No instrumentation other than standard liquid transfer robotics is needed. Induction of gene expression by as little as 2-

fold can reliably be detected, with an apparently very low false-positive rate. Hence, the screen possesses both high sensitivity and specificity. The method is also adaptable to measuring any gene of interest and, in principle, to cells other than the glioblastoma cells used in this study.

There have been limited studies on splicing factor expression and functional correlation in a tissue-specific manner (Barker et al., 1993; Xu et al., 2002). Since I have found a number of factors that could possibly modulate PKM isoform expression in a tissue specific manner, it is possible that the factors themselves are expressed at different levels in different tissues and cell lines and regulate function and splicing of other targets important for tumorigenesis. In my screen, I have detected various proteins that have not been conventionally characterized as splicing factors; however, they do bind to the emerging transcript and could potentially change splicing by acting as a direct splicing factor, or indirectly by other mechanisms, such as hindering export of the pre-mRNA into the cytoplasm or by changing the secondary structure. Most of them bind to RNA, but the primary screen also gave hits that have a role in chromatin regulation and histone modification that would be interesting to further investigate as PK-M splicing modulators. Our data links the Warburg effect to the spliceosomal machinery (see at previous chapters). These findings are relevant to basic mechanisms of proliferation and cancer metabolism that are poorly defined at present, and the exploitation of these pathways in cancer therapy.

4.4 MATERIALS AND METHODS

4.4.1 Library preparation

A custom shRNA library targeting 420 RNA-binding proteins was designed using miR30-adapted BIOPREDsi predictions (six shRNAs per gene) and constructed by PCR-cloning a pool of oligonucleotides synthesized on 55k customized arrays (Agilent Technologies) as previously described (Zuber et al., 2011).

4.4.2 High-Throughput DNA Production

Transfection quality DNA was prepped with 96 well Purelink kits (Invitrogen) with average yields of 4g DNA/well. DNA was quantified by PicoGreen assay (Molecular Probes) using a HT plate reader (Molecular Systems). DNA concentrations were normalized robotically (Biomek Robot) across plates. Relative transfection efficiencies varied by <2-fold across a single plate, as measured by GFP fluorescence under the microscope.

4.4.3 High-Throughput Lentiviral Production

Lentiviruses were made by transfecting packaging cells (293T) with a 4-plasmid system using 50 ng each of Rev, Tat and PMZ plasmid, 150 ng of VSVG, and 300 ng of PGIPZ per well. Transfections were performed in 96-well plates to generate lenti-viruses in a high-throughput manner. Packaging cells were seeded with a multichannel pipette at a density of 2.2 x 10^4 cells per well in 100 ml media (DMEM/10% FBS/no antibiotics) 24 hours before transfection and grown at 37^0C/5 % CO_2. DNA for transfections was prepared with a mixture of 50ml Opti-MEM (Gibco) and 3ml Mirus LTE (Mirus Bio LLC)

and added to the DNA, this mixture was incubated for 15 min before addition to the packaging cells. Cells were incubated for 24 h, and the media was changed very carefully without disturbing the cells to remove any remaining transfection reagent. Lentiviral supernatants were collected at 48 and 60h post-transfection. The supernatants from the 48 and 60 h time points were then pooled and re-arrayed into 96-well plates for the final screen.

4.4.4 High-Throughput Lentiviral Infections and cDNA Extraction

Infection conditions were optimized in 96-well plates for growth conditions, plate types, viral dose and assay times, prior to large-scale screening. Seeding U-118 cells at a density of 1200 cells/well in a 96-well assay plate (Costar 3712) was optimal for extracting cDNA 4 days post-infection. This resulted in cells being ~90% confluent at the time of assay. Target cells were seeded in 96-well plates in 50 ml media (DMEM/10%FBS/antibiotics) and plates were kept at room temperature for 1 h prior to incubation at $37^{o}C/5\%CO_2$. After 24 h, 25µl of the medium was removed from each well and 3µL of polybrene was added to each well to achieve a final polybrene concentration of 8µg/mL. Following this, 100µL of the shRNA lentivirus was added and the well contents were mixed gently. The plates were then spun at 2250 rpm for 90 min at $25^{o}C$. The medium was then removed and replaced with fresh medium (50 µL).

4.4.5 High-throughput qPCR Assay and Data Analysis

Four days post-infection, target cells were lysed with 10 mM KCl, 10 mM Tris pH8, 1.5 mM MgCl2 and 1% NP-40. cDNA was prepared using Ambion's Cells to Ct kit according

to the manufacturers protocol. cDNA from 96-well plates of target cells were analyzed for PK-M1 transcript using QPCR analysis. Quantitative PCR reactions were performed using Applied Biosystem FAM and VIC-MGB primer/probe sets and Agilent III fast QPCR Master Mix on an ABI Prism 7900HT Real-Time PCR machine (Applied Biosystems). Constitutive PKM levels in the same cDNA samples were measured in the same qPCR reactions using multiplexing, which served as an endogenous control for splicing. qPCR reactions for PK-M1 plasmids were run as standards, and single Ct (cycles to threshold) values were used in the comparative Ct method (ABI User Bulletin #2) for relative quantification of PK-M1 gene expression. Control infections using either a shRNA targeting luciferase or a shRNA not targeting any human gene were used to define 100 % expression. Data for each lentiviral sample was rejected unless the Ct values were in the range of 18-35, on grounds that noise levels are too high beyond that range to allow reliably estimating changes in PKM level.

4.4.6 Lentiviral Production and Infections for Hit Follow-up Experiments

DNA for selected hairpins was prepared using mini- or maxi-prep kits (Invitrogen). Packaging cells (293T) were seeded onto 60 mm dishes at a density of 8 x 10^5 cells 24 h prior to transfection. A mixture containing 100mL OptiMEM (GIBCO), 0.5µg Rev, Tat, PMZ respectively, 1.5 µg VSVG, 2µg pGIPZ and 10µL Mirus LTE was added to a 1.5 mL Eppendorf tube and incubated for 15 min at room temperature. This transfection mixture was then transferred to 60 mm dishes containing packaging cells and incubated at 37^0C/ 5% CO_2. At 36 h post-transfection, lentiviral supernatants were removed from

plates of producer cells. These supernatants were stored at 4^{o}C and 5 mL of fresh medium (DMEM/10% FBS/pen-strep/glutamine) was added and the dishes were incubated for an additional 12 h, followed by a second lentiviral supernatant collection. The 36 and 48 hour lentiviral supernatants were pooled and stored at -20^{o}C until required. For infections, target cells (2.5 x 10^5 U118 and A-172) were seeded onto 60 mm dishes and allowed to grow at 37^{o}C/5% CO_2 for 24 hours. Lentiviral supernatants were gently transferred to dishes containing the target cells, polybrene (Sigma) was added to the dishes to a final concentration of 8μg/mL, and the cells were incubated 4-6 h at 37^{o}C/5% CO_2. The lentiviral supernatants were then removed and replaced with fresh medium (DMEM/10% FBS/pen-strep/glutamine). The target cells were grown at 37^{o}C/5% CO_2 for 12-24 h prior to being split into two 60 mm dishes. Puromycin was added 24 h after splitting to a final concentration of 2 μg/mL and cells were incubated for 3 additional days at 37^{o}C/5% CO_2. The total incubation time post-infection was 4 days.

4.4.7 Immunoblot Analyses

Cells were rinsed twice with phosphate buffered saline (PBS), collected by scraping, and harvested by centrifugation (1250 rpm/4 minutes/25^{0}C). Cell pellets were then re-suspended in 200 μL of chilled lysis buffer [50mM Tris pH8.0, 150 mM NaCl, 1 % NP-40, 0.5 % sodium deoxycholate, 0.1 % SDS, 1 mM Na_3VO_4, 25 mM NaF, 5 mM sodium pyrophosphate, 5mM sodium β-glycerophosphate and a cocktail of protease inhibitors

(Roche)], transferred to 1.5 mL Eppendorf tubes, vortexed thrice for 5 sec and incubated on ice for 30 min. Cell lysates were then centrifuged at 16000 x *g* (10 min/4^{o}C) and supernatants transferred to fresh 1.5 mL tubes. Protein concentrations were determined by Bradford assay (BioRad). Protein extracts were separated by SDS-PAGE and immunoblotting was performed, probing with the indicated antibodies, and quantifying with an Odyssey infrared-imaging system (LI-COR Biosciences). Primary antibodies were: tubulin (Genscript rAb, 1:5000); SRSF1 (mAb AK96 culture supernatant, 1:100 (28)); RBFOX2(sigma rAb 1:1000); SRSF6 (mAb 9126 culture supernatant, 1:100)); PTB (mAb SH54 culture supernatant, 1:100 (30) or Abcam rAb83897, 1:1000); secondary antibodies were IRdye 800 or 680 anti-rabbit, anti-mouse, or anti-goat (LI-COR Biosciences, 1:10,000).

4.4.8 Quantitative RT-PCR

Total RNA was harvested from cells in 6 cm tissue culture plates using Trizol (Invitrogen). Reverse transcription reactions were carried out using a Promega II RT Kit (Promega). Quantitative PCR reactions were performed using Applied Biosystems FAM-MGB primer/probe sets and Agilent II fast PCR Master Mix or using Power Sybr Green system (Applied Biosystems) on an ABI Prism 7900HT Real-Time PCR machine (Applied Biosystems). Quantification of actin levels in the same cDNA samples measured in separate qPCR reactions served as an endogenous control. All qPCR reactions were run in triplicate, and the average Ct (cycles to threshold) were used in the comparative Ct

method (ABI User Bulletin #2) for relative quantification of target gene expression. Control infections using a shRNA targeting luciferase were used to define 100% expression.

4.4.9 Titering Assay

Viruses were titered using U118 cells, plated in 6 well dishes at 10^5 cells per well. The next day, cells were infected with 1 ml of highly diluted virus (1:5-1:3665) using a standard spin infection protocol with 8µg/ml polybrene. 24 hours post infection, GFP expression was observed and cells were counted 4 days after infection and the M.O.I calculated as previously described (Zhang et al., 2004).

Figure 4.1 Vector Features and Application Scheme

PGIPZ lentivirus vector was used for the screen, which had a CMV promoter, GFP as the fluorescent marker, puromycin resistance and a mir22 shRNA cassette.

(A) The shRNA screen workflow for detection of factors affecting PKM-1 isoform.

(B) Different dilutions of virus were transduced in U-118 cells, and cells with GFP were counted 96 hours after infection and the M.O.I determined. An M.O.I 10 was used for the final screening, which gave 100% transduction and did not require puromycin selection.

(C) Representative images of GFP immunofluorescence after infection with virus at MOI=10 in three independent 96 well plates, 96 hours after infection.

(A)

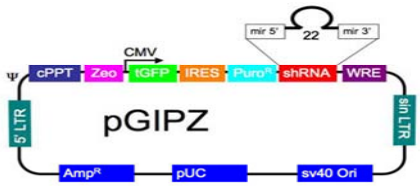
mir 5'
22
mir 3'
CMV
Ψ
cPPT
Zeo
tGFP
IRES
Puro^R
shRNA
WRE
5' LTR
pGIPZ
sin LTR
Amp^R
pUC
sv40 Ori

(B)

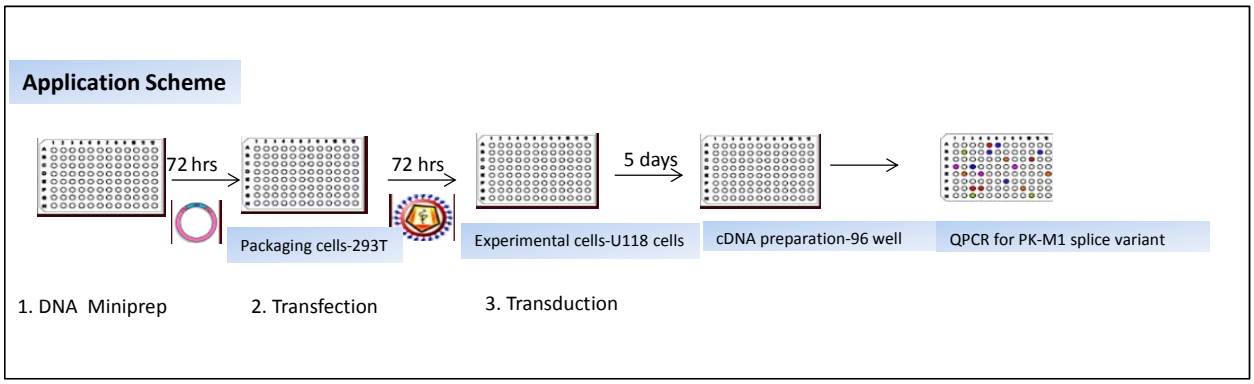
Application Scheme
72 hrs
72 hrs
5 days
Packaging cells-293T
Experimental cells-U118 cells
cDNA preparation-96 well
QPCR for PK-M1 splice variant
1. DNA Miniprep
2. Transfection
3. Transduction

(C)

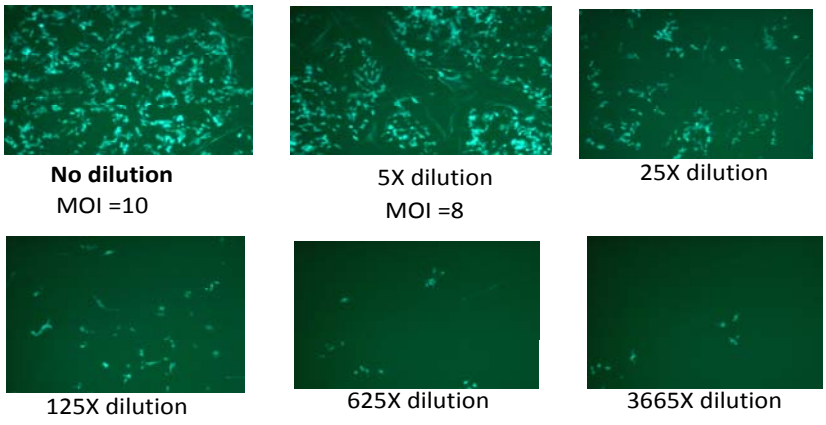
No dilution
MOI =10
5X dilution
MOI =8
25X dilution
125X dilution
625X dilution
3665X dilution

(D)

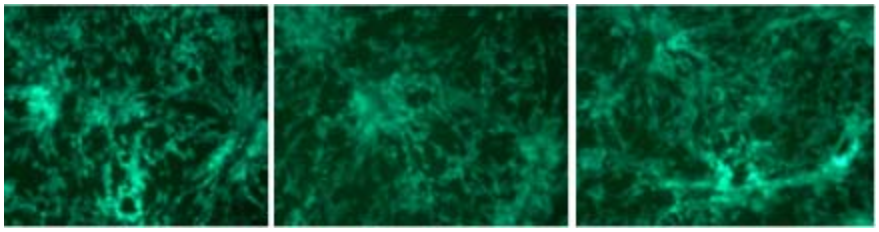

Fig 4.2 Knockdown Performance of HT-Generated Lentivirus in U-118 Cells

(A) Knockdown performance of lentiviruses representing 58 shRNAs targeting 6 different splicing factors (SRSF1, SRSF2, SRSF6, RBFOX2, hnRNPM, SRSF10). Protein levels for duplicate experiments were measured by western blot and are reported for each shRNA hairpin relative to average protein levels for control infections (i.e., a shRNA targeting scrambled sequence). Knockdown for the first set of infections is shown by black bars and the second set of infections by grey bars. Total protein levels in control cell lines infected with luciferase is shown with the black line at 100%.

(B) Knockdown performance of lentiviruses representing 30 shRNAs targeting 4 different splicing factors (SRSF3, SRSF4, SRSF5, hnRNPH3). Transcript levels for triplicate experiments were measured by qRT-PCR and are reported for each shRNA hairpin relative to average transcript levels for control infections (i.e., a shRNA targeting a scrambled sequence). Error bars show S.D.

(A)

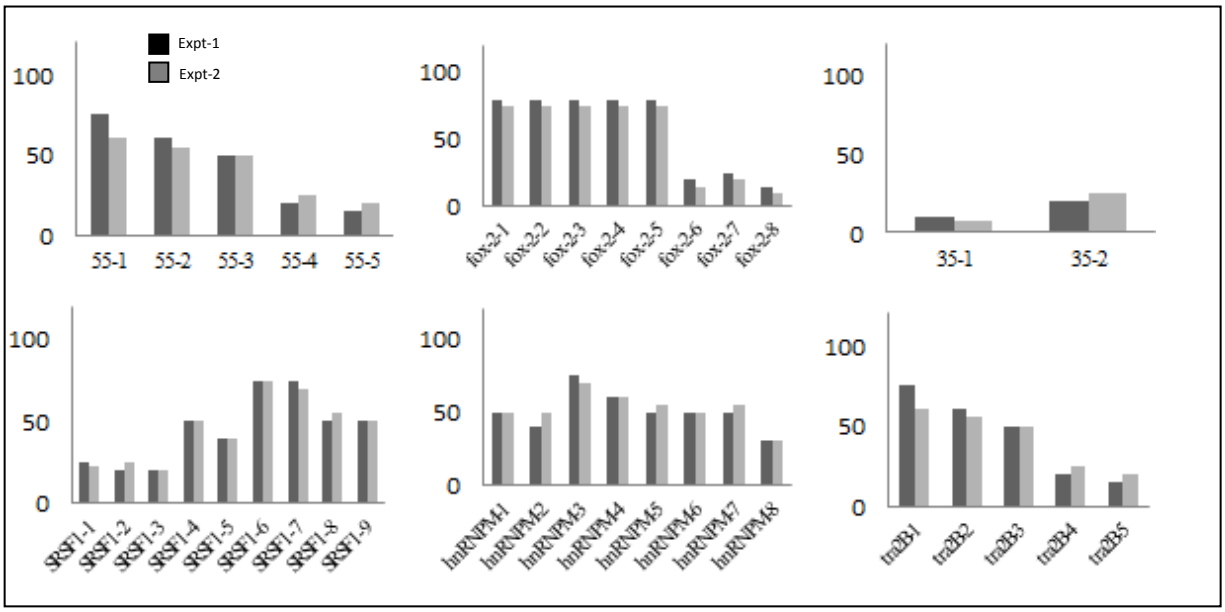
Expt-1
Expt-2
100
50
0
55-1
55-2
55-3
55-4
55-5
fox-2-1
fox-2-2
fox-2-3
fox-2-4
fox-2-5
fox-2-6
fox-2-7
fox-2-8
35-1
35-2
SRSF1-1
SRSF1-2
SRSF1-3
SRSF1-4
SRSF1-5
SRSF1-6
SRSF1-7
SRSF1-8
SRSF1-9
hnRNPM1
hnRNPM2
hnRNPM3
hnRNPM4
hnRNPM5
hnRNPM6
hnRNPM7
hnRNPM8
tra2B1
tra2B2
tra2B3
tra2B4
tra2B5

(B)

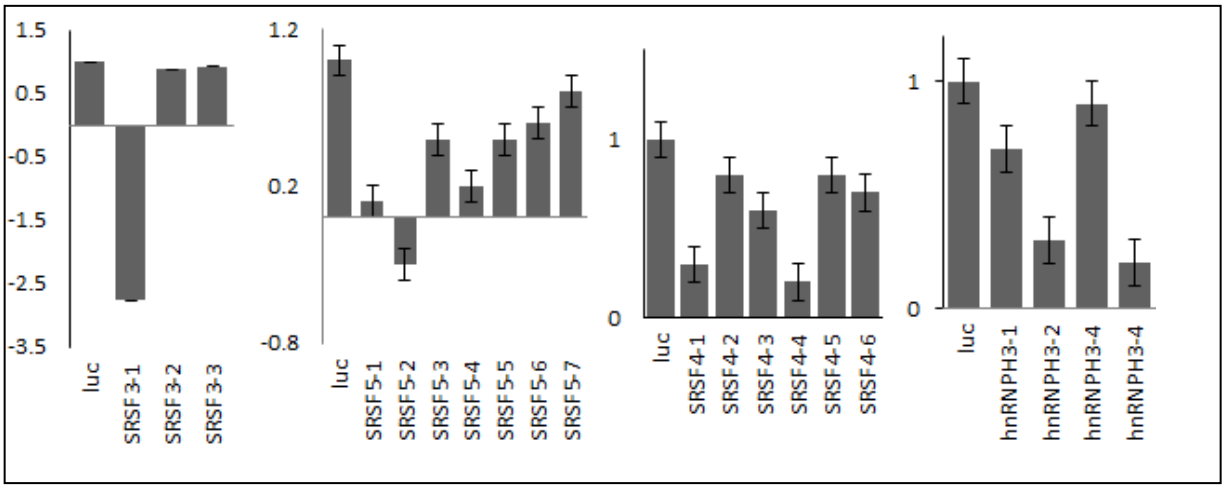
1.5
0.5
-0.5
-1.5
-2.5
-3.5
luc
SRSF3-1
SRSF3-2
SRSF3-3
1.2
0.2
-0.8
luc
SRSF5-1
SRSF5-2
SRSF5-3
SRSF5-4
SRSF5-5
SRSF5-6
SRSF5-7
1
0
luc
SRSF4-1
SRSF4-2
SRSF4-3
SRSF4-4
SRSF4-5
SRSF4-6
1
0
luc
hnRNPH3-1
hnRNPH3-2
hnRNPH3-3
hnRNPH3-4

Fig 4.3 Screen for RNA Binding Proteins that Increase PKM-1 Transcript Level Upon Knockdown

(A) Scheme for the QPCR based multiplex splicing screen. Primers annealing to exon 8 and exon 11, and VIC-MGB probe annealing to exon 9, respectively, were used to amplify human PK-M1 transcript. The alternative exons that encode the distinctive segments of PK-M1 and PK-M2 are indicated in black and grey, respectively. Primers annealing to exon 11 and exon 12 and FAM-NFQ probe annealing to exon 12 were used to amplify constitutively spliced region of PKM1/2 transcript, which served as the internal control for the splicing qPCR assay. Nucleotide sequence alignments of ME exons 9 (M1) and 10 (M2). Primer on exon 9 anneals to the region with highest mismatch between exon 9 and exon 10, as shown by the red box. Representative graph of qPCR amplification curves detecting PK-M1 mRNA levels from one 384-well qPCR plate of the screen. (*Inset*) The complete curves are shown.

(B) Change in PKM-1 levels in various cell lines and different positive and negative controls, as seen by the qPCR. The change in PKM-1 levels correlates with the changes seen by semi-quantitative PCR, as discussed before (data not shown). Results are Mean +/- S.D shown from three independent experiments.

(A)

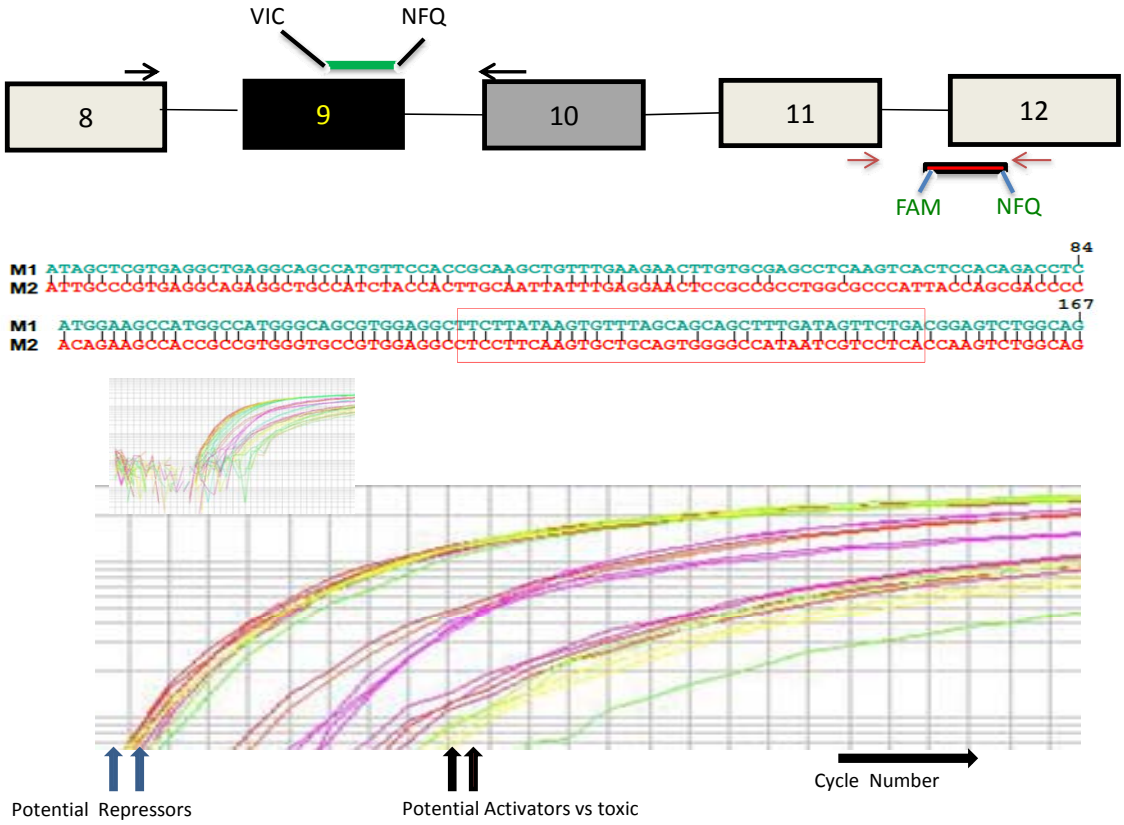
VIC
NFQ
8
9
10
11
12
FAM
NFQ
M1 ATAGCTCGTGAGGCTGAGGCAGCCATGTTCCACCGCAAGCTGTTTGAAGAACTTGTGCGAGCCTCAAGTCACTCCACAGACCTC
M2 ATTGCCCGTGAGGCAGAGGCTGCCATCTACCACTTGCAATTATTTGAGGAACTCCGCCGCCTGGCGCCCATTACCAGCGACCCC
84
167
M1 ATGGAAGCCATGGCCATGGGCAGCGTGGAGGCTTCTTATAAGTGTTTAGCAGCAGCTTTGATAGTTCTGACGGAGTCTGGCAG
M2 ACAGAAGCCACCGCCGTGGGTGCCGTGGAGGCCTCCTTCAAGTGCTGCAGTGGGGCCATAATCGTCCTCACCAAGTCTGGCAG
Potential Repressors
Potential Activators vs toxic
Cycle Number

(B)

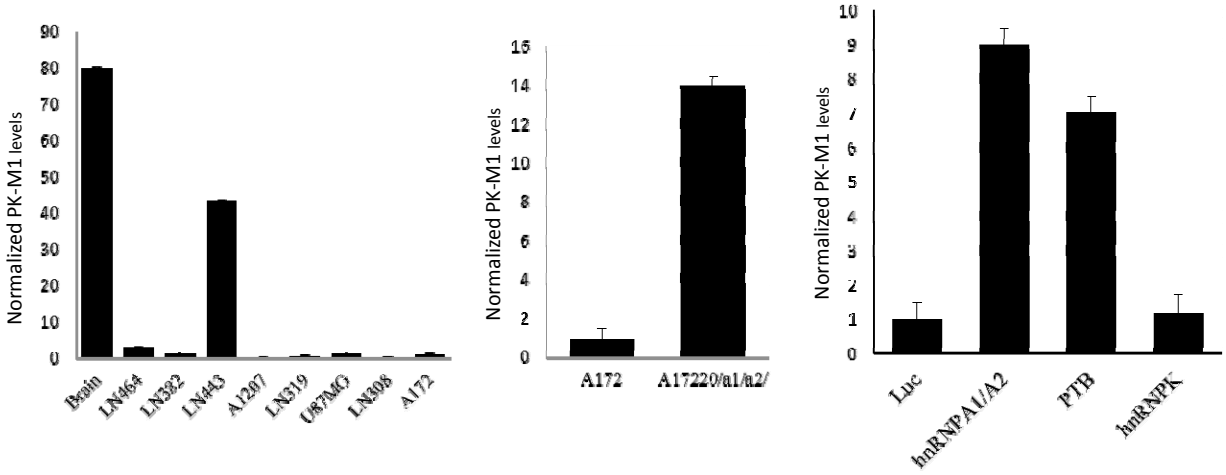
Normalized PK-M1 levels
90
80
70
60
50
40
30
20
10
0
Brain
LN464
LN382
LN443
A1207
LN319
U87MG
LN308
A172
Glioblastoma cells lines
Normalized PK-M1 levels
16
14
12
10
8
6
4
2
0
A172
A17220/a1/a2/
A172 cells
Normalized PK-M1 levels
10
9
8
7
6
5
4
3
2
1
0
Luc
hnRNPA1/A2
PTB
hnRNPK
U118 cells

Fig 4.4 Scatter plot for raw Ct values.

(A) Scatter plot showing raw Ct values from the entire library plotted against total well numbers. Blue represents Ct values for PK-M1 transcript and pink represents Ct values for PK-M constitutive region.

(B) Scatter plot showing raw Ct values from the entire library plotted against shRNA plates. Black represents Ct values for PK-M1 transcript and pink represents Ct values for PK-M constitutive transcript.

Both plots depict the relatively disciplined variation in Ct values and the raw result output from the entire screen, which increases confidence in the primary screen results.

(A)

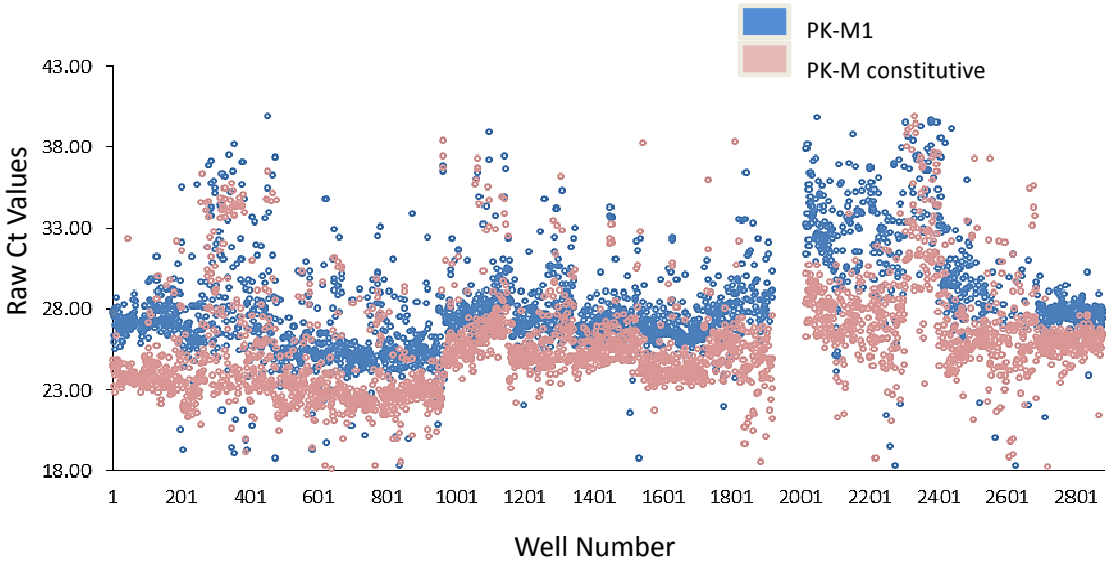
PK-M1
PK-M constitutive
43.00
38.00
33.00
28.00
23.00
18.00
Raw Ct Values
1
201
401
601
801
1001
1201
1401
1601
1801
2001
2201
2401
2601
2801
Well Number

(B)

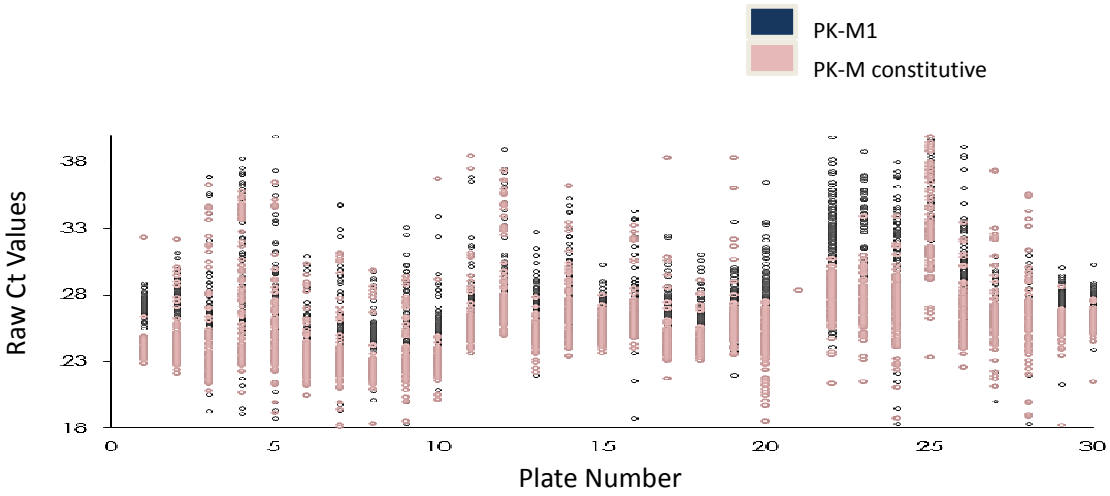
PK-M1
PK-M constitutive
38
33
28
23
18
Raw Ct Values
0
5
10
15
20
25
30
Plate Number

Fig 4.5 shRNA qPCR screen identifies mediators of the PKM-splicing.

(A) Analysis of the Ct values of shRNAs from the QPCR screen experiment for outlier identification. Data are normalized against the internal control PKM constitutive and plotted as the $\log_2$(ratio FAM/VIC) versus $\log_2$(√intensity FAM×VIC)). The red dots represent select enriched shRNAs that exhibited > 2.5-sigma increase in PK-M1 levels in the screen.

(B) Bin diagram of fold induction of PK-M1 in randomly scattered positive-control wells from the screen, that correlate with changes seen previously in our earlier studies with semi-quantitative PCR discussed in previous chapters.

(A)

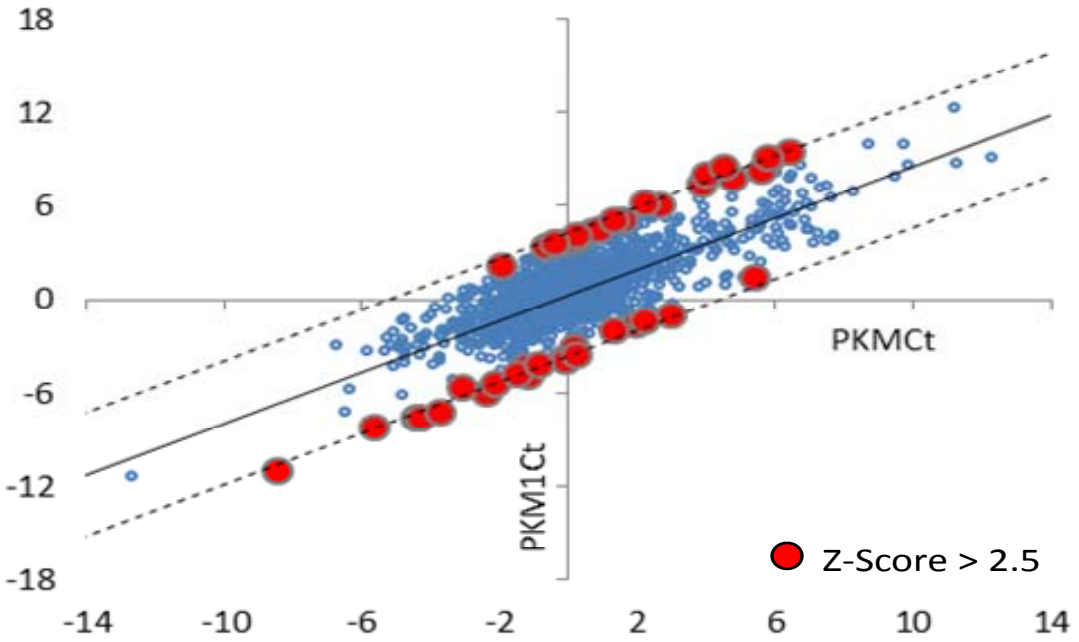
18
12
6
0
-6
-12
-18
-14
-10
-6
-2
2
6
10
14
PKMCt
PKM1Ct
Z-Score > 2.5

(B)

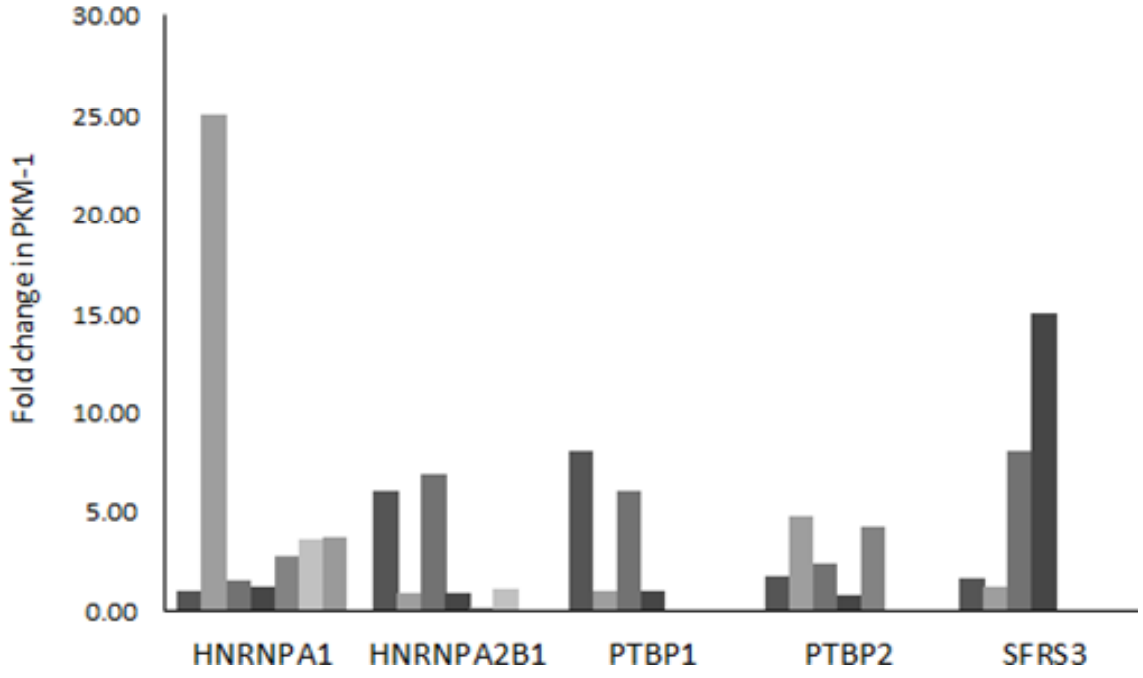
30.00
25.00
20.00
15.00
10.00
5.00
0.00
Fold change in PKM-1
HNRNPA1
HNRNPA2B1
PTBP1
PTBP2
SFRS3

Table 1: Top RNA Binding Proteins that changed PKM-1 levels > 5 fold

THOC6	THO complex subunit 6 homolog;THOC6	mRNA processing factor
SMNDC1	Survival of motor neuron-related-splicing factor 3	mRNA processing factor
KHSRP	Far upstream element-binding protein 2;KHSRP	mRNA processing factor
PABPC1	Polyadenylate-binding protein 1;PABPC1	mRNA processing factor
SFRS3 a b	Splicing factor, arginine/serine-rich 3;SFRS3	mRNA processing factor
SFRS5 a	Splicing factor, arginine/serine-rich 5;SFRS5	mRNA processing factor
FUBP1 b	Far upstream element-binding protein 1;FUBP1	mRNA processing factor
BRUNOL4 a c	CUG-BP- and ETR-3-like factor 4;BRUNOL4	mRNA processing factor
SFRS10 a	Splicing factor, arginine/serine-rich 10;SFRS10	mRNA processing factor
SFRS8 a	Splicing factor, arginine/serine-rich 8;SFRS8	mRNA processing factor
TRA2A a b	Transformer-2 protein homolog;TRA2A	mRNA processing factor
ROD1	Regulator of differentiation 1;ROD1	mRNA processing factor
SNRPA	U1 small nuclear ribonucleoprotein A;SNRPA	mRNA processing factor
BCAS2 a b	Pre-mRNA-splicing factor SPF27;BCAS2	mRNA processing factor
CDC40	Pre-mRNA-processing factor 17;CDC40	mRNA processing factor
SNRPD3	Small nuclear ribonucleoprotein Sm D3;SNRPD3	mRNA processing factor
NCBP1	Nuclear cap-binding protein subunit 1;NCBP1	mRNA processing factor
LSM5	U6 snRNA-associated Sm-like protein LSm5;LSM5	mRNA processing factor
PCBP3	Poly(rC)-binding protein 3;PCBP3	mRNA processing factor
PCBP4	Poly(rC)-binding protein 4;PCBP4	mRNA processing factor

ZCCHC8	Zinc finger CCHC domain-containing protein 8;ZC	nucleic acid binding
THOC1	THO complex subunit 1;THOC1	nucleic acid binding
SRP68	Signal recognition particle 68 kDa protein;SRP68	nucleic acid binding
RBM7	RNA-binding protein 7;RBM7	nucleic acid binding
CLK4	Dual specificity protein kinase CLK4;CLK4	protein kinase
CLK3	Dual specificity protein kinase CLK3;CLK3	protein kinase
RBM42	RNA-binding protein 42;RBM42	replication origin binding pro
HNRNPF [a] [b]	Heterogeneous nuclear ribonucleoprotein F;HNR	ribosomal protein
HNRNPH3 [a]	Heterogeneous nuclear ribonucleoprotein H3;HI	ribosomal protein
GRSF1	G-rich sequence factor 1;GRSF1	ribosomal protein
HNRNPH1 [a] [b]	Heterogeneous nuclear ribonucleoprotein H;HNI	ribosomal protein
RBM5 [a]	RNA-binding protein 5;RBM5	RNA binding protein
NCBP2	Nuclear cap-binding protein subunit 2;NCBP2	RNA binding protein
RBMX2	RNA-binding motif protein, X-linked 2;RBMX2	RNA binding protein
DHX38	Pre-mRNA-splicing factor ATP-dependent RNA hel	RNA helicase
DDX21	Probable ATP-dependent RNA helicase DDX56;DI	RNA helicase
DHX8	ATP-dependent RNA helicase DHX8;DHX8	RNA helicase
DDX21	Nucleolar RNA helicase 2;DDX21	RNA helicase
CCNK	Cyclin-K;CCNK	transcription cofactor
RUVBL2	RuvB-like 2;RUVBL2	transcription cofactor
KLHDC8A	Kelch domain-containing protein 8A;KLHDC8A	transcription cofactor
KHDRBS3 [c]	KH domain-containing, RNA-binding, signal trans	transcription cofactor
FUS [c]	RNA-binding protein FUS;FUS	transcription factor
TARDBP	TAR DNA-binding protein 43;TARDBP	transcription factor
ANXA2	Annexin A2;ANXA2	transfer/carrier protein
FRG1	Protein FRG1;FRG1	transfer/carrier protein
QPCT	Glutaminyl-peptide cyclotransferase;QPCT	transferase

YWHAQ	14-3-3 protein theta;YWHAQ	chaperone
ACIN1	Apoptotic chromatin condensation inducer in the	chromatin/chromatin-bindin
SMARCA5	SWI/SNF-related matrix-associated actin-depend	DNA helicase
SKIV2L2	Superkiller viralicidic activity 2-like 2;SKIV2L2	DNA helicase
TOP1	DNA topoisomerase 1;TOP1	DNA topoisomerase
EXOSC8	Exosome complex exonuclease RRP43;EXOSC8	exoribonuclease
TOPORS	E3 ubiquitin-protein ligase Topors;TOPORS	isomerase
CCNA1	Cyclin-A1;CCNA1	kinase activator
CCDC55	Coiled-coil domain-containing protein 55;CCDC55	
GPATCH1	G patch domain-containing protein 1;GPATCH1	
LSM10	U7 snRNA-associated Sm-like protein LSm10;LSM10	
SFRS17A	Splicing factor, arginine/serine-rich 17A;SFRS17A	
TDRD3	Tudor domain-containing protein 3;TDRD3	
CROP	Cisplatin resistance-associated overexpressed protein;CROP	
KIN	DNA/RNA-binding protein KIN17;KIN	
TET1	Protein TET1;TET1	

a- Known regulators of mammalian splicing
b- Implicated in tumorigenesis
c- Known expression in differentiated tissues: muscle, brain, testis

Chapter 5

Concluding Remarks

5.1 Introduction

Alternative splicing of Pyruvate Kinase M (PK-M) confers distinctive metabolic properties to cancer cells (the Warburg effect). The M1 and M2 pyruvate-kinase isozymes are expressed from a single gene through alternative splicing of a pair of mutually exclusive exons. Considering that PK-M splicing is a key regulator of the Warburg effect, I sought to elucidate the mechanisms of PK-M alternative splicing. I focused my studies on *trans*-acting factors that bind to their cognate *cis*-acting elements in the PK-M pre-mRNA. Here, I summarize my findings and discuss potential directions of future research.

By measuring the expression of M1 and M2 mRNA and protein isoforms in mouse tissues, tumor cell lines, and during terminal differentiation of muscle cells, I verified that alternative splicing regulation is sufficient to account for the levels of expressed protein isoforms. I further demonstrated that the M1-specific exon is actively repressed in cancer-cell lines, and that the related splicing repressors hnRNP A1 and A2, as well as the polypyrimidine-tract-binding protein PTB, contribute to this control. Down-regulation of these splicing repressors in cancer-cell lines using shRNAs rescues M1 isoform expression and decreases the extent of lactate production. These findings extended the link between alternative splicing and cancer, and began to define some of the factors responsible for the switch to aerobic glycolysis. The detailed results were

presented in Chapter 2.

By studying the expression pattern of PK-M splicing in cells with SRSF3 knockdown, I also demonstrated that SRSF3 functions as an activator of exon 10 of the PK-M gene. SRSF3 acts in an additive fashion with the previously characterized exon 9 repressors hnRNPA1/A2 and PTB. SRSF3 was recently shown to be an oncogenic SR protein, and I found overexpression of SRSF3 in multiple cancer cell lines, which also expressed high levels of PK-M2 (exon 10 inclusion). These findings were presented in Chapter 3.

It was not possible to revert cancer cells to exclusively expressing the PK-M1 isoform by knocking down all the above factors together – hnRNPA1, hnRNPA2, PTB, and SRSF3. This observation suggested that there are additional levels of control that play a role in PK-M splicing. In general, individual AS events are thought to be controlled combinatorially by multiple *trans*-acting factors. Therefore, as a more exhaustive approach to identifying other factors involved in PK-M alternative splicing, I carried out a directed lentivirus shRNA screen. Our lab had designed and obtained a focused lentiviral shRNA library in PGIPZ, with an average of seven hairpins for each of ~400 factors involved or at least implicated in constitutive and/or alternative splicing, including many RNA-binding proteins, spliceosome components, RNA helicases, and modifying enzymes. I used this shRNA library to investigate additional factors involved in the splicing control of PK-M.

I transduced U118 glioblastoma cells with individual constructs, and generated cDNA for analysis. Initial results showed that unlike most cell lines, U118 cells express detectable

levels of PK-M1 (~30%) at the mRNA and protein level, in addition to PK-M2. Therefore, using these cell lines in a shRNA screen provides the advantage that changes in expression in either direction towards the M1 and M2 isoforms are more likely to be detected. I accomplished the following: a) I validated the initial knockdown efficiency of the library using western blotting (in the case of factors for which antibodies are available) and qPCR, and tested knockdown efficiency for pooled versus unpooled vectors; b) I optimized the lentivirus transduction protocol and cDNA synthesis in 96-well format; c) I optimized QPCR protocols for identifying the two alternatively spliced PK-M isoforms, with each sample initially tested for PK-M isoform expression at the mRNA level using the RT-PCR plus cleavage assay established during our previous work on this project (as a control); and d) I undertook the shRNA library screening in U-118 cells. The screen identified 45 candidates that increase PK-M1 isoform levels, and potentially play a role in modulating the PK-M1/PK-M2 ratio in glioblastoma cells.

5.2 Summary and Future Perspective

In summary, by studying the *trans*-acting factors that regulate the PK-M splicing ratio in proliferating versus differentiated cells, my dissertation underscores the importance of splicing in regulating one of the hallmarks of cancer. My studies are consistent with a model that posits that cancer cells display mis-regulation of various RNA-binding proteins, which in turn causes downstream splicing defects. By studying *trans*-acting factors, my work describes the role of specific splicing factors in control of cancer-cell metabolism or the Warburg effect. However, further research will be necessary to

understand all levels of control of the mutually exclusive alternative splicing of PK-M, and the role of various *trans*-acting factors in this process.

hnRNPs and SRSF3 regulating the mutual exclusivity of PK-M in a tissue-specific manner is a starting point for understanding the complex regulation of this gene. The outcome of the shRNA screen suggests that there are various other RNA-binding and splicing-related factors that could play important roles in splicing regulation. Candidate factors that I identified in the primary screen need to be validated using semi-quantitative PCR. Thereafter, top hits need to be categorized based on their p-values determined in the initial screen, tested for reciprocal effects by overexpression, and their mechanism of action characterized, e.g., by RNA-binding assays and functional studies in the context of glucose metabolism. Functional analysis will involve overexpression studies in glioblastoma cell lines and investigating metabolic changes, such as lactate production. Candidate factors that have additional cell lines environment specificity will need to be addressed, as the precise mechanisms of PK-M splicing regulation may be context-dependent.

Though most of the protein hits from the qPCR screen are known splicing factors responsible for mediating alternative splicing, my screen also found protein kinases, such as CLK3/4, ribosomal proteins, helicases, transcriptional cofactors and chromatin-binding proteins as potential mediators of PK-M alternative splicing. In the future, to examine the total network of controls on PK-M splicing, it will be necessary to perform a genome wide screen, which would implicate factors which have not been investigated in splicing till now. Only a few of the factors found in my focused screen, have, so far been

investigated in cancer and tissue-specific alternative splicing. Therefore, future studies should involve experiments to investigate the role of the above-mentioned factors not only in PK-M splicing, but also in tumor initiation and progression.

It should be mentioned here that my primary screen found chromatin-binding factors as a class of regulators of PK-M splicing. A recent string of papers have suggested that transcription and splicing influence each other (Carrillo Oesterreich et al., 2010; Gornemann et al., 2005; Shukla et al., 2011). It has been known for some time that chromatin modification plays an important role in transcription, but the role of chromatin and histone modification in pre-mRNA splicing is only slowly coming to light now. It is intriguing to consider that PK-M splicing regulation could be a co-transcriptional process. It has been shown that splicing can induce pausing of RNA pol II during transcription, and RNA pol II pausing influenced by zinc-finger binding proteins like CTCF, increases the time window for co-transcriptional alternative splicing. One possibility is that one or more of the chromatin regulators found in my screen are overexpressed in certain cell lines~~,~~ and by binding to exon 9, promotes RNA pol II pausing and thereby mediates weaker exon 9 inclusion. This could explain the expression of PK-M1 in certain cell lines and not others. Although extensive literature has been devoted to the role of RNA-binding proteins in alternative splicing, only a few examples have hitherto been found to mediate alternative splicing via mutually exclusive exons in mammalian systems. Given that PK-M splicing has consequences for tumor maintenance, the isolation of factors that selectively mediate exon 10 splicing in cancer cells would not only advance our knowledge of alternative splicing but would

also give us important insights about tumor maintenance and proliferation in general, and tumor metabolism in particular.

Appendix 1

Table showing raw Ct values obtained from the qPCR screen

Destination plate	Destination row	Destination column	Gene Symbol (only first string)	PKM1Ct	PKMCt
A001	a	1	RBBP7	Undetermined	30.94702
A001	a	2	PRPF38A	27.71435	24.55254
A001	a	3	PRPF18	27.8317	24.41447
A001	a	4	SRPK3	27.8673	24.82695
A001	a	5	ROD1	25.97299	23.22708
A001	a	6	CCNA1	27.4881	24.11491
A001	a	7	SF3B14	26.32376	23.25008
A001	a	8	WTAP	28.03156	24.51155
A001	a	9	IK	27.86287	24.55383
A001	a	10	SFRS7	26.99128	23.86771
A001	a	11	CPSF2	25.48396	22.87009
A001	a	12	PLRG1	27.53966	24.88059
A001	b	1	DDX23	Undetermined	Undetermined
A001	b	2	TDRD3	27.47233	24.45599
A001	b	3	KIN	28.71756	26.3485
A001	b	4	DDX39	27.14167	24.29472
A001	b	5	SMU1	28.11001	24.83565
A001	b	6	QPCT	26.98236	23.95048
A001	b	7	KHDRBS1	26.93807	24.11726
A001	b	8	SNRNP48	26.85768	24.06385
A001	b	9	CCNK	27.82193	24.74432
A001	b	10	POLR2B	26.60191	23.26825
A001	b	11	C2orf3	27.31984	24.62144
A001	b	12	EXOSC4	25.6885	23.8936
A001	c	1	EXOSC9	27.52269	24.55727
A001	c	2	C14orf166	26.98575	23.49734
A001	c	3	DGCR14	26.04291	23.41789
A001	c	4	FMR1	26.47105	23.44498
A001	c	5	HNRNPK	27.44838	23.30084
A001	c	6	SNRNP40	26.57735	23.07944
A001	c	7	SF4	26.761	23.43842
A001	c	8	SFRS4	27.25996	23.98971
A001	c	9	DHX15	26.69447	23.55634
A001	c	10	RAVER1	25.92831	23.58304
A001	c	11	FIP1L1	26.96229	23.9599

A001	c	12	ZRANB2	27.24734	24.6347
A001	d	1	MYEF2	28.25916	23.56198
A001	d	2	MFSD11	26.8266	23.40636
A001	d	3	CCDC94	26.94469	23.88333
A001	d	4	ILF2	27.39921	23.8744
A001	d	5	DIDO1	27.4593	23.52691
A001	d	6	SFRS4	26.41891	23.84708
A001	d	7	LOC643167	26.31228	23.83391
A001	d	8	DHX9	26.71881	23.59758
A001	d	9	LOC119358	26.75144	23.61842
A001	d	10	PPM1G	27.13467	23.93195
A001	d	11	FUBP1	27.47702	24.54676
A001	d	12	EXOSC4	27.05051	23.90472
A001	e	1	SMN1	Undetermined	32.3097
A001	e	2	SNRNP40	27.48922	24.40042
A001	e	3	ZCCHC8	27.02287	23.82056
A001	e	4	SFRS10	27.05702	23.81872
A001	e	5	RNF113A	27.37502	23.50518
A001	e	6	HNRNPH1	26.81591	23.72305
A001	e	7	TOP1	26.68849	23.59832
A001	e	8	HNRNPC	27.26483	23.47094
A001	e	9	TOP1	26.82796	23.56284
A001	e	10	POLR2A	26.96546	23.85826
A001	e	11	SNRPA	27.20914	24.09412
A001	e	12	PHF5A	27.33674	24.59114
A001	f	1	EXOSC9	27.68292	23.48276
A001	f	2	LOC100130003	27.0093	23.85155
A001	f	3	SMARCA5	28.52744	23.94741
A001	f	4	KIN	27.67166	23.88264
A001	f	5	TNRC4	27.47296	23.41695
A001	f	6	RBMXL2	26.93104	23.58451
A001	f	7	ELAVL3	27.79538	24.10277
A001	f	8	ILF2	28.88566	23.29418
A001	f	9	ZRANB2	28.49573	23.39586
A001	f	10	CPSF6	28.16953	23.57859
A001	f	11	CWC22	27.24745	23.35816
A001	f	12	DHX15	27.0579	23.90627
A001	g	1	SFRS7	Undetermined	Undetermined
A001	g	2	ROD1	Undetermined	Undetermined
A001	g	3	QKI	Undetermined	Undetermined
A001	g	4	RP9	Undetermined	Undetermined
A001	g	5	KIAA1429	Undetermined	Undetermined
A001	g	6	LUC7L2	Undetermined	Undetermined

A001	g	7	SFRS6	Undetermined	Undetermined
A001	g	8	XRCC6	Undetermined	Undetermined
A001	g	9	PRPF31	Undetermined	Undetermined
A001	g	10	THOC5	Undetermined	Undetermined
A001	g	11	BAT1	Undetermined	Undetermined
A001	g	12	CLK1	Undetermined	Undetermined
A001	h	1	PRPF3	Undetermined	Undetermined
A001	h	2	CCDC12	25.87673	22.84953
A001	h	3	LOC100128974	26.68313	23.77395
A001	h	4	C14orf166	26.89822	23.96921
A001	h	5	ELAVL3	26.22617	23.12479
A001	h	6	SFRS5	27.32393	23.42048
A001	h	7	EIF3M	26.5856	23.75683
A001	h	8	XRN2	26.51226	23.27966
A001	h	9	HNRNPU	27.20467	23.51781
A001	h	10	RALYL	27.09689	24.10961
A001	h	11	BUD13	27.10958	23.64125
A001	h	12	EXOSC8	27.3945	23.96734
A002	a	1	PRPF38A	28.18409	24.36004
A002	a	2	GRSF1	27.61517	25.08005
A002	a	3	HMGB1	28.14751	24.96934
A002	a	4	MYEF2	27.38667	24.87519
A002	a	5	A2BP1	27.1543	24.69133
A002	a	6	PPIL1	26.74361	23.79512
A002	a	7	SFPQ	27.41357	24.79764
A002	a	8	MLL	26.8564	23.0337
A002	a	9	BRUNOL6	26.92335	23.608
A002	a	10	CRNKL1	27.31628	24.46829
A002	a	11	PHF5A	26.87417	23.5003
A002	a	12	PCBP4	26.19382	23.24563
A002	b	1	SFRS1	27.06669	25.58927
A002	b	2	GPATCH1	29.6325	27.10703
A002	b	3	SFRS6	28.53844	25.15907
A002	b	4	SYNCRIP	27.66324	24.79609
A002	b	5	YBX1	29.70866	27.81431
A002	b	6	LOC728554	27.59894	24.13214
A002	b	7	HNRNPH2	29.87267	27.5503
A002	b	8	HNRPLL	27.9255	24.03799
A002	b	9	DNAJC8	28.3687	24.38751
A002	b	10	HTATSF1	28.43827	23.37853
A002	b	11	LSM10	27.49799	22.96947
A002	b	12	RBM10	27.65193	24.19125
A002	c	1	POLR2B	27.55162	24.76838

A002	c	2	RBBP7	27.1594	24.39708
A002	c	3	TAF15	27.1064	24.30153
A002	c	4	SNW1	27.16089	23.8492
A002	c	5	EIF2S2	27.15759	23.84322
A002	c	6	PRPF40A	27.07971	23.68817
A002	c	7	LOC100129566	27.2119	23.57234
A002	c	8	WDR25	26.87747	23.50324
A002	c	9	TOPORS	28.08657	24.55777
A002	c	10	SRPK2	31.20224	28.64503
A002	c	11	SAFB	29.71632	25.75388
A002	c	12	C16orf80	28.07621	23.28933
A002	d	1	EXOSC8	29.9372	24.73354
A002	d	2	PABPC1	29.0824	30.01706
A002	d	3	PSEN1	28.0509	24.53623
A002	d	4	XRN2	27.90568	22.85829
A002	d	5	HNRNPU	27.20423	23.07628
A002	d	6	NUMA1	27.3013	23.65739
A002	d	7	PRPF4	28.21799	23.66673
A002	d	8	PRPF19	28.86994	23.52818
A002	d	9	SNRNP35	26.55278	24.1116
A002	d	10	PSEN1	28.81898	22.38684
A002	d	11	NCBP1	Undetermined	22.10997
A002	d	12	MSI2	29.25786	25.0641
A002	e	1	C2orf3	27.99255	25.12866
A002	e	2	RNPS1	27.34324	23.83824
A002	e	3	FUS	27.26903	24.10816
A002	e	4	LNX1	27.3437	23.31791
A002	e	5	DGCR14	27.00198	23.38618
A002	e	6	NUDT21	26.76627	23.56655
A002	e	7	HNRNPA2B1	27.27192	23.6464
A002	e	8	TPR	27.56027	23.09471
A002	e	9	SCNM1	28.17716	24.31642
A002	e	10	FMR1	26.97566	23.03581
A002	e	11	DHX16	28.20711	23.4558
A002	e	12	KLHDC8A	29.22015	29.46769
A002	f	1	CCNK	28.03193	24.43814
A002	f	2	MYEF2	27.96802	24.12494
A002	f	3	SRPK1	26.99863	23.79164
A002	f	4	SRPK2	26.38392	23.32075
A002	f	5	EIF3A	27.61647	23.60221
A002	f	6	STRBP	26.32816	23.11479
A002	f	7	TAF15	27.10294	23.50651
A002	f	8	TCERG1	27.40212	23.46783

A002	f	9	IGF2BP3	28.42181	24.95751
A002	f	10	CLK2	28.58486	24.00741
A002	f	11	RBM15	28.51159	23.41801
A002	f	12	THOC6	29.18739	29.7726
A002	g	1	EXOSC8	27.02785	22.69399
A002	g	2	AKAP8	27.32644	23.93969
A002	g	3	CDC5L	26.73583	23.11898
A002	g	4	SFRS6	26.9851	23.17383
A002	g	5	RBM26	27.36279	22.88971
A002	g	6	BUD13	26.42108	23.2369
A002	g	7	BUD13	27.94413	23.1148
A002	g	8	YBX1	28.14963	22.76908
A002	g	9	HNRNPM	27.12346	23.27829
A002	g	10	ZNF207	29.24933	23.09845
A002	g	11	NCBP1	29.88491	24.24548
A002	g	12	HNRNPC	28.81428	28.99484
A002	h	1	HMG1L6	27.48066	24.18561
A002	h	2	SNIP1	29.14651	26.20278
A002	h	3	PPWD1	27.70145	24.25946
A002	h	4	LSM3	27.65819	24.28538
A002	h	5	PSEN1	26.66034	23.78597
A002	h	6	TMEM149	28.07707	25.41439
A002	h	7	STRBP	26.98396	23.61991
A002	h	8	SYNCRIP	Undetermined	32.17721
A002	h	9	NOSIP	27.35675	23.58011
A002	h	10	CPSF2	27.64762	23.27919
A002	h	11	LOC389465	30.79168	23.01491
A002	h	12	PRCC	28.14661	25.8567
A003	a	1	LOC389465	26.83833	24.54224
A003	a	2	RBM17	26.89283	23.59299
A003	a	3	RBM47	27.20265	25.12433
A003	a	4	USP39	28.97386	26.07978
A003	a	5	CHERP	26.04771	23.701
A003	a	6	MFSD11	20.51424	28.16946
A003	a	7	EIF3A	29.73137	25.30962
A003	a	8	C21orf66	28.95227	24.82462
A003	a	9	EXOSC10	27.89686	24.87847
A003	a	10	HNRPLL	32.10456	28.08737
A003	a	11	SF3B2	Undetermined	Undetermined
A003	a	12	PRCC	35.48457	31.61203
A003	b	1	EFTUD2	26.72697	24.36047
A003	b	2	CUGBP1	19.26476	23.53804
A003	b	3	EXOSC10	26.29778	23.05432

A003	b	4	SNRPF	25.32588	21.85909
A003	b	5	MOV10	25.71265	22.06373
A003	b	6	PRPF38B	25.52136	22.02708
A003	b	7	ISY1	24.43199	22.21906
A003	b	8	KIAA1429	Undetermined	21.73621
A003	b	9	C21orf66	26.50613	23.46401
A003	b	10	SAFB	26.77399	23.30431
A003	b	11	LSM3	16.09158	26.37609
A003	b	12	CCDC55	27.92465	24.77801
A003	c	1	HNRNPC	27.10047	25.10571
A003	c	2	MAGOHB	26.70277	22.66096
A003	c	3	DDX26B	26.93268	21.75484
A003	c	4	SNRPF	26.91738	21.87968
A003	c	5	GTF2I	26.18282	22.02289
A003	c	6	IGF2BP3	26.18767	21.31997
A003	c	7	CPSF1	26.91958	21.37781
A003	c	8	SYF2	24.99328	21.9522
A003	c	9	TAF6	25.75502	22.93888
A003	c	10	HNRNPF	25.40807	23.67825
A003	c	11	MSI1	26.64682	22.83786
A003	c	12	IQGAP1	27.13421	24.36165
A003	d	1	KPNA2	25.69124	22.43937
A003	d	2	NCL	25.92249	22.61279
A003	d	3	NXF1	26.09038	22.56764
A003	d	4	MOV10	26.45578	21.90134
A003	d	5	SNRNP70	31.24842	21.46008
A003	d	6	PPP1R8	28.15195	21.87802
A003	d	7	ELAVL2	Undetermined	16.93763
A003	d	8	TET1	23.49439	23.17212
A003	d	9	C19orf43	25.91643	22.23883
A003	d	10	AKAP8	15.02985	24.76034
A003	d	11	SFRS1	25.98215	22.52023
A003	d	12	APC	26.13276	23.18172
A003	e	1	ZFR	28.1802	23.06188
A003	e	2	PCBP3	24.80825	22.79284
A003	e	3	CDC40	25.93358	22.81246
A003	e	4	IGF2BP1	25.73522	22.79505
A003	e	5	HNRNPM	25.92647	23.64291
A003	e	6	THOC7	26.28389	22.10964
A003	e	7	LUC7L2	25.95245	23.0479
A003	e	8	LOC100128223	35.62568	21.56245
A003	e	9	DDX26B	26.63042	22.83317
A003	e	10	EFTUD2	25.48804	23.47599

A003	e	11	PHF5A	26.1575	23.44965
A003	e	12	EXOSC8	28.14445	25.13944
A003	f	1	HNRNPC	27.55813	23.73082
A003	f	2	WDR33	25.91569	22.75982
A003	f	3	ZFR	25.18257	22.5421
A003	f	4	ZNF207	25.96647	22.92342
A003	f	5	HNRNPL	28.33052	24.05595
A003	f	6	XRN2	26.71547	23.94835
A003	f	7	RBM38	27.26756	24.65379
A003	f	8	POLR2A	29.62793	20.81596
A003	f	9	SR140	Undetermined	Undetermined
A003	f	10	HNRPDL	Undetermined	34.54522
A003	f	11	NCL	Undetermined	36.29094
A003	f	12	SFRS12	28.86545	27.10354
A003	g	1	POLDIP3	26.68353	24.68484
A003	g	2	HNRNPD	25.96102	24.04737
A003	g	3	EXOSC10	26.08517	24.21599
A003	g	4	PHF5A	28.18908	25.51378
A003	g	5	KIAA1429	28.12131	25.19921
A003	g	6	EWSR1	27.02999	24.69299
A003	g	7	PTBP2	26.1799	23.67521
A003	g	8	RBMXL2	25.88962	23.49607
A003	g	9	C14orf166	28.62561	24.94052
A003	g	10	SFRS9	Undetermined	34.07609
A003	g	11	DNAJC6	Undetermined	34.53131
A003	g	12	SMU1	27.50083	25.12085
A003	h	1	BUD13	29.67959	26.9274
A003	h	2	RBM7	Undetermined	31.7827
A003	h	3	C14orf166	Undetermined	30.43246
A003	h	4	RBM4	Undetermined	30.02999
A003	h	5	SF3A2	31.77659	28.02881
A003	h	6	EIF4A3	Undetermined	33.62565
A003	h	7	PHRF1	36.85048	33.62273
A003	h	8	LUC7L2	14.15298	26.33761
A003	h	9	DHX9	36.87431	34.6446
A003	h	10	RNF113A	27.01956	24.86013
A003	h	11	RBMS1	34.0916	32.39198
A003	h	12	DDX3Y	29.4159	28.1213
A004	a	1	HNRNPUL1	37.1591	31.2449
A004	a	2	LNX1	35.71298	30.18699
A004	a	3	GTF2I	34.22459	30.17092
A004	a	4	ELAVL2	33.70254	29.71232
A004	a	5	CLK4	30.86117	27.88265

A004	a	6	DIDO1	28.57751	25.79134
A004	a	7	LSM7	27.06524	23.87387
A004	a	8	LUC7L	25.98422	23.25577
A004	a	9	SMU1	26.05393	22.68285
A004	a	10	TOPORS	25.26192	23.26415
A004	a	11	THOC2	35.91166	32.74184
A004	a	12	SMNDC1	29.20487	26.71041
A004	b	1	LSM8	35.40344	30.65367
A004	b	2	LOC728554	35.16802	28.98054
A004	b	3	U2AF1L4	31.68528	29.09411
A004	b	4	FIP1L1	32.02636	29.23846
A004	b	5	SFRS7	29.40339	26.51646
A004	b	6	C8orf58	28.01539	25.06917
A004	b	7	TNRC4	27.56649	24.78082
A004	b	8	DHX8	25.01916	22.91386
A004	b	9	SLU7	26.78691	23.18614
A004	b	10	LSM2	26.4321	22.83649
A004	b	11	LOC100130003	25.61663	23.24695
A004	b	12	SFRS2IP	28.75472	24.1097
A004	c	1	SFRS7	Undetermined	31.60467
A004	c	2	LOC646517	32.25633	27.65728
A004	c	3	SFRS5	32.77247	29.82933
A004	c	4	SMARCA5	34.39197	34.83612
A004	c	5	SFRS10	31.25437	27.94057
A004	c	6	PCBP4	26.50251	23.1288
A004	c	7	EXOSC9	Undetermined	33.58677
A004	c	8	EIF4G3	Undetermined	34.51863
A004	c	9	TDRD3	36.34386	34.0666
A004	c	10	EXOSC8	21.72096	23.5466
A004	c	11	CDC40	Undetermined	34.28136
A004	c	12	THOC2	28.12916	23.9052
A004	d	1	TPR	31.04164	27.57686
A004	d	2	HNRNPA1	Undetermined	31.99785
A004	d	3	INTS6	Undetermined	35.42429
A004	d	4	RNPS1	28.67124	25.4338
A004	d	5	DDX23	36.16694	34.77058
A004	d	6	DNAJC17	Undetermined	33.68556
A004	d	7	CCNK	26.37399	23.61524
A004	d	8	DNAJC8	25.75636	23.6614
A004	d	9	DDX17	27.23805	22.93473
A004	d	10	CSDA	27.72096	25.0816
A004	d	11	PRPF8	Undetermined	34.03155
A004	d	12	CCNK	24.16099	24.65229

A004	e	1	SNRPA	29.92968	26.75792
A004	e	2	PRPF4B	33.41087	29.86003
A004	e	3	SNRNP35	37.50487	34.00616
A004	e	4	HNRNPA0	28.14422	23.2199
A004	e	5	SF3B3	29.25508	22.25383
A004	e	6	PIAS4	35.21803	34.66425
A004	e	7	LUC7L	26.2418	23.04824
A004	e	8	LSM1	26.27111	23.29179
A004	e	9	HNRNPH3	23.21668	23.14715
A004	e	10	FUBP3	Undetermined	34.22587
A004	e	11	RBM9	19.47378	23.93263
A004	e	12	RBM9	31.80747	20.64658
A004	f	1	DIDO1	Undetermined	35.70651
A004	f	2	ELAVL4	36.45795	35.29329
A004	f	3	ZMAT2	30.55951	28.16489
A004	f	4	KHSRP	27.30511	24.3088
A004	f	5	RBMS1	27.91268	23.15296
A004	f	6	PRCC	Undetermined	34.35227
A004	f	7	KIN	38.21121	33.80056
A004	f	8	CSDA	19.1064	24.11095
A004	f	9	ZNF207	Undetermined	33.72958
A004	f	10	SF3B4	Undetermined	34.43729
A004	f	11	DDX21	21.16024	22.33801
A004	f	12	TIA1	26.47514	24.37192
A004	g	1	SNIP1	Undetermined	28.32809
A004	g	2	XAB2	30.7718	28.53559
A004	g	3	SNRNP27	Undetermined	34.30266
A004	g	4	INTS1	28.35382	24.01627
A004	g	5	SRRM2	26.83108	23.69237
A004	g	6	CWF19L1	26.26259	23.03714
A004	g	7	WDR33	26.8202	22.74839
A004	g	8	SR140	26.83903	23.80356
A004	g	9	CRKRS	27.48295	23.43732
A004	g	10	THOC5	Undetermined	34.83009
A004	g	11	HNRNPU	26.23096	23.82257
A004	g	12	PPIL3	25.42287	24.28766
A004	h	1	MBNL3	32.30703	27.16724
A004	h	2	RBBP7	29.78696	26.35915
A004	h	3	HNRNPR	Undetermined	34.56442
A004	h	4	HRNBP3	31.07573	28.05277
A004	h	5	GTF2I	35.67838	34.3128
A004	h	6	HNRPDL	31.06869	27.51574
A004	h	7	CIR	37.05979	34.4085

A004	h	8	EXOSC8	14.40801	25.57519
A004	h	9	CCNK	21.70887	23.63954
A004	h	10	SNRPA	37.04956	35.05084
A004	h	11	THOC4	Undetermined	Undetermined
A004	h	12	POLDIP3	34.76339	33.93717
A005	a	1	LSM4	29.59043	25.83901
A005	a	2	PSIP1	29.61885	27.03759
A005	a	3	GRSF1	25.47588	23.89135
A005	a	4	PPIL2	29.18889	23.25456
A005	a	5	HNRNPM	Undetermined	19.1702
A005	a	6	CLK2	19.91399	26.3431
A005	a	7	BUB3	Undetermined	19.94118
A005	a	8	FAM120A	28.43575	23.25215
A005	a	9	SFRS8	28.23356	24.7404
A005	a	10	CCNA1	19.31089	24.68649
A005	a	11	LSM1	26.863	24.35595
A005	a	12	THOC1	23.83159	22.95716
A005	b	1	TIA1	29.77669	26.71028
A005	b	2	RBBP7	27.55661	25.21835
A005	b	3	PRPF19	29.14555	24.97082
A005	b	4	EIF4A3	28.61293	24.93016
A005	b	5	XRN2	27.65237	24.83708
A005	b	6	SKIV2L2	24.78011	22.42349
A005	b	7	SFRS14	25.6994	23.88034
A005	b	8	PPWD1	Undetermined	16.58388
A005	b	9	TXNL4A	26.71448	22.97331
A005	b	10	NCBP2	24.92355	22.26313
A005	b	11	CCNK	33.64556	21.3993
A005	b	12	RBM5	20.75263	23.05881
A005	c	1	MBNL1	Undetermined	31.00878
A005	c	2	IGF2BP3	29.67874	27.59779
A005	c	3	C19orf29	27.22062	24.17058
A005	c	4	LSM1	27.89174	25.05784
A005	c	5	A2BP1	27.94459	25.56079
A005	c	6	THOC7	26.54138	24.31583
A005	c	7	BAT1	25.75347	23.81711
A005	c	8	CTNNBL1	Undetermined	23.40254
A005	c	9	SNRNP200	33.37892	21.2327
A005	c	10	HNRNPL	26.81744	23.03658
A005	c	11	PUF60	26.73163	23.36643
A005	c	12	DDX41	25.72553	23.15404
A005	d	1	PRPF3	31.95353	25.91382
A005	d	2	DGCR14	31.2944	29.1585

A005	d	3	DDX3Y	27.63896	24.9974
A005	d	4	HNRNPM	28.26714	25.98391
A005	d	5	DDX3Y	28.5175	26.01919
A005	d	6	SF3B14	26.91999	25.10143
A005	d	7	SFPQ	25.94113	23.92716
A005	d	8	QPCT	26.01691	23.3048
A005	d	9	TET1	26.46545	23.53002
A005	d	10	RBM3	25.15451	22.88335
A005	d	11	LOC644811	25.7098	23.52461
A005	d	12	SFRS1	26.11985	23.58538
A005	e	1	BUD31	31.84402	28.21917
A005	e	2	ANXA2	25.61827	24.43778
A005	e	3	EXOSC4	28.43774	25.77068
A005	e	4	C1QBP	28.16425	25.19528
A005	e	5	FUSIP1	30.05112	27.47849
A005	e	6	RBM9	28.41588	25.90908
A005	e	7	SLU7	26.68453	23.69579
A005	e	8	YWHAG	23.93434	23.76957
A005	e	9	SMN1	26.70616	24.10166
A005	e	10	DIDO1	24.70789	23.22605
A005	e	11	DDX3Y	24.67889	23.7459
A005	e	12	BRUNOL5	27.63339	23.356
A005	f	1	SMU1	27.97717	26.13098
A005	f	2	IQGAP1	29.58069	26.74674
A005	f	3	PSPC1	33.55938	29.2086
A005	f	4	SFRS2IP	28.11002	25.85029
A005	f	5	MAGOH	26.87944	24.81955
A005	f	6	PCBP2	Undetermined	34.77204
A005	f	7	KLHDC8A	27.57207	23.06524
A005	f	8	MBNL3	39.87429	36.48964
A005	f	9	SF1	26.12405	22.82272
A005	f	10	ZMAT5	14.80479	26.05278
A005	f	11	PRPF4B	35.47028	34.72534
A005	f	12	EIF2S2	26.06079	23.1912
A005	g	1	CDC5L	30.30249	26.88597
A005	g	2	PNN	28.64095	27.36628
A005	g	3	INTS3	33.98364	29.0442
A005	g	4	HNRNPD	26.98973	25.05911
A005	g	5	SNW1	27.4997	24.99111
A005	g	6	PABPN1	26.54995	23.53719
A005	g	7	DDX3Y	26.58153	23.01072
A005	g	8	TIAL1	25.77188	23.1801
A005	g	9	HNRNPUL1	26.50644	23.46551

A005	g	10	HNRNPA2B1	24.07251	23.65016
A005	g	11	SFPQ	Undetermined	34.60023
A005	g	12	DDX3X	36.25532	35.13352
A005	h	1	PPAN	31.26419	29.89161
A005	h	2	PRPF40A	25.90599	23.17747
A005	h	3	PRPF18	24.81563	22.73124
A005	h	4	C8orf58	25.50086	24.4833
A005	h	5	PPIL3	28.61257	23.26505
A005	h	6	HNRNPH3	28.78149	25.97241
A005	h	7	LOC387703	37.34926	22.44475
A005	h	8	RBM42	27.3314	24.36288
A005	h	9	TOPORS	29.72134	26.80457
A005	h	10	SF3B3	18.75428	28.55347
A005	h	11	RBM39	Undetermined	34.71059
A005	h	12	CCDC55	28.28981	25.57824
A006	a	1	SF1	25.13698	22.28613
A006	a	2	CPSF6	24.24146	22.02998
A006	a	3	KHSRP	25.36044	21.30936
A006	a	4	PRPF38B	28.58965	22.01623
A006	a	5	MYEF2	24.24366	21.48917
A006	a	6	THOC1	15.95237	23.38122
A006	a	7	POLDIP3	25.18519	21.19584
A006	a	8	CDC40	24.48591	20.47019
A006	a	9	CRNKL1	24.14853	22.44112
A006	a	10	DDX46	23.42516	22.33011
A006	a	11	DDX21	23.14947	23.7081
A006	a	12	CD2BP2	27.20342	25.09518
A006	b	1	POLR2B	28.58473	22.08546
A006	b	2	WBP11	24.79965	22.03761
A006	b	3	PRPF3	25.1603	22.18851
A006	b	4	SFRS2B	24.98385	22.6155
A006	b	5	KPNA2	24.25875	21.85181
A006	b	6	RBM8A	25.55225	21.92578
A006	b	7	PLRG1	26.15874	21.53526
A006	b	8	EWSR1	24.1718	21.43075
A006	b	9	GPATCH1	25.25572	22.29723
A006	b	10	IGF2BP1	25.05322	22.02382
A006	b	11	DEK	25.01372	21.72051
A006	b	12	FIP1L1	24.18194	21.79048
A006	c	1	PPP1R8	26.22134	23.83751
A006	c	2	C2orf49	25.27416	23.18672
A006	c	3	RBM39	24.97487	24.27781
A006	c	4	LSM10	24.68318	23.39432

A006	c	5	CPSF6	25.12141	23.66639
A006	c	6	SDCCAG10	26.22644	23.88181
A006	c	7	KHDRBS3	25.57753	23.35142
A006	c	8	SFRS2IP	25.48628	23.4398
A006	c	9	KHDRBS1	25.21498	23.46477
A006	c	10	ELAVL4	25.58527	23.28434
A006	c	11	SF3A2	26.45318	24.42377
A006	c	12	RBM25	27.46602	25.17617
A006	d	1	RBM25	25.35375	23.32359
A006	d	2	PCBP1	24.41657	23.08941
A006	d	3	MATR3	26.09484	22.03351
A006	d	4	LOC644422	Undetermined	21.85711
A006	d	5	LOC644422	25.7928	22.97541
A006	d	6	SFRS1	26.23628	23.49489
A006	d	7	SNRNP48	24.97167	23.35184
A006	d	8	MATR3	25.33482	22.62328
A006	d	9	FRG1	25.58776	23.62235
A006	d	10	LSM8	25.39694	23.03438
A006	d	11	TNPO1	26.90306	25.43197
A006	d	12	MAGOH	26.95377	26.0534
A006	e	1	PPP1R8	25.32609	23.75216
A006	e	2	MAGOHB	24.05167	22.26109
A006	e	3	ADAR	25.36399	22.76427
A006	e	4	SNRNP25	25.93733	23.30873
A006	e	5	SPEN	25.1293	23.07812
A006	e	6	RBM3	25.11165	22.43123
A006	e	7	PLRG1	25.14501	23.20764
A006	e	8	NUMA1	25.13181	22.61442
A006	e	9	DDX1	24.21843	21.851
A006	e	10	SRPK2	25.04711	22.44237
A006	e	11	FUS	25.12351	23.14626
A006	e	12	SRPK1	30.32233	28.76899
A006	f	1	RBM24	25.04963	23.60737
A006	f	2	PCBP2	23.89418	22.33058
A006	f	3	BAT1	25.3713	23.39789
A006	f	4	HNRNPA1	24.83242	22.67431
A006	f	5	SART3	24.87741	22.48642
A006	f	6	PRPF4B	25.05057	22.44056
A006	f	7	SRP19	24.75835	22.13052
A006	f	8	SNRNP200	24.62532	22.57129
A006	f	9	SFRS6	25.07733	22.9562
A006	f	10	ZC3H18	24.59242	22.71405
A006	f	11	DHX8	28.37045	28.67438

A006	f	12	WTAP	30.16609	30.34501
A006	g	1	CWC15	25.56751	23.88825
A006	g	2	HNRNPA0	24.87304	24.11719
A006	g	3	DIDO1	26.25446	23.27854
A006	g	4	CRKRS	26.13448	22.8268
A006	g	5	ELAVL1	27.12186	25.8883
A006	g	6	INTS6	25.95167	23.63931
A006	g	7	DHX38	25.43754	23.47245
A006	g	8	DDX17	26.23838	23.94628
A006	g	9	DDX17	25.47309	23.32805
A006	g	10	LGALS3	26.3029	23.47193
A006	g	11	ILF3	26.56815	24.2214
A006	g	12	THOC5	26.56424	24.95922
A006	h	1	U2AF2	30.90693	26.23053
A006	h	2	DDX41	25.59276	24.05478
A006	h	3	FMR1	28.88052	21.4761
A006	h	4	FUSIP1	25.4504	21.77871
A006	h	5	PARP1	26.52301	24.4974
A006	h	6	ZC3H18	24.14696	21.9435
A006	h	7	HNRNPA1	25.3779	22.32927
A006	h	8	RNPC3	26.39064	23.06778
A006	h	9	EIF3A	28.7352	28.23798
A006	h	10	SFRS12	25.44852	24.07439
A006	h	11	C21orf66	29.84867	29.49717
A006	h	12	PLEKHA5	30.30674	28.99557
A007	a	1	U2AF1	28.2499	26.97169
A007	a	2	CLK4	17.49815	26.08054
A007	a	3	XRN2	24.18205	23.02918
A007	a	4	PABPC1	26.69968	22.723
A007	a	5	BCAS2	21.48967	22.18483
A007	a	6	LOC100131556	15.79599	23.0028
A007	a	7	SRPK3	26.03712	19.40788
A007	a	8	CDC5L	19.31415	23.22536
A007	a	9	HNRNPUL1	25.29348	21.15556
A007	a	10	TOPORS	25.12809	23.62013
A007	a	11	KIAA1429	25.06808	21.99908
A007	a	12	SFRS2IP	Undetermined	Undetermined
A007	b	1	POLR2B	25.50223	23.53983
A007	b	2	NCBP2	24.91129	22.59386
A007	b	3	SFRS3	25.45943	21.06115
A007	b	4	EIF3A	25.36776	23.27079
A007	b	5	MBNL3	24.89479	22.32827
A007	b	6	PTBP2	24.10948	21.89973

A007	b	7	CWF19L1	24.93242	22.18994
A007	b	8	AKAP8	24.41559	22.27312
A007	b	9	YBX1	25.11628	22.4184
A007	b	10	PSIP1	24.37577	22.8564
A007	b	11	ERG	28.03427	26.9767
A007	b	12	FUBP3	23.17328	21.96883
A007	c	1	LSM5	25.88121	24.41329
A007	c	2	WDR33	25.17181	23.26048
A007	c	3	C21orf66	25.91348	22.84374
A007	c	4	IGF2BP1	25.18852	22.44052
A007	c	5	DHX35	25.118	22.78458
A007	c	6	LOC652595	26.38338	22.04209
A007	c	7	GTF2I	26.55742	23.6813
A007	c	8	FMR1	25.27719	23.37322
A007	c	9	STRBP	25.81713	23.58884
A007	c	10	TCERG1	26.54854	23.66859
A007	c	11	C1QBP	26.44854	24.66869
A007	c	12	HMG1L1	29.43624	29.6297
A007	d	1	SFRS10	25.2084	21.96999
A007	d	2	CWC22	24.61968	22.85386
A007	d	3	MBNL2	24.73262	22.87969
A007	d	4	KHSRP	22.30397	22.81704
A007	d	5	SNRPD1	30.70968	16.02386
A007	d	6	CLK4	25.8546	22.40748
A007	d	7	TPR	26.43999	22.62263
A007	d	8	SART1	15.39467	24.01298
A007	d	9	C2orf3	24.92319	22.8779
A007	d	10	PRPF18	34.7888	18.29344
A007	d	11	FUBP1	25.1757	23.19031
A007	d	12	RBM22	34.74927	17.62263
A007	e	1	MFSD11	26.51797	23.98494
A007	e	2	LSM6	19.71431	21.01508
A007	e	3	HNRNPM	25.45911	23.01008
A007	e	4	RALY	25.13026	22.5218
A007	e	5	HNRNPUL1	24.78286	22.53475
A007	e	6	WBP4	25.1981	23.47561
A007	e	7	DHX38	25.87907	22.57563
A007	e	8	NCBP1	24.68165	22.58596
A007	e	9	DIDO1	25.07884	22.84436
A007	e	10	CIRBP	26.16128	24.0111
A007	e	11	HNRNPR	27.10443	24.97699
A007	e	12	TET1	25.40741	23.89085
A007	f	1	LOC643387	22.97994	21.95509

A007	f	2	HNRNPR	24.01299	22.07472
A007	f	3	P2RY11	24.06469	22.17885
A007	f	4	SF3A1	Undetermined	18.07294
A007	f	5	CRNKL1	24.96059	22.37843
A007	f	6	PPIL3	25.49726	22.37218
A007	f	7	HNRNPUL2	12.92268	26.66748
A007	f	8	QKI	31.09827	21.67121
A007	f	9	ILF3	28.0016	21.38395
A007	f	10	DIDO1	32.93924	21.08311
A007	f	11	DDX21	29.88168	31.13833
A007	f	12	CLK4	29.66838	31.14023
A007	g	1	HNRNPK	29.10819	22.82908
A007	g	2	DHX8	26.30727	24.14284
A007	g	3	RBM39	25.68954	23.01014
A007	g	4	IK	25.7124	22.99575
A007	g	5	PRPF8	27.51256	26.28131
A007	g	6	PARP1	24.8348	22.80116
A007	g	7	SNRNP40	24.91995	22.78238
A007	g	8	HNRNPH3	25.67081	22.95989
A007	g	9	GRSF1	25.20835	23.81737
A007	g	10	HCFC1	28.81862	27.72992
A007	g	11	SMNDC1	29.36294	30.5358
A007	g	12	SFRS8	29.42946	30.93074
A007	h	1	BUD13	27.81844	22.64762
A007	h	2	ZMAT2	32.37755	21.54029
A007	h	3	ELAVL2	25.3376	23.43423
A007	h	4	EIF4A3	25.96808	23.19778
A007	h	5	ZC3H18	24.62254	23.24363
A007	h	6	HNRPLL	24.9349	22.79235
A007	h	7	QKI	24.25998	22.51066
A007	h	8	CLK1	25.89972	23.35467
A007	h	9	HNRNPU	26.3549	23.94452
A007	h	10	MYEF2	28.96075	26.33439
A007	h	11	FRG1	30.17011	30.437
A007	h	12	THOC1	29.9012	30.65382
A008	a	1	CTNNBL1	8.54863	19.92985
A008	a	2	THOC1	25.21127	22.22241
A008	a	3	PPWD1	26.04875	21.46425
A008	a	4	DIS3	25.76409	22.39929
A008	a	5	PPM1G	24.14334	22.6398
A008	a	6	RBM4	25.50017	23.2019
A008	a	7	CDC40	25.53223	23.02409
A008	a	8	DDX5	25.60453	22.46034

A008	a	9	RBM26	25.11904	22.75405
A008	a	10	CIR	25.12483	22.94165
A008	a	11	FRG1	25.39874	22.73351
A008	a	12	TOP1MT	25.43076	22.81576
A008	b	1	SRPK2	24.13675	21.61292
A008	b	2	TRA2A	23.70409	22.70354
A008	b	3	WDR25	25.88475	20.93411
A008	b	4	TPR	24.0256	22.04343
A008	b	5	DDX46	25.30719	21.60101
A008	b	6	PCBP3	25.07931	22.07265
A008	b	7	SMU1	24.42066	22.10745
A008	b	8	HNRNPR	24.74451	22.11089
A008	b	9	SFRS11	25.31398	23.10096
A008	b	10	DHX8	25.00748	22.44483
A008	b	11	HNRNPA1	20.77243	22.41544
A008	b	12	WBP11	24.73035	21.82063
A008	c	1	PABPN1	25.7977	21.42051
A008	c	2	RP9	24.42859	22.3726
A008	c	3	CWC15	24.85413	22.36859
A008	c	4	DDX3X	24.7399	21.71196
A008	c	5	TET1	28.51814	28.3337
A008	c	6	SFRS2B	24.88885	22.41421
A008	c	7	GPATCH1	24.96505	22.23241
A008	c	8	EIF4A3	25.91928	22.49032
A008	c	9	RNPC3	24.93722	21.86816
A008	c	10	PPP1R8	24.91392	22.09596
A008	c	11	FASTK	25.07987	22.68267
A008	c	12	INTS3	25.73332	24.20641
A008	d	1	CLK4	23.93196	22.1406
A008	d	2	TNPO1	25.04641	22.30276
A008	d	3	SF4	25.03043	22.90568
A008	d	4	SFRS12	25.42787	22.52112
A008	d	5	TOP1	24.85846	22.51269
A008	d	6	HRNBP3	24.75458	22.28922
A008	d	7	RBMX2	24.86173	22.30629
A008	d	8	DHX38	25.08428	22.48998
A008	d	9	WBP4	25.26418	22.43368
A008	d	10	DHX9	25.56768	22.05187
A008	d	11	DEK	25.11194	22.18306
A008	d	12	HNRNPD	29.23251	28.60299
A008	e	1	SF3B2	25.31928	22.03381
A008	e	2	RBM24	24.95566	22.59714
A008	e	3	QPCT	24.23827	22.46114

A008	e	4	BUD31	24.6494	22.80178
A008	e	5	DIDO1	24.19152	22.14445
A008	e	6	SNW1	25.03199	22.29984
A008	e	7	DDX26B	24.49516	22.31518
A008	e	8	DNAJC8	24.92213	22.32277
A008	e	9	ZC3H18	25.53603	22.28226
A008	e	10	SFRS4	25.17931	22.06739
A008	e	11	RBM17	24.99725	22.47966
A008	e	12	ARS2	24.32804	23.05206
A008	f	1	GRSF1	20.1455	22.68583
A008	f	2	DIS3	24.58712	22.5661
A008	f	3	SFRS12	25.40016	22.53251
A008	f	4	SRP68	25.16812	21.71575
A008	f	5	SFRS2	25.42801	21.77049
A008	f	6	SFRS10	25.02134	22.08694
A008	f	7	PPIL1	24.87637	22.03418
A008	f	8	IGF2BP3	24.97638	21.90223
A008	f	9	SAFB	24.68927	22.02347
A008	f	10	HNRNPA1	24.85158	22.38911
A008	f	11	EIF3M	28.70985	27.79006
A008	f	12	IGF2BP3	24.35356	22.34623
A008	g	1	ZFR	25.48607	21.23655
A008	g	2	TAF15	25.05631	22.29701
A008	g	3	ZRANB2	25.8488	22.56234
A008	g	4	DDX3X	25.32	21.90251
A008	g	5	NCBP2	28.1553	26.70643
A008	g	6	BAT1	25.11913	21.91353
A008	g	7	LOC643387	27.62238	22.07407
A008	g	8	C2orf49	26.9955	22.43287
A008	g	9	PPIL1	Undetermined	21.77652
A008	g	10	HTATSF1	22.75078	22.08893
A008	g	11	LUC7L2	24.09945	22.01331
A008	g	12	PPP1R8	29.11259	28.06242
A008	h	1	LOC652607	25.00239	21.84619
A008	h	2	DIDO1	24.62226	23.25969
A008	h	3	RBM38	29.808	20.94242
A008	h	4	THOC5	24.50219	22.48988
A008	h	5	ZMAT2	24.32609	22.41736
A008	h	6	CPSF6	24.76594	22.3441
A008	h	7	DIS3	17.0435	24.22079
A008	h	8	HNRNPD	7.580393	18.35558
A008	h	9	C19orf43	14.69781	23.58265
A008	h	10	SNRNP35	26.57912	21.76945

A008	h	11	LSM2	24.48704	22.19895
A008	h	12	RNF113A	25.05736	22.21519
A009	a	1	FUBP1	29.77778	29.88306
A009	a	2	DDX17	28.30042	27.03495
A009	a	3	DDX5	29.4742	27.48373
A009	a	4	SFPQ	30.17656	28.6972
A009	a	5	SNIP1	30.25027	29.1017
A009	a	6	GRSF1	32.4781	27.23391
A009	a	7	DDX39	27.64433	25.84251
A009	a	8	DIDO1	25.83219	22.9719
A009	a	9	MYEF2	28.30894	23.97081
A009	a	10	DDX46	25.78477	24.00374
A009	a	11	C2orf3	26.05	24.19823
A009	a	12	ZCRB1	16.70015	27.82688
A009	b	1	TET1	33.0615	27.39323
A009	b	2	HNRNPF	28.95961	26.31856
A009	b	3	CSDA	25.20547	21.94303
A009	b	4	DDX41	28.23799	26.18921
A009	b	5	TDRD3	25.09262	22.67171
A009	b	6	PARP1	25.95817	23.77907
A009	b	7	MAGOH	26.7108	22.53722
A009	b	8	U2AF2	25.26644	21.59864
A009	b	9	RBM24	25.9909	21.47
A009	b	10	HNRNPD	27.39837	22.41203
A009	b	11	C1orf55	24.82902	22.45628
A009	b	12	CPSF1	24.96424	21.93217
A009	c	1	FUSIP1	29.8067	27.58478
A009	c	2	PCBP2	25.5581	22.85043
A009	c	3	ILF3	26.58697	22.99258
A009	c	4	HCFC1	24.33965	21.52865
A009	c	5	DHX9	24.58951	21.48367
A009	c	6	IQGAP1	25.47559	21.88315
A009	c	7	TET1	25.46255	22.59195
A009	c	8	HNRNPH1	27.21687	21.44668
A009	c	9	NHP2L1	25.26401	22.31753
A009	c	10	SMU1	23.93844	22.59626
A009	c	11	SNRNP48	25.14135	22.71819
A009	c	12	RALYL	17.25207	23.8056
A009	d	1	KHDRBS1	29.079	27.83593
A009	d	2	LOC100129566	25.4182	22.63237
A009	d	3	CTNNBL1	25.0877	22.91317
A009	d	4	SLU7	26.12912	22.657
A009	d	5	RALYL	23.67529	23.12374

A009	d	6	EIF3A	26.90228	22.20411
A009	d	7	LOC646517	25.98791	22.25179
A009	d	8	EIF2S2	25.5368	22.95798
A009	d	9	CIR	15.47727	22.65818
A009	d	10	YBX1	16.12477	23.19413
A009	d	11	FAM71D	24.81533	22.56619
A009	d	12	CRKRS	24.34541	21.54838
A009	e	1	TARDBP	24.2412	25.13632
A009	e	2	NOSIP	25.22838	21.76328
A009	e	3	SFRS10	22.53541	23.48243
A009	e	4	LOC100130289	31.037	19.98569
A009	e	5	CDC5L	28.77721	21.83524
A009	e	6	SSB	25.06832	22.72034
A009	e	7	SRRM1	25.55207	22.7369
A009	e	8	TRA2A	25.66755	22.93735
A009	e	9	RBM7	20.09217	22.19009
A009	e	10	ISY1	25.04776	22.65925
A009	e	11	CPSF4	24.54855	21.16942
A009	e	12	SNRPA1	24.25787	22.76854
A009	f	1	XAB2	26.42689	19.95808
A009	f	2	SKIV2L2	25.31299	22.40985
A009	f	3	HNRNPA1	24.25829	21.50871
A009	f	4	GRSF1	24.87849	22.56534
A009	f	5	AQR	25.0144	22.74357
A009	f	6	HNRNPC	25.23497	22.53482
A009	f	7	C22orf28	26.24582	22.77048
A009	f	8	C2orf49	27.52178	22.18536
A009	f	9	DEK	24.19385	22.78066
A009	f	10	C19orf29	5.921665	20.33035
A009	f	11	HNRPDL	18.34246	25.51785
A009	f	12	RBMS1	28.60247	18.5317
A009	g	1	NUMA1	24.88783	23.03421
A009	g	2	RBMX2	27.52274	20.86125
A009	g	3	DHX15	24.4032	21.94811
A009	g	4	WBP4	17.59277	23.28064
A009	g	5	TRA2A	23.79042	25.00861
A009	g	6	PTBP2	Undetermined	17.21883
A009	g	7	BUD31	26.16024	22.31408
A009	g	8	LSMD1	24.61614	22.505
A009	g	9	DDX1	25.0463	22.2924
A009	g	10	DDX41	25.19744	22.67929
A009	g	11	DDX39	24.3576	22.66288
A009	g	12	LOC646517	28.5829	29.36394

A009	h	1	SNRNP70	15.2068	29.10136
A009	h	2	ZRANB2	28.0618	25.27267
A009	h	3	SFRS17A	27.2359	24.87039
A009	h	4	EXOSC4	24.42068	21.79777
A009	h	5	DHX38	25.34784	23.19494
A009	h	6	C1orf55	27.59537	22.26196
A009	h	7	SFRS1	25.90791	23.4844
A009	h	8	SRRM2	14.42866	24.86232
A009	h	9	DDX26B	25.19195	22.97185
A009	h	10	HNRPLL	25.59134	23.08288
A009	h	11	YWHAG	19.92731	23.42884
A009	h	12	PSIP1	24.93812	22.81035
A010	a	1	LSM6	25.59045	22.92131
A010	a	2	CUGBP1	26.62349	22.97069
A010	a	3	RBM42	25.20939	22.75272
A010	a	4	DDX1	25.4973	22.94424
A010	a	5	PLRG1	Undetermined	17.60884
A010	a	6	LSM2	25.16925	22.60429
A010	a	7	CCNA1	24.44961	22.3112
A010	a	8	LSM3	25.40586	23.24135
A010	a	9	SRP68	25.03252	23.13257
A010	a	10	RBMX2	33.87574	20.18153
A010	a	11	FUBP3	25.88293	23.94624
A010	a	12	SART1	26.71854	24.9105
A010	b	1	RBM9	25.04753	22.79647
A010	b	2	LSM5	24.86346	23.45013
A010	b	3	EXOSC10	25.05152	22.58663
A010	b	4	SMARCA5	24.3591	22.71409
A010	b	5	DDX39	25.00405	22.91752
A010	b	6	SFRS9	25.7945	23.14666
A010	b	7	SMNDC1	25.28833	23.12003
A010	b	8	POLR2A	25.07358	23.0122
A010	b	9	LOC119358	25.85364	22.42549
A010	b	10	MYEF2	26.36815	23.75568
A010	b	11	SNRNP70	26.01412	23.12277
A010	b	12	LOC643167	28.41482	23.18699
A010	c	1	MSI2	24.68517	22.74674
A010	c	2	SNRNP27	25.77836	22.85595
A010	c	3	PRPF18	25.4607	22.89047
A010	c	4	USP39	26.06221	23.4907
A010	c	5	TIA1	25.70362	23.267
A010	c	6	KHDRBS1	25.46253	23.69838
A010	c	7	WBP11	24.53944	23.37105

A010	c	8	SART3	26.19682	23.74569
A010	c	9	RNF113A	25.27009	23.19853
A010	c	10	LOC100130003	25.68259	24.06512
A010	c	11	CLK4	26.42301	24.08249
A010	c	12	PLRG1	24.17245	22.84398
A010	d	1	MSI2	26.38945	22.7418
A010	d	2	SRPK1	25.69619	23.09479
A010	d	3	XRN2	24.76974	22.49431
A010	d	4	RALYL	25.25216	22.6118
A010	d	5	PRPF6	25.45722	22.74996
A010	d	6	TNPO1	26.48284	23.31966
A010	d	7	PQBP1	25.07765	23.30624
A010	d	8	SNRPF	24.94089	23.02577
A010	d	9	SNW1	25.35232	22.75705
A010	d	10	MBNL3	24.96631	23.46769
A010	d	11	SFRS3	25.64706	23.28074
A010	d	12	SART1	25.35379	23.06567
A010	e	1	MAGOHB	28.31078	23.25676
A010	e	2	RBM15	29.55493	22.12232
A010	e	3	HNRNPH3	26.78937	21.53495
A010	e	4	SNRPD3	29.21674	23.11344
A010	e	5	SR140	24.75872	22.15082
A010	e	6	PLEKHA5	32.37926	20.55217
A010	e	7	IK	27.07256	22.71783
A010	e	8	NUDT21	16.67427	23.12381
A010	e	9	CLK1	25.33241	22.21422
A010	e	10	TXNL4A	5.315302	20.12587
A010	e	11	KHDRBS1	24.89523	22.93525
A010	e	12	ELAVL3	24.28219	21.78937
A010	f	1	PRPF38B	25.30408	22.25611
A010	f	2	RBM7	24.32731	23.49413
A010	f	3	TNPO1	25.34554	22.12211
A010	f	4	PABPC1	24.9378	22.56894
A010	f	5	PARP1	26.24653	24.75591
A010	f	6	SCAF1	24.89883	22.83805
A010	f	7	SYF2	25.08253	22.81962
A010	f	8	DIDO1	24.89616	22.82759
A010	f	9	PCBP3	24.54281	22.70766
A010	f	10	CD2BP2	25.14011	21.96639
A010	f	11	CCDC94	24.46491	22.665
A010	f	12	FASTK	24.0903	23.34466
A010	g	1	CIRBP	25.48264	22.94238
A010	g	2	CTNNBL1	25.3064	23.4366

A010	g	3	SYF2	26.26022	22.11099
A010	g	4	CDC5L	25.74487	22.95864
A010	g	5	CPSF6	26.20831	24.76609
A010	g	6	U2AF1	23.56986	20.43711
A010	g	7	BCAS2	25.86667	23.51649
A010	g	8	PRPF18	25.30046	22.07884
A010	g	9	SFRS17A	22.22066	23.04419
A010	g	10	SNRNP25	24.61527	22.64286
A010	g	11	DDX1	24.5409	23.02679
A010	g	12	PRPF8	20.86735	23.9253
A010	h	1	HNRNPH3	25.58917	21.69535
A010	h	2	TOP1	27.84736	22.49434
A010	h	3	DIDO1	28.05222	22.80996
A010	h	4	SF3B14	28.86946	24.41303
A010	h	5	CHERP	24.26602	23.31738
A010	h	6	USP39	26.23352	22.13865
A010	h	7	YWHAQ	24.68611	21.93859
A010	h	8	DDX3X	24.18202	22.91661
A010	h	9	DDX21	25.15942	22.57136
A010	h	10	LSM5	23.04749	23.47615
A010	h	11	INTS6	28.74413	29.15736
A010	h	12	TAF15	23.96302	22.4186
A011	a	1	ILF3	Undetermined	36.71981
A011	a	2	HRNBP3	27.71483	24.82566
A011	a	3	BUD13	36.84974	38.41605
A011	a	4	SKIV2L2	36.49773	37.42645
A011	a	5	PSPC1	27.8015	23.88776
A011	a	6	SFRS8	25.77029	24.94007
A011	a	7	LOC644035	24.89592	23.96336
A011	a	8	TOP1	23.65186	24.70923
A011	a	9	SR140	Undetermined	30.9998
A011	a	10	SF3A2	27.46344	24.56755
A011	a	11	SNIP1	27.15165	25.31274
A011	a	12	CLK3	Undetermined	Undetermined
A011	b	1	DDX23	27.14214	25.80197
A011	b	2	SF3B4	27.59355	24.85196
A011	b	3	DHX16	27.20208	24.9955
A011	b	4	C14orf166	27.16641	25.22541
A011	b	5	PRPF4B	28.01565	25.46081
A011	b	6	SNRPA	27.15791	24.48146
A011	b	7	SNRNP48	26.54261	24.46479
A011	b	8	LSM2	27.50558	25.50481
A011	b	9	RALYL	27.2812	26.15075

A011	b	10	SLU7	28.54947	26.31297
A011	b	11	RBM24	28.27283	26.02986
A011	b	12	BAT1	30.36807	28.17977
A011	c	1	SF4	30.10894	28.39226
A011	c	2	RUVBL2	28.0378	26.51243
A011	c	3	KHSRP	26.76758	25.19012
A011	c	4	PARP1	26.93288	24.82576
A011	c	5	DHX8	32.32554	30.79979
A011	c	6	LOC729200	26.74296	24.88619
A011	c	7	PARP1	27.40115	24.77351
A011	c	8	HRNBP3	Undetermined	26.3396
A011	c	9	PRCC	27.66585	24.59331
A011	c	10	DIDO1	Undetermined	25.39276
A011	c	11	SFRS6	27.57143	26.15364
A011	c	12	SMNDC1	31.00392	29.4338
A011	d	1	RBM38	26.64603	25.6455
A011	d	2	SNRNP35	26.63706	24.82653
A011	d	3	LOC100129492	26.62839	25.44232
A011	d	4	FMR1	26.92346	25.28674
A011	d	5	RBM7	26.72361	24.22934
A011	d	6	IGF2BP1	27.32638	25.23624
A011	d	7	KHSRP	26.11764	24.57475
A011	d	8	PPP1R8	27.20516	25.61451
A011	d	9	CROP	27.39262	25.778
A011	d	10	EIF4A3	31.56738	28.56604
A011	d	11	C1orf55	27.59887	26.24221
A011	d	12	PRPF6	27.78357	26.16494
A011	e	1	DDX3Y	31.69209	31.19789
A011	e	2	PCBP2	28.24423	25.72211
A011	e	3	TCERG1	27.16022	25.41704
A011	e	4	PNN	27.2729	24.46592
A011	e	5	ISY1	27.23748	25.17172
A011	e	6	CPSF2	27.2166	25.34107
A011	e	7	DDX1	27.13085	25.4664
A011	e	8	HIST2H2AA3	26.7865	25.56128
A011	e	9	LSM5	27.33315	26.56706
A011	e	10	MYEF2	27.98963	26.39908
A011	e	11	SF4	27.66865	25.63974
A011	e	12	NOVA2	27.19445	25.38152
A011	f	1	SLU7	28.38013	23.66301
A011	f	2	ZRANB2	28.22075	26.11758
A011	f	3	FUSIP1	27.81158	25.11336
A011	f	4	CLK1	27.3285	25.18896

A011	f	5	LOC653155	27.27908	25.90361
A011	f	6	POLDIP3	28.15188	25.42705
A011	f	7	NOSIP	27.8071	25.77295
A011	f	8	SCAF1	27.19356	25.01032
A011	f	9	HTATSF1	27.43104	24.88
A011	f	10	SMARCA5	28.04072	25.94579
A011	f	11	SNW1	28.15429	26.04143
A011	f	12	CSDA	29.06616	26.76722
A011	g	1	SNRNP35	27.39215	25.61788
A011	g	2	XRN2	31.0187	29.0627
A011	g	3	SFRS7	27.00278	25.31548
A011	g	4	DDX41	27.32329	25.15049
A011	g	5	RBM22	27.25789	25.97124
A011	g	6	MSI2	28.93843	27.42297
A011	g	7	ZFR	27.70524	25.18042
A011	g	8	C2orf49	27.43726	25.21156
A011	g	9	HNRNPU	26.77453	25.06975
A011	g	10	SDCCAG10	27.63564	25.3387
A011	g	11	C16orf80	27.85354	26.30089
A011	g	12	RBM25	29.47155	26.92268
A011	h	1	INTS3	26.79442	24.93391
A011	h	2	DDX23	26.96916	25.08309
A011	h	3	MYEF2	27.38604	24.87618
A011	h	4	SART1	26.69909	25.61207
A011	h	5	APC	26.41896	24.11931
A011	h	6	DDX17	26.25686	24.48136
A011	h	7	SRPK2	27.29748	25.41792
A011	h	8	POLR2A	26.02206	24.12867
A011	h	9	THOC7	27.9661	25.52612
A011	h	10	LOC100127915	28.09728	26.52799
A011	h	11	GPATCH1	27.95927	25.91787
A011	h	12	PCBP3	27.26188	25.35374
A012	a	1	PRPF6	28.37471	26.96349
A012	a	2	SCNM1	27.54452	25.81904
A012	a	3	CIR	Undetermined	35.65075
A012	a	4	SART3	36.04276	35.93795
A012	a	5	THOC2	28.61922	27.38665
A012	a	6	INTS1	Undetermined	Undetermined
A012	a	7	NUMA1	26.77552	25.34651
A012	a	8	FUSIP1	Undetermined	36.65979
A012	a	9	HNRNPC	Undetermined	37.2945
A012	a	10	LOC119358	36.36383	36.59481
A012	a	11	CRNKL1	27.3696	25.91257

A012	a	12	IQGAP1	34.89204	34.50707
A012	b	1	SYF2	26.98386	26.2189
A012	b	2	PQBP1	28.9438	26.69824
A012	b	3	BRUNOL4	28.30166	26.30593
A012	b	4	ADAR	26.97166	25.29218
A012	b	5	SNRPD3	27.92675	27.28732
A012	b	6	HNRNPK	28.02788	24.97357
A012	b	7	MOV10	27.73212	26.07857
A012	b	8	PIAS4	28.25008	27.07958
A012	b	9	HNRNPH3	28.30509	25.87487
A012	b	10	ACIN1	27.55646	26.55617
A012	b	11	SNRNP27	28.58897	26.63756
A012	b	12	ADAR	33.20217	30.34668
A012	c	1	SFRS1	27.74632	26.00524
A012	c	2	HCFC1	28.12345	27.24988
A012	c	3	DHX8	28.62693	26.7406
A012	c	4	HNRNPH1	27.65075	26.16025
A012	c	5	SRP19	27.81276	26.46366
A012	c	6	KIN	34.3378	32.84427
A012	c	7	PPP1R8	27.21095	26.16841
A012	c	8	PPIL1	27.75244	25.85934
A012	c	9	SRPK3	29.11245	27.50655
A012	c	10	DDX41	28.01797	25.16277
A012	c	11	YWHAG	28.31174	26.74777
A012	c	12	TCERG1	Undetermined	35.54082
A012	d	1	MSI1	27.88043	27.23335
A012	d	2	C16orf80	37.21215	33.04039
A012	d	3	TARDBP	38.92744	34.72105
A012	d	4	CIR	27.87924	26.39817
A012	d	5	YBX1	28.04258	26.61241
A012	d	6	ZFR	28.42363	26.74483
A012	d	7	LGALS3	27.90361	25.46862
A012	d	8	BRUNOL5	28.31858	26.94112
A012	d	9	MOV10	28.47701	27.07006
A012	d	10	RBM22	27.83434	26.62937
A012	d	11	SRPK3	28.12207	26.59218
A012	d	12	SF3A3	26.41962	25.22877
A012	e	1	DEK	30.92717	27.65888
A012	e	2	U2AF1	28.57628	27.59779
A012	e	3	C16orf80	29.90094	29.09157
A012	e	4	FAU	28.99101	27.42003
A012	e	5	SR140	27.811	26.24554
A012	e	6	RBBP7	28.08118	26.51211

A012	e	7	LSM2	27.47787	26.85688
A012	e	8	SMN1	29.40586	27.22646
A012	e	9	PRPF4B	29.10119	27.92669
A012	e	10	INTS6	28.6532	26.4063
A012	e	11	ARS2	28.80634	27.65855
A012	e	12	DGCR14	33.75898	32.90967
A012	f	1	KIN	30.47191	28.00015
A012	f	2	ZNF207	29.57645	27.28663
A012	f	3	PHF5A	29.01911	26.95272
A012	f	4	BUD13	28.01415	25.02005
A012	f	5	LOC100130289	28.68434	26.59006
A012	f	6	RBMXL2	29.94909	27.94929
A012	f	7	DHX38	29.34243	27.897
A012	f	8	ZRSR2	30.06498	28.86912
A012	f	9	BAT1	28.91971	27.1552
A012	f	10	LOC100130190	28.24808	27.31278
A012	f	11	LOC100127915	28.14935	26.79895
A012	f	12	SDCCAG10	28.09305	26.42062
A012	g	1	PUF60	30.33355	27.161
A012	g	2	SNRPD3	27.58248	27.42152
A012	g	3	RALYL	28.64604	26.23743
A012	g	4	INTS6	28.90839	26.77748
A012	g	5	PRPF8	29.73439	28.58687
A012	g	6	SPEN	Undetermined	34.88197
A012	g	7	PPIL2	29.83998	27.42967
A012	g	8	SDCCAG10	31.03696	29.75635
A012	g	9	CCNK	29.8314	28.48814
A012	g	10	SNRNP40	27.0185	26.23171
A012	g	11	ROD1	28.71385	26.52256
A012	g	12	PSIP1	28.32271	26.70275
A012	h	1	CD2BP2	34.93744	33.88138
A012	h	2	EXOSC8	37.44827	34.75945
A012	h	3	XRN2	28.73296	28.03651
A012	h	4	EIF4G3	30.26227	29.40676
A012	h	5	MYEF2	36.61959	33.184
A012	h	6	TNPO1	29.65156	27.81294
A012	h	7	RBM4	30.37702	29.01338
A012	h	8	HNRNPH2	Undetermined	Undetermined
A012	h	9	DHX38	28.84518	27.11157
A012	h	10	RBMX2	30.51159	28.05279
A012	h	11	SF3B3	28.68858	26.63636
A012	h	12	PPP1R8	32.30713	32.47207
A013	a	1	TOP1	28.32295	25.76462

A013	a	2	XAB2	5.925935	23.54121
A013	a	3	LOC402026	30.39806	23.63744
A013	a	4	THOC7	28.61888	25.62417
A013	a	5	BRUNOL5	30.98324	23.64958
A013	a	6	PCBP3	29.47062	23.08117
A013	a	7	AKAP8	28.4678	27.14837
A013	a	8	SKIV2L2	28.33191	25.00618
A013	a	9	HNRNPA2B1	28.47539	25.2577
A013	a	10	WBP11	Undetermined	27.06045
A013	a	11	HRNBP3	27.07101	25.34042
A013	a	12	SDCCAG10	26.21891	24.6898
A013	b	1	LOC644035	29.16364	24.78799
A013	b	2	LOC644422	26.31482	25.27416
A013	b	3	ZFR	25.31068	25.27984
A013	b	4	CTNNBL1	27.21833	25.01073
A013	b	5	SNRPB	26.21972	24.60946
A013	b	6	LOC728554	27.22989	24.32657
A013	b	7	U2AF1	29.77087	23.80223
A013	b	8	SAFB	27.06503	25.15547
A013	b	9	TNPO1	26.67281	24.44531
A013	b	10	MOV10	26.66312	25.26999
A013	b	11	XRN2	27.70536	25.66866
A013	b	12	LSM5	27.12914	22.20849
A013	c	1	INTS3	28.15138	24.65128
A013	c	2	HMG1L10	25.75991	25.6134
A013	c	3	CLK4	26.60307	24.54239
A013	c	4	RBM17	27.08148	24.92611
A013	c	5	BRUNOL4	26.89545	24.90959
A013	c	6	TNPO1	26.57841	24.49177
A013	c	7	SMARCA5	27.55989	24.80489
A013	c	8	WDR25	27.94976	25.5541
A013	c	9	LOC100130178	27.1448	25.18082
A013	c	10	SCAF1	27.42082	25.35209
A013	c	11	CWF19L1	26.75133	25.00183
A013	c	12	SNIP1	26.74501	25.56413
A013	d	1	TDRD3	29.09241	27.8471
A013	d	2	FUBP3	11.47175	24.51665
A013	d	3	SFRS17A	26.31873	24.80449
A013	d	4	HNRNPCL1	26.92916	24.95354
A013	d	5	HNRNPL	26.93633	25.11322
A013	d	6	SFRS2B	27.11009	24.68508
A013	d	7	NCL	25.63255	24.685
A013	d	8	CPSF1	22.00947	25.13339

A013	d	9	CPSF3	26.50629	24.55672
A013	d	10	TFIP11	27.66437	25.30512
A013	d	11	RBM15	24.93888	24.78721
A013	d	12	PPIE	27.11208	24.48222
A013	e	1	DIS3	28.50419	24.82676
A013	e	2	LUC7L2	27.20683	25.91257
A013	e	3	EWSR1	27.97678	24.40632
A013	e	4	PARP1	26.4891	25.01745
A013	e	5	C21orf66	27.05147	24.6978
A013	e	6	DHX15	27.16561	24.73221
A013	e	7	FUBP1	26.9416	25.19914
A013	e	8	C14orf166	26.88645	25.02679
A013	e	9	CWF19L1	27.35771	26.01435
A013	e	10	SFRS5	26.99342	25.58055
A013	e	11	SMN1	26.43074	25.70139
A013	e	12	C21orf66	28.04021	25.66596
A013	f	1	SNRNP70	31.51377	26.33001
A013	f	2	SF4	26.90846	24.67495
A013	f	3	GPATCH1	27.87387	25.10218
A013	f	4	CHERP	25.89304	23.97481
A013	f	5	TNPO1	26.38776	24.17207
A013	f	6	DDX5	27.10208	24.93375
A013	f	7	DDX39	28.04015	25.80446
A013	f	8	DGCR14	28.91584	26.34402
A013	f	9	SFPQ	26.38878	24.72688
A013	f	10	LSM4	27.14591	25.47417
A013	f	11	PRPF3	27.34533	24.99578
A013	f	12	MBNL3	27.39768	25.20613
A013	g	1	TXNL4A	27.85986	24.96262
A013	g	2	SNRNP35	28.10807	25.05933
A013	g	3	LOC643167	27.61376	24.95488
A013	g	4	STRBP	27.15232	25.21429
A013	g	5	EIF2S2	28.98405	25.76094
A013	g	6	ELAVL4	27.94378	25.56444
A013	g	7	ADAR	27.35632	25.05356
A013	g	8	C1orf55	27.84714	25.51722
A013	g	9	DHX8	28.31832	26.60496
A013	g	10	ARS2	27.47719	24.86997
A013	g	11	RUVBL2	24.24805	25.407
A013	g	12	RBM4	26.95908	25.05691
A013	h	1	RP9	27.57947	24.80381
A013	h	2	CUGBP2	28.77433	26.46373
A013	h	3	RBM3	27.33992	24.66158

A013	h	4	HNRNPL	27.36414	23.69751
A013	h	5	CWC15	26.26165	24.05584
A013	h	6	MAGOH	26.66055	22.54508
A013	h	7	EXOSC9	26.7606	24.88571
A013	h	8	THOC2	26.65937	24.29038
A013	h	9	HMGB1	29.0619	27.78654
A013	h	10	EXOSC8	Undetermined	Undetermined
A013	h	11	RNPC3	32.76043	22.92414
A013	h	12	SF3B14	11.78658	Undetermined
A014	a	1	PSPC1	25.7873	26.05936
A014	a	2	CCDC12	26.71815	24.32978
A014	a	3	DHX38	27.35564	25.1372
A014	a	4	INTS3	28.70434	25.87874
A014	a	5	TET1	27.75564	24.39996
A014	a	6	PCBP2	28.79127	26.78363
A014	a	7	SRPK1	27.58645	25.09741
A014	a	8	MATR3	29.41758	27.55918
A014	a	9	ELAVL2	25.5015	24.75952
A014	a	10	HTATSF1	26.8893	24.75568
A014	a	11	SRRM2	34.76942	28.77182
A014	a	12	XRN2	26.02799	24.31945
A014	b	1	PRCC	27.70578	26.10213
A014	b	2	RALYL	27.6752	24.96895
A014	b	3	DNAJC17	27.66756	25.54318
A014	b	4	PRPF38A	27.34936	24.31336
A014	b	5	SMN1	27.20362	24.43165
A014	b	6	PCBP1	Undetermined	24.79705
A014	b	7	CHERP	26.68609	24.59469
A014	b	8	SCAF1	30.0842	27.58586
A014	b	9	SYNCRIP	27.44606	25.19591
A014	b	10	DDX26B	26.68294	25.30585
A014	b	11	SMN2	28.24826	26.06317
A014	b	12	QPCT	30.67242	29.08417
A014	c	1	YWHAG	30.51557	26.03884
A014	c	2	NOVA2	26.55396	23.43905
A014	c	3	SF3B5	25.65275	23.99171
A014	c	4	SNRNP48	27.00027	24.5013
A014	c	5	KIN	27.48986	24.44377
A014	c	6	HNRNPUL1	27.33971	24.36669
A014	c	7	PUF60	26.16447	24.75275
A014	c	8	LOC728554	Undetermined	33.42291
A014	c	9	CRKRS	30.20164	28.77991
A014	c	10	HNRNPUL2	26.47707	24.865

A014	c	11	CLK1	31.52099	29.61325
A014	c	12	CWC15	32.37815	29.72197
A014	d	1	RBM17	27.30664	24.82074
A014	d	2	SNRNP200	28.21975	26.42263
A014	d	3	HNRPDL	28.14232	26.42013
A014	d	4	KHDRBS1	28.42739	26.39764
A014	d	5	PQBP1	26.47313	23.95301
A014	d	6	XRCC6	34.18406	31.33286
A014	d	7	DDX23	26.93323	25.17986
A014	d	8	CSDA	34.15573	33.11552
A014	d	9	SFRS3	27.58419	24.82052
A014	d	10	HNRNPK	30.62681	27.6933
A014	d	11	MSI2	29.9825	28.13781
A014	d	12	PPIL2	31.10155	26.88052
A014	e	1	TMEM149	27.49313	24.92094
A014	e	2	LOC728554	27.71663	25.31468
A014	e	3	SNRPB2	27.81765	25.67448
A014	e	4	RP9	27.96582	26.30172
A014	e	5	ILF3	30.58464	29.16616
A014	e	6	SMNDC1	25.88261	24.10907
A014	e	7	LSM6	26.41848	23.40081
A014	e	8	EIF4G3	Undetermined	36.18094
A014	e	9	LOC729200	26.54289	24.82855
A014	e	10	LSMD1	29.47487	27.42147
A014	e	11	PRPF19	28.55213	26.79749
A014	e	12	PPM1G	35.29624	32.84765
A014	f	1	XRCC6	27.10656	25.11534
A014	f	2	SF3B1	27.43861	25.48858
A014	f	3	NUDT21	28.12885	26.63166
A014	f	4	LOC644422	27.58606	25.95526
A014	f	5	SART1	28.80674	27.02666
A014	f	6	TRA2A	30.29239	28.81578
A014	f	7	LOC728554	27.12944	24.27441
A014	f	8	LSM4	29.04105	27.29001
A014	f	9	FUS	26.96562	27.52958
A014	f	10	TPR	28.99131	26.66673
A014	f	11	BRUNOL6	27.95161	26.17094
A014	f	12	C2orf3	29.48412	28.23474
A014	g	1	WBP4	27.17634	24.70024
A014	g	2	DDX17	27.20299	24.87722
A014	g	3	SART3	28.94216	26.82408
A014	g	4	FAM120A	29.06471	27.72081
A014	g	5	DDX41	30.20375	28.45101

A014	g	6	ZFR	28.69324	26.51975
A014	g	7	EIF3M	28.67924	26.1707
A014	g	8	EXOSC10	28.30006	26.21527
A014	g	9	ROD1	27.5857	25.03365
A014	g	10	CCNA1	27.64796	24.75664
A014	g	11	PARP1	27.861	24.96842
A014	g	12	FUBP3	28.73467	26.89791
A014	h	1	PPM1G	31.82195	30.1329
A014	h	2	NCBP1	28.42857	26.54113
A014	h	3	MBNL3	29.49415	26.94022
A014	h	4	C14orf166	30.57977	28.35576
A014	h	5	ZMAT2	29.38459	27.32488
A014	h	6	RP9	28.3759	25.06591
A014	h	7	SYNCRIP	28.42734	25.93737
A014	h	8	C1QBP	29.76342	28.18179
A014	h	9	HMGB3	28.25204	26.02399
A014	h	10	PABPN1	28.13676	26.79377
A014	h	11	DDX21	32.356	29.93475
A014	h	12	BAT1	33.02773	30.40233
A015	a	1	ZCCHC8	25.75611	23.99465
A015	a	2	PRPF40B	25.94045	24.39818
A015	a	3	SFRS17A	26.14093	24.30178
A015	a	4	EIF3A	26.74121	25.01042
A015	a	5	INTS6	25.73295	24.39668
A015	a	6	PQBP1	25.93059	24.47713
A015	a	7	SNRNP70	26.83967	24.78556
A015	a	8	RALYL	26.88717	25.02241
A015	a	9	SFRS10	26.71411	25.114
A015	a	10	CD2BP2	25.95536	24.62531
A015	a	11	CPSF3	25.742	23.66535
A015	a	12	HNRNPH1	26.01256	25.5305
A015	b	1	DGCR14	26.54401	23.92177
A015	b	2	PTBP2	25.73608	24.98615
A015	b	3	KIAA1429	26.63748	24.71993
A015	b	4	KHDRBS1	26.85712	24.88884
A015	b	5	HTATSF1	26.59082	25.11181
A015	b	6	ZRSR2	26.95952	25.05974
A015	b	7	CD2BP2	26.56949	25.37266
A015	b	8	DDX23	27.68219	25.94896
A015	b	9	KLHDC8A	26.44399	25.0487
A015	b	10	NOSIP	26.06486	24.94789
A015	b	11	GRSF1	26.05555	24.79882
A015	b	12	PPIH	25.12767	24.44939

A015	c	1	HNRNPH2	26.10496	25.22555
A015	c	2	EFTUD2	26.24781	25.68141
A015	c	3	CIRBP	26.57803	24.89119
A015	c	4	U2AF1L4	27.25789	24.90433
A015	c	5	CPSF2	26.85895	24.85634
A015	c	6	DEK	27.90836	26.80789
A015	c	7	CWC22	26.44521	24.49623
A015	c	8	RBM39	26.88447	25.92526
A015	c	9	LSMD1	25.9025	25.05819
A015	c	10	HNRNPA1	26.04505	24.48028
A015	c	11	HNRNPU	27.87097	26.67968
A015	c	12	SRPK2	26.63716	24.82014
A015	d	1	SNRPA	25.88832	25.41292
A015	d	2	MAGOHB	26.8288	24.96326
A015	d	3	PPM1G	26.37808	25.14393
A015	d	4	SYF2	27.59487	26.05851
A015	d	5	LOC100128469	28.19297	26.46944
A015	d	6	SNRPD2	26.37513	25.09606
A015	d	7	SRPK1	25.68397	24.11558
A015	d	8	BCAS2	26.43401	24.40515
A015	d	9	SF3A1	26.45701	24.8865
A015	d	10	ILF2	28.7212	25.08213
A015	d	11	INTS3	26.70417	25.05796
A015	d	12	SMNDC1	27.91727	26.0617
A015	e	1	PSPC1	25.5867	25.02213
A015	e	2	SF3A1	26.2523	25.11442
A015	e	3	FRG1	26.93407	25.42391
A015	e	4	CTNNBL1	27.05203	25.98335
A015	e	5	SFRS16	27.52731	25.09921
A015	e	6	LSM6	25.31567	24.25707
A015	e	7	CDC40	26.73376	25.34868
A015	e	8	PPM1G	26.06054	24.9847
A015	e	9	PRPF4B	26.93678	25.61575
A015	e	10	SKIV2L2	26.7758	25.90588
A015	e	11	CCDC55	26.87003	25.34503
A015	e	12	SNRNP35	26.59274	24.93333
A015	f	1	QKI	27.03799	26.42751
A015	f	2	TPR	28.03826	26.60318
A015	f	3	HNRNPA3	26.88277	24.53303
A015	f	4	NXF1	27.37459	25.97767
A015	f	5	TRA2A	28.89237	26.93461
A015	f	6	C14orf166	26.5777	25.63157
A015	f	7	PCBP4	26.79731	25.67543

A015	f	8	RBM24	27.38417	25.73175
A015	f	9	ELAVL2	26.88796	25.14495
A015	f	10	RUVBL2	27.50662	26.32329
A015	f	11	CXCL12	27.39235	25.07298
A015	f	12	ZMAT5	26.74174	25.1206
A015	g	1	HNRNPH3	26.70179	24.49736
A015	g	2	SNRPD2	26.47517	26.01617
A015	g	3	HNRNPA1	26.05982	24.88729
A015	g	4	DDX5	30.22666	27.97112
A015	g	5	DDX26B	27.07459	25.5051
A015	g	6	LOC100130102	27.4423	26.23118
A015	g	7	SNRNP25	27.6821	25.68437
A015	g	8	POLR2B	26.54562	24.96437
A015	g	9	MBNL2	27.13136	25.72772
A015	g	10	PLRG1	27.7175	26.07465
A015	g	11	PPWD1	28.46894	26.95023
A015	g	12	LOC644035	27.0127	25.55772
A015	h	1	PRPF19	25.97851	24.58435
A015	h	2	LOC643446	26.9629	24.81274
A015	h	3	LOC652607	26.36742	24.68517
A015	h	4	PPIH	26.22934	24.97739
A015	h	5	FASTK	26.51249	25.04136
A015	h	6	GRSF1	26.93922	25.67496
A015	h	7	HNRNPL	26.442	25.04486
A015	h	8	PSPC1	26.83035	25.00918
A015	h	9	HNRNPCL1	27.75119	26.85464
A015	h	10	CPSF6	29.03041	27.25024
A015	h	11	QKI	26.48494	24.61688
A015	h	12	LOC652147	27.4686	26.5037
A016	a	1	EIF4A3	27.39781	25.30753
A016	a	2	SF3B3	27.40063	26.14284
A016	a	3	HIST2H2AA3	27.84205	25.69802
A016	a	4	PSEN1	26.47256	24.90014
A016	a	5	PSEN1	28.34193	26.98404
A016	a	6	TIA1	27.49144	25.77231
A016	a	7	LOC652607	27.31847	26.4557
A016	a	8	ZMAT5	33.74739	32.00056
A016	a	9	INTS1	34.26859	32.32736
A016	a	10	LOC100133872	28.20622	26.91995
A016	a	11	LSM4	33.61728	32.13657
A016	a	12	SR140	33.6694	33.2454
A016	b	1	LSM10	27.2901	25.45685
A016	b	2	DDX26B	25.86944	24.82833

A016	b	3	PUF60	27.55187	25.74467
A016	b	4	THOC2	26.70767	25.5614
A016	b	5	KPNA2	27.51642	26.31869
A016	b	6	SFRS14	28.97329	27.16478
A016	b	7	DIDO1	26.72883	25.5049
A016	b	8	WTAP	27.02726	26.02507
A016	b	9	AQR	27.14205	25.47094
A016	b	10	NXF1	26.62489	25.5367
A016	b	11	LOC644035	27.25322	25.94093
A016	b	12	RBM5	31.04226	28.48287
A016	c	1	SF1	25.90782	24.93958
A016	c	2	ZRANB2	28.16519	25.60094
A016	c	3	PCBP3	27.75149	25.91141
A016	c	4	KLHDC8A	28.64739	27.60126
A016	c	5	RBM5	27.33243	25.43704
A016	c	6	SNRNP27	26.10391	25.10002
A016	c	7	ZMAT5	26.6556	25.13345
A016	c	8	LOC643446	28.04293	26.84832
A016	c	9	ZMAT2	27.8559	25.96024
A016	c	10	TRA2A	27.63265	26.3585
A016	c	11	LSM7	27.11498	25.53538
A016	c	12	KIAA1429	Undetermined	25.16924
A016	d	1	DHX8	26.69786	25.59941
A016	d	2	SMC1A	27.39727	25.80487
A016	d	3	HNRNPM	26.53667	24.93809
A016	d	4	FMR1	26.00056	25.21121
A016	d	5	PPIL2	27.46905	25.42183
A016	d	6	KLHDC8A	25.83478	24.77932
A016	d	7	PQBP1	26.76705	25.62776
A016	d	8	PHRF1	27.11714	26.19116
A016	d	9	PCBP2	29.0006	27.68607
A016	d	10	TAF15	27.83657	26.55325
A016	d	11	SNRNP40	27.93676	25.65756
A016	d	12	ZMAT5	28.6675	25.57526
A016	e	1	C19orf43	26.2305	25.55693
A016	e	2	C16orf80	27.19266	25.62497
A016	e	3	CHERP	26.18719	25.12421
A016	e	4	PCBP4	27.01582	24.89246
A016	e	5	CPSF3	26.28218	25.38658
A016	e	6	WDR33	Undetermined	25.46741
A016	e	7	RP9	27.52902	26.59474
A016	e	8	PRPF3	27.5988	25.87415
A016	e	9	RBM38	30.06208	27.21822

A016	e	10	KIAA1429	Undetermined	27.24943
A016	e	11	SFRS8	28.64486	25.85015
A016	e	12	HNRNPCL1	Undetermined	26.21191
A016	f	1	CDC5L	27.38394	24.83745
A016	f	2	RBM22	25.89691	24.79376
A016	f	3	KHDRBS3	24.77514	25.29193
A016	f	4	ELAVL2	24.91558	25.42417
A016	f	5	DGCR14	27.42834	25.48934
A016	f	6	DDX39	21.55399	25.45934
A016	f	7	SFPQ	Undetermined	26.43827
A016	f	8	PRPF19	27.67965	26.11702
A016	f	9	POLR2B	27.84509	26.70123
A016	f	10	ELAVL1	Undetermined	27.43224
A016	f	11	SRP68	25.72597	26.45589
A016	f	12	PPIL3	23.61703	26.25849
A016	g	1	FUBP3	26.02647	23.99794
A016	g	2	MBNL3	26.46326	24.79705
A016	g	3	PRPF31	26.05072	25.12103
A016	g	4	ILF2	27.09205	25.72562
A016	g	5	TOPORS	26.87492	25.7874
A016	g	6	MBNL3	27.36719	25.92238
A016	g	7	SFRS7	28.55585	26.11943
A016	g	8	KPNA2	Undetermined	26.71383
A016	g	9	BUD31	28.67773	27.31629
A016	g	10	NOVA1	29.2548	27.45045
A016	g	11	NOSIP	28.14175	26.64198
A016	g	12	BCAS2	27.30363	25.44732
A016	h	1	SF3A2	32.19643	30.44611
A016	h	2	PSIP1	26.71307	24.03046
A016	h	3	RBM24	31.6019	30.66328
A016	h	4	TOPORS	25.22802	25.87254
A016	h	5	PPIE	28.96802	28.12363
A016	h	6	FAM120A	26.94356	25.30672
A016	h	7	SFRS9	26.78943	25.00831
A016	h	8	SFRS8	27.47549	25.56561
A016	h	9	DDX41	18.77459	Undetermined
A016	h	10	RBBP7	27.08337	26.25386
A016	h	11	LOC100131556	27.69746	25.96821
A016	h	12	CWF19L1	32.34907	32.73703
A017	a	1	PNN	26.83098	24.27477
A017	a	2	ZNF207	27.80558	24.66964
A017	a	3	DDX3X	26.9805	24.46682
A017	a	4	TRA2A	27.1315	24.17537

A017	a	5	CRNKL1	26.50232	24.05527
A017	a	6	CPSF6	28.41655	24.94921
A017	a	7	BCAS2	27.9798	24.55082
A017	a	8	LSM3	Undetermined	38.27818
A017	a	9	THOC7	29.40014	26.0753
A017	a	10	PABPN1	26.33825	24.31111
A017	a	11	THOC2	26.9346	24.04942
A017	a	12	NXF1	27.0124	23.57749
A017	b	1	SFPQ	26.98676	24.61965
A017	b	2	C2orf3	27.37178	25.32418
A017	b	3	SNRPD3	26.73063	24.17634
A017	b	4	TRA2A	26.61622	24.2282
A017	b	5	PRPF18	26.36172	23.82643
A017	b	6	ZMAT5	25.76385	23.96108
A017	b	7	SFRS16	27.83801	24.70752
A017	b	8	HTATSF1	27.35928	24.92162
A017	b	9	PRPF31	25.31788	24.09647
A017	b	10	SFPQ	26.66548	24.14029
A017	b	11	PPIH	26.54671	23.8059
A017	b	12	HNRNPUL1	27.30696	23.05633
A017	c	1	SRPK3	25.99751	24.29077
A017	c	2	HCFC1	26.63984	24.97547
A017	c	3	DDX3Y	28.14277	24.14358
A017	c	4	CCNK	26.48129	24.57377
A017	c	5	SFRS10	26.80568	23.83718
A017	c	6	WDR25	26.30321	23.4091
A017	c	7	PRPF6	26.19207	24.17544
A017	c	8	HNRNPC	26.17227	23.52098
A017	c	9	HNRPDL	26.02691	23.25233
A017	c	10	RBM22	25.0446	23.48593
A017	c	11	PRPF38B	26.13554	24.18508
A017	c	12	LUC7L2	27.26268	24.53814
A017	d	1	SMU1	27.1279	25.11321
A017	d	2	NCBP2	26.7209	24.61924
A017	d	3	RBM42	26.45556	24.13969
A017	d	4	HNRNPF	26.87437	24.26567
A017	d	5	ERG	27.53966	21.73596
A017	d	6	RUVBL2	25.93462	23.17619
A017	d	7	ZFR	26.294	23.82105
A017	d	8	INTS1	25.81344	23.57155
A017	d	9	USP39	26.29959	23.93453
A017	d	10	MSI1	27.93234	24.92863
A017	d	11	LOC652595	26.87893	24.62114

A017	d	12	CTNNBL1	27.35237	25.08323
A017	e	1	ZCRB1	26.17202	23.51378
A017	e	2	LSM8	26.87822	24.43397
A017	e	3	C22orf28	26.52041	23.9278
A017	e	4	RBM10	24.96723	23.45387
A017	e	5	LOC728448	26.21275	23.66423
A017	e	6	DNAJC8	27.62137	25.10169
A017	e	7	CCDC12	26.70049	23.74179
A017	e	8	NUMA1	26.8485	24.23021
A017	e	9	U2AF1	25.71593	23.75617
A017	e	10	PIAS4	28.4114	25.95411
A017	e	11	HNRNPU	25.01477	24.08713
A017	e	12	C21orf110	29.82575	26.95728
A017	f	1	SDCCAG10	26.42847	24.03216
A017	f	2	RALYL	26.99434	25.03205
A017	f	3	EXOSC8	26.49664	25.0528
A017	f	4	PHF5A	25.76274	23.54454
A017	f	5	CPSF6	26.43509	24.92151
A017	f	6	USP39	28.01957	25.41309
A017	f	7	LOC100128402	26.82159	23.94438
A017	f	8	CUGBP1	26.92408	25.23265
A017	f	9	TNRC4	27.5666	24.73627
A017	f	10	FIP1L1	25.17764	23.11225
A017	f	11	CLK3	26.80011	24.754
A017	f	12	ZFR	27.27652	24.71258
A017	g	1	TARDBP	26.9899	24.21507
A017	g	2	STRBP	26.42626	24.15678
A017	g	3	CRKRS	26.86803	24.81297
A017	g	4	RBM9	26.91754	23.58054
A017	g	5	LUC7L	26.58105	23.6132
A017	g	6	ZMAT2	26.77928	24.20404
A017	g	7	TRA2A	26.47357	23.57324
A017	g	8	SNRNP40	27.75839	24.97162
A017	g	9	SNRNP70	27.1653	25.55854
A017	g	10	C2orf3	30.50767	29.48938
A017	g	11	HMG4L	26.75505	24.95639
A017	g	12	AKAP8	26.53005	24.27105
A017	h	1	MOV10	27.67668	23.91883
A017	h	2	THOC6	26.55652	24.08022
A017	h	3	LSM8	26.4113	24.74807
A017	h	4	CWC15	26.46569	23.74918
A017	h	5	FAU	26.59104	24.17633
A017	h	6	SNRPD2	27.65315	25.88912

A017	h	7	ZNF207	28.34339	24.78832
A017	h	8	DIS3	30.25712	28.55882
A017	h	9	DDX5	28.58404	27.50058
A017	h	10	HNRNPM	32.28655	30.85842
A017	h	11	KHDRBS3	27.54127	24.73885
A017	h	12	SF3B2	32.42495	30.58517
A018	a	1	RBMXL2	26.22281	23.62358
A018	a	2	TFIP11	26.37219	24.43802
A018	a	3	BRUNOL5	27.22846	25.11758
A018	a	4	PLRG1	26.45684	23.94435
A018	a	5	RBM5	26.54553	23.58838
A018	a	6	C21orf66	26.54879	23.64693
A018	a	7	BUD13	27.07653	24.14375
A018	a	8	HNRNPR	29.78794	28.13919
A018	a	9	ARS2	27.60499	25.00478
A018	a	10	SF3B2	14.85425	28.09745
A018	a	11	DHX38	26.77251	24.66034
A018	a	12	SFRS11	25.8682	24.31441
A018	b	1	DIDO1	26.54588	23.85189
A018	b	2	PCBP2	25.22306	23.81958
A018	b	3	RBM25	26.59424	23.97614
A018	b	4	CPSF6	26.16939	23.07106
A018	b	5	KIN	26.65672	23.79906
A018	b	6	SF3B5	27.1985	24.02245
A018	b	7	DHX9	26.0011	23.86198
A018	b	8	TIA1	26.4726	23.94324
A018	b	9	HNRNPUL2	26.3953	24.19845
A018	b	10	SSB	25.72999	23.85565
A018	b	11	THOC6	28.38963	25.36661
A018	b	12	LOC643446	26.2688	23.99454
A018	c	1	ADAR	26.48772	24.21053
A018	c	2	LOC100129329	26.13672	24.33289
A018	c	3	RBMX	27.19898	25.12252
A018	c	4	SNRNP35	27.24089	23.90255
A018	c	5	BCAS2	26.03671	23.50769
A018	c	6	HNRNPR	25.74369	24.09741
A018	c	7	RBM26	30.06847	27.3031
A018	c	8	EIF2S2	26.20318	24.30209
A018	c	9	SF3A2	27.78605	25.59603
A018	c	10	SFRS11	27.70145	25.24367
A018	c	11	ILF2	26.17606	24.24093
A018	c	12	SYF2	26.24608	24.69141
A018	d	1	ACIN1	25.93115	23.93969

A018	d	2	DDX1	27.07437	24.95427
A018	d	3	PRPF40A	27.57049	24.5795
A018	d	4	SRPK1	25.97345	23.71276
A018	d	5	STRBP	26.08567	23.58226
A018	d	6	FRG1	25.17267	24.06135
A018	d	7	DDX17	25.98888	23.41733
A018	d	8	DDX46	26.31712	23.61474
A018	d	9	AQR	26.18982	24.45797
A018	d	10	KHDRBS1	25.99898	23.6259
A018	d	11	EIF3M	26.33206	23.73027
A018	d	12	RBM8A	26.1364	23.92545
A018	e	1	GTF2I	27.0923	24.48549
A018	e	2	XAB2	26.85764	24.65287
A018	e	3	PRPF38A	26.66826	24.53346
A018	e	4	RNPC3	26.03702	23.63743
A018	e	5	PSIP1	25.62088	23.25227
A018	e	6	LSM5	26.49829	24.26208
A018	e	7	DDX1	25.58954	23.77839
A018	e	8	PCBP4	26.22746	25.05096
A018	e	9	ELAVL4	26.22744	24.69298
A018	e	10	PRPF38B	26.38909	24.31792
A018	e	11	RBBP7	25.92592	24.15698
A018	e	12	SF3B3	27.27122	24.36208
A018	f	1	SLU7	26.747	24.20968
A018	f	2	SR140	26.13856	24.4511
A018	f	3	LOC100131482	26.6702	23.99767
A018	f	4	QPCT	27.14366	23.85788
A018	f	5	HNRNPF	26.02906	23.49045
A018	f	6	C19orf43	28.12832	24.78121
A018	f	7	SFPQ	27.13655	24.72692
A018	f	8	SFRS12	26.00183	24.13784
A018	f	9	GRSF1	27.92425	25.52749
A018	f	10	NCBP1	26.83598	23.88432
A018	f	11	SFRS4	26.72752	24.048
A018	f	12	NOSIP	26.33789	23.48714
A018	g	1	PRPF38B	26.36669	23.62608
A018	g	2	ZCRB1	27.36491	24.07294
A018	g	3	ELAVL4	27.01189	23.98563
A018	g	4	DIDO1	26.81143	24.55326
A018	g	5	C1QBP	26.09446	24.26809
A018	g	6	CPSF6	28.86206	24.93669
A018	g	7	SNW1	26.92981	24.17682
A018	g	8	SNRPF	26.76324	24.52986

A018	g	9	KPNA2	26.8885	24.12646
A018	g	10	DNAJC8	26.38055	23.421
A018	g	11	MOV10	26.65601	24.11076
A018	g	12	THOC5	25.58114	23.52192
A018	h	1	EXOSC4	25.19057	23.27085
A018	h	2	ELAVL1	26.13379	23.60098
A018	h	3	WDR25	27.88993	24.79418
A018	h	4	RBM24	26.80038	24.04629
A018	h	5	PABPN1	25.40675	23.94729
A018	h	6	KIN	30.57255	26.99845
A018	h	7	LOC643446	28.77152	26.8308
A018	h	8	LOC100129492	28.41825	25.58622
A018	h	9	FIP1L1	26.9567	24.71785
A018	h	10	DDX21	26.28187	23.7665
A018	h	11	PRPF18	26.40928	23.60601
A018	h	12	SFRS5	31.00851	29.10212
A019	a	1	PHF5A	Undetermined	Undetermined
A019	a	2	CPSF3	26.92896	24.56853
A019	a	3	LOC652595	28.71623	27.37013
A019	a	4	HNRNPA1	28.05116	35.97388
A019	a	5	LOC92755	28.06726	25.16514
A019	a	6	SFRS8	29.80965	31.65727
A019	a	7	SPEN	26.76935	25.51518
A019	a	8	SRPK3	27.70858	25.43296
A019	a	9	PLRG1	27.74064	26.08665
A019	a	10	PPAN	26.40362	25.52075
A019	a	11	SCAF1	27.59293	25.48538
A019	a	12	MSI2	29.01535	29.00654
A019	b	1	PRPF38A	26.61653	25.04281
A019	b	2	RBM4	26.78718	25.76959
A019	b	3	DHX15	26.90122	25.50359
A019	b	4	RBBP7	25.44691	23.48276
A019	b	5	HNRNPH2	27.76506	25.53251
A019	b	6	SNIP1	28.23655	25.32904
A019	b	7	PRPF40A	29.48857	26.49602
A019	b	8	SART3	27.98553	25.38514
A019	b	9	SFRS17A	27.66492	26.62468
A019	b	10	SAFB	26.67157	25.55015
A019	b	11	CUGBP1	27.42093	26.42587
A019	b	12	SF3B2	27.17691	25.57086
A019	c	1	ZNF207	24.58756	24.72813
A019	c	2	CLK3	24.28093	24.59727
A019	c	3	RBM5	27.44996	24.12858

A019	c	4	RBM26	27.12283	25.36899
A019	c	5	LOC100129492	27.16423	24.0752
A019	c	6	THOC7	27.98915	26.06902
A019	c	7	SFRS11	28.1627	25.74416
A019	c	8	PTBP2	27.76374	26.01576
A019	c	9	TAF6	27.23258	25.24975
A019	c	10	SAFB	25.94695	24.59207
A019	c	11	TNPO1	30.03039	25.76208
A019	c	12	CDC40	26.28815	24.5533
A019	d	1	SNRPC	28.40781	26.62447
A019	d	2	TARDBP	26.06389	24.79863
A019	d	3	AKAP8	28.06143	25.44171
A019	d	4	U2AF1	27.06075	24.55184
A019	d	5	LOC100130003	27.64425	25.53819
A019	d	6	RNPC3	27.65027	26.50757
A019	d	7	CD2BP2	27.62758	25.73386
A019	d	8	DDX26B	28.68465	26.2484
A019	d	9	MAGOHB	28.22138	26.29429
A019	d	10	CDC40	27.838	24.87538
A019	d	11	EIF2S2	26.43599	23.57431
A019	d	12	CCDC12	27.34474	25.60238
A019	e	1	HNRNPA2B1	23.77426	23.54959
A019	e	2	QPCT	21.97431	23.94294
A019	e	3	KHDRBS1	26.30741	26.29344
A019	e	4	NUMA1	27.0917	25.6471
A019	e	5	CLK1	28.0248	26.97196
A019	e	6	THOC6	25.77133	28.01221
A019	e	7	LSM6	27.78805	26.5411
A019	e	8	IQGAP1	28.27342	26.51773
A019	e	9	C19orf29	28.08864	26.64506
A019	e	10	DHX9	27.15716	26.00991
A019	e	11	ARS2	27.82064	26.44599
A019	e	12	RBM10	29.2649	26.12811
A019	f	1	PRPF8	24.61615	24.54167
A019	f	2	LUC7L	24.74427	23.95954
A019	f	3	KLHDC8A	26.66439	25.72952
A019	f	4	RBM15	26.20879	24.69364
A019	f	5	HNRNPA2B1	29.05049	25.79823
A019	f	6	PQBP1	26.78012	24.46916
A019	f	7	RBM26	28.23706	25.16967
A019	f	8	RNF113A	28.42513	25.53429
A019	f	9	SNRPA1	28.31192	26.79801
A019	f	10	NUDT21	26.87416	26.48563

A019	f	11	LSM7	26.26993	25.77497
A019	f	12	PRPF6	29.84785	Undetermined
A019	g	1	RNF113A	25.72214	24.82254
A019	g	2	ACIN1	25.09666	26.16309
A019	g	3	SCAF1	27.20073	25.57138
A019	g	4	HMG1L10	27.59708	25.45602
A019	g	5	RALY	29.45206	26.11371
A019	g	6	CRKRS	28.20378	25.53796
A019	g	7	LOC644035	29.01379	25.38293
A019	g	8	THOC7	27.87057	26.1667
A019	g	9	ROD1	28.94688	27.03666
A019	g	10	CCDC55	25.41733	25.3629
A019	g	11	SR140	26.70774	25.255
A019	g	12	KLHDC8A	28.3886	38.33048
A019	h	1	GPATCH1	23.73434	24.14157
A019	h	2	GPATCH1	27.35663	26.00108
A019	h	3	LNX1	27.48609	26.24991
A019	h	4	RBM25	27.1681	25.10058
A019	h	5	LOC100130109	28.29394	25.52409
A019	h	6	PPAN	28.90072	30.66758
A019	h	7	BCAS2	29.91483	26.14818
A019	h	8	EIF4A3	29.70898	26.8602
A019	h	9	IGF2BP1	28.48096	25.77685
A019	h	10	PRPF31	33.50185	32.18886
A019	h	11	FMR1	26.51958	25.26749
A019	h	12	PHRF1	Undetermined	Undetermined
A020	a	1	RBM5	28.00677	27.38124
A020	a	2	RBMXL2	29.21442	26.98577
A020	a	3	ELAVL2	Undetermined	23.43059
A020	a	4	LUC7L2	26.41094	25.57767
A020	a	5	SMC1A	28.32349	23.85498
A020	a	6	DDX41	Undetermined	17.5971
A020	a	7	SNW1	33.44561	26.79911
A020	a	8	RAVER1	30.74269	24.07358
A020	a	9	RALY	29.41631	27.41981
A020	a	10	LOC387703	29.12695	25.89513
A020	a	11	ZC3H18	Undetermined	23.96482
A020	a	12	HNRNPA1	27.83649	26.70504
A020	b	1	FIP1L1	27.72212	24.87895
A020	b	2	SFRS1	33.49703	24.4354
A020	b	3	TAF6	Undetermined	20.67138
A020	b	4	FAM120A	8.739712	19.64768
A020	b	5	PPIH	Undetermined	16.76367

A020	b	6	DNAJC17	30.05173	25.77066
A020	b	7	CPSF2	28.65824	23.68266
A020	b	8	FRG1	36.43408	24.29683
A020	b	9	PPIL1	Undetermined	20.903
A020	b	10	PRPF8	31.25902	24.4708
A020	b	11	DDX23	27.81464	26.58385
A020	b	12	CPSF2	28.51479	24.16702
A020	c	1	DHX9	27.7858	24.35606
A020	c	2	CCDC94	Undetermined	21.26414
A020	c	3	TFIP11	Undetermined	23.59469
A020	c	4	HNRPDL	31.41884	24.36091
A020	c	5	C2orf3	27.23743	24.36815
A020	c	6	LSM2	28.46752	25.66834
A020	c	7	ZCRB1	31.57651	25.70742
A020	c	8	CHERP	9.920181	23.47508
A020	c	9	PRPF40B	29.29664	26.52279
A020	c	10	DDX46	29.37457	25.52596
A020	c	11	WTAP	28.48553	26.61855
A020	c	12	INTS3	33.28719	25.07953
A020	d	1	MAGOH	Undetermined	21.63705
A020	d	2	SLC43A2	Undetermined	Undetermined
A020	d	3	U2AF2	Undetermined	20.4525
A020	d	4	RBM25	Undetermined	21.47824
A020	d	5	HCFC1	27.72647	24.74065
A020	d	6	SMC1A	28.84877	25.84231
A020	d	7	HIST2H2AA3	30.72914	26.80787
A020	d	8	DNAJC6	29.68915	26.33471
A020	d	9	ZCCHC8	29.65814	25.78145
A020	d	10	SRRM2	28.9791	25.3182
A020	d	11	TDRD3	28.10801	26.31752
A020	d	12	RBMS1	27.8805	25.07682
A020	e	1	POLR2A	Undetermined	22.77309
A020	e	2	U2AF2	29.80558	24.51511
A020	e	3	DDX3X	Undetermined	24.71924
A020	e	4	SLC43A2	Undetermined	22.83754
A020	e	5	RBM3	Undetermined	16.93203
A020	e	6	DHX38	32.33711	25.0571
A020	e	7	PUF60	27.59249	25.64134
A020	e	8	SLC43A2	27.31714	26.10465
A020	e	9	PPAN	28.58422	26.75516
A020	e	10	IQGAP1	14.54189	Undetermined
A020	e	11	SRRM2	26.57715	24.97096
A020	e	12	SMARCA5	26.99068	24.80863

A020	f	1	IK	26.05694	24.74534
A020	f	2	PCBP2	Undetermined	18.56891
A020	f	3	RBM10	Undetermined	23.66995
A020	f	4	RBMS1	Undetermined	23.92146
A020	f	5	BUD13	28.55819	25.47787
A020	f	6	PPP1R8	27.33505	25.39988
A020	f	7	SF4	27.85342	25.5729
A020	f	8	TFIP11	27.99438	24.96572
A020	f	9	SF1	28.44655	26.91236
A020	f	10	YWHAQ	Undetermined	24.0242
A020	f	11	MSI2	28.89414	23.7528
A020	f	12	RBM38	28.18152	25.437
A020	g	1	CCDC94	26.60508	23.24847
A020	g	2	LGALS3	Undetermined	20.07824
A020	g	3	HNRNPF	27.92667	25.9073
A020	g	4	SF3B4	27.61328	26.08086
A020	g	5	LSM10	31.02915	26.06895
A020	g	6	LOC644811	28.67378	26.15676
A020	g	7	PRPF38B	29.60898	23.71248
A020	g	8	PABPC1	28.39003	24.19621
A020	g	9	SNRNP40	28.89385	26.47268
A020	g	10	CPSF2	31.39655	24.86639
A020	g	11	PSEN1	Undetermined	25.75677
A020	g	12	SSB	32.06569	24.91047
A020	h	1	NUDT21	27.59987	26.75064
A020	h	2	TAF15	27.19725	24.86202
A020	h	3	IGF2BP3	Undetermined	24.63733
A020	h	4	RDBP	Undetermined	21.76084
A020	h	5	SFRS4	Undetermined	22.37721
A020	h	6	SFRS16	29.0744	24.49086
A020	h	7	FIP1L1	Undetermined	24.85612
A020	h	8	CPSF6	Undetermined	23.6935
A020	h	9	MBNL3	Undetermined	21.1884
A020	h	10	CLK3	30.31209	23.07637
A020	h	11	TPR	28.66718	24.92971
A020	h	12	LSM10	29.14523	27.56938
A021	a	1	C21orf66		
A021	a	2	MATR3		
A021	a	3	PRPF40A		
A021	a	4	RBMX2		
A021	a	5	PPIL1		
A021	a	6	WDR33		
A021	a	7	POLR2A		

A021	a	8	POLR2A
A021	a	9	POLDIP3
A021	a	10	STRBP
A021	a	11	BRUNOL4
A021	a	12	CIR
A021	b	1	SRPK2
A021	b	2	SAFB
A021	b	3	TET1
A021	b	4	SFRS3
A021	b	5	PHRF1
A021	b	6	POLR2A
A021	b	7	PPIE
A021	b	8	PTBP1
A021	b	9	WBP4
A021	b	10	FAM120A
A021	b	11	HRNBP3
A021	b	12	LOC442308
A021	c	1	SFRS2IP
A021	c	2	FAM120A
A021	c	3	HNRNPF
A021	c	4	KHSRP
A021	c	5	CLK4
A021	c	6	RBM42
A021	c	7	ACIN1
A021	c	8	RBM3
A021	c	9	DNAJC8
A021	c	10	CCDC94
A021	c	11	PPM1G
A021	c	12	SFRS14
A021	d	1	ZRSR2
A021	d	2	SFRS5
A021	d	3	SNW1
A021	d	4	RBMXL2
A021	d	5	WDR33
A021	d	6	SMN1
A021	d	7	PPWD1
A021	d	8	SLC43A2
A021	d	9	RBMX2
A021	d	10	CTNNBL1
A021	d	11	SRP68
A021	d	12	PPIE
A021	e	1	RBMX2
A021	e	2	RBM4

A021	e	3	RBMS1
A021	e	4	DHX35
A021	e	5	EIF4G3
A021	e	6	CLK2
A021	e	7	WBP11
A021	e	8	BUB3
A021	e	9	C1orf55
A021	e	10	ZNF207
A021	e	11	HTATSF1
A021	e	12	CLK1
A021	f	1	SMU1
A021	f	2	SPEN
A021	f	3	CDC40
A021	f	4	LOC643167
A021	f	5	NOVA1
A021	f	6	LOC644811
A021	f	7	CCDC12
A021	f	8	NOVA2
A021	f	9	NOVA1
A021	f	10	DHX15
A021	f	11	EXOSC4
A021	f	12	RBMX2
A021	g	1	FMR1
A021	g	2	SFRS2IP
A021	g	3	SLC43A2
A021	g	4	CWC15
A021	g	5	PLRG1
A021	g	6	FIP1L1
A021	g	7	SNW1
A021	g	8	CRNKL1
A021	g	9	SFRS7
A021	g	10	C2orf49
A021	g	11	NOVA2
A021	g	12	LSM8
A021	h	1	EIF3M
A021	h	2	SFRS11
A021	h	3	LSM5
A021	h	4	ZRANB2
A021	h	5	RALY
A021	h	6	DHX9
A021	h	7	RBM47
A021	h	8	ZCCHC8
A021	h	9	SNRPF

A021	h	10	FUBP3		
A021	h	11	C2orf3		
A021	h	12	GPATCH1		
A022	a	1	SNRNP35	33.21738	28.34058
A022	a	2	MSI1	31.3445	26.27399
A022	a	3	MATR3	37.85616	30.14335
A022	a	4	BUB3	38.20185	28.51125
A022	a	5	SNRNP200	33.05591	27.17252
A022	a	6	SFRS7	33.86089	28.65587
A022	a	7	LOC100128974	32.27817	28.25804
A022	a	8	TOPORS	31.90862	27.31897
A022	a	9	LSM8	35.65616	29.16853
A022	a	10	YBX1	35.39467	30.69119
A022	a	11	SF3A3	34.48562	29.00025
A022	a	12	C19orf29	34.93161	29.76332
A022	b	1	TIAL1	36.42604	30.11646
A022	b	2	DDIT3	34.56157	29.5653
A022	b	3	CRKRS	36.24048	29.76864
A022	b	4	BCAS2	33.25425	28.76852
A022	b	5	DNAJC8	34.34071	29.22008
A022	b	6	SRRM1	33.67304	28.69119
A022	b	7	PRPF4	33.76993	28.77211
A022	b	8	RAVER1	34.0116	28.31229
A022	b	9	CCDC55	37.10227	29.36056
A022	b	10	ELAVL4	33.79445	28.70858
A022	b	11	HNRNPCL1	34.05806	28.9497
A022	b	12	CWC15	32.30562	27.99835
A022	c	1	RBMS1	33.45468	27.01166
A022	c	2	EFTUD2	32.58075	27.25721
A022	c	3	TUBB	34.7644	29.55046
A022	c	4	SRPK3	30.90312	26.40421
A022	c	5	HNRNPL	37.25543	29.7608
A022	c	6	BRUNOL6	32.60761	26.24133
A022	c	7	HMGB3	39.7971	30.70348
A022	c	8	HNRNPA2B1	32.65925	26.60037
A022	c	9	PRPF4B	32.22014	27.46828
A022	c	10	RAVER1	35.85318	29.2259
A022	c	11	PRPF3	32.50956	27.82746
A022	c	12	C19orf43	31.8936	28.21928
A022	d	1	RBM15	33.21817	29.04437
A022	d	2	MFSD11	35.02655	30.13964
A022	d	3	RBM47	35.16238	29.35808
A022	d	4	PPAN	34.27295	28.24768

A022	d	5	TOP1MT	32.59723	27.78001
A022	d	6	WBP4	32.09341	26.47239
A022	d	7	AKAP8	33.08688	26.29665
A022	d	8	SF3A3	31.63026	26.7637
A022	d	9	PRPF4	31.80543	27.27748
A022	d	10	RP9	32.53791	28.35294
A022	d	11	PRPF31	35.54949	29.02137
A022	d	12	WDR25	31.41794	28.50178
A022	e	1	ZMAT2	35.00765	28.18582
A022	e	2	HRNBP3	34.31848	28.11549
A022	e	3	NOVA2	33.99775	28.37787
A022	e	4	PRPF40B	32.13395	27.4163
A022	e	5	TAF15	31.83409	26.82959
A022	e	6	LSM4	31.8711	29.23718
A022	e	7	BUB3	32.16685	25.56232
A022	e	8	SNIP1	33.37407	27.05988
A022	e	9	HNRNPUL1	31.04906	26.0262
A022	e	10	HNRNPK	32.47099	27.43673
A022	e	11	RBM7	32.53072	28.22795
A022	e	12	KPNA2	30.8131	26.79403
A022	f	1	SNRPF	33.0521	28.31094
A022	f	2	FMR1	31.66431	28.06978
A022	f	3	PPIL3	32.39947	27.52142
A022	f	4	HNRNPH3	31.2413	26.30493
A022	f	5	PRPF38A	31.64693	27.05217
A022	f	6	PPWD1	34.62339	28.70554
A022	f	7	SNRNP70	31.96413	26.45248
A022	f	8	TOP1MT	35.8875	29.65882
A022	f	9	TIA1	32.62456	27.00164
A022	f	10	HMG4L	31.4686	27.47251
A022	f	11	IGF2BP1	33.17225	27.96337
A022	f	12	PNN	32.8134	26.71923
A022	g	1	SMU1	30.6075	26.74583
A022	g	2	IK	30.99338	26.32123
A022	g	3	TXNL4A	32.81592	28.31144
A022	g	4	PRPF4	32.937	28.33134
A022	g	5	EXOSC10	32.93098	28.39645
A022	g	6	DDIT3	32.29298	27.9617
A022	g	7	SNRPC	34.1004	28.18711
A022	g	8	FUSIP1	30.78557	27.7487
A022	g	9	CIRBP	32.55253	27.33393
A022	g	10	RBM7	30.31436	26.08514
A022	g	11	SMN2	30.50576	26.42579

A022	g	12	NCL	29.19751	26.22585
A022	h	1	MBNL1	30.46157	28.21919
A022	h	2	NCBP2	25.17706	25.699
A022	h	3	CLK4	26.85865	24.68571
A022	h	4	THOC2	31.5695	30.73158
A022	h	5	HNRNPCL1	24.13353	23.72616
A022	h	6	DIDO1	29.79214	26.27047
A022	h	7	RBM9	27.95544	25.8468
A022	h	8	SFRS2	32.44453	28.96245
A022	h	9	NCBP1	25.35931	21.29574
A022	h	10	SNRPA	25.08856	26.25959
A022	h	11	THOC6	27.82481	26.29607
A022	h	12	PPWD1	24.91662	23.48206
A023	a	1	IQGAP1	Undetermined	26.51437
A023	a	2	EFTUD2	36.94117	29.6877
A023	a	3	CROP	33.86273	26.66783
A023	a	4	FAM120A	35.64672	28.60865
A023	a	5	SNRPB2	29.37882	26.58431
A023	a	6	RBM24	35.83221	28.46074
A023	a	7	DNAJC8	29.8123	26.18259
A023	a	8	C19orf29	29.36448	26.05658
A023	a	9	QKI	29.60523	26.31872
A023	a	10	POLR2A	30.01082	26.81739
A023	a	11	ILF3	33.08312	29.19714
A023	a	12	LOC392510	31.6142	27.6453
A023	b	1	HNRNPA1	Undetermined	24.82169
A023	b	2	LUC7L	32.66926	26.64382
A023	b	3	TIAL1	Undetermined	21.48581
A023	b	4	SF3A1	Undetermined	24.53074
A023	b	5	PRPF19	Undetermined	28.14258
A023	b	6	HNRNPL	Undetermined	23.08952
A023	b	7	C2orf49	15.50161	23.39315
A023	b	8	CPSF4	11.02074	15.6233
A023	b	9	POLR2B	Undetermined	25.72445
A023	b	10	IGF2BP1	33.68478	26.9425
A023	b	11	RUVBL2	30.60567	26.95624
A023	b	12	PHRF1	30.45916	27.02077
A023	c	1	DGCR14	29.68721	26.3712
A023	c	2	C8orf58	34.31869	27.22631
A023	c	3	DNAJC6	35.1223	29.01352
A023	c	4	PLRG1	33.4441	28.06239
A023	c	5	CCDC94	36.99678	27.73246
A023	c	6	STRBP	34.60213	26.7541

A023	c	7	NXF1	33.43818	26.71621
A023	c	8	FUS	Undetermined	33.87087
A023	c	9	HNRNPR	32.75027	27.07748
A023	c	10	DNAJC6	33.62368	27.63261
A023	c	11	CCDC12	33.26559	27.20251
A023	c	12	TDRD3	33.62833	28.28799
A023	d	1	PRPF38A	Undetermined	28.67504
A023	d	2	SNRNP40	33.73046	30.1974
A023	d	3	U2AF2	Undetermined	26.65151
A023	d	4	RBM47	Undetermined	26.02411
A023	d	5	YWHAQ	Undetermined	27.66815
A023	d	6	HNRPLL	38.75846	28.11672
A023	d	7	CPSF4	Undetermined	26.07871
A023	d	8	PCBP3	Undetermined	27.03063
A023	d	9	QPCT	30.31335	26.72905
A023	d	10	SNIP1	Undetermined	27.3237
A023	d	11	YWHAQ	27.2749	26.24204
A023	d	12	RBM3	36.77138	30.98406
A023	e	1	FUS	31.5461	27.19986
A023	e	2	WBP11	31.53053	27.47495
A023	e	3	HNRNPUL2	35.19611	28.33741
A023	e	4	RBM26	30.36145	28.09799
A023	e	5	SF3B14	33.77869	28.27473
A023	e	6	C1orf55	34.06833	27.58106
A023	e	7	SF3B1	33.7723	28.60671
A023	e	8	DDIT3	34.1013	28.48512
A023	e	9	C16orf80	33.08774	25.15732
A023	e	10	LGALS3	29.31049	28.18403
A023	e	11	RBM7	31.53063	29.60173
A023	e	12	ZMAT2	32.91164	29.07468
A023	f	1	SF3B14	30.80672	29.97338
A023	f	2	DHX9	30.61379	27.27377
A023	f	3	FAU	Undetermined	26.64806
A023	f	4	SNRPC	Undetermined	24.86228
A023	f	5	TOP1MT	33.99315	26.00204
A023	f	6	INTS6	6.590147	Undetermined
A023	f	7	PRPF19	Undetermined	27.04477
A023	f	8	PRPF4	35.29833	29.62511
A023	f	9	RBM42	35.84051	27.96254
A023	f	10	SFRS17A	33.87171	25.81133
A023	f	11	PRPF40B	34.54189	28.03709
A023	f	12	SFRS12	29.30553	25.53635
A023	g	1	MBNL1	Undetermined	Undetermined

A023	g	2	KPNA2	Undetermined	Undetermined
A023	g	3	STRBP	Undetermined	Undetermined
A023	g	4	HNRNPAB	Undetermined	Undetermined
A023	g	5	THOC5	Undetermined	Undetermined
A023	g	6	HNRNPC	Undetermined	Undetermined
A023	g	7	BRUNOL4	Undetermined	Undetermined
A023	g	8	SF3B3	Undetermined	Undetermined
A023	g	9	TFIP11	Undetermined	Undetermined
A023	g	10	CUGBP2	Undetermined	Undetermined
A023	g	11	TET1	Undetermined	Undetermined
A023	g	12	CIRBP	Undetermined	Undetermined
A023	h	1	SFRS1	Undetermined	30.06637
A023	h	2	NOVA1	35.54535	28.05128
A023	h	3	KHDRBS3	7.639278	17.56219
A023	h	4	SRP68	14.30791	27.46331
A023	h	5	BUD13	34.6844	30.58958
A023	h	6	SRP68	Undetermined	26.07839
A023	h	7	PABPN1	Undetermined	25.1013
A023	h	8	SYNCRIP	36.59005	24.95724
A023	h	9	LOC728554	36.74749	26.64649
A023	h	10	PPWD1	34.49315	26.83694
A023	h	11	SFRS14	35.8271	30.03692
A023	h	12	RBM15	35.16263	28.19596
A024	a	1	SNRPD3	34.61526	25.89083
A024	a	2	EIF2S2	Undetermined	26.27253
A024	a	3	HMG1L10	33.99801	28.87783
A024	a	4	ELAVL1	34.20608	24.45087
A024	a	5	FAM120A	29.8223	26.98166
A024	a	6	HNRNPK	35.37048	29.19577
A024	a	7	SNRNP27	31.9553	28.45628
A024	a	8	ELAVL4	31.44622	25.51379
A024	a	9	RUVBL2	Undetermined	26.21079
A024	a	10	TFIP11	31.81941	27.93754
A024	a	11	WDR25	7.413547	18.7371
A024	a	12	U2AF1	28.83921	25.93864
A024	b	1	SFRS11	Undetermined	31.8434
A024	b	2	DNAJC8	Undetermined	26.85483
A024	b	3	TPR	32.07103	27.82883
A024	b	4	HNRNPCL1	33.91639	28.37466
A024	b	5	CWF19L1	35.13291	28.67006
A024	b	6	PRPF18	32.41322	28.28633
A024	b	7	HNRNPR	36.11985	27.41434
A024	b	8	TIA1	31.43747	27.51792

A024	b	9	EXOSC4	30.85592	27.89874
A024	b	10	ZCCHC8	28.65032	29.2632
A024	b	11	LOC652595	32.95357	27.75425
A024	b	12	RBMS1	31.67435	29.12268
A024	c	1	BRUNOL4	32.82854	27.62865
A024	c	2	LOC644035	Undetermined	26.09704
A024	c	3	TOPORS	33.03619	27.12773
A024	c	4	NUDT21	32.59157	24.72818
A024	c	5	THOC6	30.17652	27.81039
A024	c	6	SRRM1	29.33866	26.14705
A024	c	7	SLU7	Undetermined	24.63556
A024	c	8	SF3A1	33.02297	26.91227
A024	c	9	FIP1L1	Undetermined	24.35836
A024	c	10	CPSF2	32.35603	27.28936
A024	c	11	TIA1	Undetermined	25.17127
A024	c	12	LOC644422	Undetermined	31.62343
A024	d	1	TAF15	33.967	28.27884
A024	d	2	ROD1	27.03557	29.49834
A024	d	3	HNRNPH3	32.60643	27.67918
A024	d	4	RBMXL2	21.47152	28.64382
A024	d	5	LSM8	30.73619	26.69365
A024	d	6	HTATSF1	30.70971	24.22118
A024	d	7	DNAJC6	Undetermined	22.82487
A024	d	8	PPIH	30.25553	26.1573
A024	d	9	SMN1	33.4091	26.17925
A024	d	10	XAB2	32.12734	28.7297
A024	d	11	YBX1	Undetermined	26.78702
A024	d	12	PSIP1	31.48994	31.61972
A024	e	1	SNRNP40	33.65595	28.51551
A024	e	2	CCDC55	Undetermined	29.39784
A024	e	3	LOC653889	32.68448	30.25064
A024	e	4	EIF2S2	28.76998	24.90736
A024	e	5	NCBP2	19.47904	24.65526
A024	e	6	STRBP	31.38158	25.07092
A024	e	7	ISY1	7.86438	21.07878
A024	e	8	CWC15	29.14228	25.49933
A024	e	9	XRN2	Undetermined	24.48826
A024	e	10	CUGBP2	30.56781	26.60383
A024	e	11	SNRPC	Undetermined	22.68172
A024	e	12	LOC643167	33.41523	27.55406
A024	f	1	PUF60	33.44724	28.54869
A024	f	2	LSM10	Undetermined	25.83287
A024	f	3	SFRS10	16.63881	28.52263

A024	f	4	SNRNP70	36.85217	29.54077
A024	f	5	PPIE	36.98344	27.35691
A024	f	6	LSMD1	Undetermined	24.29911
A024	f	7	THOC2	Undetermined	25.48824
A024	f	8	PRPF3	27.20886	26.47355
A024	f	9	HNRNPA1	18.36626	26.50371
A024	f	10	HNRNPUL2	25.85098	23.14728
A024	f	11	HNRNPU	12.64165	27.02008
A024	f	12	TNRC4	31.18545	31.0486
A024	g	1	PPIL3	30.17821	27.10518
A024	g	2	TAF6	32.57086	26.19784
A024	g	3	HNRNPA0	29.97918	25.59975
A024	g	4	SNRNP27	30.55359	28.13829
A024	g	5	QKI	33.37887	28.63207
A024	g	6	NOVA1	31.40865	27.62563
A024	g	7	ZCRB1	32.33978	28.00044
A024	g	8	PPAN	37.22853	29.36438
A024	g	9	SF3A2	34.47147	27.29274
A024	g	10	PCBP2	22.11728	29.38733
A024	g	11	PABPC1	Undetermined	33.88579
A024	g	12	HNRNPCL1	6.533351	22.36967
A024	h	1	C1QBP	37.97445	27.95648
A024	h	2	HNRNPC	Undetermined	24.13361
A024	h	3	PSIP1	Undetermined	27.96472
A024	h	4	KPNA2	32.46933	28.14864
A024	h	5	BRUNOL5	28.95488	27.29453
A024	h	6	RBM4	30.26283	28.61654
A024	h	7	DDX3X	35.14639	28.4138
A024	h	8	USP39	32.46225	25.34928
A024	h	9	SFRS2IP	33.38376	27.64626
A024	h	10	TXNL4A	36.79641	29.54357
A024	h	11	SFRS2	Undetermined	24.55094
A024	h	12	SFRS11	Undetermined	29.26593
A025	a	1	IGF2BP1	Undetermined	29.91992
A025	a	2	CCNK	Undetermined	31.02423
A025	a	3	DNAJC8	39.53079	32.79499
A025	a	4	DHX16	Undetermined	31.05567
A025	a	5	RBMX2	Undetermined	Undetermined
A025	a	6	DDX23	Undetermined	38.00185
A025	a	7	DDX23	Undetermined	38.79506
A025	a	8	SAFB	Undetermined	39.0303
A025	a	9	POLR2A	Undetermined	33.32503
A025	a	10	CROP	38.64621	31.0723

A025	a	11	EXOSC8	33.38586	29.85329
A025	a	12	SR140	Undetermined	Undetermined
A025	b	1	CWC22	36.64512	31.46492
A025	b	2	BUD31	Undetermined	31.19573
A025	b	3	DHX35	Undetermined	32.74606
A025	b	4	YWHAQ	Undetermined	39.20276
A025	b	5	PCBP2	Undetermined	Undetermined
A025	b	6	WBP4	Undetermined	Undetermined
A025	b	7	SNRNP40	Undetermined	33.45601
A025	b	8	HMGB3	Undetermined	Undetermined
A025	b	9	PTBP1	35.486	32.47286
A025	b	10	RBMXL2	Undetermined	37.82055
A025	b	11	THOC5	Undetermined	35.73782
A025	b	12	CPSF2	38.37209	33.23742
A025	c	1	HNRPDL	Undetermined	33.01121
A025	c	2	PLEKHA5	35.11902	34.41033
A025	c	3	SNRNP35	Undetermined	39.86335
A025	c	4	FAM120A	Undetermined	Undetermined
A025	c	5	RAVER1	33.99715	29.37182
A025	c	6	INTS3	33.58463	29.17232
A025	c	7	QKI	Undetermined	38.83827
A025	c	8	SRP68	Undetermined	Undetermined
A025	c	9	SFRS3	37.43686	39.44946
A025	c	10	SFRS17A	37.22651	Undetermined
A025	c	11	HNRNPC	Undetermined	Undetermined
A025	c	12	CUGBP1	Undetermined	33.02314
A025	d	1	MSI2	Undetermined	31.27779
A025	d	2	GPATCH1	Undetermined	29.32418
A025	d	3	PPIH	Undetermined	31.33067
A025	d	4	PSPC1	Undetermined	Undetermined
A025	d	5	HNRNPK	37.53602	32.39
A025	d	6	FUSIP1	35.99751	31.63726
A025	d	7	AQR	30.12474	26.60235
A025	d	8	CRKRS	Undetermined	37.14682
A025	d	9	TAF6	Undetermined	34.03423
A025	d	10	LOC653889	33.61958	29.24133
A025	d	11	SF3B5	39.263	35.1271
A025	d	12	SRRM2	Undetermined	37.35052
A025	e	1	LOC644035	34.82031	31.31301
A025	e	2	EXOSC8	Undetermined	32.85009
A025	e	3	SRPK2	Undetermined	36.70401
A025	e	4	SF3A2	Undetermined	Undetermined
A025	e	5	PARP1	32.65798	27.06817

A025	e	6	PHRF1	33.94792	36.85808
A025	e	7	ZNF207	32.95848	26.18379
A025	e	8	SFRS4	37.09176	30.59148
A025	e	9	TMEM149	Undetermined	32.21105
A025	e	10	SART3	36.57152	34.66494
A025	e	11	CDC5L	Undetermined	23.33986
A025	e	12	QPCT	34.95971	35.38054
A025	f	1	NOSIP	Undetermined	30.39628
A025	f	2	PTBP1	Undetermined	32.79812
A025	f	3	SNRPB	36.63179	31.39005
A025	f	4	RBM17	Undetermined	Undetermined
A025	f	5	PPIL3	36.51558	30.20876
A025	f	6	SFRS2IP	37.8928	31.04657
A025	f	7	RBM22	33.82589	29.40595
A025	f	8	MOV10	35.31795	29.82435
A025	f	9	FUBP1	37.09206	32.74047
A025	f	10	SMU1	36.53296	32.45603
A025	f	11	QKI	Undetermined	32.89586
A025	f	12	PCBP4	37.67435	31.03545
A025	g	1	PSIP1	Undetermined	29.20135
A025	g	2	SFPQ	Undetermined	31.51955
A025	g	3	LUC7L2	Undetermined	32.76535
A025	g	4	RBM47	Undetermined	Undetermined
A025	g	5	C8orf58	38.13199	34.70597
A025	g	6	CPSF2	39.51615	30.91486
A025	g	7	STRBP	39.62067	31.16838
A025	g	8	ELAVL4	32.02472	35.95498
A025	g	9	CIR	34.6988	30.85314
A025	g	10	LSM2	Undetermined	37.37862
A025	g	11	ACIN1	Undetermined	33.3617
A025	g	12	A2BP1	Undetermined	37.67432
A025	h	1	ELAVL4	Undetermined	29.90709
A025	h	2	EIF3M	36.11133	33.69723
A025	h	3	PRPF40A	Undetermined	32.15763
A025	h	4	TOP1	37.47987	31.38073
A025	h	5	SNRPD3	Undetermined	34.46745
A025	h	6	THOC7	Undetermined	31.48587
A025	h	7	C1QBP	39.51103	32.59767
A025	h	8	DDX26B	32.63839	30.00318
A025	h	9	PRCC	34.31876	36.45933
A025	h	10	RBM17	Undetermined	36.9173
A025	h	11	RBM8A	Undetermined	37.59122
A025	h	12	CPSF4	35.37342	34.39697

A026	a	1	THOC1	30.49042	26.90833
A026	a	2	DHX35	33.7244	27.83126
A026	a	3	NOVA2	33.54751	25.74912
A026	a	4	RALY	30.69495	26.53211
A026	a	5	RBM47	28.38285	24.44467
A026	a	6	SR140	33.12632	28.82093
A026	a	7	FUS	38.52948	30.84061
A026	a	8	SF1	32.66718	28.9329
A026	a	9	SFRS2B	37.35428	31.09667
A026	a	10	SF3B14	34.89892	30.12963
A026	a	11	MBNL2	29.47251	26.18629
A026	a	12	EIF3A	33.12723	25.87324
A026	b	1	DNAJC6	6.869308	28.31736
A026	b	2	LOC389901	29.66855	25.90928
A026	b	3	XRN2	29.24782	26.97735
A026	b	4	SNW1	29.43714	25.87933
A026	b	5	SF1	29.3978	25.5638
A026	b	6	SMARCA5	38.27763	31.93379
A026	b	7	PRPF40A	30.81836	30.19097
A026	b	8	BRUNOL5	32.8234	29.01952
A026	b	9	DHX15	29.77582	26.46722
A026	b	10	LOC389901	32.87972	28.21152
A026	b	11	ZMAT5	30.41256	27.3775
A026	b	12	MFSD11	29.77974	25.78572
A026	c	1	C8orf58	27.71748	24.489
A026	c	2	LGALS3	Undetermined	28.81287
A026	c	3	PPIL1	33.00684	27.28021
A026	c	4	HNRNPH1	30.60894	23.95212
A026	c	5	P2RY11	29.60412	23.9581
A026	c	6	HNRNPM	28.75808	24.7238
A026	c	7	SNRNP35	28.02408	24.34255
A026	c	8	LOC643446	30.21348	26.44586
A026	c	9	RBM4	29.38821	24.88349
A026	c	10	CIR	30.08362	26.35822
A026	c	11	SFRS10	29.46389	24.02686
A026	c	12	SMN1	31.05554	25.78058
A026	d	1	TET1	28.50789	24.16531
A026	d	2	CROP	39.10674	32.14616
A026	d	3	DDX5	28.1728	25.49501
A026	d	4	LSMD1	29.3597	25.87177
A026	d	5	RBM24	29.37357	25.50451
A026	d	6	SRPK2	27.96814	24.25448
A026	d	7	LNX1	28.58146	24.73232

A026	d	8	POLR2B	26.63598	25.0482
A026	d	9	BUB3	26.91042	24.83779
A026	d	10	USP39	29.89628	26.81789
A026	d	11	BAT1	29.68173	26.73772
A026	d	12	PARP1	30.30675	27.00868
A026	e	1	RALYL	27.51177	24.04016
A026	e	2	HTATSF1	32.86805	28.54471
A026	e	3	DDX3Y	31.06499	25.97445
A026	e	4	MBNL2	28.32457	24.15183
A026	e	5	DDX21	27.62733	23.55042
A026	e	6	SFRS17A	30.15715	25.94676
A026	e	7	SFRS9	29.35248	25.19981
A026	e	8	THOC2	28.26106	25.32479
A026	e	9	RDBP	29.10646	25.54902
A026	e	10	ELAVL4	29.5118	26.00013
A026	e	11	SRPK3	30.76168	27.68266
A026	e	12	LOC389465	30.49768	26.53974
A026	f	1	EIF4G3	27.69023	25.5035
A026	f	2	C14orf166	32.31108	24.55471
A026	f	3	SF3A3	28.12469	25.02712
A026	f	4	NCBP2	28.05737	24.96955
A026	f	5	LOC646517	28.69851	25.28807
A026	f	6	LSM3	30.48665	27.51975
A026	f	7	SRRM2	28.11285	25.09619
A026	f	8	SFRS2	30.88332	28.02017
A026	f	9	ANXA2	26.46927	26.61285
A026	f	10	RBM8A	31.55033	27.91041
A026	f	11	PCBP4	27.96438	27.6491
A026	f	12	PHRF1	29.8769	25.83868
A026	g	1	SF3B2	26.25449	22.60472
A026	g	2	SFRS12	27.27111	25.02418
A026	g	3	ZRSR1	29.01966	25.43284
A026	g	4	PPP1R8	26.13696	24.76215
A026	g	5	TRA2A	27.57513	25.30896
A026	g	6	DNAJC17	28.88528	25.59172
A026	g	7	EXOSC8	31.29566	25.16702
A026	g	8	SF3A3	29.19817	25.21332
A026	g	9	PTBP2	30.75709	27.31613
A026	g	10	CRKRS	30.03342	27.48906
A026	g	11	EXOSC10	35.96353	33.45173
A026	g	12	TOPORS	28.47267	25.68577
A026	h	1	SCNM1	Undetermined	25.96887
A026	h	2	PSEN1	29.27759	25.65685

A026	h	3	IGF2BP3	33.36858	26.72416
A026	h	4	MBNL2	32.07874	25.78593
A026	h	5	RBM7	30.62402	25.53358
A026	h	6	HMG1L10	31.84653	26.31291
A026	h	7	IQGAP1	31.16691	26.54677
A026	h	8	SF3B3	29.37922	25.6889
A026	h	9	CCBL2	29.39477	25.40918
A026	h	10	MBNL3	30.70476	28.02568
A026	h	11	ADAR	29.83061	24.94334
A026	h	12	PRPF8	28.59042	25.4258
A027	a	1	RBM3	14.26484	13.62654
A027	a	2	PCBP4	14.7967	32.5634
A027	a	3	WDR25	14.44065	32.38589
A027	a	4	HNRNPH3	15.76786	Undetermined
A027	a	5	PPAN	5.94462	Undetermined
A027	a	6	ZNF207	Undetermined	21.13168
A027	a	7	SFRS10	Undetermined	25.65947
A027	a	8	ZCCHC8	Undetermined	Undetermined
A027	a	9	LOC100133872	Undetermined	37.31525
A027	a	10	CDC5L	Undetermined	14.86237
A027	a	11	PRPF4B	26.52394	27.03397
A027	a	12	EIF4A3	27.34669	25.81118
A027	b	1	CDC40	29.19337	25.93084
A027	b	2	ZMAT5	28.89492	26.46011
A027	b	3	SFRS1	29.68926	26.56549
A027	b	4	MAGOHB	30.86057	25.9821
A027	b	5	MBNL1	Undetermined	Undetermined
A027	b	6	INTS6	Undetermined	Undetermined
A027	b	7	PRPF19	Undetermined	26.47429
A027	b	8	PHRF1	Undetermined	33.0242
A027	b	9	DHX9	28.3033	26.60312
A027	b	10	SFRS2IP	29.44955	26.72401
A027	b	11	CD2BP2	27.28971	26.29181
A027	b	12	MBNL3	26.41605	26.41285
A027	c	1	TDRD3	22.17826	24.94829
A027	c	2	HNRNPA0	17.0919	Undetermined
A027	c	3	CLK2	Undetermined	26.11585
A027	c	4	BRUNOL5	Undetermined	25.7797
A027	c	5	LSM8	Undetermined	17.6229
A027	c	6	SART3	Undetermined	26.09216
A027	c	7	BRUNOL4	29.8798	25.64014
A027	c	8	NCL	28.99218	25.67873
A027	c	9	SMNDC1	Undetermined	27.20899

A027	c	10	KHDRBS1	27.6865	26.65679
A027	c	11	LOC729200	27.69792	26.43606
A027	c	12	PCBP3	26.96689	27.02725
A027	d	1	DHX15	28.21001	26.05411
A027	d	2	LSM10	29.27231	25.88997
A027	d	3	HIST2H2AA3	28.1994	26.51931
A027	d	4	THOC5	27.93295	26.63175
A027	d	5	SLC43A2	28.96659	26.14852
A027	d	6	SNRNP70	29.43088	27.32549
A027	d	7	PUF60	28.73164	25.87776
A027	d	8	HNRPDL	27.85866	25.66938
A027	d	9	DDX46	27.96496	26.48525
A027	d	10	LOC643167	28.12479	26.14349
A027	d	11	PRPF4	28.13928	26.55481
A027	d	12	DDIT3	27.05298	27.0312
A027	e	1	KHDRBS1	Undetermined	22.24554
A027	e	2	ELAVL2	13.63844	30.159
A027	e	3	LOC100131556	Undetermined	32.23311
A027	e	4	SSB	Undetermined	28.13701
A027	e	5	SFRS3	Undetermined	25.5035
A027	e	6	ILF3	Undetermined	23.02577
A027	e	7	INTS3	Undetermined	37.25826
A027	e	8	SNRPD1	Undetermined	26.78189
A027	e	9	C1QBP	Undetermined	24.67664
A027	e	10	A2BP1	Undetermined	24.54339
A027	e	11	C14orf166	Undetermined	23.8777
A027	e	12	HMGB3	27.93819	26.47282
A027	f	1	SFRS16	28.76414	25.1728
A027	f	2	NOVA1	28.42082	25.92855
A027	f	3	KIAA1429	Undetermined	25.15427
A027	f	4	FRG1	Undetermined	25.84474
A027	f	5	XRN2	30.25057	25.68465
A027	f	6	PCBP1	Undetermined	29.47447
A027	f	7	NUMA1	Undetermined	29.01405
A027	f	8	FAM120A	Undetermined	26.34718
A027	f	9	HMG4L	Undetermined	24.22767
A027	f	10	RNPS1	Undetermined	27.17728
A027	f	11	FRG1	20.01567	26.05195
A027	f	12	SNW1	27.91472	26.53485
A027	g	1	C1QBP	Undetermined	26.45158
A027	g	2	THOC6	14.5247	Undetermined
A027	g	3	SRPK2	Undetermined	25.03396
A027	g	4	SNRPD3	Undetermined	21.67995

A027	g	5	QPCT	Undetermined	28.31699
A027	g	6	PSEN1	Undetermined	25.60238
A027	g	7	SMC1A	Undetermined	25.32693
A027	g	8	KHSRP	Undetermined	24.40767
A027	g	9	SKIV2L2	Undetermined	27.24046
A027	g	10	LNX1	Undetermined	32.19724
A027	g	11	DDX46	30.88649	26.2224
A027	g	12	KHDRBS3	29.39601	25.87561
A027	h	1	RBM22	Undetermined	21.89307
A027	h	2	SNRNP25	Undetermined	23.91226
A027	h	3	SYNCRIP	Undetermined	24.38015
A027	h	4	RNF113A	Undetermined	27.71357
A027	h	5	FRG1	Undetermined	25.17771
A027	h	6	SNRPF	Undetermined	30.20264
A027	h	7	SYF2	Undetermined	30.89959
A027	h	8	A2BP1	Undetermined	27.66072
A027	h	9	MOV10	Undetermined	24.36956
A027	h	10	NOVA2	27.35497	26.77819
A027	h	11	HNRNPAB	28.21903	26.1673
A027	h	12	LOC653889	27.02078	26.17305
A028	a	1	DDX1	Undetermined	32.07204
A028	a	2	PPWD1	Undetermined	23.89121
A028	a	3	SFRS2B	Undetermined	23.01226
A028	a	4	KIN	Undetermined	Undetermined
A028	a	5	RALYL	5.708316	Undetermined
A028	a	6	HNRNPU	Undetermined	23.53066
A028	a	7	TET1	Undetermined	24.67995
A028	a	8	PRPF8	Undetermined	Undetermined
A028	a	9	KPNA2	Undetermined	25.97662
A028	a	10	AKAP8	Undetermined	26.18628
A028	a	11	CCNA1	8.605816	17.73528
A028	a	12	RBM42	29.98892	26.61624
A028	b	1	PHF5A	Undetermined	24.14653
A028	b	2	RNPC3	Undetermined	18.87281
A028	b	3	ZC3H18	7.951105	25.82965
A028	b	4	DDX17	6.143886	19.84266
A028	b	5	DIDO1	9.738521	24.21435
A028	b	6	BCAS2	Undetermined	26.93091
A028	b	7	PRPF3	Undetermined	26.99645
A028	b	8	TIAL1	27.59708	26.74757
A028	b	9	SRPK1	Undetermined	26.86883
A028	b	10	BRUNOL6	3.629615	Undetermined
A028	b	11	SCNM1	Undetermined	31.33926

A028	b	12	CPSF1	Undetermined	18.98233
A028	c	1	PRPF4B	31.34927	19.98298
A028	c	2	RBBP7	14.28985	29.03364
A028	c	3	PPIL1	27.8446	26.65559
A028	c	4	CPSF6	Undetermined	28.00235
A028	c	5	SMARCA5	Undetermined	26.95573
A028	c	6	POLDIP3	17.87802	Undetermined
A028	c	7	PPIL2	Undetermined	24.23899
A028	c	8	PCBP2	Undetermined	Undetermined
A028	c	9	SF3B5	18.34178	29.72606
A028	c	10	INTS6	Undetermined	24.66001
A028	c	11	EXOSC10	Undetermined	24.86922
A028	c	12	ACIN1	29.65961	27.00623
A028	d	1	DDX5	Undetermined	24.85356
A028	d	2	SNRNP200	Undetermined	27.42602
A028	d	3	SNRNP35	Undetermined	27.02542
A028	d	4	SNW1	Undetermined	25.7344
A028	d	5	NOVA2	Undetermined	30.07057
A028	d	6	SFRS3	Undetermined	26.87502
A028	d	7	PRPF38B	Undetermined	24.6106
A028	d	8	SF3A3	Undetermined	29.41564
A028	d	9	PRPF40B	Undetermined	23.73065
A028	d	10	PTBP2	13.58114	29.06344
A028	d	11	PPIH	Undetermined	24.35019
A028	d	12	MBNL3	5.317996	22.78509
A028	e	1	DDX21	27.5994	25.28288
A028	e	2	SR140	30.00408	25.21384
A028	e	3	HNRNPF	30.37407	26.44262
A028	e	4	EIF4A3	Undetermined	25.40053
A028	e	5	DDX21	Undetermined	27.3816
A028	e	6	SFRS9	27.34086	26.21437
A028	e	7	YWHAQ	Undetermined	24.92167
A028	e	8	PRPF38B	Undetermined	26.38115
A028	e	9	HTATSF1	7.918369	25.6288
A028	e	10	DGCR14	Undetermined	22.05011
A028	e	11	MFSD11	Undetermined	24.80932
A028	e	12	MSI1	28.4734	26.96407
A028	f	1	IK	26.81144	24.16422
A028	f	2	LOC100129329	Undetermined	25.68333
A028	f	3	LOC644811	Undetermined	27.59702
A028	f	4	DHX38	Undetermined	28.32403
A028	f	5	SNRNP27	Undetermined	23.81979
A028	f	6	RBM25	9.663167	23.85729

A028	f	7	CIRBP	Undetermined	23.85236
A028	f	8	CUGBP1	Undetermined	27.6342
A028	f	9	NUDT21	Undetermined	27.27802
A028	f	10	HNRNPK	Undetermined	25.42596
A028	f	11	PRCC	22.00494	26.68217
A028	f	12	PRPF38A	30.96401	25.59099
A028	g	1	TDRD3	Undetermined	Undetermined
A028	g	2	LSM2	Undetermined	35.42557
A028	g	3	SNRPB	Undetermined	Undetermined
A028	g	4	U2AF2	Undetermined	25.36642
A028	g	5	RALY	Undetermined	27.15344
A028	g	6	CPSF6	Undetermined	25.81044
A028	g	7	GTF2I	Undetermined	24.0956
A028	g	8	TARDBP	Undetermined	24.16743
A028	g	9	HNRNPH3	Undetermined	27.53206
A028	g	10	PPP1R8	Undetermined	28.93134
A028	g	11	DHX38	13.12805	33.15104
A028	g	12	PSIP1	Undetermined	25.73583
A028	h	1	HNRNPH1	Undetermined	34.28567
A028	h	2	RBM26	14.93018	Undetermined
A028	h	3	PRPF4	Undetermined	35.55651
A028	h	4	HNRNPC	Undetermined	33.71281
A028	h	5	LGALS3	Undetermined	27.11598
A028	h	6	PPIL2	Undetermined	27.26145
A028	h	7	SRRM1	Undetermined	27.48332
A028	h	8	MAGOHB	Undetermined	29.21556
A028	h	9	NCBP1	12.38913	22.47158
A028	h	10	PCBP3	29.62768	26.22939
A028	h	11	CRNKL1	29.3715	24.7829
A028	h	12	INTS6	28.84228	26.13018
A029	a	1	TCERG1	Undetermined	26.01406
A029	a	2	ILF3	26.93814	26.71738
A029	a	3	LSM3	28.33268	25.84961
A029	a	4	THOC2	28.21844	25.95648
A029	a	5	RAVER1	27.86191	25.83975
A029	a	6	INTS1	27.24386	25.13901
A029	a	7	CHERP	28.20237	25.64729
A029	a	8	C21orf66	28.18134	25.66021
A029	a	9	RBM26	30.04576	25.55668
A029	a	10	LOC92755	28.2141	25.77712
A029	a	11	SMNDC1	27.75145	26.19968
A029	a	12	PABPN1	27.01909	26.84389
A029	b	1	C8orf58	28.0328	25.95114

A029	b	2	DDX41	27.40884	25.60439
A029	b	3	MSI2	26.64051	26.2832
A029	b	4	LOC100130003	27.09618	25.52846
A029	b	5	HNRNPA2B1	28.23431	25.38409
A029	b	6	LSM4	25.77167	25.33269
A029	b	7	PRPF19	27.97051	25.64645
A029	b	8	CCNK	28.05071	25.22698
A029	b	9	LOC652595	27.90463	26.07847
A029	b	10	LUC7L2	27.17036	26.45769
A029	b	11	KHDRBS1	21.27513	28.59116
A029	b	12	YWHAG	27.05841	26.19009
A029	c	1	RBM42	27.80688	26.71657
A029	c	2	EIF3M	27.63687	25.92111
A029	c	3	LOC100130003	27.74361	25.75348
A029	c	4	PTBP2	26.28922	25.36353
A029	c	5	THOC7	26.29887	25.19364
A029	c	6	NOVA1	13.26481	18.24501
A029	c	7	KIAA1429	27.00912	25.98329
A029	c	8	SF3B2	26.22511	25.89306
A029	c	9	CCDC55	26.35502	26.37567
A029	c	10	HNRNPK	27.411	25.16435
A029	c	11	LOC644035	26.62028	25.88685
A029	c	12	MFSD11	29.03742	25.96507
A029	d	1	MYEF2	27.91454	26.51961
A029	d	2	RBM15	28.01702	25.27112
A029	d	3	PPIL3	27.99554	25.82655
A029	d	4	ZCRB1	27.53817	26.02187
A029	d	5	POLR2B	27.65877	25.53824
A029	d	6	SNRPB2	27.68591	25.05053
A029	d	7	ZC3H18	27.90203	24.5353
A029	d	8	MOV10	27.4484	25.32799
A029	d	9	POLR2A	27.21976	25.73889
A029	d	10	HIST2H2AA3	27.25275	26.20681
A029	d	11	BRUNOL6	27.58726	26.11954
A029	d	12	RP9	27.7097	25.38617
A029	e	1	PABPC1	28.06889	26.14714
A029	e	2	DHX38	26.56435	26.80535
A029	e	3	TOP1MT	27.36712	26.47803
A029	e	4	PLRG1	27.62307	25.98978
A029	e	5	CDC5L	28.18292	25.87334
A029	e	6	SF3B1	27.91381	25.083
A029	e	7	CWF19L1	27.30591	26.41074
A029	e	8	CTNNBL1	27.47044	26.19697

A029	e	9	PQBP1	29.17021	25.81291
A029	e	10	SNRPA	27.58419	25.79742
A029	e	11	NCBP1	27.68835	25.74339
A029	e	12	SFRS1	27.38827	26.06945
A029	f	1	CLK3	28.96711	26.6498
A029	f	2	WDR33	27.58535	26.65941
A029	f	3	CD2BP2	27.63536	25.78827
A029	f	4	XAB2	27.94785	25.6288
A029	f	5	LOC389465	27.50609	26.06083
A029	f	6	TNPO1	27.12663	24.98257
A029	f	7	SNRPB	27.43123	25.72244
A029	f	8	EIF4A3	29.32155	26.22878
A029	f	9	AKAP8	28.80646	26.028
A029	f	10	LOC654340	28.11844	23.43424
A029	f	11	DDX39	27.26096	26.7353
A029	f	12	DHX9	28.60566	23.89516
A029	g	1	YBX1	28.29053	26.31091
A029	g	2	CCNK	28.41492	25.90496
A029	g	3	RBM7	28.25615	25.7776
A029	g	4	MOV10	27.60399	25.56001
A029	g	5	LOC92755	28.0394	26.16689
A029	g	6	MBNL2	27.98568	25.26201
A029	g	7	C2orf3	28.03463	25.35169
A029	g	8	C8orf58	27.9986	25.51021
A029	g	9	SNRNP200	28.35629	24.01948
A029	g	10	PRPF4B	28.93548	25.77096
A029	g	11	WDR33	29.43078	25.26652
A029	g	12	NXF1	27.97043	24.6553
A029	h	1	TAF6	27.7519	26.41747
A029	h	2	CLK2	27.61403	26.47851
A029	h	3	LUC7L	27.34992	25.63261
A029	h	4	CTNNBL1	27.67625	26.31267
A029	h	5	SNIP1	27.43277	26.20913
A029	h	6	RBM24	27.92533	25.88919
A029	h	7	IK	27.76431	25.94528
A029	h	8	ANXA2	27.80365	26.27146
A029	h	9	TDRD3	27.53655	26.70623
A029	h	10	CLK3	27.73605	26.25006
A029	h	11	FASTK	27.90193	25.85206
A029	h	12	BCAS2	26.799	24.35456
A030	a	1	AQR	27.90748	25.53359
A030	a	2	RBBP7	27.75649	25.99041
A030	a	3	PIAS4	27.60826	25.83105

A030	a	4	LOC728554	27.2527	25.92769
A030	a	5	LSM6	28.06318	24.47076
A030	a	6	MSI1	27.67847	25.83846
A030	a	7	SRPK2	28.07799	26.29808
A030	a	8	LSM6	28.41934	25.12477
A030	a	9	GTF2I	28.14154	26.25993
A030	a	10	SNRNP25	28.59531	25.93385
A030	a	11	LOC729200	28.22147	25.33778
A030	a	12	CLK2	27.40634	25.7474
A030	b	1	HNRNPUL1	27.54962	25.96833
A030	b	2	CSDA	27.33784	25.98072
A030	b	3	MSI2	27.10925	26.42595
A030	b	4	SRP19	26.69052	26.48209
A030	b	5	SF3B3	27.14823	26.33228
A030	b	6	LOC100127915	26.24121	26.33932
A030	b	7	RP9	27.08641	25.10841
A030	b	8	LSM6	27.20527	26.31146
A030	b	9	LSMD1	27.71246	25.6796
A030	b	10	SNRPD2	27.21565	26.41825
A030	b	11	SF1	27.55426	26.42209
A030	b	12	PABPN1	27.26187	26.86526
A030	c	1	KHDRBS3	27.59102	27.54862
A030	c	2	POLR2B	28.04225	26.55758
A030	c	3	EIF4G3	28.16548	25.52741
A030	c	4	SDCCAG10	28.24885	25.21142
A030	c	5	DIDO1	27.94135	26.50772
A030	c	6	CSDA	28.53983	26.56717
A030	c	7	PSPC1	27.7486	25.6774
A030	c	8	SFPQ	28.36406	25.70962
A030	c	9	HNRNPD	28.73002	25.26502
A030	c	10	PHF5A	28.81381	24.79349
A030	c	11	C1orf55	28.59505	25.63964
A030	c	12	WBP11	27.34274	26.55873
A030	d	1	PRPF19	27.92085	27.08968
A030	d	2	SFRS1	27.22076	25.81309
A030	d	3	EXOSC9	26.83407	26.32005
A030	d	4	PCBP1	26.99575	26.01116
A030	d	5	C8orf58	27.36296	26.4328
A030	d	6	RNF113A	28.07309	25.27775
A030	d	7	EXOSC4	27.11826	24.99891
A030	d	8	MAGOHB	26.99771	26.57429
A030	d	9	EXOSC4	27.6808	25.90669
A030	d	10	PABPN1	27.16022	26.70393

A030	d	11	SNRNP70	27.30481	26.66545
A030	d	12	EIF3A	27.26768	26.18711
A030	e	1	INTS3	30.23484	27.53108
A030	e	2	RAVER1	28.12976	27.64175
A030	e	3	CHERP	27.97956	26.03738
A030	e	4	PPIL1	27.51306	25.73808
A030	e	5	HNRNPD	23.91525	27.09398
A030	e	6	SF4	27.25067	26.23163
A030	e	7	KHSRP	27.92651	25.58649
A030	e	8	DDX5	27.81603	25.75114
A030	e	9	CWC22	27.74213	25.82983
A030	e	10	TNPO1	27.87841	26.31539
A030	e	11	MATR3	27.74464	26.56444
A030	e	12	SFRS8	27.55619	26.83527
A030	f	1	LOC100128974	27.39783	25.72248
A030	f	2	CLK4	27.65719	25.92709
A030	f	3	CPSF4	27.35385	26.61094
A030	f	4	DEK	27.7142	25.72833
A030	f	5	RBM9	27.55207	25.97396
A030	f	6	LOC441722	27.21941	25.46619
A030	f	7	IGF2BP3	27.70757	25.71929
A030	f	8	SF3B2	27.78431	25.59792
A030	f	9	TOP1	27.74836	26.08145
A030	f	10	RBMS1	28.17571	26.19358
A030	f	11	TFIP11	26.90552	26.50753
A030	f	12	IK	27.6456	26.19442
A030	g	1	LSM7	26.80534	26.26534
A030	g	2	U2AF2	27.52774	25.26889
A030	g	3	YBX1	27.58608	25.78694
A030	g	4	HNRNPU	28.02493	25.6741
A030	g	5	TCERG1	27.68086	25.83171
A030	g	6	PABPC1	27.96224	25.76789
A030	g	7	RBM47	27.75428	26.38579
A030	g	8	DNAJC6	28.08604	26.02335
A030	g	9	LUC7L2	27.97882	25.9981
A030	g	10	HNRNPR	27.75526	26.42893
A030	g	11	CUGBP1	28.91339	26.2371
A030	g	12	RBM25	27.68501	21.4483
A030	h	1	RBM38	27.78137	25.47319
A030	h	2	SFRS10	27.6288	25.16572
A030	h	3	PABPN1	27.60413	25.72785
A030	h	4	LOC644811	27.34456	26.76963
A030	h	5	DHX9	27.79954	26.17763

A030	h	6	RBM3	28.1208	25.57063
A030	h	7	DEK	26.90811	26.64996
A030	h	8	ANXA2	27.10135	26.11162
A030	h	9	MBNL1	27.72029	26.29737
A030	h	10	RUVBL2	27.35187	26.40518
A030	h	11	RBMS1	27.43375	26.45281
A030	h	12	SFRS12	27.94985	26.40112

Appendix 2

The work presented in Chapter 2 and Chapter 3 of this thesis resulted in the following peer-reviewed publications attached in this appendix:

- Clower, C.V., **Chatterjee, D**., Wang, Z., Cantley, L.C., Vander Heiden, M.G., and Krainer, A.R. (2010). The alternative splicing repressors hnRNP A1/A2 and PTB influence pyruvate kinase isoform expression and cell metabolism. Proceedings of the National Academy of Sciences of the United States of America *107*, 1894-1899.**(co-first author)**

- Wang Z, **Chatterjee D**, Akerman M, Vander Heiden MG, Cantley LC, and Krainer AR (2011) Exon-centric regulation of pyruvate kinase M alternative splicing via mutually exclusive exons. J Mol Cell Biol. 2012 Apr;4(2):79-87

The alternative splicing repressors hnRNP A1/A2 and PTB influence pyruvate kinase isoform expression and cell metabolism

Cynthia V. Clower[a,1], Deblina Chatterjee[b,c,1], Zhenxun Wang[b,d], Lewis C. Cantley[a], Matthew G. Vander Heiden[a,e], and Adrian R. Krainer[b,c,2]

[a]Division of Signal Transduction, Beth Israel Deaconess Medical Center and Department of Systems Biology, Harvard Medical School, Boston, MA 02115; [b]Cold Spring Harbor Laboratory, Cold Spring Harbor, NY 11724; [c]Graduate Program in Molecular and Cellular Biology, Stony Brook University, Stony Brook, NY 11794; [d]Watson School of Biological Sciences, Cold Spring Harbor, NY 11724; and [e]Department of Medical Oncology, Dana-Farber Cancer Institute, Boston, MA 02115

Communicated by Tom Maniatis, Harvard University, Cambridge, MA, December 22, 2009 (received for review December 2, 2009)

Cancer cells preferentially metabolize glucose by aerobic glycolysis, characterized by increased lactate production. This distinctive metabolism involves expression of the embryonic M2 isozyme of pyruvate kinase, in contrast to the M1 isozyme normally expressed in differentiated cells, and it confers a proliferative advantage to tumor cells. The M1 and M2 pyruvate-kinase isozymes are expressed from a single gene through alternative splicing of a pair of mutually exclusive exons. We measured the expression of M1 and M2 mRNA and protein isoforms in mouse tissues, tumor cell lines, and during terminal differentiation of muscle cells, and show that alternative splicing regulation is sufficient to account for the levels of expressed protein isoforms. We further show that the M1-specific exon is actively repressed in cancer-cell lines—although some M1 mRNA is expressed in cell lines derived from brain tumors—and demonstrate that the related splicing repressors hnRNP A1 and A2, as well as the polypyrimidine-tract-binding protein PTB, contribute to this control. Downregulation of these splicing repressors in cancer-cell lines using shRNAs rescues M1 isoform expression and decreases the extent of lactate production. These findings extend the links between alternative splicing and cancer, and begin to define some of the factors responsible for the switch to aerobic glycolysis.

aerobic glycolysis | cancer | RNA splicing

Cancer cells exhibit a metabolic phenotype characterized by increased glycolysis with lactate generation, regardless of oxygen availability—a phenomenon termed the Warburg effect. Recent work demonstrated that expression of the type II isoform of the pyruvate-kinase-M gene (*PKM2*, referred to here as PK-M) is a critical determinant of this metabolic phenotype, and confers a selective proliferative advantage to tumor cells in vivo (1). This finding adds to the growing body of evidence that alterations in alternative prem-RNA splicing play important roles in different aspects of cancer progression (2, 3).

Pyruvate-kinase (PK) is the enzyme that catalyzes the final step in glycolysis, generating pyruvate and ATP from phosphoenolpyruvate and ADP (4). The resulting pyruvate can be converted to lactate or it can be incorporated into the tricarboxylic acid (TCA) cycle to drive oxidative phosphorylation. PK is encoded by two paralogous genes, each of which is alternatively spliced, such that four PK isoforms are expressed in mammals. The L and R isozymes, derived from the *PKLR* gene, show tissue-specific expression in the liver and red-blood cells, respectively. They have different first exons, defined by tissue-specific promoters (5). The *PKM2* (PK-M) gene consists of 12 exons, of which exons 9 and 10 are alternatively spliced in a mutually exclusive fashion to give rise to the PK-M1 and PK-M2 isoforms, respectively (6). Exons 9 and 10 each encode a 56 amino acid variable segment that confers distinctive properties to the regulation and activity of PK-M1 and PK-M2 enzymes; as a result, PK-M1 is constitutively active, whereas the activity of PK-M2 is allosterically regulated by fructose-1,6-bisphosphate levels and interaction with tyrosine-phosphorylated proteins (1).

The ability of PK-M2 activity to be regulated is thought to provide a mechanism for cells to control the availability of metabolites for anabolic processes, and to confer a proliferative advantage during tumorigenesis (7). Despite increasing evidence demonstrating the significance of PK-M2 isoform expression in cancer-cell metabolism and tumorigenesis, the mechanisms governing alternative splicing of the PK-M gene are not understood. PK-M2 is expressed in a range of cancer cells, as well as in fetal and undifferentiated adult tissues, whereas PK-M1 is expressed predominantly in terminally differentiated tissues (1, 8).

Alternative splicing involving pairs of mutually exclusive exons represents only ~2% of all alternative splicing events in human genes (9). In terms of gene structure, the regulated exons in such genes are often closely related in sequence—as in the case of PK-M exons 9 and 10—indicating that they originally arose by exon duplication (10). Well characterized examples of this alternative splicing pattern in mammals include the tropomyosins, fibroblast growth factor receptor 2, and α-actinin [reviewed in (11)]. Although some of the trans-acting factors involved in the recognition of individual mutually exclusive exons in these genes have been identified, it remains unclear how these pairs of exons are coordinately regulated in a way that maintains their mutually exclusive properties (11).

We have begun to dissect the molecular mechanisms underlying PK-M2 alternative splicing regulation. Previous work implicated the splicing-repressor paralogs PTB and nPTB in the repression of exon 9 (12). In addition, other splicing repressors, such as hnRNP A1 and hnRNP A2, and activators, such as SF2/ASF, have been implicated in oncogenic transformation (2, 3), and hence could potentially play a role in PK-M alternative splicing. Here we characterize the expression of PK-M isoforms at the mRNA and protein level in primary tissues and cancer-cell lines, as well as during terminal differentiation of muscle cells in culture. We show that hnRNP A1/A2, in addition to PTB, repress the use of exon 9, such that knocking down expression of these splicing repressors allows expression of PK-M1, accompanied by a decrease in lactate production.

Author contributions: C.V.C., D.C., Z.W., L.C.C., M.G.V.H., and A.R.K. designed research; C.V.C., D.C., Z.W., and M.G.V.H. performed research; C.V.C., D.C., Z.W., L.C.C., M.G.V.H., and A.R.K. analyzed data; C.V.C., D.C., Z.W., L.C.C., M.G.V.H., and A.R.K. wrote the paper.

The authors declare a conflict of interest. L.C.C. and M.G.V.H. are associated with Agios Pharmaceuticals.

[1]C.V.C. and D.C. contributed equally to this work.

[2]To whom correspondence should be addressed. E-mail: krainer@cshl.edu.

[3]Present address: Koch Institute for Integrative Cancer Research at MIT, Cambridge, MA 02139.

www.pnas.org/cgi/doi/10.1073/pnas.0914845107

Results

Relative PK-M1 and PK-M2 Expression in Tissues and Cell Lines Correlates with hnRNP A1/A2 and PTB Expression. Proliferating cells and cancer cells preferentially express PK-M2 over PK-M1 at the protein level (1, 13). To determine if the expressed protein isozymes are a direct reflection of differences in alternative splicing—as opposed to, e.g., being affected by mRNA stability or translational control—we measured the levels of mRNA and protein isoforms expressed in various tissues and cell lines. Representative organs/tissues isolated from adult mice were perfused with saline, and total protein and RNA were isolated and analyzed. The relative expression of PK-M1 and PK-M2 protein isoforms was organ/tissue-specific: Brain and skeletal muscle preferentially expressed PK-M1, whereas spleen and lung expressed mainly PK-M2, as detected by Western blotting with isoform-specific antibodies (Fig. 1*A*). As previously reported (1), several human cell lines expressed PK-M2 protein with no detectable PK-M1 (Fig. 1*B*). Among the cell lines tested, however, two brain-tumor-derived cell lines, namely U-118MG and A-172 glioblastoma cells, expressed detectable levels of PK-M1 protein, in addition to PK-M2, reminiscent of the protein pattern in mouse brain, where both isoforms are also readily detectable (cf. Fig. 1*B*, Fig. 1*A*).

To accurately measure the relative levels of PK alternatively spliced mRNA isoforms, we simultaneously detected both isoforms by radioactive RT-PCR with a single pair of primers corresponding to the flanking constitutive exons 8 and 11. Because exons 9 and 10 are identical in length (167 nt), the resulting cDNA amplicons were digested with restriction enzymes that cleave either exon 9 or 10 to distinguish the two isoforms (Fig. 1*C*; see also (14)). PK-M1 mRNA was the predominant isoform in striated muscle and brain—tissues that are enriched in terminally differentiated, nonproliferating cells. In contrast, PK-M2 mRNA was the major isoform in lung and spleen, presumably reflecting the abundance of proliferating cells in these organs. PK-M2 mRNA was invariably the major isoform in all cancer or transformed cell lines we assayed, consistent with the previous finding that PK-M2 expression at the protein level is strongly correlated with, and facilitates, proliferation and tumorigenesis (1)). However, PK-M1 mRNA was readily detectable in brain-tumor-derived cancer-cell lines, including glioblastoma (U-118MG and A-172) and neuroblastoma (SK-N-BE) cell lines. This finding is consistent with PK-M1 protein being detectable in U-118MG cells and to a lesser extent in A-172 cells (Fig. 1*B*). In general, we observed a strong correlation between PK-M1/M2 isoform ratios measured at the protein and mRNA levels, in both tissues and cell lines.

To facilitate studies of the mechanism underlying the PK-M2 to PK-M1 isoform switch during terminal differentiation, we examined several established systems for cell differentiation in culture. We found that proliferating mouse C2C12 myoblasts induced to terminally differentiate into myotubes (15) switched protein and mRNA isoform expression from almost exclusively PK-M2 to predominantly PK-M1 (Fig. 2). Consistent with PK-M2 being the predominant isoform in proliferating cells, and PK-M1 being the predominant isoform in muscle (Fig. 1*A*), this switch in PK-M isoform accompanied the morphological differentiation of the C2C12 myoblasts into myotubes (Fig. 2*A*). Normalizing to total PK-M protein expression, it is readily apparent that there was a pronounced increase in PK-M1 upon differentiation, at the expense of the PK-M2 isoform (Fig. 2*B*). Likewise, at the mRNA level, the proportion of the M1 isoform changed from 5% to 55% over a differentiation time course (Fig. 2*C*).

We also measured the protein levels of representative alternative splicing factors, including some known to have oncogenic activities (3). In the C2C12 differentiation model, as well as in mouse or human tissues and cancer-cell lines, we observed a correlation between high levels of the alternative splicing factors hnRNP A1/A2 and PTB, and reduced expression of the PK-M1 isoform (Fig. 2*B*, *D*, and *E*). In contrast, there was little or no change in several other splicing factors, such as SF2/ASF and

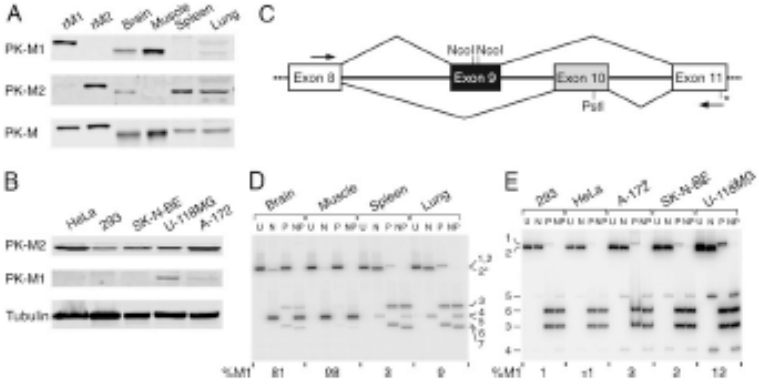

Fig. 1. Protein and transcript expression patterns of pyruvate kinase M1/M2 isoforms in cells and tissues. (*A*) Total adult-mouse organ/tissue homogenates were used for Western blotting with the indicated antibodies. rM1 and rM2: Flag-tagged purified recombinant human PK isoforms. (*B*) Total cell lysates of five human cancer-cell lines were used for Western blotting with the indicated antibodies. (*C*) Primers annealing to exon 8 and exon 11, respectively were used to amplify mouse or human PK-M transcripts. The alternative exons that encode the distinctive segments of PK-M1 and PK-M2 are indicated in (*black*) and (*gray*), respectively. To distinguish between PK-M1 (exon 9 included) and PK-M2 (exon 10 included) isoforms, the PCR products were cleaved with NcoI, PstI, or both. There is an additional NcoI site (*) 11 bp away from the 3′ end of mouse exon 11. (*D*) Mouse organs were freshly dissected and perfused with saline. Total RNA was analyzed by radioactive RT-PCR followed by digestion with NcoI (N), PstI (P), or both enzymes (NP), plus an uncut control (U). Numbered bands are as follows: 1: Uncut M1 (502 bp); 2: uncut M2 (502 bp); 2*: M2 cleaved with NcoI in exon 11 (491 bp); 3: PstI-cleaved M2 5′ fragment (286 bp); 4: NcoI-cleaved M1 5′ fragment (245 bp); 5: NcoI-cleaved M1 3′ fragment (240 bp); 6: PstI-cleaved M2 3′ fragment (216 bp); 7: PstI + NcoI-cleaved M2 3′ fragment (205 bp). The %M1 was quantified from band 1 (M1) and bands 3 and 6 (M2) in each P lane. (*E*) RT-PCR and restriction digest analysis of total RNA from the indicated human cell lines. The bands are numbered as for the mouse RT-PCR products, but the sizes are different because of the positions of the primers; the sizes are as follows: 1: 398 bp; 2: 398 bp; 3: 185 bp; 4: 144 bp; 5: 248 bp; 6: 213 bp. Note that the PK-M1 bands in the P and U lanes migrate slightly above the PK-M2 bands, which is also the case for the mouse PK-M1 transcripts.

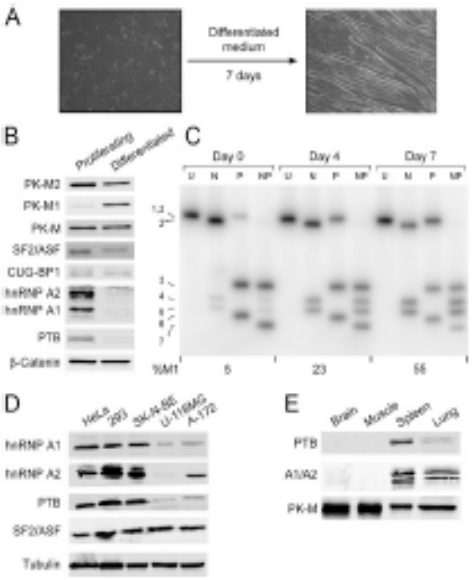

Fig. 2. Expression of pyruvate-kinase isoforms and selected splicing factors in cell lines and tissues. (*A*) Differentiation of mouse C2C12 myoblasts into myotubes. The left field shows proliferating myoblasts, and the right field shows cells after seven days in differentiation medium, when most of the cells have fused into myotubes. (*B*) Western blot of proliferating myoblasts versus AraG-treated myotubes with the indicated antibodies against selected splicing factors, β-catenin, total PK-M, and PK-M1 or PK-M2. (*C*) Radioactive RT-PCR analysis of PK-M1 and PK-M2 expression in C2C12 cells over a differentiation time course. Bands are numbered as in Fig. 1*D*. (*D*) Total cell lysates of five human-tumor or transformed cell lines were used for Western blotting with the indicated specific antibodies. Tubulin was used as an internal control for loading. HeLa (cervical carcinoma); HEK293 (transformed embryonic kidney cells); SK-NB-E (neuroblastoma); U-118MG (glioma); A-172 (glioblastoma). (*E*) Mouse tissues were analyzed as in Fig. 1*A*, with the indicated antibodies.

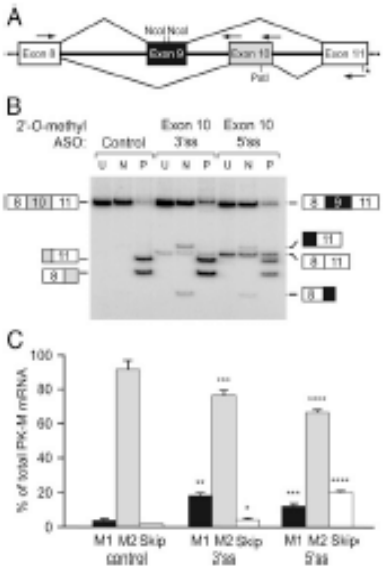

Fig. 3. Exon 9 is partially rescued in HEK293 cells when exon 10 is blocked. (*A*) Schematic representation of the strategy used to block exon 10 with 2′-O-methyl antisense oligonucleotides. The two arrows above exon 10 denote the oligonucleotides complementary to the 3′ splice site and 5′ splice site regions. (*B*) Radioactive RT-PCR assay to measure PK-M1/PK-M2 levels after blocking each of the exon 10 splice sites with antisense oligonucleotides. An abnormal isoform arising from skipping of both exons 9 and 10 is indicated. (*C*) Quantitation of multiple experiments. (Error bars show s.d.; $n = 3$; p-values: $^{*}0.007$; $^{**}0.005$; $^{***}0.004$; $^{****}0.001$; Student's paired *t*-test).

CUG-BP1 (Fig. 2*B*). U-118MG and A-172 cells, which expressed detectable levels of PK-M1, both at mRNA and protein levels (Fig. 1*B*, *E*), had less hnRNP A1/A2 and PTB compared to HeLa, HEK293, and SK-N-BE cells, whereas SF2/ASF was expressed at similar levels in these cell lines (Fig. 2*D*). Both hnRNP A/B and PTB (also known as hnRNP I) protein family members are well characterized splicing repressors, which led us to hypothesize that these factors might be partly responsible for repressing the use of exon 9 during prem-RNA splicing.

Blocking the 3′ Splice Site of Exon 10 Causes Abnormal Skipping of Both Exons 9 and 10. To determine if exon 9 is actively repressed in cancer-cell lines, or simply fails to compete effectively with exon 10, we blocked the 3′ or 5′ splice sites of exon 10 using 2′-O-methyl, phosphorothioate antisense oligonucleotides complementary to these regions (16) (Fig. 3*A*). The oligonucleotides were transfected into HEK293 cells and the endogenous PK mRNA isoforms were analyzed by radioactive RT-PCR (Fig. 3*B*). As expected, use of exon 10 was partially inhibited by the antisense oligonucleotides. However, in addition to increased use of exon 9 (PK-M1 isoform), we observed an abnormal mRNA arising from skipping of both mutually exclusive exons. These results indicate that even with reduced use of exon 10, there is residual repression of exon 9 use.

hnRNP Proteins Repress Exon 9 in a Glioblastoma Cell Line. To address whether specific hnRNP proteins are responsible for repression of exon 9, we generated stable cell lines expressing shRNAs directed against hnRNP A1, A2, or PTB (Fig. 4). We chose A-172 glioblastoma cells for this analysis, both because they already express some PK-M1 (Fig. 1*B*, *E*) and because they tolerated simultaneous stable-knockdown of hnRNP A1 and A2, in contrast to other cells we examined. We achieved ~65% knockdown of hnRNP A1 and ~50% knockdown of hnRNP A2 (Fig. 4*A*). Although individual knockdown of these proteins—which are closely related in structure and function (17)—had little effect, the combined knockdown elicited a ~6-fold increase in PK-M1 protein (Fig. 4*A*) and ~5-fold increase in PK-M1 mRNA (Fig. 4*B*).

PTB or PTB + nPTB siRNA-knockdown in HeLa cells was previously shown by quantitative 2D-gel proteomics to decrease total PK-M expression (12). Although the PK-M1 and PK-M2 spots could not be resolved, RT-PCR revealed a ~4-fold increase in the PK-M1/M2 ratio (12). We stably expressed PTB shRNA in A-172 cells and performed Western blotting and radioactive RT-PCR analyses as above, and detected a ~3-fold increase in PK-M1 protein and mRNA (Fig. 4*C*,*D*). Taken together, these results suggest that hnRNP A1/A2 and PTB directly or indirectly mediate active repression of exon 9 in cancer cells.

Knockdown of Splicing Repressors Inhibits Lactate Production in a Glioblastoma Cell Line. To test whether knockdown of hnRNP A1/A2 or PTB, which results in an increase in the PK-M1/PK-M2 protein ratio, is sufficient to affect cancer-cell metabolism, we measured the extent of lactate production in stable-knockdown versus control A-172 cells (Fig. 5). Remarkably, we ob-

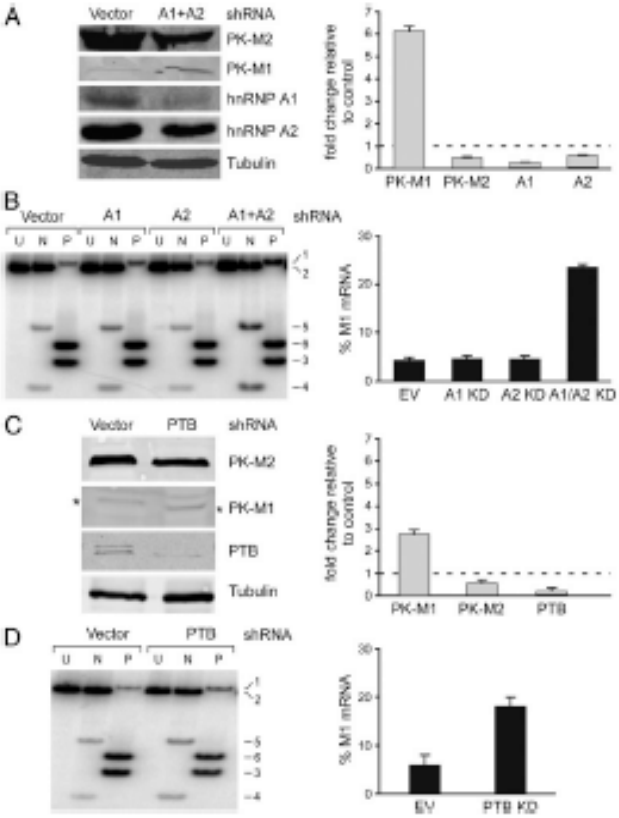

Fig. 4. Repression of exon 9 by hnRNP proteins. (*A*) A-172 glioblastoma cells were transduced with retroviruses expressing hnRNPA1 and hnRNP A2 shRNAs. Total lysates were analyzed by Western blotting with the indicated antibodies. The histogram on the right shows the quantitation of multiple experiments by infrared-imaging ($n = 4$; error bars show s.d.; $p = 0.02$ (M1); $p = 0.005$ (M2); $p = 0.05$ (A1); $p = 0.01$ (A2); Student's paired *t*-test) (*B*) Analysis of PK -M/RNA transcripts from the cells in (*A*) using radioactive RT-PCR and NcoI or PstI digestion. Bands are numbered as in Fig. 1*E*. The histogram on the right shows the quantitation from several experiments (error bars show s.d.; $n = 4$; $p = 10^{-4}$ for the A1/A2 double-knockdown; Student's paired *t*-test) (*C*) and (*D*) As in (*A*) and (*B*) but using shRNAs against PTB (hnRNP I). (*C*) The * on each side indicates the band corresponding to PK-M1. The histogram on the right shows the quantitation ($n = 4$; error bars show s.d.; $p = 0.03$ (M1); $p = 0.01$(M2); $p = 0.03$ (PTB); Student's paired *t*-test). (*D*) The histogram on the right shows the quantitation (error bars show s.d.; $n = 3$; $p = 0.001$; Student's paired *t*-test).

served a >2-fold decrease in lactate production upon combined knockdown of hnRNP A1/A2, and a ~1.5-fold reduction upon knockdown of PTB.

Discussion

We have demonstrated that downregulation of the splicing repressors hnRNP A1/A2 and PTB relieves repression of PK-M exon 9 inclusion, resulting in higher levels of PK-M1. Both types of hnRNP proteins have been implicated in cancer (2, 3, 18), consistent with their ability to promote expression of the protumorigenic PK-M2 isoform. hnRNP A1 and A2 are closely related proteins encoded by two separate genes (*HNRNPA1* and *HNRNPA2B1*), which express additional minor isoforms (19); they are splicing repressors that typically, but not always, recognize exonic splicing silencer elements, and once bound to these elements they can spread along the RNA through cooperative interactions and interfere with the binding of spliceosomal components or activator proteins (20). PTB (hnRNP I) is also an abundant RNA-binding protein that binds to polypyrimidine tracts, such as those present at or upstream of

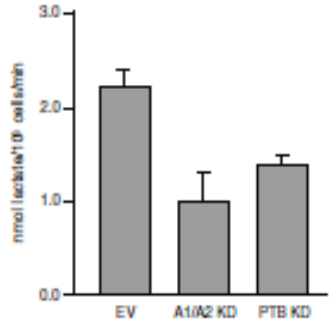

Fig. 5. Effect of splicing-repressor knockdown on metabolism of glioblastoma cells. Lactate production was measured in A-172 glioblastoma cells transduced with empty vector or with combined shRNAs against hnRNP A1 and A2, or against PTB. Error bars show s.d.; $n = 12$ for EV control, and $n = 6$ for A1/A2 ($p = 0.0034$) and PTB ($p = 0.014$) knockdowns; Student's paired *t*-test.

3′ splice sites, and it can regulate alternative splicing by creating a zone of silencing (21).

Previous analysis of PK-M splicing using a minigene suggested that inclusion of exon 10 is the default splicing pattern in proliferating cells (14). This is consistent with our observation that blocking either of the splice sites of exon 10 by means of antisense oligonucleotides leads to simultaneous skipping of both exons 9 and 10, rather than to efficient derepression of exon 9. We have shown that hnRNP A1/A2 and PTB are responsible for, or contribute to the repression of exon 9 in cells that express PK-M2. Although preferred motifs recognized by these repressors are known, we have not determined yet whether hnRNP A1/A2 and PTB regulate PK-M alternative splicing directly, and if so, where the relevant binding sites are located. However, two recent studies reported that PTB can be crosslinked in cells to several regions in intron 8 (22) and hnRNP A1 can bind in vitro to an RNA fragment encompassing the 5′ splice site of intron 9 (23). Further studies of cis-acting elements within and flanking both exon 9 and exon 10 will be necessary to uncover how individual cells achieve predominant or exclusive expression of only one of the two isoforms.

Considering that downregulation of hnRNP A1/A2 or PTB achieved only a three to fivefold increase over the low basal level of exon 9 inclusion, accompanied by a modest increase in PK-M1 protein with the persistence of PK-M2 protein, additional factors likely contribute to the usually tight control of PK-M alternative splicing. As in other instances of regulated alternative splicing [reviewed in (24)], combinatorial control by numerous RNA-binding proteins is likely operative for the PK-M gene.

The effects we observed on lactate production following combined knockdown of hnRNP A1/A2 are likely attributable to more than just the switch in PK-M isoform expression. hnRNP A1/A2 knockdown resulted in some PK-M1 protein expression, although cells continued to express appreciable amounts of PK-M2. A nearly complete switch of PK-M2 to PK-M1 using shRNA knockdown and isoform-specific rescue constructs resulted in at most a 30% decrease in lactate production (1). Thus, the >2-fold reduction in lactate production we observed following combined hnRNP A1 + A2 knockdown probably reflects changes in alternative splicing that presumably occur in addition to those involving PK-M1/M2.

Aside from PK-M, additional genes important for cancer-cell metabolism are alternatively spliced. For instance, the bifunctional enzyme phosphofructokinase/bisphophatase B3 gene (*PFKFB3*) is a key regulator of glycolysis with preferential expression in cancer cells (25, 26). The kinase activity of this gene product generates fructose 2,6 bisphosphate (F2,6BP), which activates phosphofructokinase-1, a rate-limiting and regulatory control point of glycolysis, and indirectly leads to PK-M2 activation. In addition, HIF-1α and oncoproteins such as Ras activate *PFKFB3*, leading to increased F2,6BP in tumors (26). Multiple alternatively spliced isoforms of *PFKFB3* exist, though their distinctive properties have not been characterized. There is cross-talk between cell-energy sensing and pyruvate-kinase regulation of this enzyme, suggesting that regulation of splicing to generate specific isoforms may be part of a larger metabolic program to promote proliferative metabolism (27). We speculate that hnRNP A1/A2 might modulate the expression of other alternatively spliced metabolic genes, in addition to PK-M, that collectively account for the large decrease in lactate production following double knockdown of hnRNP A1 and A2.

Materials and Methods

Cells and Transfections. HeLa, HEK293, U-118MG, A-172, SK-N-BE, and C2C12 cells were grown in DMEM, supplemented with 10% (vol) FBS, penicillin, and streptomycin. To induce differentiation, near-confluent C2C12 cultures were washed 3X with PBS and maintained for 7 d in medium containing 2% (vol) horse serum, penicillin, and streptomycin. To select for a more homogenous differentiated culture, myotubes were treated for 4 d with 25 μM cytosine β-D-arabinofuranoside hydrochloride (AraC) (Sigma) beginning on day 7 after inducing differentiation. To generate stable transductant pools, A-172 cells were infected with LMP-puro or LMP-hygro retroviral vectors (5). The medium was replaced 24 h after infection, and starting 1 d later, infected cells were selected with puromycin (2 μg·mL^{-1}) for 3 d, or hygromycin (200 μg·mL^{-1}) for 7 d. In the case of double infections, cells were treated with hygromycin for 7 d after selection with puromycin for 3 d. Short hairpin RNA sequences were as follows: hnRNP A1—5′-TGCTGTTGACAGTGAGCGAAGTGTACAACAGATTTGTGAATAGTGAAGCCACAGATGTATTCACAAATCTGTTGTAACCTGTGCCTACTGCCTCGGA-3′; hnRNP A2—5′-TGCTGTTGACAGTGAGCGCGCATGGGCTTCACTGTATAATAGTGAAGCCACAGATGTATTATACAGTGAAGCCGATGGCATGCCTACTGCCTCGGA-3′; PTB—5′-CGCGTCCCCGCAGTTGGAGTGACCTTACTTCAAGAGAGTAAGGTCACTTCAGCTGCTTTTTGGAAAT-3′.

Immunoblotting. Cells were lysed in SDS and total protein concentration was measured. 30 μg of total protein from each lysate was separated by SDS-PAGE and transferred onto a nitrocellulose membrane. This was followed by blocking with 5% milk in Tris-buffered saline with Tween, probing with the indicated antibodies, and quantitation using an Odyssey infrared-imaging system (LI-COR Biosciences). Primary antibodies were: β-catenin (Abcam rAb 6302, 1:4,000); tubulin (Genscript rAb, 1:5,000); SF2/ASF (mAb AK96 culture supernatant, 1:100 (28)); hnRNP A1 (Abcam mAb 4810, 1:1,000 or mAb UP1-55 culture supernatant (29)); hnRNP A2 (Abcam mAb D3/3, 1:1,000); hnRNP A1/A2 (A1/UP1-62 culture supernatant, 1:20 (29)); PTB (mAb SH54 culture supernatant, 1:100 (30) or Abcam rAb83897, 1:1,000); CUG-BP1 (Abcam mAb 3B1, 1:500); PK-M2 (rabbit, 1:500) and PK-M1 (rabbit, 1:2,000) (1); total PK-M (Abcam gAb6191, 1:1,000). Secondary antibodies were IRdye 800 or 680 anti-rabbit, anti-mouse, or anti-goat (LI-COR Biosciences, 1:10,000).

RT-PCR Assays. 2 μg of total RNA was extracted from freshly dissected, saline-perfused mouse tissues, and from cell lines, using Trizol reagent (Invitrogen). Contaminating DNA was removed by treatment with DNase I (Promega). Reverse transcription was carried out using ImProm-II reverse transcriptase (Promega). Semiquantitative PCR using AmpliTaq polymerase (Applied Biosystems) was performed by including [α-^{32}P]-dCTP in the reactions. The mouse- and human-specific primer sets anneal to exons 8 and 11, and their sequences are as follows: hPKMF: 5′-AGAAACACAGCCAAAGGGCACT-3′; hPKMR: 5′-CATTCATGGCAAAGTTCACG-3′ and mPKMF: 5′-ATGCTGGAGAGCATGATCAAGAAGCCACGG-3′; mPKMR: 5′-CAACATCCATGGCCAAGTT-3′. After 22 amplification cycles, the reactions were separated into four aliquots for digestion with NsiI, PstI (New England Biolabs), both, or neither. The products were analyzed on a 5% native polyacrylamide gel, visualized by autoradiography, and quantitated on a FUJIFILM FLA-5100 phosphorimager (Fuji Medical Systems) using Multi Gauge software Version 2.3 (Fujifilm). The %M1 mRNA was calculated using the GC-content-normalized intensities of the top undigested band (M1) and the bottom two digested bands (M2) in the PstI-digest lanes.

Antisense Oligonucleotides. 2′-O-methyl phosphorothioate oligonucleotides were purchased from TriLink Biotechnologies, and purity was confirmed by gel electrophoresis. 3′ splice site antisense oligonucleotide: CUGGCAATCTAGGGGAGAAAC; 5′ splice site antisense oligonucleotide: CCGCCTCCTACCTGCCAGAC. HEK293 cells were plated at 50,000 cells per well in 6-well plates in DMEM supplemented with 10% fetal calf serum, 500 units/mL penicillin, and 0.1 mg/mL streptomycin. After allowing cells to adhere, they were transfected with 500 nM oligonucleotide using Lipofectamine 2000 (Invitrogen). After 4 h at 37°C, the transfecting mixture was replaced with fresh medium with serum. After 48 h, the cells were washed three times with PBS, trypsinized, counted, and extracted RNA was analyzed by radioactive RT-PCR as described above.

Lactate Assays. Lactate production was measured using a fluorescence-based assay kit (BioVision). Fresh medium was added to a 12-well plate of subconfluent cells and aliquots of media from each well were assessed 30 min later for the amount of lactate present. The cells were counted with a hemocytometer.

ACKNOWLEDGMENTS. We thank Chaolin Zhang, Martin Ackerman, Rotem Karni, Zuo Zhang, Yimin Hua, Mads Jensen, and Shuying Sun for helpful discussions and reagents. This work was supported by a grant from the Starr Cancer Consortium to A.R.K. and L.C.C. A Ruth L. Kirschstein National Research Service Award from the National Institutes of Health was received by C.V.C. A National Science Scholarship administered by the Agency for Science, Technology, and Research, Singapore was received by Z.W.

1. Christofk HR, et al. (2008) The M2 splice isoform of pyruvate kinase is important for cancer metabolism and tumour growth. *Nature*, 452:230–233.
2. Grosso AR, Martins S, Carmo-Fonseca M (2008) The emerging role of splicing factors in cancer. *EMBO Rep*, 9:1087–1092.
3. Karni R, et al. (2007) The gene encoding the splicing factor SF2/ASF is a proto-oncogene. *Nat Struct Mol Biol*, 14:185–193.
4. Dombrauckas JD, Santarsiero BD, Mesecar AD (2005) Structural basis for tumor pyruvate kinase M2 allosteric regulation and catalysis. *Biochemistry*, 44:9417–9429.
5. Noguchi T, Yamada K, Inoue H, Matsuda T, Tanaka T (1987) The L- and R-type isozymes of rat pyruvate kinase are produced from a single gene by use of different promoters. *J Biol Chem*, 262:14366–14371.
6. Noguchi T, Inoue H, Tanaka T (1986) The M1- and M2-type isozymes of rat pyruvate kinase are produced from the same gene by alternative RNA splicing. *J Biol Chem*, 261:13807–13812.
7. Christofk HR, Vander Heiden MG, Wu N, Asara JM, Cantley LC (2008) Pyruvate kinase M2 is a phosphotyrosine-binding protein. *Nature*, 452:181–186.
8. Jurica MS, et al. (1998) The allosteric regulation of pyruvate kinase by fructose-1, 6-bisphosphate. *Structure*, 6:195–210.
9. Chacko E, Ranganathan S (2009) Comprehensive splicing graph analysis of alternative splicing patterns in chicken, compared to human and mouse. *BMC Genomics*, 10(Suppl 1):S5.
10. Letunic I, Copley RR, Bork P (2002) Common exon duplication in animals and its role in alternative splicing. *Hum Mol Genet*, 11:1561–1567.
11. Smith CW (2007) Alternative splicing—when two's a crowd. *Cell*, 123:1–3.
12. Spellman R, Llorian M, Smith CW (2007) Crossregulation and functional redundancy between the splicing regulator PTB and its paralogs nPTB and ROD1. *Mol Cell*, 27:420–434.
13. Mazurek S, Boschek CB, Hugo F, Eigenbrodt E (2005) Pyruvate kinase type M2 and its role in tumor growth and spreading. *Semin in Cancer Biology*, 15:300–308.
14. Takenaka M, et al. (1995) Alternative splicing of the pyruvate kinase M gene in a minigene system. *Eur J Biochem*, 235:366–371.
15. Kislinger T, et al. (2003) Proteome dynamics during C2C12 myoblast differentiation. *Mol Cell Proteomics*, 4:887–901.
16. Sierakowska H, Agrawal S, Kole R (2000) Antisense oligonucleotides as modulators of pre-mRNA splicing. *Methods in Molecular Biology*, 133:223–233.
17. Mayeda A, Munroe SH, Cáceres JF, Krainer AR (1994) Function of conserved domains of hnRNP A1 and other hnRNP A/B proteins. *EMBO J*, 13:5483–5495.
18. Venables JP (2006) Unbalanced alternative splicing and its significance in cancer. *Bioessays*, 28:378–386.
19. He Y, Smith R (2009) Nuclear functions of heterogeneous nuclear ribonucleoproteins A/B. *Cell Mol Life Sci*, 66:1239–1256.
20. Okunola HL, Krainer AR (2009) Cooperative-binding and splicing-repressive properties of hnRNP A1. *Mol Cell Biol*, 29:5620–5631.
21. Wagner EJ, Garcia-Blanco MA (2001) Polypyrimidine tract binding protein antagonizes exon definition. *Mol Cell Biol*, 21:3281–3288.
22. Xue Y, et al. (2009) Genome-wide analysis of PTB-RNA interactions reveals a strategy used by the general splicing repressor to positively or negatively regulate alternative splicing in mammalian cells. *Mol Cell*, 35:926–1005.
23. David CJ, Chen M, Assanah M, Canoll P, Manley JL. (2009) HnRNP proteins controlled by c-Myc deregulate pyruvate kinase mRNA splicing in cancer. *Nature*, in press.
24. Black DL (2003) Mechanisms of alternative pre-messenger RNA splicing. *Annu Rev Biochem*, 72:291–336.
25. Van Schaftingen E, Hers HG (1981) Phosphofructokinase 2: The enzyme that forms fructose 2,6-bisphosphate from fructose 6-phosphate and ATP. *Biochem Biophys Res Commun*, 101:1078–1084.
26. Atsumi T, et al. (2002) High expression of inducible 6-phosphofructo-2-kinase/fructose-2,6-bisphosphatase (IPFK-2/PFKFB3) in human cancers. *Cancer Res*, 62:5881–5887.
27. Bando H, et al. (2005) Phosphorylation of the 6-phosphofructo-2-kinase/fructose 2, 6-bisphosphatase/PFKFB3 family of glycolytic regulators in human cancer. *Clin Cancer Res*, 11:5784–5792.
28. Hanamura A, Cáceres JF, Mayeda A, Franza BR, Jr, Krainer AR (1998) Regulated tissue-specific expression of antagonistic pre-mRNA splicing factors. *RNA*, 4:430–444.
29. Hua Y, Vickers TA, Okunola HL, Bennett CF, Krainer AR (2008) Antisense masking of an hnRNP A1/A2 intronic splicing silencer corrects SMN2 splicing in transgenic mice. *Am J Hum Genet*, 82:834–848.
30. Huang S, Deerinck TJ, Ellisman MH, Spector DL (1997) The dynamic organization of the perinucleolar compartment in the cell nucleus. *J Cell Biol*, 137:965–974.

doi:10.1093/jmcb/mjr030
Published online November 1, 2011

Article

Exon-centric regulation of pyruvate kinase M alternative splicing via mutually exclusive exons

Zhenxun Wang[1,2], Deblina Chatterjee[1,3], Hyun Yong Jeon[1,3], Martin Akerman[1], Matthew G. Vander Heiden[4], Lewis C. Cantley[5], and Adrian R. Krainer[1,*]

[1] Cold Spring Harbor Laboratory, PO Box 100, Cold Spring Harbor, NY 11724, USA
[2] Watson School of Biological Sciences, Cold Spring Harbor, NY 11724, USA
[3] Graduate Program in Molecular and Cellular Biology, Stony Brook University, Stony Brook, NY 11794, USA
[4] Koch Institute for Integrative Cancer Research at MIT, Cambridge, MA 02139, USA
[5] Division of Signal Transduction, Beth Israel Deaconess Medical Center and Department of Systems Biology, Harvard Medical School, Boston, MA 02115, USA
* Correspondence to: Adrian R. Krainer, E-mail: krainer@cshl.edu

Alternative splicing of the pyruvate kinase M gene (*PK-M*) can generate the M2 isoform and promote aerobic glycolysis and tumor growth. However, the cancer-specific alternative splicing regulation of *PK-M* is not completely understood. Here, we demonstrate that *PK-M* is regulated by reciprocal effects on the mutually exclusive exons 9 and 10, such that exon 9 is repressed and exon 10 is activated in cancer cells. Strikingly, exonic, rather than intronic, *cis*-elements are key determinants of *PK-M* splicing isoform ratios. Using a systematic sub-exonic duplication approach, we identify a potent exonic splicing enhancer in exon 10, which differs from its homologous counterpart in exon 9 by only two nucleotides. We identify SRSF3 as one of the cognate factors, and show that this serine/arginine-rich protein activates exon 10 and mediates changes in glucose metabolism. These findings provide mechanistic insights into the complex regulation of alternative splicing of a key regulator of the Warburg effect, and also have implications for other genes with a similar pattern of alternative splicing.

Keywords: alternative splicing, cancer metabolism, pyruvate kinase, SRSF3

Introduction

Cancer cells exhibit a metabolic phenotype termed aerobic glycolysis, or the Warburg effect, characterized by increased glycolysis with lactate generation, regardless of oxygen availability (Vander Heiden et al., 2009). Expression of the type II isoform of the pyruvate kinase M gene (*PKM2*, referred to here as *PK-M*) mediates this metabolic phenotype, and confers a proliferative advantage to tumor cells *in vivo* (Christofk et al., 2008a).

Pyruvate kinase (PK) catalyzes the final step in glycolysis, generating pyruvate and ATP from phosphoenolpyruvate and ADP (Dombrauckas et al., 2005). The exons 9 and 10 of the *PK-M* gene can each encode a 56-amino-acid segment, and be alternatively spliced in a mutually exclusive (*ME*) fashion to give rise to M1 and M2 isoforms, respectively (Noguchi et al., 1986). PK-M1 is constitutively active and predominantly expressed in terminally differentiated tissues (Christofk et al., 2008a; Clower et al., 2010). PK-M2 is expressed in cancer cells, as well as in fetal and undifferentiated adult tissues, and is allosterically regulated by fructose-1,6-bisphosphate (FBP) and can interact with tyrosine-phosphorylated signaling proteins (Christofk et al., 2008a, b). The growth signal-mediated inhibition of PK-M2 activity contributes to cancer cell growth by decreasing carbon flux through the catabolic glycolytic pathway, allowing accumulated upstream intermediates to be shunted to anabolic pathways to facilitate cell proliferation (Hitosugi et al., 2009).

ME exons are responsible for <2% of alternative splicing (Chacko and Ranganathan, 2009). Several mechanisms involved in ME exon selection have been described, but how they are coordinately regulated in a ME fashion is not well understood (Smith, 2005). ME exons are often homologous, indicating an exon-duplication origin (Letunic et al., 2002). The exons 9 and 10 of *PK-M* are ME exons whose ME splicing mechanism might be novel, as the length (401 bp) and sequence of intron 9 rule out steric interference that could prevent double splicing due to the spacing of the branch site and the 5′ splice site (5′ss) (Smith and Nadal-Ginard, 1989).

Recently, we and others demonstrated that exon 10 is preferred in cancer and proliferating cells, and also implicated two pairs of splicing-repressor paralogs—PTB/nPTB and hnRNPA1/A2—in exon 9 repression (Clower et al., 2010; David et al., 2010). It remains unclear whether additional repressors block exon 9, and exon 10 is the 'default' exon in proliferating cells, i.e. is its selection actively promoted, or is it included simply as a consequence of exon 9 repression? Moreover, though hnRNPA1/A2 and PTB appear to bind in the intronic regions flanking exon 9 (David et al., 2010), it remains unclear where the critical *cis*-elements responsible for the

Received July 11, 2011. Revised August 9, 2011. Accepted August 21, 2011.

REFERENCES

Akerman, M., David-Eden, H., Pinter, R.Y., and Mandel-Gutfreund, Y. (2009). A computational approach for genome-wide mapping of splicing factor binding sites. Genome Biol *10*, R30.

Akgul, C., Moulding, D.A., and Edwards, S.W. (2004). Alternative splicing of Bcl-2-related genes: functional consequences and potential therapeutic applications. Cellular and molecular life sciences : CMLS *61*, 2189-2199.

Allemand, E., Guil, S., Myers, M., Moscat, J., Caceres, J.F., and Krainer, A.R. (2005). Regulation of heterogenous nuclear ribonucleoprotein A1 transport by phosphorylation in cells stressed by osmotic shock. Proceedings of the National Academy of Sciences of the United States of America *102*, 3605-3610.

Anastasiou, D., Poulogiannis, G., Asara, J.M., Boxer, M.B., Jiang, J.K., Shen, M., Bellinger, G., Sasaki, A.T., Locasale, J.W., Auld, D.S.*, et al.* (2011). Inhibition of pyruvate kinase M2 by reactive oxygen species contributes to cellular antioxidant responses. Science *334*, 1278-1283.

Arany, Z., Wagner, B.K., Ma, Y., Chinsomboon, J., Laznik, D., and Spiegelman, B.M. (2008). Gene expression-based screening identifies microtubule inhibitors as inducers of PGC-1alpha and oxidative phosphorylation. Proceedings of the National Academy of Sciences of the United States of America *105*, 4721-4726.

Atsumi, T., Chesney, J., Metz, C., Leng, L., Donnelly, S., Makita, Z., Mitchell, R., and Bucala, R. (2002). High expression of inducible 6-phosphofructo-2-kinase/fructose-2,6-bisphosphatase (iPFK-2; PFKFB3) in human cancers. Cancer research *62*, 5881-5887.

Ayroldi, E., D'Adamio, F., Zollo, O., Agostini, M., Moraca, R., Cannarile, L., Migliorati, G., Delfino, D.V., and Riccardi, C. (1999). Cloning and expression of a short Fas ligand: A new alternatively spliced product of the mouse Fas ligand gene. Blood *94*, 3456-3467.

Back, S.H., Schroder, M., Lee, K., Zhang, K., and Kaufman, R.J. (2005). ER stress signaling by regulated splicing: IRE1/HAC1/XBP1. Methods *35*, 395-416.

Bando, H., Atsumi, T., Nishio, T., Niwa, H., Mishima, S., Shimizu, C., Yoshioka, N., Bucala, R., and Koike, T. (2005). Phosphorylation of the 6-phosphofructo-2-kinase/fructose 2,6-bisphosphatase/PFKFB3 family of glycolytic regulators in human cancer. Clinical cancer research : an official journal of the American Association for Cancer Research *11*, 5784-5792.

Barker, P.A., Lomen-Hoerth, C., Gensch, E.M., Meakin, S.O., Glass, D.J., and Shooter, E.M. (1993). Tissue-specific alternative splicing generates two isoforms of the trkA receptor. The Journal of biological chemistry *268*, 15150-15157.

Bates, D.O., Cui, T.G., Doughty, J.M., Winkler, M., Sugiono, M., Shields, J.D., Peat, D., Gillatt, D., and Harper, S.J. (2002). VEGF165b, an inhibitory splice variant of vascular endothelial growth factor, is down-regulated in renal cell carcinoma. Cancer research *62*, 4123-4131.

Black, D.L. (2003). Mechanisms of alternative pre-messenger RNA splicing. Annual review of biochemistry *72*, 291-336.

Boise, L.H., Gonzalez-Garcia, M., Postema, C.E., Ding, L., Lindsten, T., Turka, L.A., Mao, X., Nunez, G., and Thompson, C.B. (1993). bcl-x, a bcl-2-related gene that functions as a dominant regulator of apoptotic cell death. Cell *74*, 597-608.

Boutz, P.L., Chawla, G., Stoilov, P., and Black, D.L. (2007). MicroRNAs regulate the expression of the alternative splicing factor nPTB during muscle development. Genes & development *21*, 71-84.

Brinkman, B.M. (2004). Splice variants as cancer biomarkers. Clinical biochemistry *37*, 584-594.

Brown, R.L., Reinke, L.M., Damerow, M.S., Perez, D., Chodosh, L.A., Yang, J., and Cheng, C. (2011). CD44 splice isoform switching in human and mouse epithelium is essential for epithelial-mesenchymal transition and breast cancer progression. The Journal of clinical investigation *121*, 1064-1074.

Cáceres, J.F., Screaton, G.R., and Krainer, A.R. (1998). A specific subset of SR proteins shuttles continuously between the nucleus and the cytoplasm. Genes Dev *12*, 55-66.

Caputi, M., Mayeda, A., Krainer, A.R., and Zahler, A.M. (1999). hnRNP A/B proteins are required for inhibition of HIV-1 pre-mRNA splicing. EMBO J *18*, 4060-4067.

Cartegni, L., Chew, S.L., and Krainer, A.R. (2002). Listening to silence and understanding nonsense: exonic mutations that affect splicing. Nature reviews Genetics *3*, 285-298.

Cascino, I., Fiucci, G., Papoff, G., and Ruberti, G. (1995). Three functional soluble forms of the human apoptosis-inducing Fas molecule are produced by alternative splicing. J Immunol *154*, 2706-2713.

Cascino, I., Papoff, G., Eramo, A., and Ruberti, G. (1996). Soluble Fas/Apo-1 splicing variants and apoptosis. Frontiers in bioscience : a journal and virtual library *1*, d12-18.

Cassago, A., Ferreira, A.P., Ferreira, I.M., Fornezari, C., Gomes, E.R., Greene, K.S., Pereira, H.M., Garratt, R.C., Dias, S.M., and Ambrosio, A.L. (2012). Mitochondrial localization and structure-based phosphate activation mechanism of Glutaminase C with implications for cancer metabolism. Proceedings of the National Academy of Sciences of the United States of America *109*, 1092-1097.

Chacko, E., and Ranganathan, S. (2009). Comprehensive splicing graph analysis of alternative splicing patterns in chicken, compared to human and mouse. BMC genomics *10 Suppl 1*, S5.

Christofk, H., Vander Heiden, M., Harris, M.H., Ramanathan, A., Gerszten, R.E., Wei, R., Fleming, M.D., Schreiber, S.L., and Cantley, L. (2008a). The M2 splice isoform of pyruvate kinase is important for cancer metabolism and tumour growth. Nature *452*, 230-233.

Christofk, H., Vander Heiden, M., Wu, N., Asara, J., and Cantley, L. (2008b). Pyruvate kinase M2 is a phosphotyrosine-binding protein. Nature *452*, 181-186.

Christofk, H.R., Vander Heiden, M.G., Harris, M.H., Ramanathan, A., Gerszten, R.E., Wei, R., Fleming, M.D., Schreiber, S.L., and Cantley, L.C. (2008c). The M2 splice isoform of pyruvate kinase is important for cancer metabolism and tumour growth. Nature *452*, 230-233.

Christofk, H.R., Vander Heiden, M.G., Wu, N., Asara, J.M., and Cantley, L.C. (2008d). Pyruvate kinase M2 is a phosphotyrosine-binding protein. Nature *452*, 181-186.

Clower, C.V., Chatterjee, D., Wang, Z., Cantley, L.C., Vander Heiden, M.G., and Krainer, A.R. (2010a). The alternative splicing repressors hnRNP A1/A2 and PTB influence pyruvate kinase isoform expression and cell metabolism. Proc Natl Acad Sci USA *107*, 1894-1899.

Clower, C.V., Chatterjee, D., Wang, Z., Cantley, L.C., Vander Heiden, M.G., and Krainer, A.R. (2010b). The alternative splicing repressors hnRNP A1/A2 and PTB influence pyruvate kinase isoform expression and cell metabolism. Proceedings of the National Academy of Sciences of the United States of America *107*, 1894-1899.

Cooper, T.A. (2005). Alternative splicing regulation impacts heart development. Cell *120*, 1-2.

David, C.J., Chen, M., Assanah, M., Canoll, P., and Manley, J.L. (2010). HnRNP proteins controlled by c-Myc deregulate pyruvate kinase mRNA splicing in cancer. Nature *463*, 364-368.

de la Mata, M., Alonso, C.R., Kadener, S., Fededa, J.P., Blaustein, M., Pelisch, F., Cramer, P., Bentley, D., and Kornblihtt, A.R. (2003). A slow RNA polymerase II affects alternative splicing in vivo. Molecular cell *12*, 525-532.

De Moerlooze, L., Spencer-Dene, B., Revest, J.M., Hajihosseini, M., Rosewell, I., and Dickson, C. (2000). An important role for the IIIb isoform of fibroblast growth factor receptor 2 (FGFR2) in mesenchymal-epithelial signalling during mouse organogenesis. Development *127*, 483-492.

Dombrauckas, J.D., Santarsiero, B.D., and Mesecar, A.D. (2005). Structural basis for tumor pyruvate kinase M2 allosteric regulation and catalysis. Biochemistry *44*, 9417-9429.

Faustino, N.A., and Cooper, T.A. (2003). Pre-mRNA splicing and human disease. Genes & development *17*, 419-437.

Ferrara, N. (2004). Vascular endothelial growth factor: basic science and clinical progress. Endocrine reviews *25*, 581-611.

Fu, R.H., Liu, S.P., Ou, C.W., Yu, H.H., Li, K.W., Tsai, C.H., Shyu, W.C., and Lin, S.Z. (2009). Alternative splicing modulates stem cell differentiation. Cell transplantation *18*, 1029-1038.

Gao, P., Tchernyshyov, I., Chang, T.C., Lee, Y.S., Kita, K., Ochi, T., Zeller, K.I., De Marzo, A.M., Van Eyk, J.E., Mendell, J.T*., et al.* (2009). c-Myc suppression of miR-23a/b enhances mitochondrial glutaminase expression and glutamine metabolism. Nature *458*, 762-765.

Ghigna, C., Valacca, C., and Biamonti, G. (2008). Alternative splicing and tumor progression. Current genomics *9*, 556-570.

Glass, C.A., Harper, S.J., and Bates, D.O. (2006). The anti-angiogenic VEGF isoform VEGF165b transiently increases hydraulic conductivity, probably through VEGF receptor 1 in vivo. The Journal of physiology *572*, 243-257.

Grosso, A.R., Martins, S., and Carmo-Fonseca, M. (2008). The emerging role of splicing factors in cancer. EMBO reports *9*, 1087-1093.

Guertin, D.A., and Sabatini, D.M. (2005). An expanding role for mTOR in cancer. Trends in molecular medicine *11*, 353-361.

Hanahan, D., and Weinberg, R.A. (2000). The hallmarks of cancer. Cell *100*, 57-70.

Hanahan, D., and Weinberg, R.A. (2011). Hallmarks of cancer: the next generation. Cell *144*, 646-674.

Harper, S.J., and Bates, D.O. (2008). VEGF-A splicing: the key to anti-angiogenic therapeutics? Nature reviews Cancer *8*, 880-887.

Hartmann, B., Castelo, R., Blanchette, M., Boue, S., Rio, D.C., and Valcarcel, J. (2009). Global analysis of alternative splicing regulation by insulin and wingless signaling in Drosophila cells. Genome biology *10*, R11.

He, X., Ee, P.L., Coon, J.S., and Beck, W.T. (2004). Alternative splicing of the multidrug resistance protein 1/ATP binding cassette transporter subfamily gene in ovarian cancer creates functional splice variants and is associated with increased expression of the splicing factors PTB and SRp20. Clin Cancer Res *10*, 4652-4660.

He, Y., and Smith, R. (2009). Nuclear functions of heterogeneous nuclear ribonucleoproteins A/B. Cellular and molecular life sciences : CMLS *66*, 1239-1256.

Hitosugi, T., Kang, S., Vander Heiden, M.G., Chung, T.W., Elf, S., Lythgoe, K., Dong, S., Lonial, S., Wang, X., Chen, G.Z*., et al.* (2009). Tyrosine phosphorylation inhibits PKM2 to promote the Warburg effect and tumor growth. Sci Signal *2*, ra73.

Hofstetter, G., Berger, A., Fiegl, H., Slade, N., Zoric, A., Holzer, B., Schuster, E., Mobus, V.J., Reimer, D., Daxenbichler, G*., et al.* (2010). Alternative splicing of p53 and p73: the novel p53 splice variant p53delta is an independent prognostic marker in ovarian cancer. Oncogene *29*, 1997-2004.

Hua, Y., Vickers, T.A., Okunola, H.L., Bennett, C.F., and Krainer, A.R. (2008). Antisense masking of an hnRNP A1/A2 intronic splicing silencer corrects SMN2 splicing in transgenic mice. Am J Hum Genet *82*, 834-848.

Hughes, D.P., and Crispe, I.N. (1995). A naturally occurring soluble isoform of murine Fas generated by alternative splicing. The Journal of experimental medicine *182*, 1395-1401.

Inglese, J., Johnson, R.L., Simeonov, A., Xia, M., Zheng, W., Austin, C.P., and Auld, D.S. (2007). High-throughput screening assays for the identification of chemical probes. Nature chemical biology *3*, 466-479.

Jia, R., Liu, X., Tao, M., Kruhlak, M., Guo, M., Meyers, C., Baker, C.C., and Zheng, Z.M. (2009). Control of the papillomavirus early-to-late switch by differentially expressed SRp20. J Virol *83*, 167-180.

Jones, R.B., Wang, F., Luo, Y., Yu, C., Jin, C., Suzuki, T., Kan, M., and McKeehan, W.L. (2001). The nonsense-mediated decay pathway and mutually exclusive expression of alternatively spliced FGFR2IIIb and -IIIc mRNAs. J Biol Chem *276*, 4158-4167.

Jones, R.G., and Thompson, C.B. (2009). Tumor suppressors and cell metabolism: a recipe for cancer growth. Genes & development *23*, 537-548.

Kalluri, R., and Weinberg, R.A. (2009). The basics of epithelial-mesenchymal transition. The Journal of clinical investigation *119*, 1420-1428.

Karam, R., Carvalho, J., Bruno, I., Graziadio, C., Senz, J., Huntsman, D., Carneiro, F., Seruca, R., Wilkinson, M.F., and Oliveira, C. (2008). The NMD mRNA surveillance pathway downregulates aberrant E-cadherin transcripts in gastric cancer cells and in CDH1 mutation carriers. Oncogene *27*, 4255-4260.

Karni, R., de Stanchina, E., Lowe, S.W., Sinha, R., Mu, D., and Krainer, A.R. (2007). The gene encoding the splicing factor SF2/ASF is a proto-oncogene. Nature structural & molecular biology *14*, 185-193.

Karni, R., Hippo, Y., Lowe, S.W., and Krainer, A.R. (2008). The splicing-factor oncoprotein SF2/ASF activates mTORC1. Proceedings of the National Academy of Sciences of the United States of America *105*, 15323-15327.

Kelloff, G.J., Hoffman, J.M., Johnson, B., Scher, H.I., Siegel, B.A., Cheng, E.Y., Cheson, B.D., O'Shaughnessy, J., Guyton, K.Z., Mankoff, D.A.*, et al.* (2005). Progress and promise of FDG-PET imaging for cancer patient management and oncologic drug development. Clinical cancer research : an official journal of the American Association for Cancer Research *11*, 2785-2808.

Kerbel, R.S. (2008). Tumor angiogenesis. The New England journal of medicine *358*, 2039-2049.

Kislinger, T., Gramolini, A.O., Pan, Y., Rahman, K., MacLennan, D.H., and Emili, A. (2005). Proteome dynamics during C2C12 myoblast differentiation. Molecular & cellular proteomics : MCP *4*, 887-901.

Koppenol, W.H., Bounds, P.L., and Dang, C.V. (2011). Otto Warburg's contributions to current concepts of cancer metabolism. Nature reviews Cancer *11*, 325-337.

Krainer, A.R., Conway, G.C., and Kozak, D. (1990a). The essential pre-mRNA splicing factor SF2 influences 5' splice site selection by activating proximal sites. Cell *62*, 35-42.

Krainer, A.R., Conway, G.C., and Kozak, D. (1990b). Purification and characterization of pre-mRNA splicing factor SF2 from HeLa cells. Genes & development *4*, 1158-1171.

Ladomery, M.R., Harper, S.J., and Bates, D.O. (2007). Alternative splicing in angiogenesis: the vascular endothelial growth factor paradigm. Cancer letters *249*, 133-142.

Letunic, I., Copley, R.R., and Bork, P. (2002a). Common exon duplication in animals and its role in alternative splicing. Human molecular genetics *11*, 1561-1567.

Letunic, I., Copley, R.R., and Bork, P. (2002b). Common exon duplication in animals and its role in alternative splicing. Human Molecular Genetics *11*, 1561-1567.

Luco, R.F., Pan, Q., Tominaga, K., Blencowe, B.J., Pereira-Smith, O.M., and Misteli, T. (2010). Regulation of alternative splicing by histone modifications. Science *327*, 996-1000.

Makeyev, E.V., Zhang, J., Carrasco, M.A., and Maniatis, T. (2007). The MicroRNA miR-124 promotes neuronal differentiation by triggering brain-specific alternative pre-mRNA splicing. Molecular cell *27*, 435-448.

Matlin, A.J., Clark, F., and Smith, C.W. (2005). Understanding alternative splicing: towards a cellular code. Nature reviews Molecular cell biology *6*, 386-398.

Mayeda, A., and Krainer, A.R. (1992). Regulation of alternative pre-mRNA splicing by hnRNP A1 and splicing factor SF2. Cell *68*, 365-375.

Mazurek, S., Boschek, C.B., Hugo, F., and Eigenbrodt, E. (2005). Pyruvate kinase type M2 and its role in tumor growth and spreading. Seminars in cancer biology *15*, 300-308.

Misteli, T., and Spector, D.L. (1999). RNA polymerase II targets pre-mRNA splicing factors to transcription sites in vivo. Molecular cell *3*, 697-705.

Moore, M.J., and Proudfoot, N.J. (2009). Pre-mRNA processing reaches back to transcription and ahead to translation. Cell *136*, 688-700.

Moore, M.J., Wang, Q., Kennedy, C.J., and Silver, P.A. (2010). An alternative splicing network links cell-cycle control to apoptosis. Cell *142*, 625-636.

Nasim, M.T., and Eperon, I.C. (2006). A double-reporter splicing assay for determining splicing efficiency in mammalian cells. Nature protocols *1*, 1022-1028.

Noguchi, T., Inoue, H., and Tanaka, T. (1986). The M1- and M2-type isozymes of rat pyruvate kinase are produced from the same gene by alternative RNA splicing. The Journal of biological chemistry *261*, 13807-13812.

Noguchi, T., Yamada, K., Inoue, H., Matsuda, T., and Tanaka, T. (1987). The L- and R-type isozymes of rat pyruvate kinase are produced from a single gene by use of different promoters. The Journal of biological chemistry *262*, 14366-14371.

Novak, B., Tyson, J.J., Gyorffy, B., and Csikasz-Nagy, A. (2007). Irreversible cell-cycle transitions are due to systems-level feedback. Nature cell biology *9*, 724-728.

Nowak, D.G., Woolard, J., Amin, E.M., Konopatskaya, O., Saleem, M.A., Churchill, A.J., Ladomery, M.R., Harper, S.J., and Bates, D.O. (2008). Expression of pro- and anti-angiogenic isoforms of VEGF is differentially regulated by splicing and growth factors. Journal of cell science *121*, 3487-3495.

Okunola, H.L., and Krainer, A.R. (2009). Cooperative-binding and splicing-repressive properties of hnRNP A1. Molecular and cellular biology *29*, 5620-5631.

Ozaki, T., and Nakagawara, A. (2005). p73, a sophisticated p53 family member in the cancer world. Cancer science *96*, 729-737.

Pasanen, A., Heikkila, M., Rautavuoma, K., Hirsila, M., Kivirikko, K.I., and Myllyharju, J. (2010). Hypoxia-inducible factor (HIF)-3alpha is subject to extensive alternative splicing in human tissues

and cancer cells and is regulated by HIF-1 but not HIF-2. The international journal of biochemistry & cell biology *42*, 1189-1200.

Paz, I., Akerman, M., Dror, I., Kosti, I., and Mandel-Gutfreund, Y. (2010). SFmap: a web server for motif analysis and prediction of splicing factor binding sites. Nucleic Acids Research *38 Suppl*, W281-285.

Ponta, H., Sherman, L., and Herrlich, P.A. (2003). CD44: from adhesion molecules to signalling regulators. Nature reviews Molecular cell biology *4*, 33-45.

Pradervand, S., Weber, J., Thomas, J., Bueno, M., Wirapati, P., Lefort, K., Dotto, G.P., and Harshman, K. (2009). Impact of normalization on miRNA microarray expression profiling. RNA *15*, 493-501.

Prinos, P., Garneau, D., Lucier, J.F., Gendron, D., Couture, S., Boivin, M., Brosseau, J.P., Lapointe, E., Thibault, P., Durand, M*., et al.* (2011). Alternative splicing of SYK regulates mitosis and cell survival. Nature structural & molecular biology *18*, 673-679.

Sakharkar, M.K., Chow, V.T., and Kangueane, P. (2004). Distributions of exons and introns in the human genome. In silico biology *4*, 387-393.

Schaal, T.D., and Maniatis, T. (1999). Selection and characterization of pre-mRNA splicing enhancers: identification of novel SR protein-specific enhancer sequences. Mol Cell Biol *19*, 1705-1719.

Sharma, P.M., Reddy, G.R., Babior, B.M., and McLachlan, A. (1990). Alternative splicing of the transcript encoding the human muscle isoenzyme of phosphofructokinase. The Journal of biological chemistry *265*, 9006-9010.

Shin, K.H., Kim, R.H., Kang, M.K., and Park, N.H. (2008). hnRNP G elicits tumor-suppressive activity in part by upregulating the expression of Txnip. Biochemical and biophysical research communications *372*, 880-885.

Smith, C.W. (2005). Alternative splicing--when two's a crowd. Cell *123*, 1-3.

Smith, C.W., and Nadal-Ginard, B. (1989). Mutually exclusive splicing of alpha-tropomyosin exons enforced by an unusual lariat branch point location: implications for constitutive splicing. Cell *56*, 749-758.

Spellman, R., Llorian, M., and Smith, C.W. (2007). Crossregulation and functional redundancy between the splicing regulator PTB and its paralogs nPTB and ROD1. Molecular cell *27*, 420-434.

Stamm, S. (2008). Regulation of alternative splicing by reversible protein phosphorylation. The Journal of biological chemistry *283*, 1223-1227.

Takenaka, M., Yamada, K., Lu, T., Kang, R., Tanaka, T., and Noguchi, T. (1996). Alternative splicing of the pyruvate kinase M gene in a minigene system. European journal of biochemistry / FEBS *235*, 366-371.

Tang, X.X., Pleasure, D.E., Brodeur, G.M., and Ikegaki, N. (1998). A variant transcript encoding an isoform of the human protein tyrosine kinase EPHB2 is generated by alternative splicing and alternative use of polyadenylation signals. Oncogene *17*, 521-526.

Tarn, W.Y., and Steitz, J.A. (1996). Highly diverged U4 and U6 small nuclear RNAs required for splicing rare AT-AC introns. Science *273*, 1824-1832.

Thiery, J.P., Acloque, H., Huang, R.Y., and Nieto, M.A. (2009). Epithelial-mesenchymal transitions in development and disease. Cell *139*, 871-890.

Thiery, J.P., and Sleeman, J.P. (2006). Complex networks orchestrate epithelial-mesenchymal transitions. Nature reviews Molecular cell biology *7*, 131-142.

Valacca, C., Bonomi, S., Buratti, E., Pedrotti, S., Baralle, F.E., Sette, C., Ghigna, C., and Biamonti, G. (2010). Sam68 regulates EMT through alternative splicing-activated nonsense-mediated mRNA decay of the SF2/ASF proto-oncogene. The Journal of cell biology *191*, 87-99.

Vander Heiden, M., Cantley, L., and Thompson, C.B. (2009). Understanding the Warburg effect: the metabolic requirements of cell proliferation. Science *324*, 1029-1033.

Venables, J.P. (2006). Unbalanced alternative splicing and its significance in cancer. BioEssays : news and reviews in molecular, cellular and developmental biology *28*, 378-386.

Wagner, E.J., and Garcia-Blanco, M.A. (2001). Polypyrimidine tract binding protein antagonizes exon definition. Molecular and cellular biology *21*, 3281-3288.

Wagner, E.J., and Garcia-Blanco, M.A. (2002). RNAi-mediated PTB depletion leads to enhanced exon definition. Molecular cell *10*, 943-949.

Wang, D., Zavadil, J., Martin, L., Parisi, F., Friedman, E., Levy, D., Harding, H., Ron, D., and Gardner, L.B. (2011). Inhibition of nonsense-mediated RNA decay by the tumor microenvironment promotes tumorigenesis. Molecular and cellular biology *31*, 3670-3680.

Wang, E.T., Sandberg, R., Luo, S., Khrebtukova, I., Zhang, L., Mayr, C., Kingsmore, S.F., Schroth, G.P., and Burge, C.B. (2008). Alternative isoform regulation in human tissue transcriptomes. Nature *456*, 470-476.

Warburg, O. (1956). On the origin of cancer cells. Science *123*, 309-314.

Warzecha, C.C., Sato, T.K., Nabet, B., Hogenesch, J.B., and Carstens, R.P. (2009). ESRP1 and ESRP2 are epithelial cell-type-specific regulators of FGFR2 splicing. Molecular cell *33*, 591-601.

Weinberg, F., and Chandel, N.S. (2009). Mitochondrial metabolism and cancer. Annals of the New York Academy of Sciences *1177*, 66-73.

Xu, Q., Modrek, B., and Lee, C. (2002). Genome-wide detection of tissue-specific alternative splicing in the human transcriptome. Nucleic acids research *30*, 3754-3766.

Xue, Y., Zhou, Y., Wu, T., Zhu, T., Ji, X., Kwon, Y.S., Zhang, C., Yeo, G., Black, D.L., Sun, H.*, et al.* (2009). Genome-wide analysis of PTB-RNA interactions reveals a strategy used by the general splicing repressor to modulate exon inclusion or skipping. Molecular cell *36*, 996-1006.

Yoshida, K., Sanada, M., Shiraishi, Y., Nowak, D., Nagata, Y., Yamamoto, R., Sato, Y., Sato-Otsubo, A., Kon, A., Nagasaki, M.*, et al.* (2011). Frequent pathway mutations of splicing machinery in myelodysplasia. Nature *478*, 64-69.

Zhang, B., Metharom, P., Jullie, H., Ellem, K.A., Cleghorn, G., West, M.J., and Wei, M.Q. (2004). The significance of controlled conditions in lentiviral vector titration and in the use of multiplicity of infection (MOI) for predicting gene transfer events. Genetic vaccines and therapy *2*, 6.

Zscharnack, K., Kessler, R., Bleichert, F., Warnke, J.P., and Eschrich, K. (2009). The PFKFB3 splice variant UBI2K4 is downregulated in high-grade astrocytomas and impedes the growth of U87 glioblastoma cells. Neuropathology and applied neurobiology *35*, 566-578.

Zuber, J., McJunkin, K., Fellmann, C., Dow, L.E., Taylor, M.J., Hannon, G.J., and Lowe, S.W. (2011). Toolkit for evaluating genes required for proliferation and survival using tetracycline-regulated RNAi. Nature biotechnology *29*, 79-83.

Carrillo Oesterreich, F., Preibisch, S., and Neugebauer, K.M. (2010). Global analysis of nascent RNA reveals transcriptional pausing in terminal exons. Molecular cell *40*, 571-581.

Gornemann, J., Kotovic, K.M., Hujer, K., and Neugebauer, K.M. (2005). Cotranscriptional spliceosome assembly occurs in a stepwise fashion and requires the cap binding complex. Molecular cell *19*, 53-63.

Shukla, S., Kavak, E., Gregory, M., Imashimizu, M., Shutinoski, B., Kashlev, M., Oberdoerffer, P., Sandberg, R., and Oberdoerffer, S. (2011). CTCF-promoted RNA polymerase II pausing links DNA methylation to splicing. Nature *479*, 74-79.